Palaeogene carbonate platforms under climatic and tectonic stress – case studies from Egypt and Spain

Dissertation
zur Erlangung des Doktorgrades der Naturwissenschaften
(Dr. rer. nat.)
am Fachbereich Geowissenschaften
der Universität Bremen

Stefan Höntzsch

Bremen, März 2011

University of Bremen
Department of Geosciences
PhD thesis
Supervisor: Prof. Dr. Hans-Joachim Kuss

Hiermit erkläre ich, dass ich die vorliegende Doktorarbeit selbstständig und ohne Zuhilfenahme unerlaubter Hilfsmittel erstellt habe. Weder diese noch eine ähnliche Arbeit wurde an einer anderen Abteilung oder Hochschule im Rahmen eines Prüfungsverfahrens vorgelegt, veröffentlicht oder zur Veröffentlichung vorgelegt. Ferner versichere ich, dass die Arbeit unter Einhaltung der Regeln guter wissenschaftlicher Praxis der Deutschen Forschungsgemeinschaft entstanden ist.

Stefan Höntzsch

ACKNOWLEDGEMENTS

I am really grateful to many people who have encouraged me during my PhD times and kept me away from procrastinating. Especially, I want to thank my working group, Jochen Kuss, Christian Scheibner, Maria Petrogiannis, Hussam Ghanem, Ralf Bätzel, Salwa Bey, Ahmed Abdel Naby, Jens Wendler and Matthias Heldt for their professional and amicable support and the relaxing working atmosphere.

The present work significantly benefited from collaboration and discussion with Michael Rasser, Akmal Marzouk, Elisa Guasti, Robert Speijer, Peter Stassen, John Reijmer, Ralph Groen, Luuk Kleipool, Peter Schulte, Christoph Vogt, Abdel Monem Soltan, Abdel Mohsen Morsi, Mohamed Boukhary, Karin Gesierich, Gauvain Wiemer and Johannes Brock. Christian Sommerfeld, Patrick Simundic, Sarah Romahn, Brit Kockisch and Monika Segl are thanked for the assiduos preparation and processing of the samples.

In more than three years in Bremen I met numerous people who made my life beyond science much more entertaining: Enno Zymelka, Anna Richter, Johannes Lindtke, Franziska Kersten, Ulrike Proske, Dörte Dittjen, Tanja Feiel and the “Tuesday Soccer Squad” have contributed many hours of recreation and fun.

Furthermore, I want to address Jorge Cham from “Piled Higher and Deeper”, who has shown me that it is not impossible to finish a PhD in less than seven years.

Special thanks go to Egbert, Manja, Ellen, Dietmar and all the friends who have managed a trip to Bremen for a weekend or two. Susan is thanked for everything else, especially for tolerating my bad mood between 7 and 9 am.

This work is dedicated to my parents for their invaluable support during the last three decades.

This study has been funded by the DFG-Project Ku 642/221 “Platform evolution around the Early Eocene Climatic Optimum (EECO) in a low latitude setting”.

ABSTRACT

Two Palaeogene carbonate platforms were studied in the Eastern Mediterranean (Egypt) and Western Mediterranean (Spain) in order to reconstruct the evolution of the shelves during times of high climatic and tectonic variability. Reconstructions are based on field observations, high-resolution microfacies (e.g., larger benthic foraminifera, corals) and geochemical data (e.g., bulk carbon isotopes).

The Paleocene to Early Eocene succession of the Galala Mountains in the Eastern Desert (Egypt) represents an excellent example for an isolated carbonate platform at the SE Tethyan shelf. Deposition at the platform is controlled by syn-depositional tectonism, climate and sea-level changes. Microfacies and geochemical analyses reveal repeated phases of tectonic uplift during the Early Eocene, which are linked to the massive deposition of siliciclastics and an increasing restriction of the Egyptian shelf. The termination of tectonic uplift is indicated by the shift to pure carbonate deposition and the recovery to open ocean conditions in the latest Early Eocene. Increased nutrient availability at the Galala platform throughout the Early Eocene is interpreted as a coupled effect of climatically-induced nutrient discharge from the African continent and tectonically-controlled eutrophication.

Carbon isotope data document three significant negative carbon isotope excursions in the Galala succession. Those excursions are related to transient global hyperthermal events. The most prominent hyperthermal event, the Paleocene-Eocene Thermal Maximum (PETM), witnesses a prominent turnover of the larger benthic foraminifera species and a shift from coral-dominated assemblages to larger benthic foraminifera-dominated assemblages at the platform. During the Early Eocene corals are not recorded in the Galala succession, which has been attributed to the coupled impact of global warming and local nutrient excess.

Further post-PETM hyperthermal events were documented in the Galala succession for the first time in a shallow-marine tropical environment. The negative carbon isotope excursions of Eocene Thermal Maximum 2 and 3 show a significantly smaller magnitude and do not demonstrate a biotic impact to shallow-benthic assemblages.

In a second study, a compiled Paleocene – Early Oligocene succession of the Prebetic platform in SE Spain has been used to document the distribution of larger benthic foraminifera and corals during the Eocene global cooling interval. High resolution microfacies data reveal a recovery of the Prebetic coral fauna during the Late Eocene. The comparision with other Tethyan carbonate successions demonstrates that coral recovery is strongly dependend on latitude: Global cooling yielded to the recovery of coral communities in the northern Tethyan realm during the Bartonian. A prominent cooling event at the Bartonian-Priabonian boundary, associated with a demise of many symbiont-bearing larger foraminifera causes the proliferation of coral reefs in the northern Tethys and the recovery of corals in the southern Tethys. The massive temperature drop related to the Oi-1 glaciation at the Eocene-Oligocene boundary caused a transient decline in coral abundance, followed by the Tethyan-wide proliferation of major coral built-ups. Local differences regarding the timing of coral recovery are amongst others related to syn-depositional tectonic activity or temporal nutrient excess.

ZUSAMMENFASSUNG

Die vorliegende Studie beschäftigt sich mit der Rekonstruktion zweier paläogener Karbonatplattformen im östlichen und westlichen Mittelmeerraum (Ägypten und Spanien). Das Paläogen repräsentiert dabei ein Zeitintervall in der Erdgeschichte, das durch starke klimatische und tektonische Umwälzung gekennzeichnet ist. Die Rekonstruktion der vorherrschenden Umweltbedingungen basiert auf hochauflösender Mikrofaziesdaten (z. B. Großforaminiferen und Korallen) sowie geochemischen Analysen (Kohlenstoffisotopie).

Sedimentationsprozesse und Plattformentwicklung an der Paleozänen bis frühen Eozänen isolierten Karbonatplattform der Galala Berge (östliche ägyptische Wüste) wurden vor allem durch tektonische Prozesse, Meeresspiegelschwankungen und Klimaänderung gesteuert. Mikrofazies und geochemische Analysen weisen auf wiederholte tektonische Hebungsereignisse während des frühen Eozäns hin, die an die verstärkte Sedimentation von siliziklastischen Ablagerungen und die zunehmende Restriktion der Galala Plattform und des ägyptischen Schelfs gekoppelt sind. Das Ende der tektonischen Hebung ist durch den Übergang zu rein karbonatischer Sedimentation und offen-marinen Verhältnissen im späten Frühen Eozän gekennzeichnet. Das verstärkte Auftreten von Organismen, die erhöhte Nährstoffgehalte anzeigen, wurde als gekoppelter Effekt klimatisch gesteuerten Nährstoffeintrags vom afrikanischen Kontinent und tektonisch verursachtem Nährstoffeintrag durch Hebung interpretiert.

Stabile Kohlenstoffisotopendaten der Galala-Abfolge weisen auf drei signifikante negative Exkursionen hin, die als hyperthermale Ereignisse interpretiert werden. Das bedeutendste hyperthermale Ereignis, das Paleozäne-Eozäne Temperatur Maximum, definiert die Paleozän-Eozän Grenze und ist durch einen bedeutenden spezifischen Übergang innerhalb der Großforaminiferenfauna gekennzeichnet. Ferner lässt sich ein Übergang von Korallen-dominierten zu Großforaminiferen-dominierten Faziesassoziationen auf der Plattform feststellen. Weitere aufgenommene hyperthermale Ereignisse wurden zum ersten Mal im flachmarinen Milieu nachgewiesen, zeigen jedoch keinerlei Einfluss auf die Organismen der Galala-Plattform.

Im zweiten Teil der Studie wurden vier Profile der Prebetischen Karbonatplattform in Südost-Spanien aufgenommen, um die Verteilung von Großforaminiferen und Korallen während der globalen Abkühlung und dem Übergang vom Treibhaus- zum Eishausklima zu dokumentieren. Hochauflösende Mikrofaziesdaten zeigen ein Wiederkehren der Korallenfauna auf der Prebetischen Plattform im späten Eozän. Der Vergleich mit anderen Karbonatplattformen verdeutlicht, dass das Wiederkehren der Korallenfauna in der Tethys stark durch die geographische Breite beeinflusst wird. Während in der nördlichen Tethys bereits im Barton erste Korallen gefunden wurden, konnten sie in der südlichen Tethys erst nach einem massiven Abkühlungsereignis an der Barton-Priabon Grenze nachgewiesen werden. Dieses Abkühlungsereignis führte ebenso zu einem massiven Rückgang photo-autotropher Großforaminiferen. Größere Tethys-weite Korallenassoziationen werden dagegen erst nach einem weiteren Abkühlungsereignis (Oi-1 Vereisung) im frühen Oligozän gefunden. Regionale Unterschiede im zeitlichen Ablauf der wiederkehrenden der Korallenfauna gehen auf wiederholte tektonische Aktivität während der Ablagerung sowie zeitweisem Nährstoffüberangebot zurück.

TABLE OF CONTENTS

LIST OF FIGURES

LIST OF TABLES

I. PROLOGUE

Carbonate platform systems are known as excellent depositional archives, which help to understand the dynamics and processes of long-term climate change and transient environmental perturbations. During the Palaeogene the Mediterranean realm has been influenced and controlled by global, regional and local factors, which strongly vary with respect to the prevailing climatic conditions, the syn-depositional impact of tectonic processes, sea-level fluctuations and the availability of nutrient resources (Wilson and D'Argenio, 1982; Hallock and Schlager, 1986; Bosellini, 1989; Crevello et al., 1989; Masse and Montaggioni, 2001; Bosence, 2005; Fournier et al., 2005). This strongly heterogeneous evolution is, however, underexplored with respect to its impact on Mediterranean carbonate platforms and the prevailing platform organisms.

The presented study helps to understand the controlling mechanisms of deposition at shallow-marine marginal shelves, focussing on the linked impact of long-term and transient climate change and syn-depositional tectonic perturbations. Two carbonate platforms in the southern Mediterranean (Egypt) and in the northern Mediterranean realm (Spain) with crucial differences regarding regional climate, prevailing platform organisms and local tectonic regime are studied.

The project focusses on platform-to-basin transects to achive a broad data set of different environments and bathymetries. The investigation of the platform systems includes high resolution microfacies and geochemical data. Stable carbon isotope data will highlight the evolution of the long-term carbon cycle and transient carbon cycle perturbations in shallow-marine settings.

I.1 Climatic evolution and carbon cycle perturbations during the Palaeogene

Environments on Earth underwent fundamental long-term and transient climatic changes during the Palaeogene, resulting in the transition from global greenhouse to icehouse conditions. The Early Palaeogene is characterized by global greenhouse conditions and rising temperatures (Fig. I.1; Zachos et al., 2001). Anomalous warm poles and low latitudinal temperature gradients caused weakened ocean circulations, oligotrophic open ocean conditions and very low Mg/Ca-ratios (“sluggish ocean”; McGowran, 1989). This Early Palaeogene “hothouse” is, however, superimposed by multiple transient climatic perturbations, which are attributed to significant negative shifts in the global carbon cycle (“hyperthermals”; Thomas and Zachos, 2000). Those hyperthermal events are characterized by negative carbon isotope excursions (CIEs), explained by the mass release of isotopically

light carbon (^{12}C). The trigger mechanisms of this mass release are manifold and may be related to the degassing of methane hydrates (Dickens et al., 1995; Katz et al., 1999), volcanic gas expulsion in the North Atlantic (Storey et al., 2007; Nisbet et al., 2009) or the global conflagration of peatlands (Fig. I.2; Kurtz et al., 2003). The most prominent carbon cycle perturbation is the Paleocene-Eocene Thermal Maximum (PETM), resulting in a global transient temperature increase of 4 – 8°C, a shallowing of the calcite compensation depth (CCD), as well as major environmental turnover and ubiqitous biotic extinctions in nearly all environments on Earth (Kennett and Stott, 1991; Zachos et al., 1993).

Further Eocene Thermal Maxima (ETM) with minor negative $\delta^{13}C$ shifts and less severe biotic impact were recorded in the deep sea and at the deeper continental shelf (Thomas and Zachos, 2000; Cramer et al., 2003; Lourens et al., 2005; Nicolo et al., 2007; Agnini et al., 2009). Two of the most important post-PETM hyperthermals are the ETM2 or Elmo-event (Eocene layer of mysterious origin; according to Lourens et al., 2005) at 53.6 Ma and the ETM3 or x-event at 52.5 Ma (Fig. I.1; Röhl et al., 2005). The impact of those hyperthermals to the shelves is still under debate. John et al. (2008) argues, that the shelves represent large carbon sinks, which are probably decoupled from the global carbon cycle during hyperthermal events. Especially the enhanced hydrological cycle with increased nutrient and carbon fluxes from the continents to the shelves refer to a higher environmental impact of hyperthermal events to marginal shallow-marine basins (Fig. I.2).

The global warming trend during the Early Palaeogene culminated during the Early Eocene Climatic Optimum (EECO) between 53 – 49 Ma (Zachos et al., 2001). The post-EECO cooling affected especially higher latitudes, whereas the tropics remained warm (Pearson et al., 2007; Jovane et al., 2009; Creech et al., 2011). Increasing latitudinal temperature gradients in the Middle and Late Eocene strengthened global ocean currents, causing the upwelling of cooler deep ocean waters and the eutrophication of the oceans (McGowran, 1989). The Oi-1 glaciation at the Eocene-Oligocene boundary represents a major break in global climate with a sharp temperature drop of >5 °C, associated with a significant deepening of the CCD, a ~1 ‰ positive excursion in the global carbon cycle and major biotic turnovers and extinctions (Fig. I.1; Ivany et al., 2000; Zanazzi et al., 2007; Eldrett et al., 2009).

Figure I.1 (next page) **–** Overview of selected Paleocene – Lower Oligocene environmental proxies, including stable isotopes, sea surface temperatures (SST), eustatic sea level, climatic- and biotic events, as well as main tectonic events (modified after Höntzsch et al., in press). Abbreviations: O. – Oligocene, CIE – carbon isotope excursion, PETM – Paleocene-Eocene Thermal Maximum, ETM – Eocene Thermal Maximum, EECO – Early Eocene climatic optimum, MECO – Middle Eocene climatic optimum.

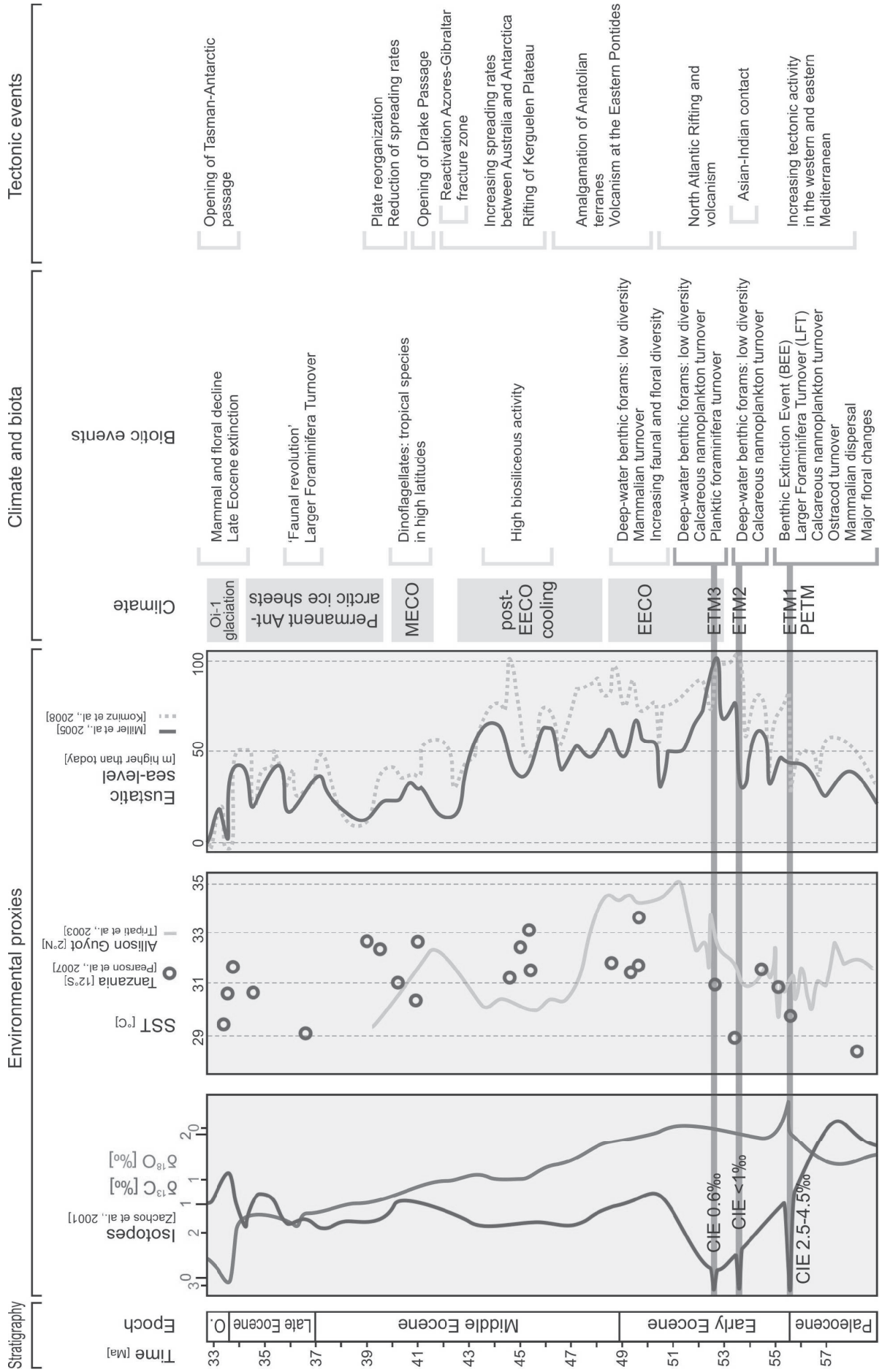
Stratigraphy
Environmental proxies
Climate and biota
Tectonic events
Time [Ma]
Epoch
Isotopes
[Zachos et al., 2001]
δ13C [‰]
δ18O [‰]
SST [°C]
Tanzania [12°S]
[Pearson et al., 2007]
Allison Guyot [2°N]
[Tripati et al., 2003]
Eustatic sea-level
[m higher than today]
[Miller et al., 2005]
[Kominz et al., 2008]
Climate
Biotic events
Tectonic events
Q.
Late Eocene
Middle Eocene
Early Eocene
Paleocene
Oi-1 glaciation
Permanent Ant-arctic ice sheets
MECO
post-EECO cooling
EECO
ETM3
ETM2
ETM1
PETM
Mammal and floral decline
Late Eocene extinction
'Faunal revolution'
Larger Foraminifera Turnover
Dinoflagellates: tropical species in high latitudes
High biosiliceous activity
Deep-water benthic forams: low diversity
Mammalian turnover
Increasing faunal and floral diversity
Deep-water benthic forams: low diversity
Calcareous nannoplankton turnover
Planktic foraminifera turnover
Deep-water benthic forams: low diversity
Calcareous nannoplankton turnover
Benthic Extinction Event (BEE)
Larger Foraminifera Turnover (LFT)
Calcareous nannoplankton turnover
Ostracod turnover
Mammalian dispersal
Major floral changes
Opening of Tasman-Antarctic passage
Plate reorganization
Reduction of spreading rates
Opening of Drake Passage
Reactivation Azores-Gibraltar fracture zone
Increasing spreading rates between Australia and Antarctica
Rifting of Kerguelen Plateau
Amalgamation of Anatolian terranes
Volcanism at the Eastern Pontides
North Atlantic Rifting and volcanism
Asian-Indian contact
Increasing tectonic activity in the western and eastern Mediterranean
CIE 0.6‰
CIE <1‰
CIE 2.5-4.5‰

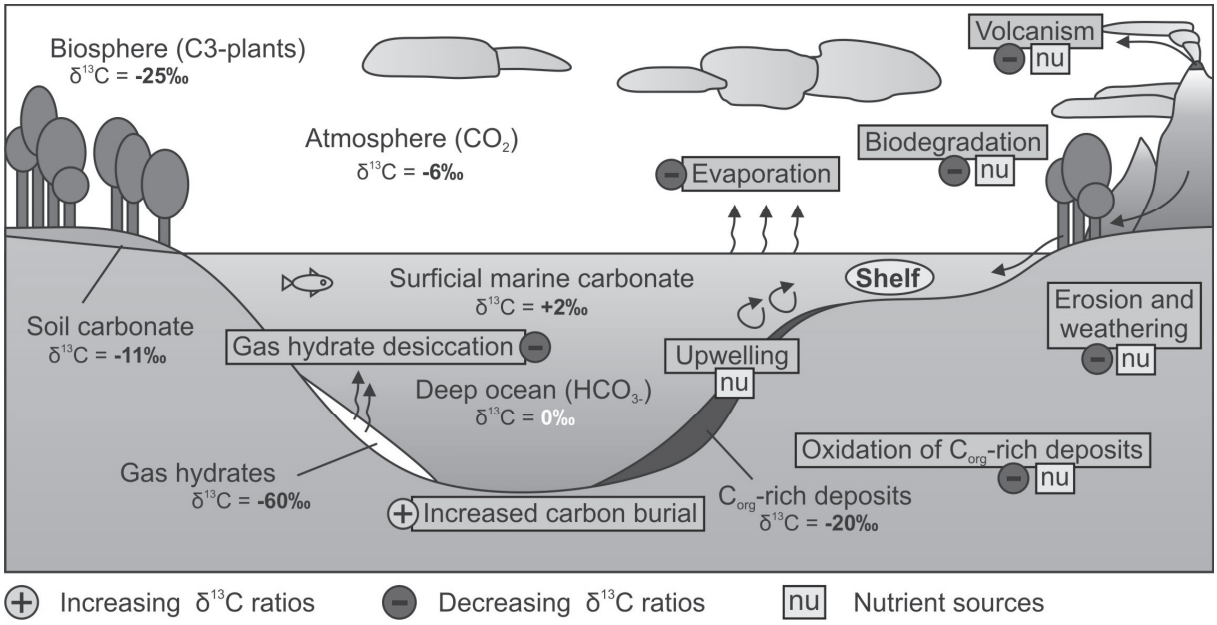

Figure I.2 – Terrestrial, marine and atmospheric carbon reservoirs and their interaction with the shallow-marine shelf. The grey rectangles indicate major carbon fluxes and their impact on δ13C ratios of shelf deposits. Major trophic resources, which cause nutrient fluxes to the shelf, are added in order to demonstrate the certain link between eutrophication and carbon input to the oceans.

I.2 Tectonic-climate coupling and reorganization of the Mediterranean realm during the Palaeogene

Long-term and transient climatic evolution is strongly influenced by the reorganization of continental plates, causing the opening and closure of ocean basins and the uplift of major mountain belts during the Palaeogene (Fig. I.1; Bohaty and Zachos, 2003). Increasing volcanic activity and the initial rifting of the North Atlantic have been associated with the release of strongly depleted carbon to the atmosphere and to the onset of the PETM (Fig. I.1; Zachos et al., 2001; Storey et al., 2007). The initial collision of India and Asia between ~55 – 50 Ma caused the closure of the Neo-Tethys and the eastern Tethyan seaway (Searle et al., 1987; Clementz et al., 2011). The continuing convergence between the African-Arabian craton, India and Eurasia resulted in the multi-phase uplift of the Alpine-Himalayan orogenic system ranging from the Pyrenees to the Himalayas (Verdel et al., 2007). Coeval North Atlantic divergence and African-Eurasian convergence resulted in the reactivation of ancient fault systems (e.g. Syrian Arc-Fold Belt, Azores-Gibraltar fracture zone), which are associated with complex tectonic deformation and frequent arc-related volcanism in the Mediterranean realm (Forster et al., 1972; Verdel et al., 2007).

Uplift, subaerial exposure and denudation of pre-orogenic carbon-rich sea floor probably forced the global cooling during the late Palaeogene. A major factor causing the isolation of Antarctica and the onset of permanent Antarctic ice sheets is demonstrated by the increasing

spreading rates between Antarctica and Australia and the rifting of the Kerguelen Plateau between 46 – 41 Ma (Bohaty and Zachos, 2003). The isolation of Antarctica yielding to the onset of a circum-Antarctic pathway was triggered by the opening of the Tasmanian-Antarctic Gateway between 41 – 31 Ma (Exon et al., 2000; Wei, 2004; Sijp et al., 2009) and the opening of the Drake Passage at 41 Ma (Scher and Martin, 2006).

I.3 Tethyan carbonate platform evolution during the Palaeogene

The evolution of circum-Tethyan carbonate platforms is strongly controlled by three major parameters: a) the occurrence of carbonate platforms in areas of high tectonic activity with strongly varying subsidence levels, causing emergence, drowning and subaerial exposure of carbonate platforms (Bosellini, 1989), b) the long-term climatic evolution during the Palaeogene, including latitudinal variations and variations in the local environmental parameters and, c) long-term and transient eustatic sea-level fluctuations. The distinct heterogeneity of the global and regional controlling mechanisms on carbonate platforms hampers an integrated classification of circum-Tethyan platform systems for the Palaeogene. However, many regional classifications on carbonate platform evolution have been established in the last decades (Spain: e.g., Pujalte et al., 2009; Egypt: e.g., Scheibner et al., 2003). A consistent model for the circum-Tethyan carbonate platform evolution based on the distribution of the main platform organisms has been established by Scheibner and Speijer (2008) for the Early Palaeogene.

Thus, the distribution of platform building biotic assemblages is strongly dependent on temperature and nutrient availability. Increasing global temperatures during the Early Palaeogene (58 – 49 Ma) with low latitudinal gradients and generally low Mg/Ca-ratios in the oceans hamper the growth of larger coral built-ups, while larger benthic foraminifera proliferate (Scheibner and Speijer, 2008). The transition from coral-dominated assemblages to larger benthic foraminifera-dominated assemblages can be observed throughout the Tethys. Timing and distribution is, however, strongly dependent on latitude. Thus, Scheibner and Speijer (2008) arranged three major circum-Tethyan platform stages from the Late Palaeocene to the Early Eocene.

Platform stage I (58.9 – 56.2 Ma)

Platform stage I is characterized by the dominance of circum-Tethyan coralgal assemblages at the platform margin, while smaller benthic foraminifera and calcareous algae dominate shallow-marine platform interior. Western Morocco (oyster dominated) and NE India (benthic foraminifera dominated) represent an exceptional facies. The onset of platform stage I is strongly connected to the prominent sea level fall at 58.9 Ma (Hardenbol et al., 1998).

Platform stage II (56.2 – 55.5 Ma)

Platform stage II represents a transitional episode between coralgal and larger foraminifera dominance in the Tethyan realm. In the northern Tethyan and Peri-Tethyan realm coralgal assemblages still dominate the platfrom margin, whereas in lower latitudes (0 – 20°) first larger foraminifera communities, composed of ranikothalids and miscellanids, proliferate.

Platform stage III (55.5 Ma – ?)

The onset of the most prominent platform stage is represented by the Paleocene-Eocene boundary and the fundamental environmental and biotic impact of the PETM. Throughout the Tethys larger foraminifera dominate the shallow-marine platform communities. Corals are either rare or completely absent. Paleocene ranikothalids and miscellanids are replaced by Eocene nummulitids and alveolinids, which developed a significant larger shell size and an adult dimorphism. This evolutionary trend, known as Larger Foraminifera Turnover (LFT), is directly coupled to the negative CIE of the PETM (Orue-Etxebarria et al., 2001; Scheibner et al., 2005).

The demise of coral-dominated platforms is rather an effect of coupled long-term climatic evolution and multiple transient environmental perturbations. With the pronounced sea-surface temperature rise at the PETM and the coeval eutrophication of shelf areas, the living conditions of corals have probably excessed a critical threshold. The timing of the recovery of the circum-Tethyan coral fauna and thus, the end of platform stage III is still under debate.

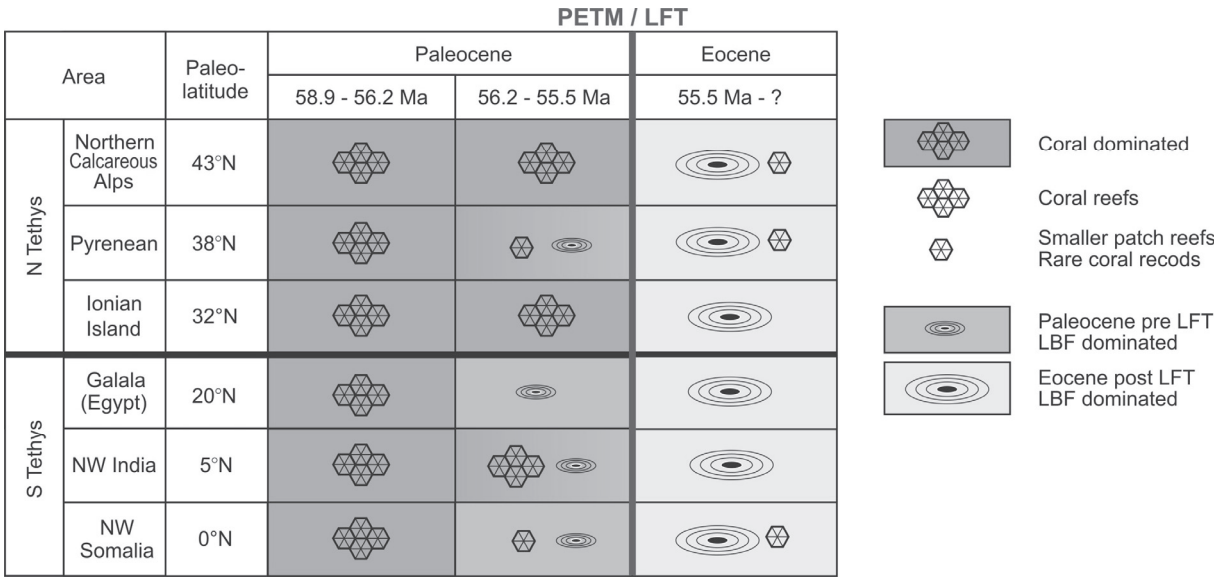

Figure I.3 – Circum-Tethyan platform evolution during the Early Palaeogene with respect to the dominating platform biota (modified after Scheibner and Speijer, 2008). The timing of the termination of the larger benthic foraminifera (LBF) dominated interval during the Eocene is under debate.

II. OBJECTIVES

Numerous case studies on Tethyan carbonate platforms have shown the complex evolution of shallow-marine environments during the Palaeogene. However, coherant platform models, which consider climate, tectonic and local controlling mechanims are still rare. Especially the impact of Early Palaeogene hyperthermals to carbonate platform has not been tested so far.
In this study two Palaeogene carbonate platform systems in different palaeogeographic settings and geotectonic regimes are analyzed in order to reconstruct the impact of long-term climate change, syn-depositional tectonism and complex local environmental perturbations to shallow-marine carbonate platforms. High-resolution microfacies, stable carbon isotopes and geochemical data as well as the comparison of the recorded successions with other Tethyan carbonate platforms will help to understand the controlling mechanims and the timing of Palaeogene platform evolution.

<u>The main aims of this study are in detail:</u>

- How do carbonate platform organisms respond to multi-source environmental stress (tectonic vs. climatic stress)? Causes environmental stress during the Palaeogene transitions in the shallow-marine benthic assemblages or on the diversity of single organism groups (e.g. LBF)?
- Previous studies demonstrated a link between the evolution of LBF and corals as well as the dramatic climatic change during the Late Paleocene – Early Eocene. Can we link the Palaeogene greenhouse-icehouse transition to changes in the LBF-coral ratio at the platforms? What are the ecological expression and the timing of this transition along a latitudinal transect?
- Tectonic activity is a major controlling mechanism of carbonate platform evolution. Can we recognize periods of increased tectonic activity in the successions and can we connect these periods to shifts in the biotic assemblages (e.g. increased eutrophication)?
- Can we record post-PETM carbon cycle perturbations (ETM2, ETM3) in shallow-marine platform environments? Is there a significant environmental impact of those perturbations? Are there differences regarding the impact along a platform-to-basin transect?
- Previous studies have shown that marginal shelf areas are decoupled from the global carbon cycle during times of increased environmental stress. What is the response of the studied carbonate platforms to repeated environmental perturbations?

III. STUDY AREA

III.1 Working area and geological setting

Galala Mountains (Eastern Desert, Egypt)

The Galala Mountains represent a Maastrichtian – Early Eocene isolated carbonate platform at the northern margin of the African-Arabian continental shelf (Figs. III.1, III.3). The mountain range is situated in the Eastern Desert of Egypt ~100 km S of Suez and comprises three main tectono-sedimentary units: a) the Northern Galala Plateau, b) Wadi Araba and, c) the Southern Galala Plateau. The fault-bounded Northern Galala Plateau or Northern Galala-Wadi Araba High (NGWA) represents the shallow-marine inner ramp and comprises of high fossiliferous limestones and dolomites. The Southern Galala Plateau is composed of fossiliferous limestones, sandstones and marls, which indicate a mid- to outer ramp setting. The rocks of the southernmost part of the Galala Mountains are dominated by marls and chalky marlstones, which represent the northern branch of the Eastern Desert Intrashelf Basin (EDIB) or Southern Galala Subbasin (SGS) (Fig. III.3; Kuss et al., 2000).

Prebetic platform (SE Spain)

The Prebetic carbonate platform is represented by a NE-SW tending facies belt north of Alicante, which comprises shallow-marine limestones, dolomites and marls (Fig. III.2). The platform demonstrates the NE branch of the Betic Cordillera, an alpine mountain belt, which is arranged in two main tectono-stratigraphic domains: a) the external zone comprises the autochthonous deposits of the South Iberian margin and, b) the internal zone, is characterized as allochthonous unit of highly metamorphous rocks (Alonso-Chaves et al., 2004).

The External Zone is represented by a heterogenous suite of Mesozoic and Early Cenozoic passive continental margin deposits (Garcia-Hernandez et al., 1980; Everts, 1991). The deposits of the External Zone are subdivided into two units with respect to their position at the shelf: a) the Prebetic domain represents the shallow-marine shelf of the South Iberian margin and, b) the Subbetic domain is characterized by deeper shelf deposits without terrigenous influence. The contact between the shallow-marine Prebetic platform (External Prebetic) and the hemipelagic Prebetics (Internal Prebetic) is represented by the Franja Anomala, a major palaeogeographic barrier (de Ruig et al., 1991; Martin-Chivelet and Chacon, 2007). The contact between Prebetic and Subbetic domain points to a major thrust fault (Garcia-Hernandez et al., 1980).

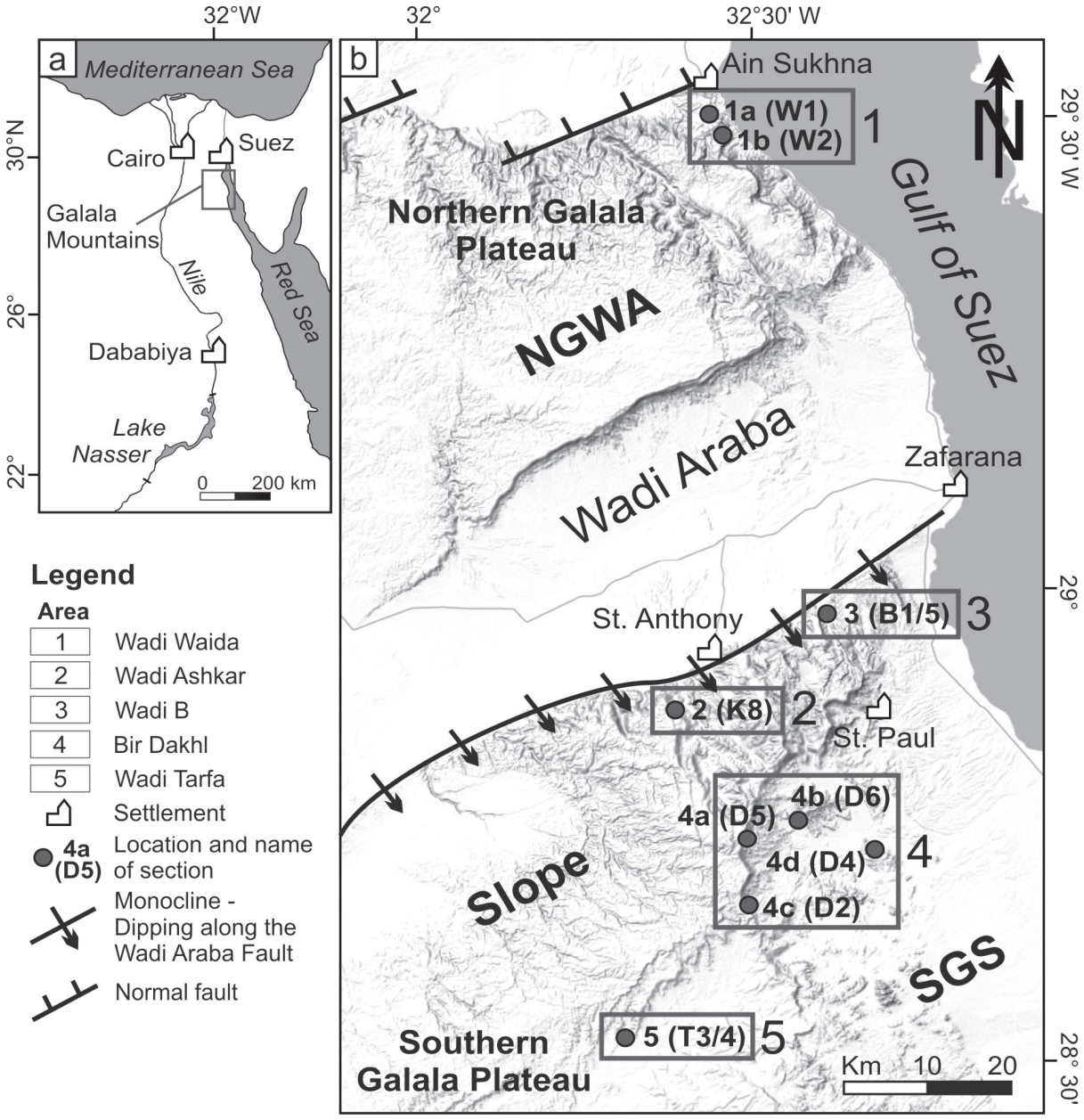

Figure III.1 – Location of the Galala Mountains and the studied sections (red circles) in the Eastern Desert of Egypt. Five areas and nine sections have been studied along an inner platform-to-basin transect. Shallow-marine inner platform deposits are recorded in area 1 at the Northern Galala-Wadi Araba High (NGWA). A transitional facies with mixed hemipelagites and shallow-marine deposits is present along the slope of the Southern Galala Plateau (areas 2, 3 and 4). Area 5 represents a hemipelagic succession of the Southern Galala Subbasin (SGS) (modified after Höntzsch et al., in press). Variations in the names of the sections result from different descriptions in the field and for publication. For example, D5 is the field description of section 4a, which has been renamed for publication.

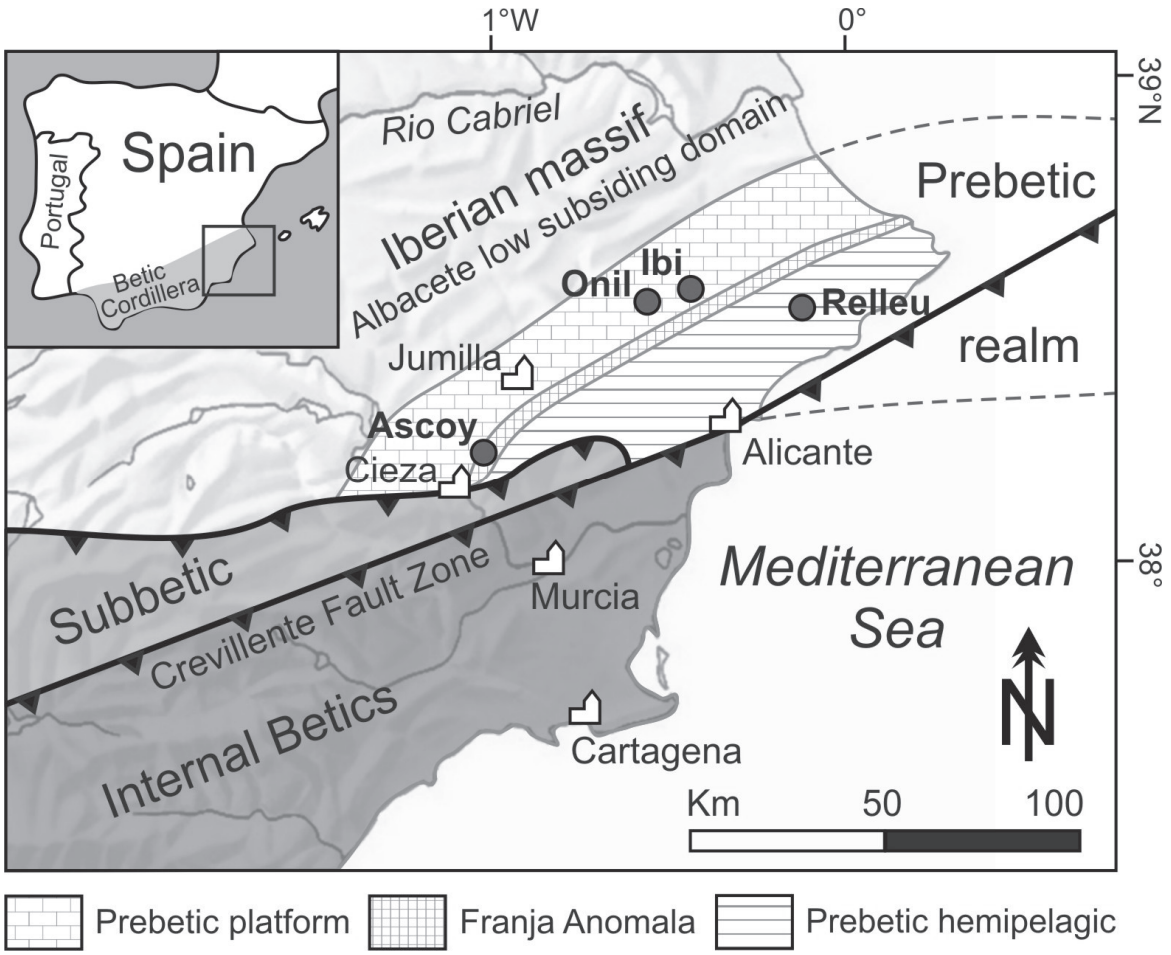

Figure III.2 – Location of the Prebetic platform and the studied section (red circles) in SE Spain (modified after Höntzsch et al., to be submitted). The Crevillente Fault Zone belongs to a palaeofault system that is related to extension along the SE Iberian continental margin (Nieto and Rey, 2004). The External zones summarizes Subbetic, Prebetic platform and the Prebetic hemipelagic realm. The palaeotectonic and palaeogeographic significance of the Franja Anomala, representing the transition of Prebetic platform and Prebetic hemipelagic realm, is still under debate.

III.2 Palaeogeography

The Mediterranean realm (or Western Tethys) is characterized by significant variations in the prevailing tectonic regime and the dimension of the northern and southern Tethyan shelves during the Palaeogene. The southern Tethyan passive continental margin of Africa is characterized by wide shelves, which extend between ~1000 km in the SE Mediterranean and up to ~3000 km in the SW Mediterranean (Fig. III.3). In contrast to the southern Mediterranean margin, the northern Mediterranean margin demonstrates a complex framework of isolated terranes, microplates and fault-bounded continental margins with narrow and patchy shelves.

The Palaeogene Galala platform represents an isolated carbonate platform ~800 km N of the African shoreline, whereas the Prebetic platform is attached to the Iberian Massif (Fig. III.3). However, both carbonate factories are influenced and controlled by syn-depositional tectonic activity in a compressional regime.

Galala platform (Eastern Desert, Egypt, ~20° N palaeolatitude)

During the Palaeogene, the Egyptian shelf demonstrates a heterogeneous framework of NE-SW tending ridges and graben structures along the African and Arabian plate margins (Fig. III.3; Moustafa and Khalil, 1995; Kuss et al., 2003). Platform evolution in those areas is strongly controlled by the syn-depositional tectonic activity along the Syrian Arc-Fold Belt, a system of en-echelon arranged, NE oriented fold-thrust structures, which extend from the Egyptian Western Desert to Syria (Fig. III.3; Krenkel, 1925; Shahar, 1994). The Syrian Arc-Fold Belt represents a complex framework of intraplate tectonic lineaments, which evolved as a result of compression during the post-Cenomanian closure of the Neo-Tethys and the coeval rifting of the North Atlantic. A main phase of compression, causing the reactivation of the Mesozoic Syrian Arc faults has affected the Egyptian shelf during the Palaeogene (Shahar, 1994; Moustafa and Khalil, 1995; Hussein and Abd-Allah, 2001).

Prebetic platform (SE Spain, 32° N palaeolatitude)

The South Iberian continental margin underwent repeated changes and deformation since the Mesozoic, culminating with the uplift and deformation of the Betic Cordillera in the Early Miocene (Fontboté and Vera, 1983; Blankenship, 1992; Geel et al., 1998; Alonso-Chaves et al., 2004). During the Palaeogene, the southern passive margin of the Iberian Craton (External Betic domain) is represented by a narrow shelf, composed of a heterogeneous framework of patchy, fault-bounded carbonate platforms (Prebetic platform; Geel et al., 1998). Towards the South, the shallow-marine deposits of the Prebetic platform pass into hemipelagic deposits of the Subbetic realm.

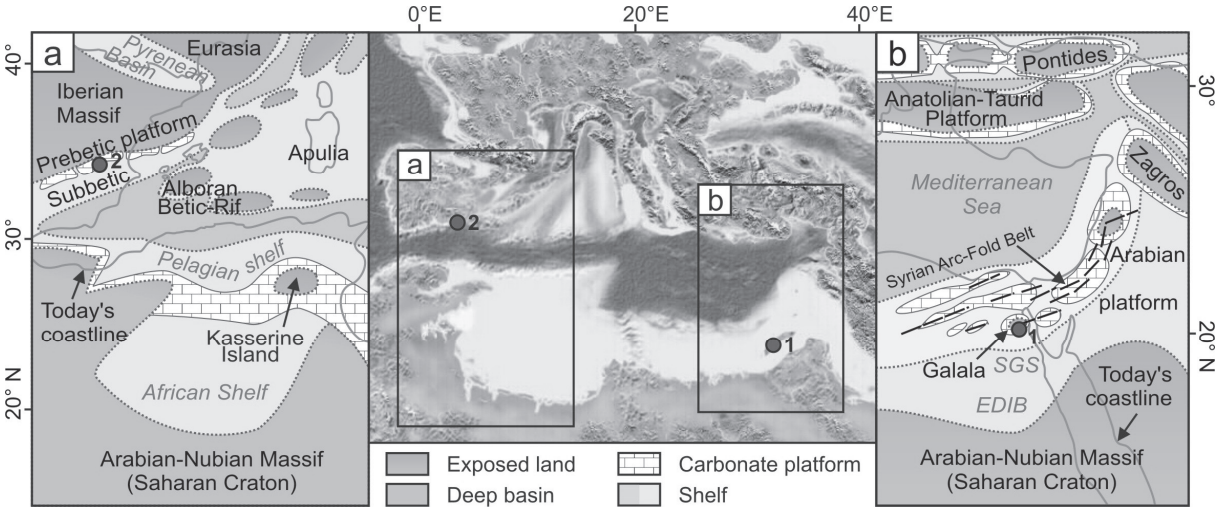

Figure III.3 – Early – Middle Eocene palaeogeography of the Mediterranean realm (modified after Blakey: http://www2.nau.edu/rcb7/eocenemed.jpg), including detailed illustrations of the Western Mediterranean realm (Figure **III.3 a**) and the Eastern Mediterranean realm (Figure **III.3 b**). The study areas are represented by red circles: 1 – Galala platform, Eastern Desert (Egypt); 2 – Prebetic platform, SE Spain. Abbreviations: SGS – Southern Galala Subbasin, EDIB – Eastern Desert Intrashelf Basin.

Highly unstable tectonic conditions with frequent subaerial exposure of the platforms prevailed during the Early Paleocene. A major sea-level rise during the Late Paleocene favoured the seaward progradation and the stabilization of platform (Alonso-Zarza et al., 2006). The largest extension of the platform is observed during the Middle and Late Eocene.

IV. METHODS

IV.1 Field work

During three field campaigns (February and November 2008: Egypt, April 2010: Spain) 13 sections were recorded and more than 1500 samples were taken (Tab. IV.1). The rock record includes a suite of hemipelagic marls, fossiliferous limestones, sandstones and dolomites. In the measured sections, depositional structures (channels, load casts, bedding), bioturbation as well as general lithological features were recorded. All recorded samples were analyzed for bulk rock carbon isotopes, total organic carbon and calcium carbonate. Limestones, sandstones and dolomites were sampled with respect to their state of preservation and fossil content in order to reconstruct microfacies evolution through time.

Table IV.1 – List of the recorded sections, including GPS coordinates, number of samples and stratigraphic range. Abbreviations: TS – samples for thin sections, loose – loose marl samples. The bold numbers indicate the total number of recorded samples.

Section	Northing	Easting	Samples	Stratigraphic range
Galala Mountains (Eastern Desert, Egypt)				
1a (W1)	N 29°32,971'	E 32°21,134'	**54** (54 TS)	Paleocene - Lower Eocene
1b (W2)	N 29°33,700'	E 32°20,873'	**21** (21 TS)	Lower Eocene
2 (K8)	N 28°52,054'	E 32°17,214'	**59** (51 TS, 8 loose)	Lower Eocene
3 (B1/5)	N 28°57,650'	E 32°28,894'	**153** (106 TS, 47 loose)	Latest Paleocene - Lower Eocene
4a (D5)	N 28°43,313'	E 32°23,657'	**230** (109 TS, 121 loose)	Latest Paleocene - ?Middle Eocene
4b (D6)	N 28°42,920'	E 32°27,569'	**134** (48 TS, 86 loose)	Latest Paleocene - upper Lower Eocene
4c (D2)	N 28°39,605'	E 32°23,585'	**99** (22 TS, 77 loose)	Latest Paleocene - upper Lower Eocene
4d (D4)	N 28°40,911'	E 32°33,515'	**103** (18 TS, 85 loose)	Latest Paleocene - upper Lower Eocene
5 (T3/4)	N 28°27,335'	E 32°13,983'	**144** (8 TS, 136 loose)	Latest Paleocene - ?Middle Eocene
Prebetic platform (SE Spain)				
Ascoy	N 38°16,250'	W 1°22,417'	**79** (67 TS, 12 loose)	Paleocene - Lower Eocene
Onil *	N 38°37,934'	E 0°39,942'	**75** (75 TS)	Lower Eocene - Middle Eocene
Ibi *	N 38°38,499'	E 0°34,725'	**131** (131 TS)	Middle Eocene - Lower Oligocene
Relleu *	N 38°38,633'	E 0°19,407'	**223** (121 TS, 102 loose)	Upper Eocene - Upper Oligocene

* recorded by G. Wiemer and J. Brock

IV.2 Biostratigraphy

Strongly varying lithologies in the recorded sections require a biostratigraphic approach, which includes marker species from deep- and shallow-marine environments.

Biostratigraphy in the hemipelagic marls of the Galala platform is based on the occurrence and distribution of calcareous nannoplankton. The Palaeogene assemblages are characterized by a great variety of different nannoplankton species and are therefore excellent biostratigraphic markers. A coherent nannoplankton zonation (NP) was compiled by Martini (1971) and Bukry (1973). Redefined NP zones based on the classification of Aubry (1995).

Planktic foraminifera biostratigraphy was performed at a basinal section in Egypt (section 5 or T3/4). Palaeogene planktic foraminifera biostratigraphy is based on the studies of Berggren (1995) and Berggren and Pearson (2005). Biostratigraphy in the sections of the Prebetic platform is also based on planktic foraminifera but was adapted from previous studies.

Shallow-marine environments without suitable marl intervals were analyzed for larger benthic foraminifera, which represent the dominant shallow-benthic species during the Palaeogene. Their occurrence throughout the Tethys and their high diversity enables a sufficient biostratigraphic classification. Hottinger (1960, 1974) introduced a biostratigraphic scheme based on alveolinids. Schaub (1960) presented a biostratigraphic classification of Palaeogene nummulitids. A standardized classification was achieved with the help of the Tethyan Paleocene-Eocene Shallow Benthic Zonation (SBZ) of Serra-Kiel et al. (1998). A correlation of the SBZ and open-marine biozonations (calcareous nannoplankton, planktic foraminifera) is still under debate.

IV.3 Microfacies and fossil assemblages

A key approach of the presented study is represented by the quantitative and qualitative analysis of the main platform organisms. Many shallow-benthic organisms at the platform are adapted to specific light conditions, depth- and trophic regimes, as well as to a well defined temperature range. The classification of the main organisms into fossil assemblages and microfacies types helps to reconstruct the prevailing environmental conditions, long- and short-term environmental perturbations, as well as sea-level changes through time. Limestones, dolomites and sandstones were prepared for geostatistical and qualitative thin section analysis via light microscope (sensu Flügel, 1978, 2004).

Larger benthic foraminifera (LBF)

In this study LBF were used as palaeoenvironmental indicators and as proxy for sea level fluctuations at the platform. LBF are one of the most common fossil groups in the shallow-marine Tethys during the Palaeogene. Their adaption to distinct photic and energetic regimes as well as their ability to host photo-autotrophic algal symbionts (Lee, 1998; Hallock, 1999, and references therein) favours a palaeoenvironmental reconstruction regarding palaeobathymetric and energetic constraints (Hohenegger, 2004, 2005). Transient climatic perturbations also show a significant impact on LBF (e.g., the LFT at the PETM). The dominating species during the Palaeogene are nummulitids, alveolinids, assilinids, discocyclinids, lepidocyclinids, soritids, miliolids, acervulinids, heterosteginids and operculinids.

Corals

Hermatypic corals play an important role in the palaeoenvironmental framework of Tethyan carbonate platforms during the Palaeogene. Their adaption to well-defined environmental conditions, with respect to light, nutrients, temperature and depth reveals the timing of Palaeogene warming and subsequent cooling. Scheibner and Speijer (2008) have shown that the coral reef demise affected first lower latitudes during the Paleocene (e.g., Egypt), whereas intermediate and high latitudes remained rather unaffected until the PETM. The record of coral built-ups in different latitudes will help to recognize the recovery of the Tethyan coral fauna during the post-EECO cooling.

Calcareous algae

Calcareous green algae proliferate especially in the restricted platform interior and are suitable palaeoenvironmental indicators for eutrophication, light regime and water depth. Kuss and Herbig (1993) established a facies scheme for the distribution of Early Palaeogene green algae from the southern Mediterranean.

Coralline red algae have been used as palaeoenvironmental indicators especially in mid- and high latitudinal Tethys (e.g., Rasser, 2000; Rasser and Piller, 2004). In intermediate and low latitudes, red algae only occur in minor portions. However, global cooling in the Upper Palaeogene favours the increasing significance of red algal limestones in the geological record (e.g., Geel, 2000).

IV.4 Carbon isotopes

Fluxes between the major carbon reservoirs on Earth are expressed in the global carbon cycle (Fig. I.2). Transient shifts in the ratio of stable carbon isotopes ($\delta^{13}C$) indicate major environmental perturbations and indicate stratigraphic intervals, which are decoupled from the global carbon cycle (Zachos et al., 2005; John et al., 2008).

Furthermore, the long-term evolution of $\delta^{13}C$ ratios supports classical biostratigraphic timescales and helps to reveal orbital-paced cyclicity (e.g., Zachos et al., 2001; Lourens et al., 2005). Bulk rock carbon isotopes are determined with a Finnigan MAT 251 mass spectrometer in the Marum Bremen.

IV.5 Calcium carbonate content and total organic carbon

Variations in the bulk rock calcium carbonate content may indicate intervals of $CaCO_3$ dissolution or dilution, caused by transient environmental perturbations. Bulk rock total organic carbon (C_{TOC}) pinpoints intervals with increased carbon burial at the shelf. Bulk rock total carbon (C_{total}) and C_{TOC} are determined with a Leco CS-300 analyzer at the University of Bremen (precision of measurement ±3 %). The bulk rock carbonate content is expressed in the formula $CaCO_3$ [%] = [(C_{total} – C_{TOC}) x 8.33].

IV.6 X-ray diffraction (XRD)

Selected sandstone samples from the Lower Eocene Galala succession were analyzed with a special focus on clay minerals, in order to reconstruct the source area of the sandstones.

IV.7 Eventstratigraphy

Eventstratigraphy represents an important tool for the correlation of transient local, regional or global perturbations to the depositional system. The recorded sections in Egypt and Spain reveal three different types of event beds: a) the increasing occurrence of quartz-rich deposits at the platforms is linked to periods of massive tectonic uplift; b) negative carbon isotope excursions are linked to transient hyperthermal events on a global scale and, c) significant transitions of the biotic assemblages are related to global climatic events.

V. THESIS OUTLINE

The results of this study are presented in three manuscripts, which are briefly introduced below. Preliminary results of the project were presented and discussed on international conferences, workshops and graduate courses. At the end of the dissertation, a summary of the main outcomes and further reasearch perspectives are presented.

1) **Tectonically driven carbonate ramp evolution at the southern Tethyan shelf – The Lower Eocene succession of the Galala Mountains, Egypt**

   The Upper Palaeocene – Lower Eocene succession of the isolated Galala platform (Eastern Desert, Egypt) is studied in order to reconstruct carbonate platform evolution in a low latitude setting. Nine sections along a platform-to-basin transect are recorded, focussing on field observations and the analysis of shallow-marine benthic biota. Microfacies data highlight the spatial distribution of the biotic assemblages and indicate intervals of syn-depositional tectonic activity by means of frequent siliciclastic deposition. The definition of local platform stages, based on the prevailing biota, sea-level fluctuations and tectonic activity summarizes the evolution of the Galala platform.

   Höntzsch S, Scheibner C, Kuss J, Marzouk AM, Rasser MW (2011) Tectonically driven carbonate ramp evolution at the southern Tethyan shelf: the Lower Eocene succession of the Galala Mountains, Egypt. Facies 57, pp. 51-72.

2) **Increasing restriction of the Egyptian shelf during the Early Eocene? – New insights from a southern Tethyan carbonate platform**

   The isolated Galala platform is studied with respect to the impact of syn-depositional climatic and tectonic perturbations during the Early Eocene. Microfacies data, carbon isotopes and geochemical data highlight the impact of repeated Early Eocene hyperthermal events at the Galala platform. Causes and consequences of increasing nutrient supply and the climatically- and tectonically-controlled restriction of the Egyptian shelf are discussed. The major outcomes are summarized in a palaeogeographic model, which reveals the impact of selected depositional processes at the shelf during the Early Palaeogene.

   Höntzsch S, Scheibner C, Guasti E, Kuss J, Marzouk AM, Rasser MW (2011, in press) Increasing restriction of the Egyptian shelf during the Early Eocene? - New insights from a southern Tethyan carbonate platform. Palaeogeography, Palaeoclimatology, Palaeoecology, pp. 1-18, doi:10.1016/j.palaeo.2011.01.022.

3) Circum-Tethyan carbonate platform evolution during the Palaeogene – the Prebetic platform as test case for climatically-controlled facies shifts

High-resolution microfacies data from four Paleocene – Late Oligocene sections along the Prebetic carbonate platform in SE Spain are compiled in order to reconstruct the evolution of shallow-marine benthic assemblages and their response to repeated tectonic perturbations. The distribution of the main platform organisms (LBF and corals) at the Prebetic platform are compared with other circum-Tethyan carbonate platforms in order to demonstrate latitudinal- and climatically-controlled facies shift during the Palaeogene.

Furthermore, high-resolution carbon isotopes from the Upper Eocene – Oligocene Relleu section are used to highlight the isotopic variations in shallow-marine limestones and hemipelagic marls as well as the increasing isolation of the Prebetic realm.

Höntzsch S, Brock JP, Scheibner C, Kuss J (to be submitted to Palaeogeography, Palaeoclimatology, Palaeoecology) Circum-Tethyan carbonate platform evolution during the Palaeogene – the Prebetic platform as test case for climatically-controlled facies shifts.

First manuscript

TECTONICALLY DRIVEN CARBONATE RAMP EVOLUTION AT THE SOUTHERN TETHYAN SHELF – THE LOWER EOCENE SUCCESSION OF THE GALALA MOUNTAINS, EGYPT

Stefan Höntzsch [a], Christian Scheibner [a], Jochen Kuss [a], Akmal M. Marzouk [b] and Michael W. Rasser [c]

[a] Department of Geosciences, Bremen University, PO Box 330440, 28359 Bremen, Germany
[b] Geology Department, Faculty of Science, Tanta University, Tanta 31527, Egypt
[c] Staatliches Museum für Naturkunde, Rosenstein 1, 70191 Stuttgart, Germany

Published in Facies (2011) Volume 57, pp. 51-72, doi:10.1007/s10347-010-0229-x
Received: 16. Dezember 2009 / Accepted: 14. August 2010

VI. TECTONICALLY DRIVEN CARBONATE RAMP EVOLUTION AT THE SOUTHERN TETHYAN SHELF – THE LOWER EOCENE SUCCESSION OF THE GALALA MOUNTAINS, EGYPT

Abstract The succession of the Galala Mountains at the southern Tethyan margin (Eastern Desert, Egypt) provides new data for the evolution of an isolated carbonate platform in the Early Eocene. Since the Late Cretaceous emergence of the Galala platform, its evolution is strongly controlled by eustatic sea-level fluctuations and the tectonic activity along the Syrian Arc-Fold-Belt. Previous studies introduce five platform stages to describe platform evolution from the Maastrichtian (stage A) to the latest Paleocene shift from a platform to ramp morphology (stage E). A first Early Eocene stage F was tentatively introduced but no described in detail. In this study we continue the work at the Galala platform, focussing on Early Eocene platform evolution, microfacies analysis and the distribution of larger benthic foraminifera on a south-dipping inner ramp to basin transect. We redefine the tentative platform stage F and introduce two new platform stages (stage G and H) by means of the distribution of 13 facies types and syn-depositional tectonism. In the earliest Eocene (stage F, NP 9b – NP 11), facies patterns indicate mainly aggradation of the ramp system. The first occurrence of isolated sandstone beds at the mid ramp reflects a post-Paleocene-Eocene Thermal Maximum (PETM) reactivation of a Cretaceous fault system, yielding to the tectonic uplift of Mesozoic and Palaeozoic siliciclastics. As a consequence, the Paleocene ramp with pure carbonate deposition shifted to a mixed carbonate-siliciclastic system during stage F. The subsequent platform stage G (NP 11 – NP 14a) is characterized by a deepening trend at the mid ramp, resulting in the retrogradation of the platform. The increasing deposition of quartz-rich sandstones at the mid ramp reflects the enhanced erosion of Mesozoic and Palaeozoic deposits. In contrast to the deepening trend at the mid ramp, the deposition of cyclic tidalites reflects a coeval shallowing and the temporarily subaerial exposure of inner ramp environments. This oppositional trend is related to the continuing uplift along the Syrian Arc-Fold-Belt in stage G. Platform stage H (NP 14a - ?) demonstrates the termination of Syrian Arc uplift the and recovery from a mixed siliciclastic carbonate platform to pure carbonate deposition.

VI.1 Introduction

The evolution of circum-Tethyan carbonate platform systems during the Early Paleogene greenhouse has been intensively studied in the last decades with respect to environmental conditions (e.g., Luterbacher, 1984; Kuss, 1986; Rasser, 1994; Wielandt, 1996; Pujalte et al., 1999; Scheibner et al., 2001a; Cosovic et al., 2004; Özgen-Erdem et al., 2005; Rasser et al., 2005; Adabi et al., 2008), shallow-benthic biostratigraphy (e.g., Schaub, 1992; Serra-Kiel et al., 1998; Scheibner and Speijer, 2009), oil potential (e.g., Loucks et al., 1998; Ahlbrandt, 2001; Baaske et al., 2008) and the response to long- and short-term palaeoclimatic change (e.g., Scheibner et al., 2005, 2007; Pujalte et al., 2009; summary by Scheibner and Speijer, 2008, and references therein). Major biotic platform contributors (e.g., corals, larger benthic foraminifera, calcareous green and red algae) play an important role in terms of the interpretation of environmental conditions and the evolution of the platform through time. Scheibner et al. (2005) compare various early Palaeogene Tethyan carbonate platforms and arrange three circum-Tethyan platform stages (stage I - III) with respect to the main biotic contributors: In the Late Paleocene platform stage I (58.9 – 56.2 Ma) corals and calcareous algae dominate carbonate platforms all over the Tethys (coralgal platforms). Platform stage II (56.2 – 55.5 Ma) is characterized by the first occurrence of larger benthic foraminifera shoals at low latitudes (below 20° N), while coralgal assemblages prevail at high latitudes (above 30° N). In platform stage III (55.5 Ma - ?) corals were replaced by larger benthic foraminifera (LBF) as major platform contributors in nearly all circum-Tethyan shallow-marine environments. The onset of platform stage III is strongly coupled to the environmental and sedimentological impact of the Paleocene-Eocene thermal maximum (PETM) at 55.5 Ma, resulting in the rapid radiation and proliferation of LBF species. This larger foraminifera turnover (LFT) also demonstrates the transition from Paleocene LBF assemblages (e.g., *Ranikothalia*, *Miscellanea*) to Eocene LBF assemblages (e.g., *Nummulites*, *Alveolina*, *Operculina*, *Orbitolites*), which are characterized by larger test sizes and adult dimorphism (e.g.; Hottinger and Schaub, 1960; Hottinger, 1998; Orue-Etxebarria et al., 2001; Scheibner and Speijer, 2009). Despite the well-known onset of platform stage III, its duration is still under debate. Multiple local circum-Tethyan studies are needed to reveal timing and trigger mechanisms with respect to the termination of platform stage III.

Additionally, the circum-Tethyan platform stages proposed by Scheibner et al. (2005) exclusively based on climatically-controlled biotic changes, while individual platform environments are affected by multiple regional factors, regarding their position on the shelf and local tectonic constraints. The importance of tectonically-controlled carbonate platform evolution has been described for various environments throughout the Phanerozoic (e.g., Lee Wilson and D'Argenio, 1982; Burchette, 1988; Bechstädt and Boni, 1989; Bosence, 2005). In the early Eocene, especially the Egyptian shelf is strongly affected by tectonism,

which is related to the northward movement of the African craton towards Eurasia as well as the reactivation of Mesozoic fault systems (e.g., Shahar, 1994; Moustafa and Khalil, 1995; Hussein and Abd-Allah, 2001). Thus, the evolution of carbonate platforms at the Egyptian shelf is controlled by those tectonic constraints and requires a regional approach beyond the general platform stages of Scheibner et al. (2005).

The Galala Mountains (Eastern Desert, Egypt) represent a key area of Cenozoic carbonate platform research. Since the mid-1980s, investigations in the Galala Mountains focused on Cretaceous to Paleocene microfacies, platform evolution, palaeoecology and the impact of the PETM (e.g., Kuss, 1986; Bandel and Kuss, 1987; Strougo and Faris, 1993; Kuss et al., 2000; Scheibner et al., 2001a, 2003; Morsi and Scheibner, 2009).

The evolution of the Galala platform is strongly coupled to the activity of the Syrian Arc-Fold-Belt, which demonstrates a NE-SW striking framework of horst and graben structures at the southern Tethyan shelf. The Syrian Arc-Fold-Belt was formed as a result of the initial collision of the African and Eurasian Plates in the Late Turonian (e.g., Moustafa and Khalil, 1995; Scheibner et al., 2003). The emergence of the Galala platform has been documented for the Campanian/Maastrichtian (Scheibner et al., 2003). Multiple pulses of tectonic uplift, which are related to the temporarily reactivation of Cretaceous fault systems caused the repeated reconfiguration of the platform morphology. A major interval of tectonic uplift along the Syrian Arc-Fold-Belt is demonstrated for the Early Eocene (e.g., Shahar, 1994).

Scheibner et al. (2003) discriminates five regional platform stages (stage A - E) from the Maastrichtian emergence of the platform system (stage A) to latest Paleocene prior to the PETM (stage E). Scheibner and Speijer (2008) introduced a sixth platform stage F, which is, however, neither defined in detail nor biostratigraphically classified.

Here we present new data from the Galala Mountains, which help to reveal the evolution of the platform system in the Early Eocene. We focus on detailed microfacies analyses, larger foraminifera assemblages and the effects of syndepositional tectonic activity on carbonate platform sedimentation. Following the studies of Scheibner et al. (2003) and Scheibner and Speijer (2008) we redefine and reevaluate the tentative introduced platform stage F. Furthermore, we introduce two new platform stages (stage G and H), which delineate the evolution of the Galala carbonate platform in the Early Eocene. Both stages G and H demonstrate major incisions in platform evolution, characterized by varying tectono-sedimentary and biotic conditions, as well as the transition from global greenhouse climate to increased cooling at the end of the Early Eocene Climatic Optimum (EECO).

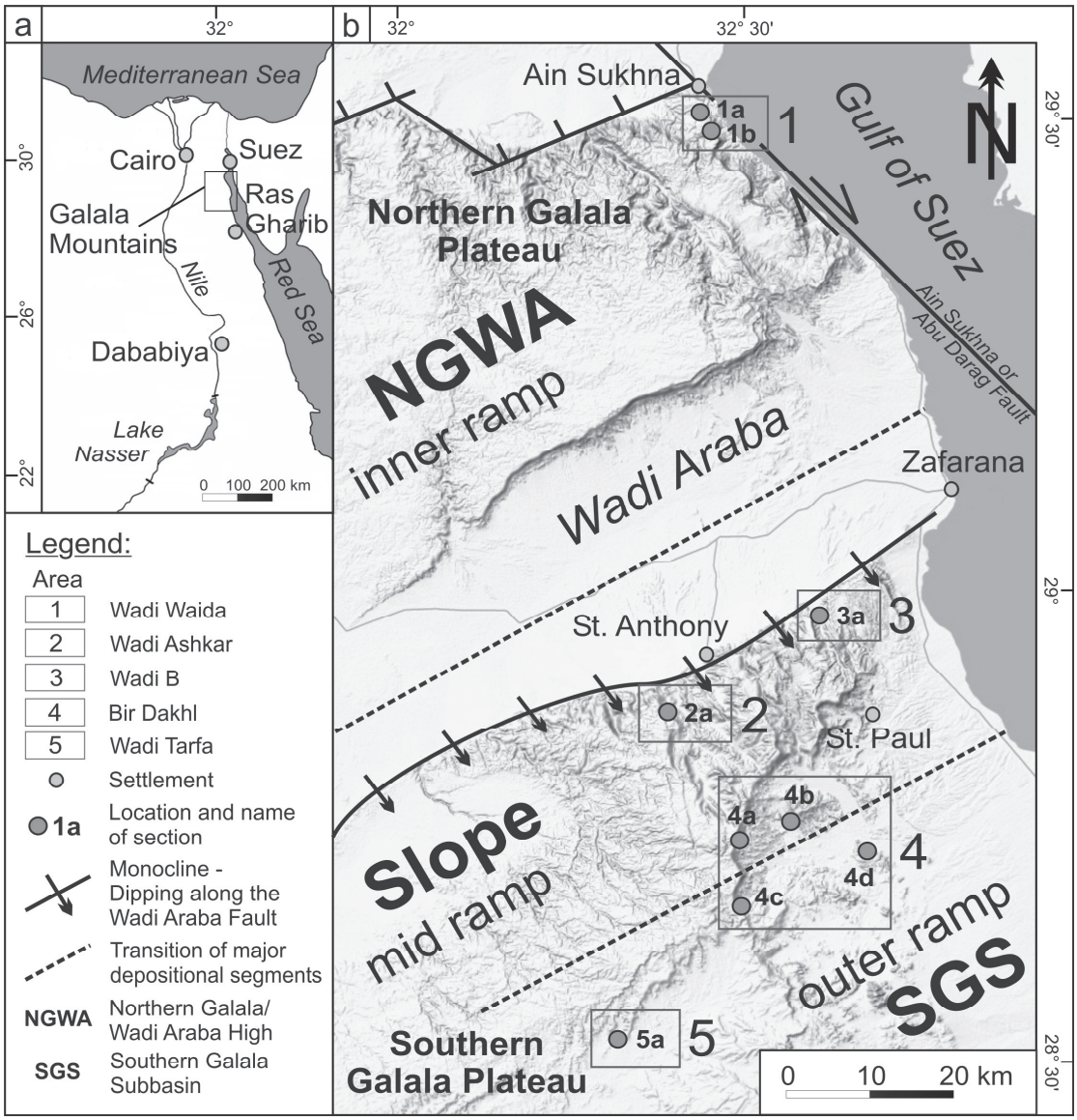

Figure VI.1 a – Simplified location map of the working area. VI.1 b – Detailed map with location of the sections, tectono-topographic features as well as the general facies belts of the carbonate platform (modified after Scheibner et al. 2001a). Tectonic elements are added according Moustafa and El-Rey (1993), Moustafa and Khalil (1995) and Schütz (1994).

VI.1.1 Geological setting

The Galala Mountains are located in the Eastern Desert of Egypt and range from Ain Sukhna near Suez 100 km to the SE (Fig. VI.1). The mountain complex represents an isolated Late Cretaceous (Maastrichtian) to Eocene carbonate platform at the southern margin of the Tethys which is referred to the unstable shelf of northern Egypt (Youssef, 2003; Fig. VI.2b). The evolution of the platform is closely connected to the tectonic activity of the ENE-WSW striking Wadi Araba Fault, which is a part of the Syrian Arc-Fold-Belt (e.g.; Krenkel, 1925; Moustafa and Khalil, 1995; Hussein and Abd-Allah, 2001). During the Early Eocene a major phase of tectonic activity occurs along the Syrian Arc-Fold-Belt (Shahar, 1994). Regional uplift and subsidence triggered the formation of ENE-WSW striking basins, submarine swells

and subaerially exposed plateaus on the unstable shelf (Said, 1990; Schütz,1994; Fig. VI.2b). Major plateaus are situated in the Cairo-Suez- and Kattamiya area as well as at the present-day coast of the Mediterranean Sea. The regional basins had a width of few tens to hundreds kilometres with a palaeobathymetry of about 100 m (Salem, 1976). However, the basinal succession of the stable shelf S of the study area comprises a palaeobathymetry of up to 600 m (Speijer and Wagner, 2002).

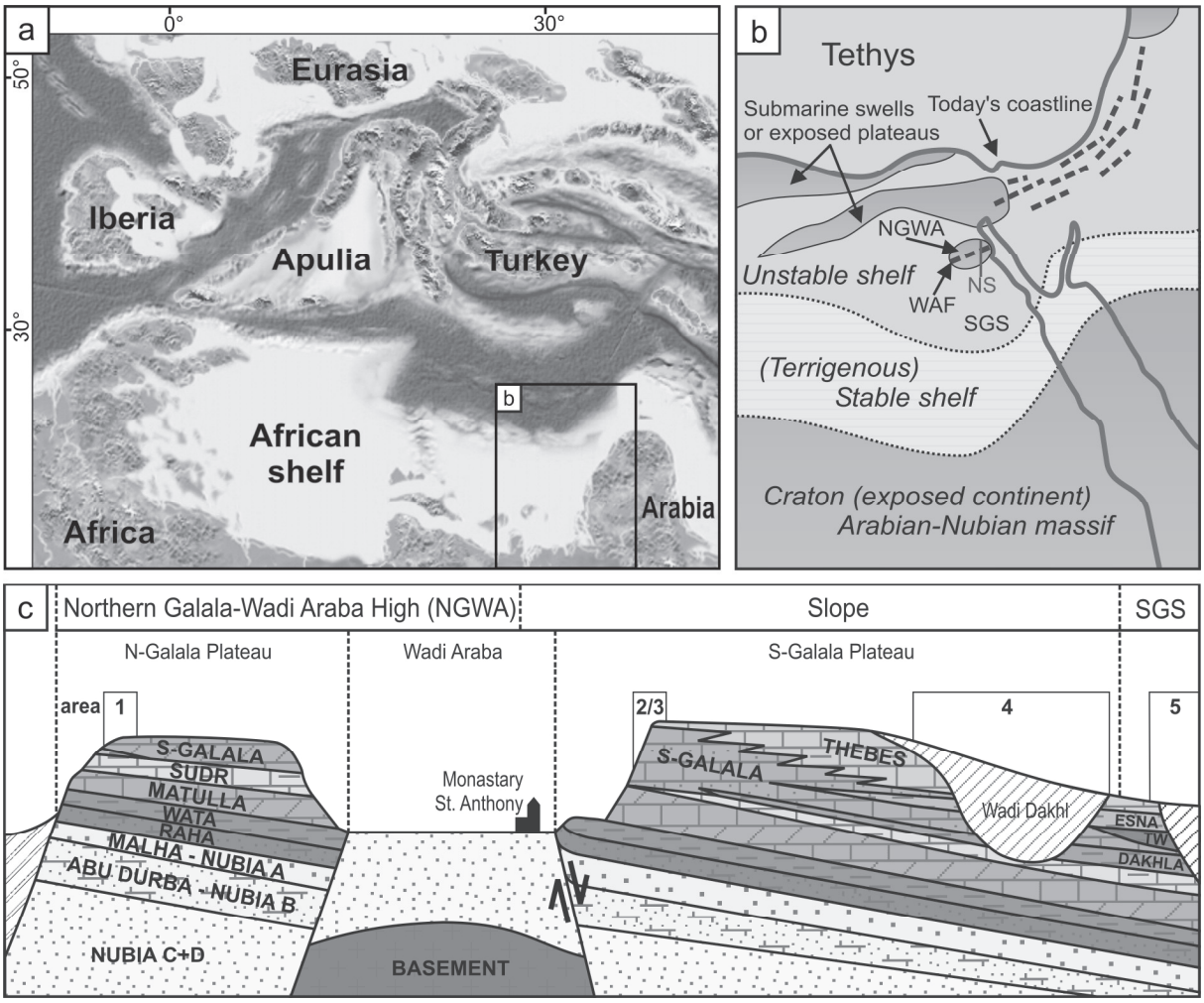

Figure VI.2 a – Palaeogeographic overview of the western Tethyan realm in the earliest Palaeogene using the maps of Blakey (http://jan.ucc.nau.edu/~rcb7/latecretmed.jpg). **VI.2 b** – Simplified map of the Early Eocene southern Tethys margin in Egypt showing the location of the Northern Galala/Wadi Araba High (*NGWA*) and the Southern Galala Subbasin (*SGS*). The Wadi Araba Fault (*WAF*) forms the southern part of the Syrian Arc-Fold-Belt (*dashed lines*). Submarine swells and plateaus are added according to Said (1990). The position of stable and unstable shelf was estimated by Meshref (1990) and was modified for the Early Palaeogene by Scheibner et al. (2001) and Speijer and Wagner (2002). The red line (*NS*) represents an NS directed cross-section shown in figure VI.2 c. **VI.2 c** – Cross-section of the Galala Mountains including the working areas (numbers 1, 2/3, 4 and 5) and main formations (modified after Schütz, 1994). Palaeozoic to Lower Cretaceous siliciclastics are represented by the Nubia Series. The Upper Cretaceous is dominated by siliciclastic marls, shales and (dolomitic) limestones (Wata, Raha, Matulla). The Sudr Formation represents the uppermost Cretaceous in the study area. Palaeogene formations (Dakhla, Tarawan, Esna, Southern Galala, Thebes) are diachronous. Their stratigraphic range is discussed in figure VI.3.

The Early Eocene Galala Mountains represent one of the southernmost plateaus of the Egyptian unstable shelf (Fig. VI.2b). According to the regional tectono-sedimentary constraints, three major depositional units can be distinguished (Fig. VI.1b): The Northern Galala/Wadi Araba High (NGWA), a transitional slope zone and the Southern Galala Subbasin (SGS). The NGWA represents shallow-marine to probably subaerially exposed inner platform environments. Due to the synsedimentary monoclinal uplift and following erosion along the Wadi Araba Fault since the Late Cretaceous, major inner-ramp deposits were eroded or intensively altered (Moustafa and Khalil, 1995). Furthermore, rocks of the northern platform interior are intensively affected by secondary dolomitization and tectonic displacement, which is a result of the Miocene opening of the Gulf of Suez. The connection between the NGWA and the Southern Galala Subbasin (SGS) is represented by a transitional slope zone (mid ramp to outer ramp). The Galala Mountains are tectonically and depositionally linked to the monoclinal structure of Gebel Somar on west-central Sinai (Moustafa and Khalil, 1995). Both structures were separated during the rifting of the Gulf of Suez in the Late Oligocene and Miocene.

VI.1.2 Lithostratigraphy

The Lower Eocene succession in the Galala Mountains encompasses three major lithostratigraphic units, which differ in their stratigraphic range and varying depositional setting within an inner platform to basin transect (Figs. VI.2c, VI.3): The Esna Formation (Beadnell, 1905) represents an interval of uppermost Paleocene to Lower Eocene basinal marls and shales (lower NP 9 to NP 12). The deposits lack shallow-marine influence and represent a palaeo-depth of 200 m in average (Speijer and Schmitz, 1998; Scheibner et al., 2001a; Fig. VI.1b). The Esna Formation is followed by alternating chalky marls, cherts and sandstones of the Thebes Formation (Hermina and Lindenberg, 1989), which represents a deep-water facies. Lithostratigraphically, the Thebes Formation is defined by the first appearance of cherts in the mid ramp to basinal sections, coinciding roughly with the initial occurrence of chalky marls in the Lower Eocene succession of the Galala Mountains (see Fig. VI.1b).

Marly sediments are rare or absent in the shallow-marine inner- to mid-ramp environments of the study area. The succession consists of platform-related, shallow-marine limestones, sandstones and conglomerates, which are represented by the Southern Galala Formation (Abdallah et al., 1970; Kuss and Leppig, 1989). Thebes Formation and Southern Galala Formation show distinct facies similarities and interfinger at different areas on the mid ramp (Scheibner et al., 2001a).

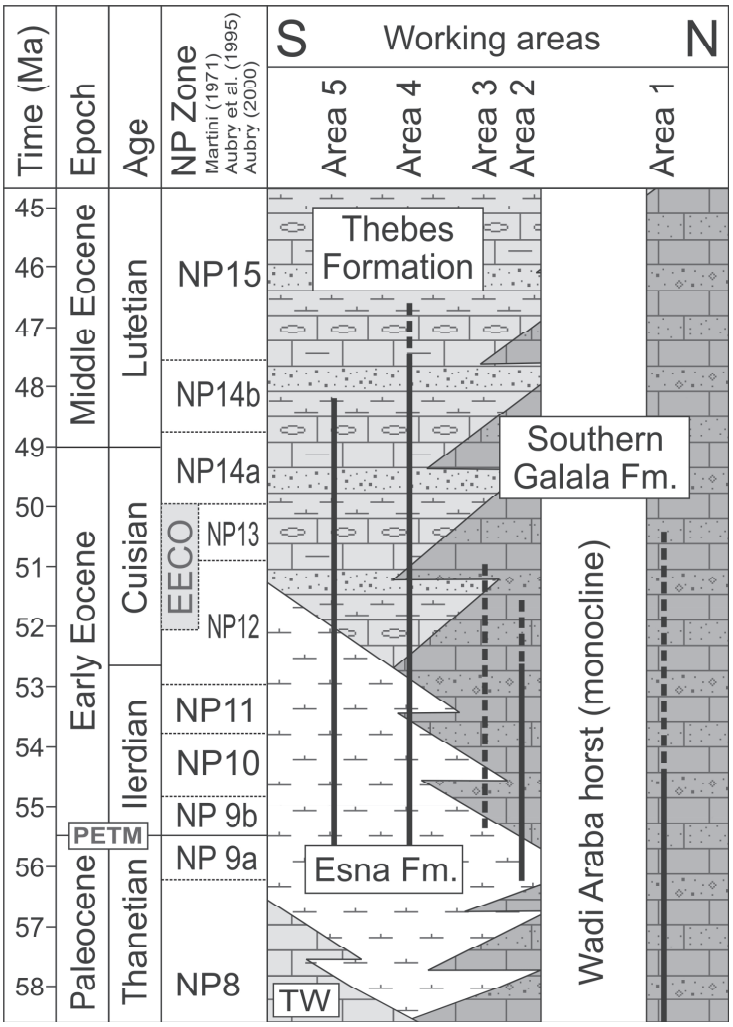

Figure VI.3 – Lithostratigraphy and biostratigraphy of the Palaeogene formations and groups in the Galala Mountains along a N-S transect (after Scheibner et al., 2001a, b; see Fig. VI.2c). The working areas (1-5) refer to Fig. VI.1b; position of PETM and EECO according to Zachos et al. (2008). *TW* Tarawan Formation. The *vertical bold lines* illustrate the stratigraphic range of the recorded sections. *Dashed lines* indicate an uncertain range.

VI.1.3 Methods

Nine stratigraphical sections, located on a platform to basin transect between Ain Sukhna and Ras Ghareb in the Galala Mountains were measured in detail (Fig. VI.1): Two exposures in the NGWA (area 1), four exposures covering the slope (area 2, 3 and 4) and three exposures in the SGS (area 4 and 5). The distance between the studied sections at the Southern Galala Plateau varies between 5 km and 20 km. The thickness of the sections ranges 70 m (section 3a) to 250 m (section 4a). The vertical sample distance varies between 20 cm in well-exposed marls and more than 1 m in sandstones, respectively, which was depending on the general condition of the outcrop and the degree of alteration. About 600 samples were taken for detailed thin section analysis of mainly litho- and biofacies. Thirteen facies types (FT) were defined according to the distribution and the assemblages of the bioclasts (smaller and larger benthic foraminifera, planktic foraminifera, calcareous green

and coralline red algae), the matrix composition (micrite, sparite, dolomite) and the quartz content. The classification of FT and facies belts (FB) follows previous studies of Paleocene successions (e.g., Scheibner et al., 2001a). The quantitative analysis was performed by estimation of components, using the comparison charts of Baccelle and Bosellini (1965) and Schäfer (1969), which provide reasonable quantitative results.

The detailed biostratigraphic assessment of the sections is based on calcareous nannoplankton (nannoplankton zonation of Martini, 1971; Aubry, 1995 and Aubry et al., 2000). Shallow-platform biostratigraphy was supported by alveolines according to the classification of Hottinger (1974) and the shallow-benthic zonation (SBZ) of Serra-Kiel et al. (1998) and Scheibner and Speijer (2009).

VI.2 Results and facies interpretation

VI.2.1 Description and biostratigraphic range of the sections

The nine studied sections represent different depositional environments along a NNE-SSW striking ramp (Figs. VI.1, VI.2c). A clear proximal-distal zonation is evident from the northern inner ramp (area 1) to the southern ramp-basin transition (area 4) and finally to the southern most basinal area 5.

The Paleocene-Eocene boundary is defined by the transition from NP 9a to NP 9b and the transition from SBZ 4 to SBZ 5 and coincides with the carbon isotope excursion (CIE) of the PETM (Scheibner et al., 2005; Scheibner and Speijer, 2009). The studied sections range from NP 9 to NP 14a whilst the lowermost Middle Eocene ones within NP 14b. A continuous biostratigraphic assessment of the respective shallow benthic zones (SBZ 6 to SBZ 13) was hindered by poorly preserved specimen in all intervals.

Area 1: The deposits of the inner ramp are characterized by alternating limestones and reworked dolostones. Marls are rare or absent. The thickness of the individual sections ranges from 110 m (section 1a) to 125 m (section 1b). The biota are dominated by larger and smaller benthic foraminifera (smaller miliolids, soritids, nummulitids, alveolinids) and green and red algae. The basal part of section 1b shows an alternating succession of LBF floatstones and fine-grained dolostones, which become more dominant towards the middle interval of the section. The upper portions of section 1b are represented by the cyclic deposition of fossiliferous dolostones (soritids, green algae, and molluscs), birdseyes limestones and reworked limestone conglomerates (Fig. VI.7). Stratigraphically, section 1a ranges from the Paleocene to NP 10. The basal 40 m of section 1b cover the lowermost Eocene (NP 9b – NP 10). A biostratigraphic assessment of the subsequent 85 m of dolomitic rocks was not possible due to lacking biostratigraphic markers.

Area 2/3: The proximal mid ramp deposits of the northern margin of the Southern Galala Plateau are represented by a mixture of highly fossiliferous sandstones and limestones, marls and dolostones. Section 2a is composed by quartz-rich allochthonous peloidal limestones with intercalated sandstones and marls. Quartz-rich sandstones and conglomerates of section 2a are poorly sorted and show high amounts of limestone and sandstone extraclasts. Strong bioturbation is common as well as sharp contacts with the underlying beds. The lower 140 m of section 3a are composed of a marly sandstone-limestone succession. Sandstones prevail as sheet-like beds or as channelized structures with strongly varying thickness. Dolostones prevail in the upper 110 m of section 3a with monotonous and almost non-fossiliferous mud- to wackestones as well as massive beds of dolomitized nummulitic float- to rudstones. Stratigraphically, section 3a ranges from the uppermost Paleocene (NP 9a) to the upper Lower Eocene (NP 13/14). Section 2a covers the lowermost Eocene NP 9b – NP 10/11).

Area 4: The four studied sections of area 4 (4a, 4b, 4c and 4d) are dominated by marls (up to 45 m thick) with intercalated sandstones and limestones. The thickness of the sandstones varies between 1 cm and more than 3 m (section 4a). The greyish to bluish marls of the lower part of the sections (Esna Formation) are replaced by white chalky marls with frequent chert nodules towards the top of the succession (Thebes Formation). Intercalated limestone beds, which are present in the lower part of the succession, decrease towards the top. Dominant components are represented by LBF, benthic green algae, shell fragments and planktic foraminifera. Biostratigraphically, the sections of area 4 range from the uppermost Paleocene (NP 9a) to the uppermost Lower Eocene (NP 14a).

Area 5: The rocks of section 5a are characterized by greyish marls and shales in the lower interval (NP 9a – NP 11) and white chalky marls with high amounts of planktic foraminifera and radiolaria as well as intercalated chert bands in the upper part of the succession (NP 11 – NP 14). Limestones or sandstones as well as larger benthic biota are absent. The total thickness of section 5a is about 90 m.

VI.2.2 Facies types

The studied rocks are attributed to 13 facies types (FT), reflecting depositional settings on a ramp from shallow-marine (FT 1) to deep-marine environments (FT 13). For the distinction of FT, microfacies data as well as field observations of sedimentary structures are used (Tab. VI.2). Description and interpretation of the FT is mainly based on the high-diverse fauna of the shallow-marine, low-latitude succession of the Galala platform (Fig. VI.4). All 13 FT were attributed to five major facies belts (FB) on an inner ramp to basin transect (Fig. VI.5): (1) restricted lagoon, (2) inner lagoon, (3) outer lagoon and shoal, (4) slope, (5) basin.

Reworked dolostones (FT 1)

Description: FT 1 is represented by a suite of massive to parallel-bedded light grey dolostones with layers of dark grey to black birdseyes and fenestral textures (Figs. VI.4a, VI.4q), followed by coarse-grained crystalline dolostones with reworked birdseyes mudstones, which are arranged in a coarsening upward succession. The individual beds have a thickness of a few centimetres up to more than 2 m. Biogenic remains are generally rare or absent. Occasionally extraclasts enriched in corals and gastropods, as well as stromatolithic textures occur in the reworked beds (e.g., bed W2-12). Desiccation cracks are present in bed W2-14 (Fig. VI.4q). The thickness of the individual cycles varies between 50 cm and more than 10 m. The thickness of the conglomerates on top of each cycle ranges from 5 cm to 20 cm; rarely up to 2 m. FT 1 is only present in section 1b and covers the upper 70 m of the succession.

Interpretation: FT 1 reflects the shallowest part of the restricted Galala platform. The succession of fossil-barren, completely altered birdseyes mudstone followed by reworked conglomerates indicates cyclicity of a tidal flat facies (Keheila and El-Ayyat, 1990). Desiccation cracks reveal periodically subaerial exposure.

Dolomitized mudstones to wackestones (FT 2)

Description: FT 2 is either represented by massive, grey dolostones with almost no macroscopic textures and by reworked nodules with remains of corals, gastropods and stromatolithic textures within FT 1 (Fig. VI.4b). Dolomite is present as inequigranular and non-rhombic crystals. Relics of miliolids and ostracods are rare. Fragments of alveolinids and smaller nummulitids are intensively affected by dolomitization. Siliciclastic material is generally absent; only few samples contain up to 20 % of well-sorted, sub-angular quartz grains (e.g., bed W2-10). Massive and coarsely recrystallized wackestones often occur in the northern part of the study area (area 1).

Interpretation: Dolomitized mudstones with very rare faunal elements occur in restricted environments of the inner ramp. Stromatolites indicate very shallow water conditions with temporarily subaerial exposure. Dolomitization is supposed to be late diagenetic and related to hypersaline brines of a tidal flat (Keheila and El-Ayyat, 1992). Samples with quartz and extraclasts probably reflect reworking by occasional storm events.

Peloidal packstones to grainstones (FT 3)

Description: Light to dark grey peloidal pack- to grainstones occur as massive or parallel-bedded limestones with sharp contacts to adjacent beds. Lumps densely packed peloids dominating this FT, the latter with volume percentages of 25 % to 50 % (Fig. VI.4c). Dominant components are miliolids (> 15 %) and micritized green algal fragments. Smaller

lenticular nummulitids, alveolinids, red algae, corals and textulariids are subordinate. Quartz is generally from rare to common. The matrix consists of xenotopic microsparite and rarely blocky sparite. Micritic parts of the matrix occur in isolated patches. Peloidal packstones to grainstones often interfinger with other facies types (e.g., nummulitid-bioclast wackestones to packstones). This FT occurs in all sections of the study area except in area 5.

Interpretation: FT 3 reflects shallow inner ramp environments. The common sparry matrix with patches of micrite and the good sorting of the components indicates high-hydrodynamic conditions and reworking. Most peloids are interpreted as micritized fragments of green algae or smaller benthic foraminifera (e.g., miliolids). Recent miliolids dominate shallow-marine lagoonal environments (e.g., Murray, 1991). It is reported, that those foraminifera are capable in tolerating high salinities and also proliferate as epiphaunal benthos within seagrass communities (e.g., Davis, 1970; Murray, 1991). Palaeoenvironmental studies on miliolid assemblages attribute the low diversity of the detected foraminifera associated with common green algal fragments to nutrient-enriched conditions in a restricted environment (e.g., Geel, 2000; Zamagni et al., 2008).

Gastropod-rich bioclastic wackestones to packstones (FT 4)

Description: The wacke- to packstones of FT 4 are present as massive light grey to bluish-grey limestones with a thickness of a 10 cm to 50 cm. Besides the frequent gastropods, fragments, alveolinids, peloids, serpulid worm tubes and miliolids occur with various ratios (Fig. VI.4d). FT 4 occurs occasionally in area 1 and 3. In section 3a (bed B5-31) quartz and peloids occur as major components. In section 1b traces of microbial stromatolithic textures are present (bed W2-12).

Interpretation: The faunal assemblage of FT 4 reflects inner ramp environments with close relations to FT 3 and FT 5. Gastropod-rich bioclastic wacke- to packstones represent shallow lagoonal conditions with moderate water circulation above fair-weather wave base (Scheibner et al., 2007). Quartz and peloids are probably storm-derived.

Nummulitid-bioclastic wackestones to packstones (FT 5)

Description: Nummulitic-bioclastic wacke- to packstones are represented by parallel-bedded or massive, grey to yellow rocks with a thickness between 10 cm and more than 1 m. This FT is characterized by an inhomogenic assemblage of smaller lenticular *Nummulites* sp., miliolids, textulariids, alveolinids, benthic green algae and peloids (Fig. VI.4e). Smaller quartz grains are present with minor amounts (< 10 %). The matrix consists of micrite or microsparite; in section 1b, FT 5 is strongly dolomitized. FT 5 occurs frequently in area 1, 2, 3 and 4.

Interpretation: FT 5 represents inner ramp environments above fair-weather wave base. The faunal assemblage reflects semi-restricted lagoonal conditions with a moderate water circulation. The occurrence of peloids and quartz grains indicates a mixture with other FT. Thus, FT 5 either occurs as *in situ* deposit at the inner ramp or as allochthonous remains in deeper realms of the ramp (e.g., section 4b).

Dasyclad-rich soritid floatstones (FT 6)

Description: Floatstones of FT 6 are represented by micritic grey to bluish-grey limestones with a bimodal distribution of elongated soritids (*Orbitolites* sp., *Opertorbitolites* sp.) and oval to round green algal fragments (mostly Dasycladacean algae). Both components make up to 55 % of the whole rock volume (Figs. VI.4f, VI.4p). Other biogenic components, as shell fragments are generally rare. FT 6 occurs only on top of section 1b (area 1).

Interpretation: The low-diverse assemblage of benthic green algae and elongated soritids, as well as the absence of quartz suggest low-hydrodynamic conditions in well-flushed backreef or backshoal environments (Hottinger, 1973, 1997; Geel, 2000). Zamagni et al. (2008) interprets the patchy cooccurrence green algae and soritids as evidence for the existence of algal meadows. Recent relatives of Palaeogene soritids proliferate in sheltered environments with 0 – 40 m water depth (Geel, 2000).

Red algae bindstones (FT 7)

Description: FT 7 occurs in dark grey to bluish-grey limestones with a stromatolitic texture. Fossil remains are represented by non-geniculate coralline red algae (*Sporolithon* sp. >50 %) as well as rare shell and green algal fragments. Red algal thalli accumulate in laminated beds with a thickness between 500 µm and 2 mm (Fig. VI.4g). FT 7 is only present in section 3a as extraclasts within a 160-cm-thick interval of alveolinid sandstones (FT 8, bed B1-50).

Interpretation: Coralline red algae bindstones occur as small patch reefs in the deeper protected inner ramp below fair-weather wave base (e.g., Gietl, 1998; Scheibner et al., 2007). The occurrence of FT 7 as extraclasts within a suite of coarse-grained alveolinid-rich sandstones suggests a deposition in the vicinity of the inner- to mid ramp transition. Gietl (1998) describes red algal patch reefs at the southern margin of the Northern Galala Plateau, reflecting an inner ramp environment. The erosion of inner ramp material containing coralline red algal bindstones is possibly related to local tectonic displacement or dramatic storm events, resulting in isolated debris flows or large-scale slumps.

Alveolinid-green algal wackestones to floatstones (FT 8)

Description: FT 8 is arranged in massive to parallel-bedded grey to bluish-grey lime- and sandstones with a thickness between 20 cm and 150 cm. Alveolinids (up to 50 %) and

benthic green algae (up to 40 %) are the dominant components (Fig. VI.4h). Peloids and miliolids are generally common and occur in various ratios and assemblages. Nummulitids, red algae (e.g., *Distychoplax biserialis*), shells and echinoderm fragments as well as *Orbitolites* are present in a minor extent. Quartz is frequent in the upper mid ramp sections (area 3, up to 40 %) but rare in the NGWA (area 1).
One sample (B1-4, Fig. VI.4o) shows a limestone conglomerate with oval-shaped extraclasts enriched in peloids and green algal fragments. Between the individual extraclasts strongly abraded alveolinids occur. The matrix is primarily sparry with local patches of micrite.

Interpretation: Alveolinids and benthic green algae are typical components of the proximal low-energetic inner ramp (Scheibner et al., 2007). The occurrence of soritids supports an environment within sheltered lagoonal or backshoal settings (Hottinger, 1973; Zamagni et al., 2008). High amounts of quartz in the vicinity of the platform margin possibly represent an allochthonous equivalent of this facies, which was reworked and transported into deeper settings (e.g., Papazzoni and Trevisani, 2006).

Nummulitid-alveolinid wackestones to floatstones (FT 9)

Description: Yellow-grey limestones, which occur as massive beds with sharp but undulating base and top surfaces, are summarized in FT 9. Stratification is generally rare, whereas fining-upward gradation occurs occasionally. *Nummulites* sp. and *Alveolina* sp. dominate this FT reaching 20 % to 40 % volume percentage (Fig. VI.4i). Other components are benthic green algae and quartz (5 % to 30 %); one sample is enriched in peloids. Miliolids, serpulid worm tubes, discoclyclinids and echinoderm fragments are present with lower percentages. The tests of all foraminifera are abraded. Especially alveolinids are often broken or squeezed. Few specimen show a strong abrasion of the outer whorls and probably lack their adult stages. Other LBF specimen show partial silicification. The poorly sorted quartz grains are generally sub-angular to sub-rounded. Micrite is the prevailing matrix of FT 9, which is replaced by sparite in a few samples. In section 1a FT 9 is frequently dolomitized with idiotopic euhedral dolomite crystals. Generally, FT 9 is one of the most frequent facies types in the study area. Floatstones occur mostly in area 1, whereas wacke- to packstones are common in the southern study areas (area 3 and 4).

Interpretation: FT 9 represents high-energy shoals (backshoal) formed at the inner/mid ramp transition. This is also evidenced by the co-occurrence of alveolinids and nummulitids, reflecting a mixing of inner- and mid ramp environments (Hohenegger et al., 1999). Immature quartz grains indicate only minor transport fractionation, whereas the eroded tests of larger foraminifera and patches of sparry cement indicate stronger currents. However, the occurrence of FT 9 at the mid ramp sections of area 4 (e.g., section 4a) is related to the transport by major mass-flows. The silicification of LBF results from diagenetic alteration

(Papazzoni and Trevisani, 2006), when calcite is replaced by autigenic silica (mostly microcrystalline quartz). Silica originates from the dissolution of biogenic material (e.g., radiolarians; see FT 13b).

Nummulitid floatstones to sandstones (FT 10)

Description: The massive, yellow-grey beds of FT 10 show commonly a sharp basis. Larger elongated nummulitids with particularly high amounts of quartz dominate this FT (Fig. VI.4j). In contrast to other FT, miliolids and alveolinids are rare or absent. Quartz grains are poor to moderately sorted; the sub-angular to sub-spherical grains are up to 5 mm in diameter. Discocyclinids, smaller rotaliids, alveolinids, echinoderm and bivalve shell fragments as well as other biogenic remains are present in varying amounts and preservations. Partial damage and deformation of larger foraminiferal tests is common and occurs intensified with increasing quartz content. The matrix consists of micrite or microsparite. In a few samples, quartz grains are overgrown by radial fibrous cements (bed D5-149; Fig. VI.3n). Nummulitid floatstones to sandstones are common in area 3 and 4. Lenticular beds with a thickness of a few metres are present in area 1.

FT 10 shows various microfacies types: 10a – dominated by *Nummulites* sp., 10b – dominated by *Ranikothalia* sp. and *Miscellanea* sp., 10c – dominated by *Assilina* sp. and *Operculina* sp.

Interpretation: FT 10 represents mixed-energetic deposits of the upper mid ramp, which were probably transported due to occasional storm events below fair-weather wave base. However, the bad sorting indicates only minor transport. *Discocyclina* sp., *Assilina* sp. and *Operculina* sp. point to a neritic environment with a water depth between 50 m and 80 m (subtype c, Beavington-Penney and Racey, 2004). True convex-shaped or lenticular shoal deposits, which are typical at the platform margin, are only present in the NGWA (area 1). Radial fibrous cement indicates high agitation and low sedimentation rates (Lighty, 1985). In the Paleocene interval of section 4a the dominating major nummulitids are represented by *Ranikothalia* sp. and *Miscellanea* sp. (subtype b), which indicate the same environment as *Nummulites* sp. (subtype a).

(Conglomeratic) quartz sandstones (FT 11)

Description: FT 11 is represented by a suite of light grey to yellow, mostly monomineralic quartz sandstones with a varying maturity (Fig. VI.4k). Rocks are massive or parallel bedded and cross stratification is rare. The thickness of the individual beds varies between 2 mm (e.g., section 4c) and several metres (e.g., section 3a). The basis of the beds is frequently undulated but sharp. Rip-up clasts of subsequent beds are common (e.g., marls). Occasionally, fining-upward is present in parallel-bedded sandstones. The sorting of the

siliciclastics is generally moderate to good; the sphericity of the quartz grains is poor to moderate. The size of the individual grains ranges from 100 µm to 3 mm. A decrease in maturity is noticeable in rocks with higher amounts of coarser grains. The matrix contains mud or is completely washed out. Relics of glauconite and weathered feldspar, as well as peloids are rare. Nummulitids, alveolinids, planktic foraminifera, bivalve shells and green algal fragments are generally rare and occur abraded or fragmented. Low fossiliferous quartz sandstones occur in a wide range in almost all sections of the study area. FT 11 is only absent in area 1 and area 5.

Interpretation: Massive to parallel bedded sandstones indicate moderate to high-hydrodynamic conditions. High amounts of siliciclastic material were probably eroded due to uplift along the Wadi Araba Fault. Sediment transport was possibly triggered by storm events or local tectonic activity (e.g., earthquakes). Massive bedding results from intensified bioturbation (Reineck and Singh, 1980), dewatering of the sediment during diagenesis (Förstner et al., 1968) or the intensified activity of microorganisms (Werner, 1963). The lack of biogenic material indicates either the transport of fossil-barren material from a point source or an intensified destruction of larger shelled biota. However, the lack of palaeoenvironmental indicators hinders the classification of FT 11 at the ramp. The occurrence of quartz sandstones at the upper and lower mid ramp suggests a source area in the vicinity of the NGWA. The repeated deposition of sandstone beds probably reflects the transport in existent distal channels or incised valleys at the mid ramp.

Bioclastic wackestones to packstones (FT 12)

Description: Bluish-grey to dark grey micritic limestones of FT 12 (Fig. VI.4l) demonstrate an inhomogeneous assemblage of densely packed aggregated grains and smaller bioclasts (miliolids, smaller rotaliids, green and red algal fragments, discocyclinids and planktic foraminifera). Peloids are present in minor amounts (rarely 25 %). Well-sorted, sub-angular to sub-sphaeric quartz grains are common in section 4a (10 % - 20 %) and occur occasionally in the area 3 as major component (bed B5-31, ~30 %). The size of the quartz grains varies between 50 µm and 300 µm. Elongated nummulitids, assilinids and discocyclinids “float” as larger components in the fine-grained matrix. The matrix consists of mud or microsparite. FT 12 is recorded in all studied areas, with the exception of area 1 and area 5.

Interpretation: Multicomponent bioclastic wackestones to packstones are interpreted as distal debris flows or turbidites, which consist of reworked material from the inner ramp (e.g., miliolids, green algae) as well as authochthonous deeper ramp biota (e.g., discocyclinids). The co-occurrence of planktic foraminifera and discocyclinids point to a deposition at the dysphotic lower mid ramp. Bassi (1998) describes large *Discocyclina* assemblages across

the inner and mid ramp transition. Good sorting and the small size of the major components indicate an advanced fractionation by transport.

Planktic foraminiferal and radiolaria-rich wackestones to packstones (FT 13)

Description: FT 13 shows two subtypes: FT 13a - Light to bluish grey planktic foraminiferal wackestones are represented by massive or parallel bedded limestones and chalky marls. The individual beds have a thickness between 30 cm up to 1 m and show no or only vague parallel stratification. FT 13a is enriched in planktic foraminifera (up to 30 %); other fossil groups like radiolarians or ostracods are generally rare (Fig. VI.3m). Biogenic material is enriched in layers of a few millimetres to centimetres or in clotted aggregates. FT 13a occurs particularly in the southern part of the study area (area 4 and 5), as well as in extraclasts in debris flow deposits in area 3.

FT 13b – Parallel bedded, laminated or massive white chalky marls and limestones represent another subtype of FT 13. The rocks are dominated by radiolarians and planktic foraminifera. A micritic matrix is generally absent. The occurrence of nodular to banded cherts with accumulated radiolarian and planktic foraminiferal remains characterizes this subtype of FT 13. Chert nodules show an elongated oval shape with a thickness of 5 cm to 20 cm. Limestones and marls, which are dominated by radiolarians occur in area 4 and area 5.

Interpretation: Planktic foraminiferal and radiolaria-rich wackestones to packstones are interpreted as typical low-hydrodynamic deep water deposits of the lower mid- to outer ramp with no or minor terrigenous input. Beds with accumulated planktic organisms indicate more condensed conditions or transient blooms. Clotted nests of planktic foraminifera and radiolarians reflect bioturbation. Chert nodules of the Lower Eocene Drunka and Thebes Formation are interpreted as product of post-depositional meteoric alteration due to shelf progradation in the Early Eocene (e.g., Keheila and El-Ayyat, 1990; McBride et al., 1999).

Table VI.2 – Summary of the facies types (FT) for the studied sections, including occurrence, main components, texture, quartz content and interpretation of the environment.

Number	Facies type (FT)	Sub FT	Occurrence, Area	Main components	Quartz	Texture	Environment, Facies belt
1	Reworked dolostones		1	-	-	Massive to parallel-bedded, fenestral textures, birdseyes	Restricted inner ramp/lagoon
2	Dolomitized mudstones to wackestones		1	Rare bioclasts	Rare, common in one sample	Massive to nodular	Restricted inner ramp/lagoon
3	Peloidal packstones to grainstones		1,2,3,4	Peloids, miliolids, green algae	Rare-common	Massive to parallel-bedded	Inner ramp, restricted lagoon
4	Gastropod-rich bioclastic wackestones to packstones		1,3	Gastropods, *Alveolina*, serpulids, peloids	Rare, common in one sample	Massive, partly stromatolithic	Inner ramp, lagoon
5	Nummulitid-bioclastic wackestones to packstones		1,2,3,4	Small *Nummulites*, miliolids, peloids, small bioclasts	Few (<10 %)	Parallel-bedded to massive	Inner ramp, semi-restricted lagoon
6	Dasyclad-rich soritid floatstones		1	Green algae, *Orbitolites*	-	Thin bedded	Inner ramp, sheltered backshoal/lagoon
7	Red algae bindstones		one sample in area 3	Red algae (*Sporolithon*)	-	Stromatolithic	Inner ramp/lagoon
8	Alveolinid-green algal wackestones to floatstones		1,2,3,4	*Alveolina*, green algae, miliolids, peloids	Rare to common (<40 %)	Massive to parallel-bedded	Inner ramp, sheltered backshoal/lagoon
9	Nummulitid-alveolinid wackestones to floatstones		Floatstones: 1, packstones: 2,3,4	Large and small *Nummulites*, *Alveolina*, green algae	Common	Massive	Inner- to mid ramp, (back)shoal
10	Nummulitid floatstones to sandstones	a	1,3,4	Large and small *Nummulites*	Common	Massive	Upper mid ramp, shoal
		b	3,4	*Ranikothalia*, *Miscellanea*	Rare	Massive	Upper mid ramp, shoal
		c	3,4	*Assilina*, *Operculina*	Rare to common	Massive	Upper mid ramp, shoal
11	(Conglomeratic) quartz sandstones		2,3,4	-	Common	Massive to parallel-bedded, fining-upward	Mid ramp, slope
12	Bioclastic wackestones to packstones		2,3,4	Small bioclasts, *Discocyclina*, planktic foraminifera, peloids	Rare to common	Massive	Mid ramp, slope
13	Planktic foraminiferal and radiolaria-rich wackestones to packstones	a	3,4,5	Planktic foraminifera	-	Massive to parallel-bedded	Mid- to outer ramp, slope
		b	4,5	Radiolarians, planktic foraminifera	-	Parallel-bedded to massive	Deeper mid- to outer ramp, slope to toe-of-slope

Main components and organisms are listed in order of decreasing abundance

VI.2.3 Foraminiferal assemblages

The following six foraminiferal assemblages are arranged on a palaeobathymetric profile, ranging from the shallow-marine inner ramp to the deep-marine basin (Fig. VI.5): (1) miliolid assemblage, (2) alveolinid assemblage, (3) nummulitid-alveolinid assemblage, (4) nummulitid assemblage, (5) nummulitid-discocyclinid assemblage and (6) planktic foraminifera assemblage.

The transitions between the individual foraminiferal assemblages are gradual and occasionally interfere with each other.

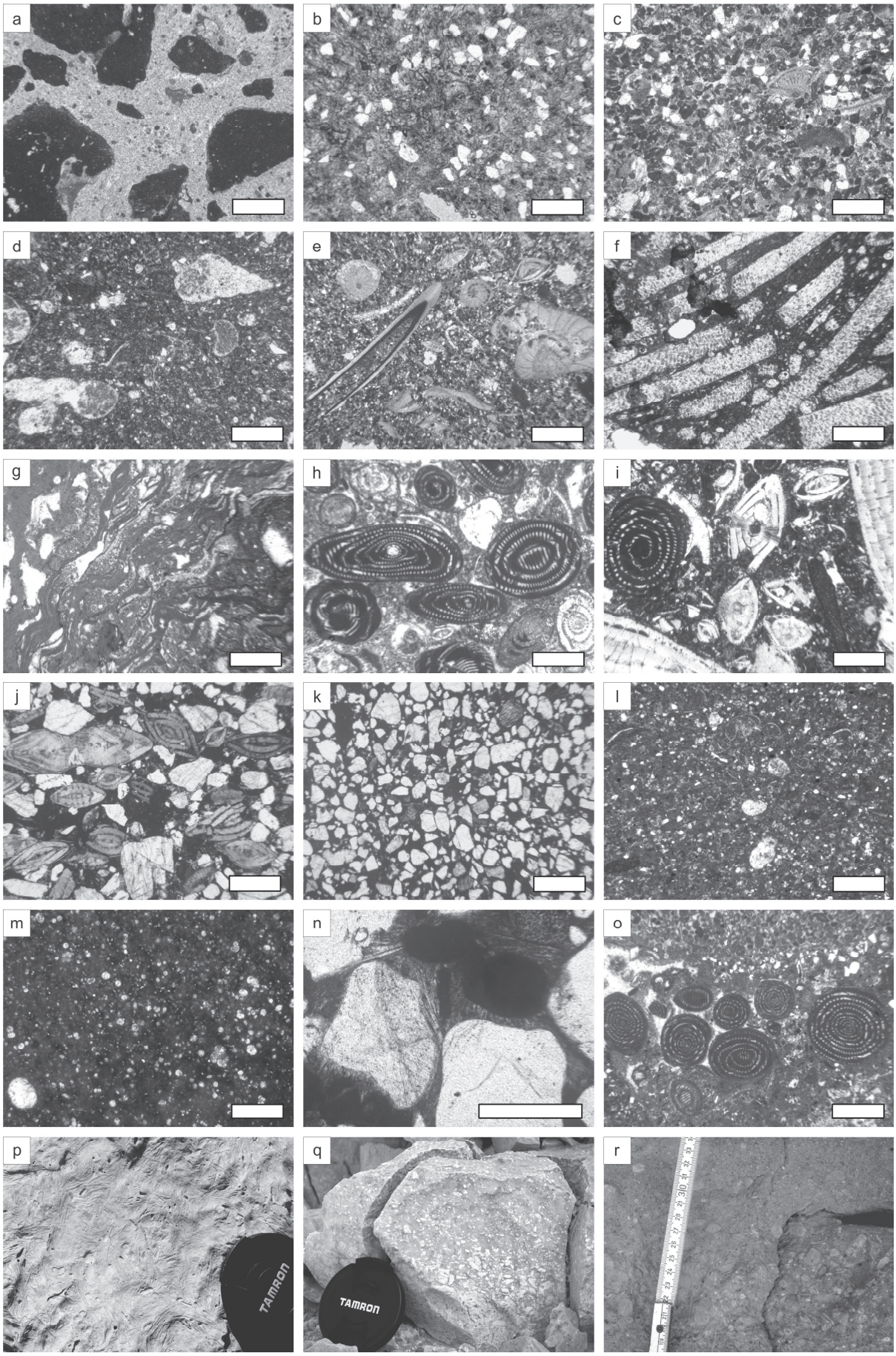
a
b
c
d
e
f
g
h
i
j
k
l
m
n
o
p
q
r
TAMRON
TAMRON

Figure VI.4 a – r (previous page) – Facies types (FT) of the studied Eocene strata: **a** Reworked dolostones (FT 1), **b** Dolomitized mudstones to wackestones (FT 2) with well-sorted quartz grains and rare bioclasts, **c** Peloidal packstones to grainstones (FT 3) with abundant smaller lenticular nummulitids and miliolids, **d** Gastropod-rich bioclastic wackestones to packstones (FT 4), **e** Nummulitid-bioclastic wackestones to packstones (FT 5) with peloids and rare serpulid worm tubes, **f** Dasyclad-rich soritid floatstones (FT 6), **g** Red algal bindstones (FT 7) consisting almost exclusively of non-geniculate red algae *Sporolithon* sp., **h** Alveolinid-green algal wackestones to floatstones (FT 8) with common silicified *Alveolina* sp. specimen, **i** Nummulitid-alveolinid wackestones to floatstones (FT 9). Note the common eroded outer whorls of the *Alveolina* specimen. Nummulites are only rarely affected by erosion. Scale bar is 1 mm, **j** Nummulitid floatstones to sandstones (FT 10) with abundant immature quartz grains, **k** (Conglomeratic) quartz sandstones (FT 11) with a high maturity and a muddy matrix, **l** Bioclastic wackestones to packstones (FT 12) dominated by planktic foraminifera and smaller bioclasts, **m** Planktic foraminiferal radiolaria-rich wackestones to packstones (FT 13), **n** radial fibrous cements in FT 4, **o** subtype of FT 6 with infraformational conglomerate composed of alveolinids, **p** weathered surface texture showing soritids and green algal relics (FT 8 in section 1b), **q** fenestral texture within dolomitized mudstones (FT 2, section 1b), **r** fining upward sequence of a debris flow in section 4a, note the high abundance of LBF. Scale bar is 1 mm

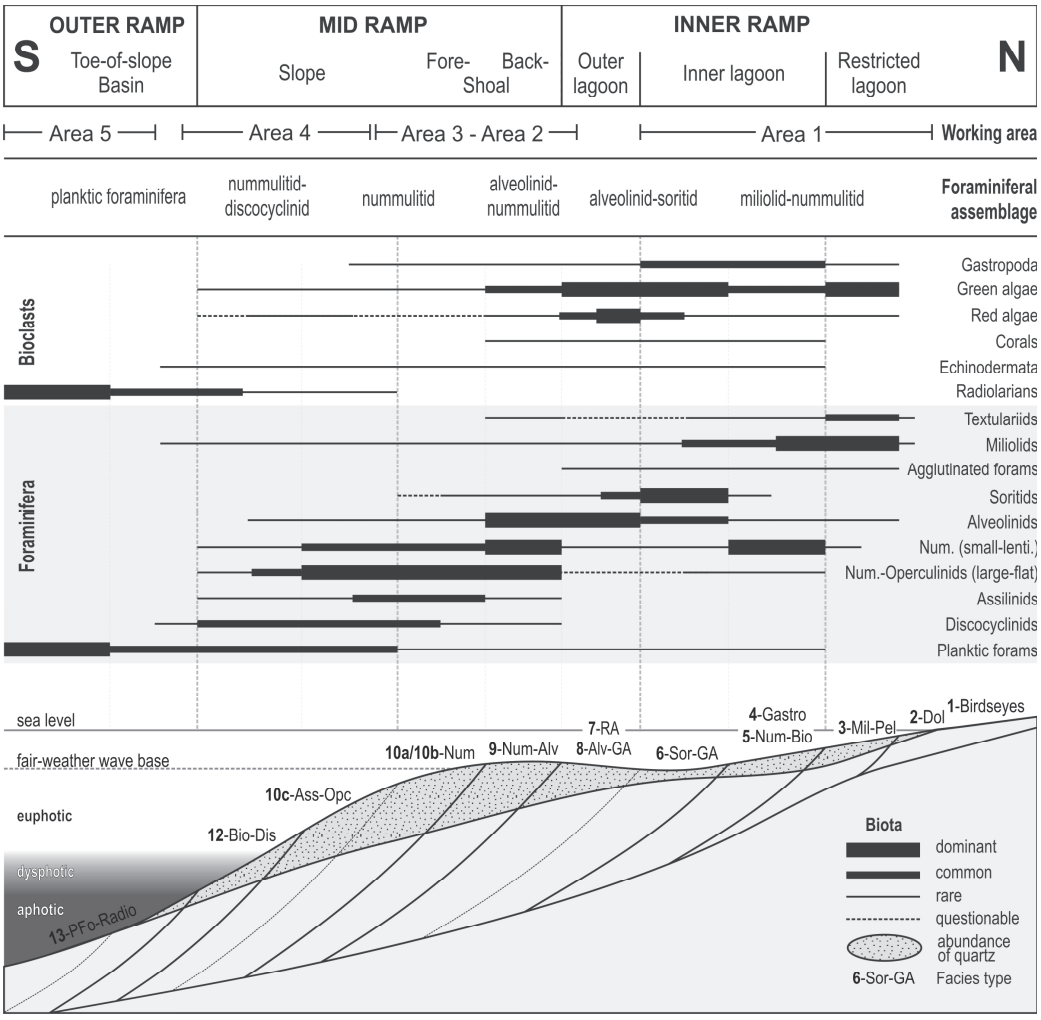

Figure VI.5 – Semi-quantitative distribution of the main microfossils combined with six foraminiferal assemblages and facies types (FT 1 – 10, 12, 13) on the Galala platform. *PFo* planktic foraminifera, *Radio* radiolarians, *Bio* bioclastic, *Dis* discocyclinids, *Ass* assilinids, *Num* nummulitids, *Opc* operculinids, *Alv* alveolinids, *GA* green algae, *RA* red algae, *Sor* soritids, *Gastro* gastropods, *Mil* miliolids, *Pel* peloids, *Dol* dolomite, *lenti.* lenticular. FT 11 (conglomeratic quartz sandstone) is not plotted and is supposed to occur on a wide range of nearly all palaeo-environments in the study area. The discrimination of inner-, mid- and outer ramp environments with the help of different bioclasts and larger foraminifera is only roughly demonstrated due to the lack of in situ deposits in the study area.

Assemblage 1: Miliolid assemblage

Description: This assemblage is dominated by smaller porcellaneous miliolids and small lenticular nummulitids. Assemblage 1 is associated with benthic red and green algae (e.g., dasycladaceans), textulariids and smaller alveolinids. Rare faunal components are echinoderm and bivalve shell fragments, as well as gastropods. The miliolid facies is common in area 2 and 3, as well as in sections 4a and 4b of area 4.

Interpretation: The dominance of miliolids and the absence of larger flattened foraminifera indicate a very shallow-marine setting of a restricted lagoon (inner ramp). Recent miliolid species prefer euryhaline, low-hydrodynamic environments on soft substrates (e.g., Murray, 1991). The association with abundant green algae fragments and smaller rotaliids reflect the occurrence of algal meadows and elevated nutrient levels in the shallow lagoon (Davies, 1970).

Assemblage 2: Alveolinid assemblage

Description: The alveolinid assemblage is characterized by the major occurrence of larger miliolid foraminifera (e.g., *Alveolina* sp.). Assemblage 2 is associated with soritids, benthic green algae and smaller miliolids. Minor bioclasts are represented by bivalve shell fragments, gastropods, discocyclinids, nummulitids, echinoderm remains and planktic foraminifera. The tests of the LBF are generally well preserved and show only occasionally abraded adult whorls. Assemblage 2 occurs in sections 2a, 3a, 4a and 4b.

Interpretation: Assemblage 2 represents illuminated shallow-water environments at the open-marine inner to upper mid ramp, characterized by low water turbulence. Dominant LBF (*Alveolina* sp., *Orbitolites* sp., *Opertorbitolites* sp.) proliferate in algal meadows (e.g., Dill et al., 2007). The occurrence of green algae and heterotrophic grazers (e.g., gastropods) indicates elevated nutrient levels.

Assemblage 3: Nummulitid-alveolinid assemblage

Description: Assemblage 3 is dominated by the cooccurrence of *Nummulites* sp. and *Alveolina* sp. *Nummulites* occur as large flattened specimen as well as small lenticular forms. Benthic green algae occur occasionally as major component. Other bioclasts are generally rare. In the Paleocene intervals of the studied sections, foraminiferal assemblage 3 is characterized by the dominance of *Ranikothalia* sp., *Miscellanea* sp. and *Glomalveolina* sp., which demonstrate the precursors of *Nummulites* sp. and *Alveolina* sp. This assemblage occurs in sections 1a, 1b, 2a and 3a and occasionally in section 4a.

Interpretation: Most of the recent alveolinids and nummulitids prevail in various environments on a carbonate ramp (Hohenegger et al., 1999). Alveolinids proliferate on the protected inner ramp within seagrass communities, whereas nummulitids can occur on a

wide range at the platform. Large-flattened fossil nummulitids dominate the deeper parts of the ramp or occur at the seaward side of shoals, whereas small-lenticular forms live together with alveolinids in more protected inner ramp environments (e.g., Geel, 2000). The coeval occurrence of large-flat nummulitids and alveolinids, reflecting two different environments either point to an offshore transport of alveolinids (Adabi et al., 2008) or to a shoal-to-inner ramp transport of nummulitids.

Assemblage 4: Nummulitid assemblage

Description: The nummulitid assemblage is characterized by the cooccurrence of large-flattened and small, lenticular forms of *Nummulites* sp. Occasionally, forms of *Assilina* sp. are present as a major component. Operculinids, discocyclinids and smaller bioclasts are rare or absent. Nummulitid-dominated rocks occur in sections 3a, 4a and rarely in section 4b.

Interpretation: Small, lenticular nummulitids reflect favourable environmental conditions, resulting in a high and quick reproduction rate but small test size (Hallock and Glenn, 1986; Beavington-Penney and Racey, 2004). Favourable conditions prevail in well-lighted shallow-marine (< 20 m) inner ramp environments with good food supply and moderate- to high water agitation. Larger flattened nummulitids are adapted to unfavourable light or food conditions at deeper parts of the ramp (Hallock, 1985). Quick reproduction is replaced by a continuing growth of the tests. The co-occurrence of small-lenticular and larger-elongated specimen concludes the post-depositional transport of shallow inner-ramp forms (small-lenticular) towards deeper realms of the ramp.

Assemblage 5: Nummulitid-discocyclinid assemblage

Description: Foraminiferal assemblage 5 is dominated by large and flat orthophragminids (*Discocyclina* sp.) and various species of nummulitids (*Operculina* sp., *Nummulites* sp., *Assilina* sp.). Planktic and agglutinated foraminifera, smaller miliolids and rotaliids as well as green and red algal fragments occur in variable amounts. The tests of the LBF show a moderate to good preservation. Adult whorls are only occasionally abraded. Assemblage 5 is present in area 4 and rarely in area 2 and 3.

Interpretation: Large flat nummulitids and orthophragminids reflect an environment in the lower euphotic to upper dysphotic zone up to 130 m water depth (Racey, 1994; Cosovic and Drobne, 1995; Zamagni et al., 2008) where decreasing light intensity requires larger test surfaces to host photo-autotrophic organisms. Flattened LBF indicate an environment with marly to sandy substrates (Zamagni et al., 2008). Notwithstanding, assilinids, operculinids and *Nummulites* can occur in the same environment, they are supposed to be dominant in different depths in the water column. Their cooccurrence in few mid ramp sections (area 4) indicates the relocation of shallower deposits towards deeper realms. Summarizing,

foraminiferal assemblage 5 was deposited in the euphotic to dysphotic mid ramp below fair-weather wave base.

Assemblage 6: Planktic foraminifera assemblage

Description: Assemblage 6 consists nearly exclusively of planktic foraminifera and radiolaria. Ostracods and smaller benthic foraminifera are rare. The low-diverse community of foraminiferal assemblage 6 occurs in all studied areas.

Interpretation: High amounts of planktic organisms and the coeval absence of storm-derived inner ramp-related bioclasts, indicate distal authochtonous depositional environments below the storm wave base. The absence of photo-autotrophic benthos (LBF, green algae) reflects aphotic conditions at the sea-floor. For tropical marine environments without major terrigenous input a depositional palaeo-water depth below 100 m, which corresponds to the distal mid- to outer ramp is suggested (Hohenegger, 2005; Renema, 2006).

Figure VI.6 (next page) **–** Summary of all investigated sections, including the general lithofacies, foraminiferal assemblages and the biostratigraphic correlation based on calcareous nannoplankton. The arrangement of the sections on the lateral inner ramp to basin transect is shown in the small map right to the legend. The basis of all sections is the PETM/LFT interval (NP 9a – NP 9b boundary). A correlation of the NGWA (area 1) and the section of the Southern Galala Plateau (area 2 to area 5) is in question, due to the assumed asymmetric tectonic activity of the Wadi Araba horst and due to erosion of major upper environments. The block diagram below the sections illustrates the regional palaeogeographic context and the position of the sections at the ramp. Generally, autochthonous inner ramp habitats (lagoon, tidal flat) are only present in area 1. Area 3 and area 4 represent environments, which are dominated by hemipelagic marls and allochthonous relocated platform allochems. Area 5 is not represented in this figure due to no significant changes in facies and foraminiferal assemblages in section 5a.

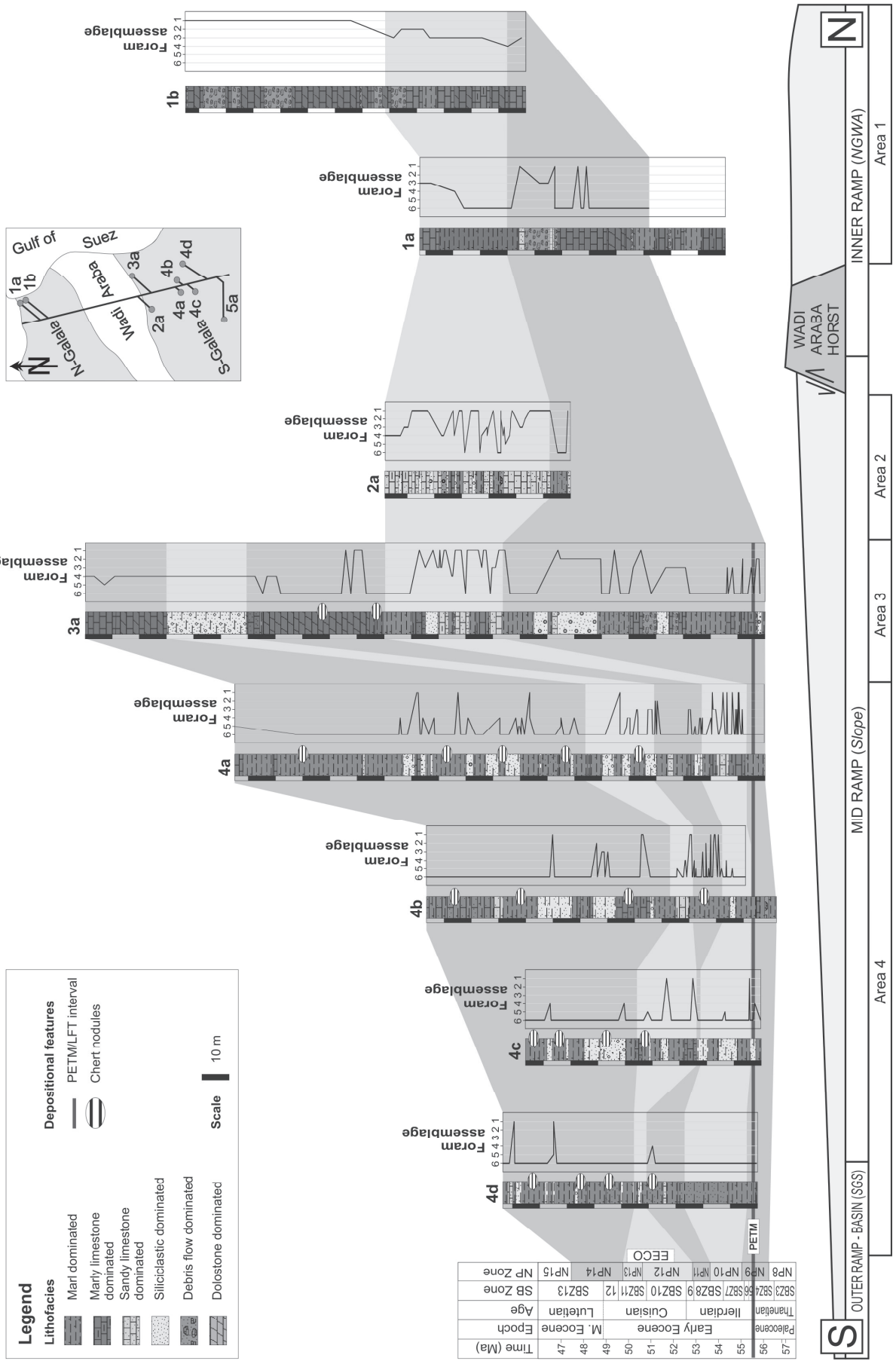
Legend
Lithofacies
Marl dominated
Marly limestone dominated
Sandy limestone dominated
Siliciclastic dominated
Debris flow dominated
Dolostone dominated
Depositional features
PETM/LFT interval
Chert nodules
Scale
10 m
Gulf of Suez
Wadi Araba
N-Galala
S-Galala
1a
1b
2a
3a
4a
4b
4c
4d
5a
Foram assemblage
6 5 4 3 2 1
WADI ARABA HORST
S
N
OUTER RAMP - BASIN (SGS)
MID RAMP (Slope)
INNER RAMP (NGWA)
Area 4
Area 3
Area 2
Area 1
Time (Ma)
47 48 49 50 51 52 53 54 55 56 57
Epoch
Paleocene
Early Eocene
M. Eocene
Thanetian
Ilerdian
Cuisian
Lutetian
Age
SB23 SB24 SB25 SBZ7 SBZ8 SBZ9 SBZ10 SBZ11 12 SBZ13
SB Zone
NP8 NP9 NP10 NP11 NP12 NP13 NP14 NP15
NP Zone
PETM
EECO

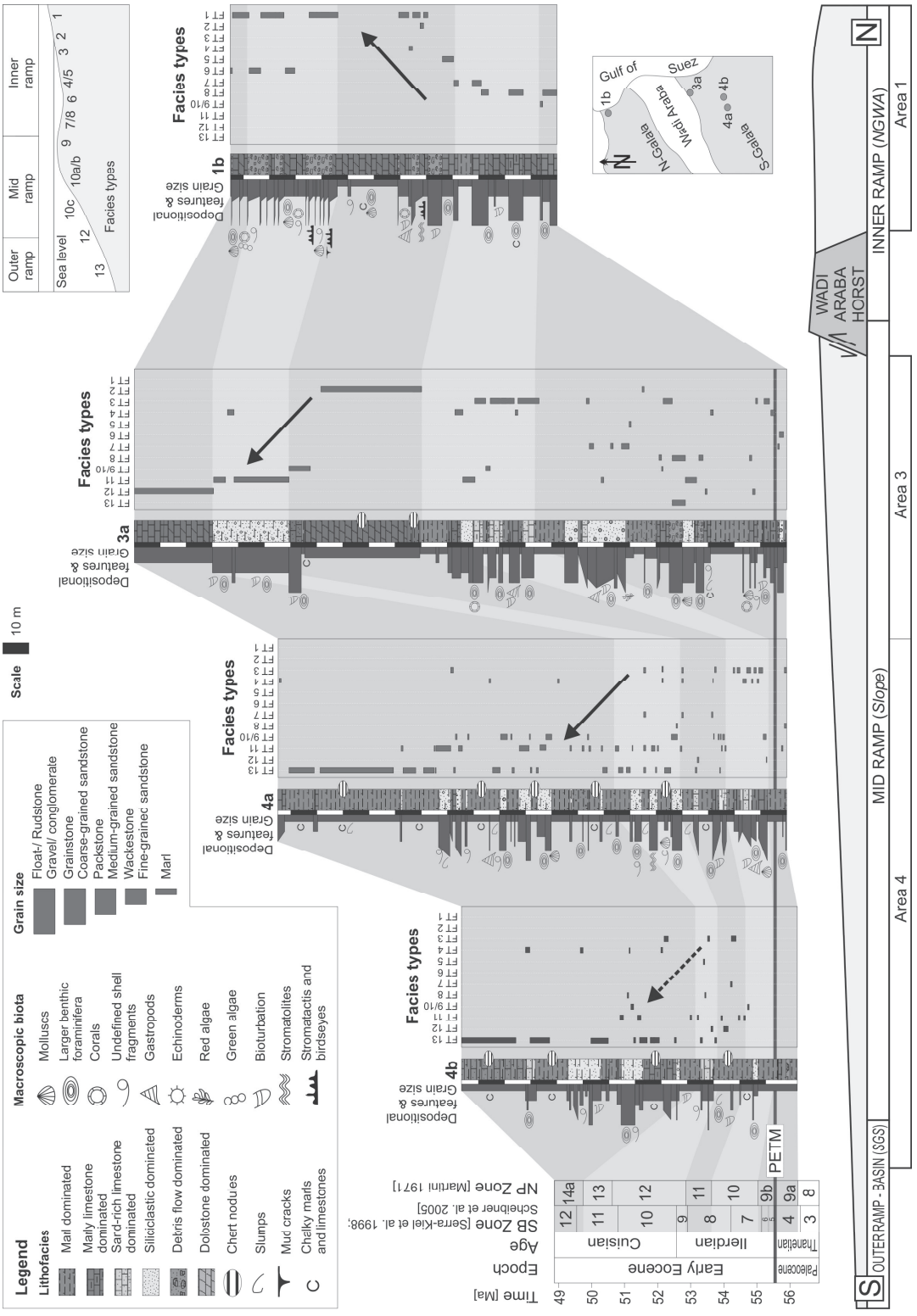

Figure VI.7 – Four selected sections of the lower mid ramp (sections 4a and 4b), the upper mid ramp (section 3a) and the inner ramp (section 1b) regarding FT changes during five stratigraphic intervals with the PETM (red line) as base of correlation. Major lithofacies (coloured), grain size, macrofossils and depositional textures are added. Detailed microfacies records of the mid ramp sections indicate a shift from shallow marine environments (FT 1 to FT 5) to deep marine environments (FT 9 to FT 13) between NP 11 and NP 12/13 (*black arrows*). However, the FT of the inner ramp area indicate a shift from open lagoonal environments (FT 8) to more restricted settings with temporarily subaerial exposure (FT 1). Both diametral facies shifts are probably related to the tectonic uplift of inner ramp environments (area 1) and a coeval sea-level rise, which is represented by a deepening upward in the tectonically uninfluenced mid- and outer ramp areas (area 3 and 4).

VI.3 Discussion

VI.3.1 Platform evolution

Formation and evolution of carbonate platform systems are strongly controlled by eustatic sea-level changes and the activity of adjacent tectonic provinces (Bosellini, 1989; Everts, 1991). Based on the Paleocene record of the Galala platform, Scheibner et al. (2003) assume a platform evolution that is more affected by local tectonic displacements than by eustatically controlled sea-level changes. Thus, the tectonic activity along the Wadi Araba Fault system triggered the initial growth of the Galala platform as a coupled effect of sea-level drop and local tectonic uplift. Furthermore, geometry and architecture of platform and slope underwent repeated changes since the Cretaceous due to the varying tectono-sedimentary constraints on the unstable Egyptian shelf (Meshref, 1990; Schütz, 1994; Youssef, 2003).

Scheibner et al. (2003) documented five platform stages regarding progradation and retrogradation of the platform margin, which encompasses the evolution of the study area from the Maastrichtian to the earliest Eocene (stages A – E, Fig. VI.8). Stages A and B describe the transition between hemipelagic and slope deposition, reflecting the initial stages (Maastrichtian to Late Paleocene, NP 5). The first progradational phase of the Galala platform is documented in the Late Paleocene (NP 5 to NP 6, stage C), which is related to uplift along the Wadi Araba Fault and a major sea-level drop. A second progradational phase (stage D) occurred during NP 7 to NP 8. Massive debris flows filled up the accommodation space at the platform rim and forced a southward shift of the platform margin. Stage E represents platform retrogradation within the latest Paleocene (NP 9) up to the PETM, reflecting a sea-level rise. Retrogradation is accompanied by the widespread deposition of marls and the onset of LBF shoals on the platform margin. Within NP 9 the slope gradient decreased, due to the subsidence of the platform interior and the coeval uplift of the SGS.

Scheibner and Speijer (2008) introduced a sixth platform stage F, which is characterized by the first occurrence of *Nummulites* and *Alveolina* in the Galala succession. The base of stage F is represented by the PETM interval, which coincides with the larger foraminifera turnover and the Paleocene – Eocene boundary (boundary NP 9a – NP 9b). The post-PETM evolution of the Galala platform is characterized by a transitional phase of aggradation. Marls and allochthonous marly limestones dominate the deposition at the slope. In NP 10 the deposition of siliciclastics increased significantly, which indicates a reactivation of the Wadi Araba Fault.

Platform stage F is terminated within NP 11, due to several fundamental shifts regarding the tectonic constraints and the trophic regime in the depositional record of the Galala Mountains. Thus, we are introducing a seventh platform stage G. The initiation of stage G

coincides approximately with the onset of the Thebes Formation in area 4 (~ NP 11/12). The evolution of the Galala platform in the newly introduced stage G is characterized by the ongoing retrogradation with a coeval significant increase of the tectonic activity along the Wadi Araba Fault. At least five major tectonic pulses, which are related to the uplift along the Wadi Araba Fault, are detected by means of the massive relocation of siliciclastic material and intervals with large slumping structures at the mid ramp. However, the lateral extension and distribution of siliciclastics at the ramp is highly heterogeneous, probably related to erosion and amalgamation of individual sandstone beds on the one hand, and undulating slope topography, that resulted from local tectonic uplift and subsidence, on the other. The frequent occurrence of sandstone and conglomerate beds at the ramp margin (area 2 and 3) probably reflects the filling of ancient channel structures, which were initialized during prior progradational stages (stage C and D). Large-scale slumps and frequent mass flows at the mid ramp (area 3 and 4) may indicate the onset of a distally steepened ramp, either within stage G or upper part of stage F. A continuing deepening in stage G that coincides with retrogradation of the southern ramp margin is demonstrated by the increasing deposition of widespread chalky marls with chert nodules and increasing amounts of planktic foraminifera and radiolaria at the former slope (area 4). Furthermore, a significant shift in the microfacies composition from shallower to deeper signatures is evidenced for areas 3 and 4 within NP 11 (Fig. VI.7).

In contrast to the described scenarios for the areas 3 and 4, inner ramp sections (area 1) do not show any evidence for a major sea-level rise during the same intervals (Fig. VI.7). This contradiction possibly results from a coeval tectonic uplift of a horst structure (NGWA), which represents the inner ramp and a continuing sea-level rise prior to the Early Eocene Climatic Optimum (EECO: ~ NP 12/13, 52 – 50 Ma, Zachos et al., 2001). Tidal related loferite cycles in area 1 indicate very shallow and temporarily subaerial exposed conditions in the restricted platform interior (Bandel and Kuss, 1987). Thus, the shallow inner-ramp areas widen during the sustained sea-level rise, while the mid ramp start to drown. However, the gradient of the slope does not show any evidence for steepening during the Early Eocene. Palaeo-water depths for Paleocene intrashelf basins in Egypt (e.g., the SGS) were interpreted between 100 m and 200 m (Salem, 1976; Speijer and Wagner, 2002). A homoclinal carbonate ramp with a slope of 100 km length would imply an average slope gradient of 0.02°. Thus, the increased deposition of mass-flows (debris flows, turbidites, slumps) must be related to local (tectonic) swells associated with steeper gradients or to a distally steepened ramp configuration. Furthermore, the facies signature of the mid ramp sections (area 4) indicate a deepening upward from the earliest Eocene (NP 10) to the uppermost Lower Eocene (NP 14a), which is manifested by decreasing proportions of inner- to mid ramp-related bioclasts (e.g. miliolids, peloids), forming mass-flow deposits. This deepening corresponds to the

global transgression in the Early Eocene, which terminates in the highest sea level in the Cenozoic (e.g., Haq et al., 1987; Rea et al., 1990; Zachos et al., 1994; Miller et al., 2005). In contrast to Scheibner et al. (2000), who interpreted the occurrence of Paleocene mass-flows as a consequence of a major sea-level drop and ramp progradation, similar processes can be excluded for the Early Eocene. An evidence for the tectonic control of the shallowing at NGWA is the continuing deposition of siliciclastic material at the mid ramp throughout stage G.

The termination of stage G is evidenced within NP 14a (uppermost Early Eocene), due to a significant decrease in the tectonic related deposition of siliciclastics. Especially in area 4 (sections 4a and 4b) the deposition of monotonous chalky chert-bearing marls without major sandstone and limestone beds demonstrates a reversal in the tectonic regime and the onset of a new platform stage, which we call stage H. Thus, sediments provided from the Wadi Araba horst were almost completely eroded and no inner ramp deposits are transported towards the SGS. Quartz-free mass flow deposits are rarely observed on top of the sections 4a and 4c. Here, well-sorted nummulitic pack- to floatstones probably indicate allochthonous equivalents of upper mid ramp LBF shoals. The exact stratigraphic range of stage H will be subject to further studies.

The dominance of larger benthic foraminifera as major platform contributing organisms suggests the continuation of the circum-Tethyan platform stage III of Scheibner et al. (2005) until NP 14a (~ 49 Ma). Our data do not indicate a recovery of major coral assemblages, which is related to a continuing warming trend throughout the Early Eocene, culminating during the Early Eocene Climatic Optimum (EECO; 53 – 49 Ma). A post-EECO cooling favours the recovery of temperature-controlled coral proliferation. However, post-EECO cooling has particularly affected high latitudes, whereas equatorial ocean basins remained warm throughout the Eocene (Tripati et al., 2003; Pearson et al., 2007). Thus, additional studies from Tethyan carbonate platforms at higher latitudes (e.g., Spain) are needed to demonstrate the impact of post-EECO cooling on platform organisms and to reveal the duration of circum-Tethyan platform stage III.

Figure VI.8 (next page) – Tectono-sedimentary evolution of the Galala platform from the Late Cretaceous (Maastrichtian) to the latest Early Eocene illustrated in six block schemes, which refer to eight platform stages (*A*-*H*). Platform stages *A* to *E* were described by Scheibner et al. (2003), platform stage *F* was introduced by Scheibner and Speijer (2008). The stages *G* and *H* are newly introduced in this paper. The initiation of the platform and its Early Eocene evolution were controlled by the tectonic activity along the Wadi Araba Fault, which superimposed sea-level fluctuations. However, the Paleocene evolution of the platform was controlled by major sea-level fluctuations. Stage *G* is again controlled by renewed tectonic activity along the Wadi Araba Fault. In contrast to stage *G*, the activity of the Wadi Araba Fault is terminated in stage *H*. The stratigraphic range of stage *H* will be explored. For a legend of the used icons see figure VI.7.

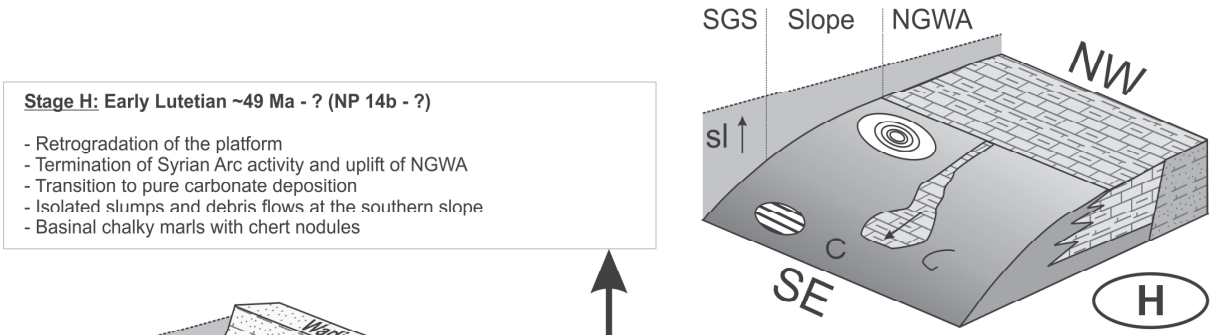

Stage H: Early Lutetian ~49 Ma - ? (NP 14b - ?)

- Retrogradation of the platform
- Termination of Syrian Arc activity and uplift of NGWA
- Transition to pure carbonate deposition
- Isolated slumps and debris flows at the southern slope
- Basinal chalky marls with chert nodules

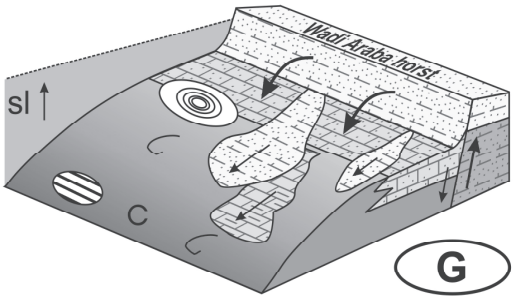

Stage G: Early - Late Ilerdian ~53,5 Ma - ~49 Ma (NP 11 - NP 14a)

- Progradation of ramp due to uplift of NGWA with massive erosion of Palaeozoic and Mesozoic siliciclastics (Nubia Series)
- Distally steepened ramp configuration with slope
- Basinal chalky marls with chert nodules
- Subaerial exposure of inner ramp intervals
- Elevated nutrient levels at the platform and the slope

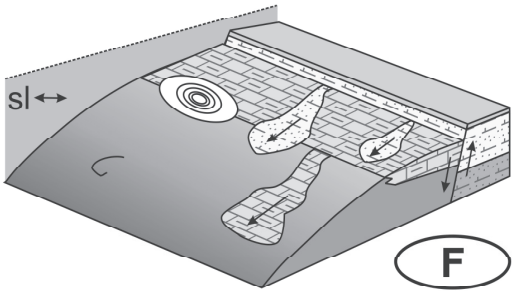

Stage F: Early Ilerdian 55,5 Ma - ~53,5 Ma (NP 9b - NP 11)

- Aggradation of the ramp
- Uplift along the Wadi Araba Fault
- Input of siliciclastics towards the S; debris flows and slumps at the slope
- Onset of a mixed carbonatic-siliciclastic depositional system
- LBF limestones and subordinate debris flows on the NGWA

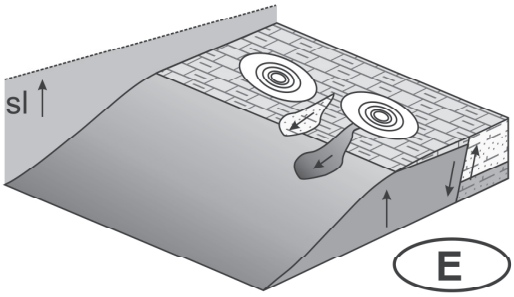

Stage E: Late Thanetian: 56,2 Ma - 55,5 Ma (NP 9a)

- Retrogradation of the platform due to sea level rise
- Transition to ramp morphology
- Rotational block movement and minor uplift along the Wadi Araba Fault
- Uplift of the slope further S
- Decrease of debris flows; increase of limestone deposition
- Coral patch reefs substituted by foraminiferal shoals and minor sand flats

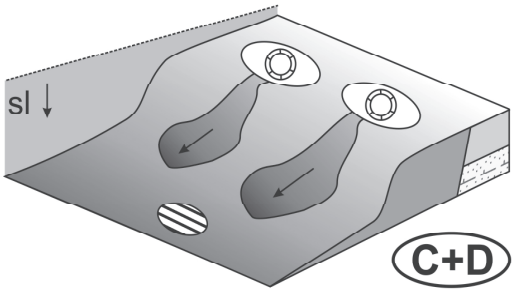

Stage C+D: Early Thanetian: 59 Ma - 56,2 Ma (NP 5 - NP 8)

- Progradation of the platform in two stages:
  Stage C) sea-level fall, initiation of coralgal patch reefs
  Stage D) basinward shift of coralgal patch reefs
- Calciturbidites and hemipelagic marls with chert nodules
- Steep platform to slope transition

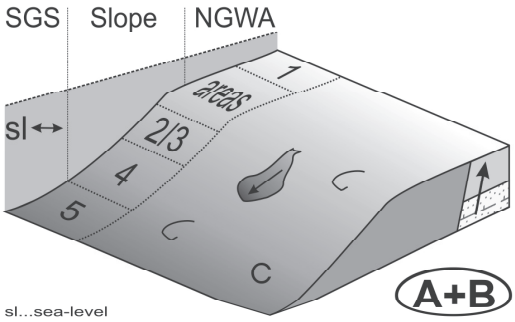

sl...sea-level

Stage A+B: Maastrichtian - Early Selandian: 69 Ma - 59 Ma

- Initiation of the platform due to local uplift along the Wadi Araba Fault; stationary platform margin
- Basinal chalks vs. phosphate-rich siliciclastic marls
- Increasing mass flows in the Early Palaeocene: debris flows and slumps vs. calciturbidites

Cretaceous marls/limestones
Mesozoic silici-clastics (Nubia A)
Palaeozoic silici-clastics (Nubia B-D)

VI.3.2 Tectonic constraints and the source of quartz

Quartz is generally rare in the Cretaceous and almost absent in the Paleocene of the Galala succession. Quartz-free carbonate mass-flow deposits were reported for the Late Paleocene, reflecting a massive sea-level drop during nannoplankton zone 5 (Lüning et al., 1998; Scheibner et al., 2000; Figs. VI.8a-d). Scheibner et al. (2003) describe first siliciclastic deposits in the latest Paleocene (NP 9a) and assume a source in the hinterland. During the Early Eocene, the abundance and frequence of sandstones and quartz-rich limestones increases, especially in the Southern Galala mid ramp sections (area 2, 3 and 4). Siliciclastic deposits from the NGWA are reported from few sections at the southern margin of the Northern Galala Plateau (Gietl, 1998). At the northern margin of the NGWA pure carbonate deposition prevailed throughout the Lower Eocene (area 1). The dominance of siliciclastic material at the Southern Galala Plateau and the coeval pure carbonate deposition at the NGWA suggest a source area of the siliciclastic material north of the Wadi Araba Fault. Furthermore, major sandstone intervals at the Southern Galala mid ramp indicate the major transport direction of quartz-rich deposits towards the South.

The deposition of siliciclastics at the isolated Galala platform is related to tectonically induced uplift and erosion of older sandstones along the Wadi Araba Fault. This was confirmed by Hussein and Abd-Allah (2001), who described increased Lower Eocene oblique convergence at the unstable Egyptian shelf resulting in the reactivation of Mesozoic fault systems and the uplift along the Syrian Arc-Fold-Belt. This tectonic reactivation resulted in an uplift of Palaeozoic and Mesozoic sandstones with a vertical displacement of more than 500 m (Schütz, 1994). Hence, the sandstones, which belong to the Nubia Series (Late Carboniferous – Early Cretaceous) were subaerial exposed and eroded in the Early Eocene (Fig. VI.8g).

The onset of a mixed carbonate-siliciclastic depositional system at the Southern Galala Plateau during the Early Eocene is reflected by increasing contents of terrigeneous quartz grains, either as distinct beds of sandstone or as disseminated components in marls and limestones. Sandstone beds accumulate in intervals of several metres to tens of metres, which are traceable throughout area 2, 3 and 4. Generally, the correlation of the siliciclastic units on the platform to basin transect is difficult, due to highly variable thicknesses of the beds and assumingly various point sources of the siliciclastic material in the vicinity of the Wadi Araba Fault (Figs. VI.6, VI.7). For this reason, the impact of various tectonic pulses is supposed to be a major trigger for the relocation of quartz-rich sediments. Major tectonic activity of the Wadi Araba Fault is estimated within NP 11 and NP 14a when thick quartz-rich packages were deposited (Fig. VI.6). Within NP 14a, the system shifted towards pure carbonate deposition (Fig. VI.8h).

VI.4 Conclusions

The biotic and abiotic evolution of the Early Eocene Galala platform is strongly influenced by regional tectonic uplift along the Wadi Araba Fault, superimposing the effects of eustatic sea-level fluctuations. The definition and interpretation of 13 facies types and six foraminiferal assemblages as well as qualitative analyses of dominating platform biota are demonstrated in the following results:

- The Early Eocene monoclinal uplift along the Wadi Araba Fault intensified with respect to the Paleocene and Late Cretaceous. Amalgamated intervals of siliciclastic material as well as slumps and coarse-grained debris flows indicate multiple tectonic pulses and local steep slope gradients. The heterogeneous distribution and irregular lateral extension of siliciclastics probably reflect a complex ramp topography, which is influenced by local uplift and subsidence, as well as pre-existent swells and troughs. The origin of those swells is probably related to pre-Eocene progradational platform stages. Although the overall ramp gradient does not indicate any steepening, frequent mass flow deposits at the lower mid ramp support the onset of a distally steepened ramp in the Early Eocene.
- Following previous studies of Scheibner et al. (2003) and Scheibner and Speijer (2008), we complete and expand the platform model with respect to the Early Eocene succession. Platform stage F, introduced and described by Scheibner and Speijer (2008) ranges from NP 9b to NP 11 and demonstrates a period of platform aggradation with the reactivation of the Wadi Araba Fault.
- We introduce two new platform stages regarding varying biotic and tectono-sedimentary constraints: Stage G (NP 11 – NP 14a) is characterized by the repeated activity along the Wadi Araba Fault and the massive input of Mesozoic siliciclastic material towards the S. The retrogradation of the platform is demonstrated by a shift in the microfacies signature of the mid- and outer ramp succession (~ NP 11/12). However, the antithetic evolution of inner ramp environments reflects a sea-level drop and the onset of tidal-related loferite cycles. This contradiction is related to the uplift of a horst structure along the Wadi Araba Fault, which formed a palaeogeographic barrier between inner- and mid ramp environments.
- In contrast to stage G, the following stage H (NP 14a) reflects the termination of tectonic activity along the Wadi Araba Fault. The horst structure initiated in stage G was completely eroded during that stage. The system shifts to pure carbonate deposition, dominated by chalky, chert-rich marls at the mid- and outer ramp. The stratigraphic range of platform stage H will be subject to further studies.

Acknowledgements The authors sincerely thank A. Freiwald (Wilhelmshaven) and an anonymous reviewer for a stimulating review of the manuscript. We thank Dr. Abdel-Mohsen Morsi and Dr. Abdel-Monem Soltan for their excellent help and organisation of our field trips in Egypt. We are grateful to Prof. Mohamed Boukhary, who has determined various nummulitids for this study. Furthermore, we thank Ralf Bätzel, Christian Sommerfeld and Karin Geserich for the preparation of the samples, as well as Steven P. Morrissey for his creative stimulation. This project was funded by the German Science Foundation (DFG-KU 642/221).

VI.5 References

Abdallah AM, Sharkawi MAE, Marzouk A (1970) Geology of Mersa Thelmet area, southern Galala, Eastern Desert A. R. E. Bull Fac Sci, Cairo Univ 44:271-280.

Adabi M, Zohdi A, Ghabeishavi A, Amiri-Bakhtiyar H (2008) Applications of nummulitids and other larger benthic foraminifera in depositional environment and sequence stratigraphy: an example from the Eocene deposits in Zagros Basin, SW Iran. Facies 54:499-512.

Ahlbrandt TS (2001) The Sirte Basin Province of Libya - Sirte-Zelten total petroleum system. US Geol Surv Bull 2202-F, pp 29.

Aubry MP (1995) Towards an upper Paleocene-lower Eocene high resolution stratigraphy based on calcareous nannofossil stratigraphy. Isr J Earth Sci 44:239-253.

Aubry MP, Cramer BS, Miller KG, Wright JD, Kent DV, Olsson RK (2000) Late Paleocene event chronology: unconformities, not diachrony. Bull Soc Géol Fr 171:367-378.

Baaske UP, Itterbeeck JV, Griffiths H, Tricker P, Mugheiry M, Burgess P (2008) The Eocene carbonate System(s) of the Sirte Basin, Libya: Implications of regional-scale observations. 2008 AAPG International Conference and Exhibition - Abstracts, October 26-29, 2008, Cape Town, South Africa.

Baccelle L, Bosellini A (1965) Diagrammi per la stima visiva della composizione percentuale nelle rocce sedimentarie. Annali dell'Università di Ferrara (Nuova Serie). Sezione IX, Sci Geol Paleontol 1:117–153.

Bandel K, Kuss J (1987) Depositional environment of the pre-rift sediments - Galala Heights (Gulf of Suez, Egypt). Berl geowiss Abh 78:1-48.

Bassi D (1998) Coralline algal facies and their palaeoenvironments in the Late Eocene of Northern Italy (Calcare di Nago, Trento). Facies 39:179-202.

Beadnell HJL (1905) The relations of the Eocene and Cretaceous systems in the Esna-Aswan reach of the Nile Valley. Q J Geol Soc Lond 61:667-678.

Beavington-Penney SJ, Racey A (2004) Ecology of extant nummulitids and other larger benthic foraminifera: applications in palaeoenvrionmental analysis. Earth Sci Rev 67:219-265.

Bechstädt T, Boni M (1989) Tectonic control on the formation of a carbonate platform: The Cambrian of Southwestern Sardinia. In: Crevello PD, Wilson JL, Sarg JF, Read JF (1989) Controls on Carbonate Platforms and Basin Development. SEPM Spec Publ 44:107-122.

Bosellini A (1989) Dynamics of Tethyan carbonate platforms. In: Crevello PD, Wilson JL, Sarg F, Read JF (eds) Controls on carbonate platform and basin development, SEPM Spec Publ 44: 3-13.

Bosence D (2005) A genetic classification of carbonate platforms based on their basinal and tectonic settings in the Cenozoic. Sedimentary Geology 175:49-72.

Burchette TP (1988) Tectonic control on carbonate platform facies distribution and sequence development: Miocene, Gulf of Suez. Sedimentary Geology 59:179-204.

Cosovic V, Drobne K (1995) Palaeoecological significance of morphology of orthophragminids from the Istrian Peninsula. Geobios 18:93-99.

Cosovic V, Drobne K, Moro A (2004) Paleoenvironmental model for Eocene foraminiferal limestones of the Adriatic carbonate platform (Istrian Peninsula). Facies 50:61-75.

Davies G (1970) Carbonate bank sedimentation, eastern Shark Bay, Western Australia. Am Assoc Petrol Geol Mem 13:85–168.

Dill HG, Wehner H, Kus J, Botz R, Berner Z, Stüben D, Al-Sayigh A (2007) The Eocene Rusayl Formation, Oman, carbonaceous rocks in calcareous shelf sediments: Environment of deposition, alteration and hydrocarbon potential. Int J Coal Geol 72:89-123.

Everts AJW (1991) Interpreting compositional variations of calciturbidites in relation to platform-stratigraphy: an example from the Paleogene of SE Spain. Sediment Geol 71:231-242.

Förstner U, Müller G, Reineck HE (1968) Sedimente und Sedimentgefüge des Rheindeltas im Bodensee. Sediments and sedimentary structures of the Rhine delta in Lake Constance. N Jahrb Miner Abh 109:33-62.

Geel T (2000) Recognition of stratigraphic sequences in carbonate platform and slope deposits: Empirical models based on microfacies analysis of Palaeogene deposits in southeastern Spain. Palaeogeogr Palaeoclimatol Palaeoecol 155:211-238.

Gietl R (1998) Biostratigraphie und Sedimentationsmuster einer nordostägyptischen Karbonatrampe unter Berücksichtigung der Alveolinen-Faunen. Ber Fachb Geowiss Univ Bremen 112:1-135.

Hallock P (1985) Why are larger foraminifera large? Paleobiology 11:195-208.

Hallock P, Glenn EC (1986) Larger foraminifera: a tool for paleoenvironmental analysis of Cenozoic carbonate depositional facies. Palaios 1:55-64.

Haq BU, Hardenbol J, Vail P (1987) Chronology of fluctuating sea levels since the Triassic. Science 235:1156-1167.

Hermina M, Lindenberg HG (1989) The Tertiary. In: Hermina M, Klitzsch E, List FK (eds) Stratigraphic lexicon and explanatory notes to the geological map of Egypt 1:500 000, Conoco Inc, Cairo, pp 141-217.

Hohenegger J, Yordanova E, Nakano Y, Tatzreiter F (1999) Habitats of larger foraminifera on the upper reef slope of Sesoko Island, Okinawa, Japan. Mar Micropaleontol 36:109-168.

Hohenegger J (2005) Estimation of environmental paleogradient values based on presence/absence data: a case study using benthic foraminifera for paleodepth estimation. Palaegeogr Palaeoclimatol Palaeoecol 217:115-130.

Hottinger L, Schaub H (1960) Zur Stufeneinteilung des Paleocaens und des Eocaens. Eclogae Geol Helv 53:453-479.

Hottinger L (1973) Selected Paleogene larger foraminifera. In: Hallam A (ed) Atlas of palaeobiogeography, Elsevier, Amsterdam, pp 443-452.

Hottinger L (1974) Alveolinids, Cretaceous Tertiary Larger Foraminifera, Exxon Research–European Laboratories. A Schudel & Co, Riehen, Basel, pp 85.

Hottinger L (1997) Shallow benthic foraminiferal assemblages as signals for depth of their deposition and their limitations. Bull Soc Géol Fr 168:491-505.

Hottinger L (1998) Shallow benthic foraminifera at the Paleocene-Eocene boundary. Strata 1 9: 61-64.

Hussein IM, Abd-Allah AMA (2001) Tectonic evolution of the northeastern part of the African continental margin, Egypt. J Afr Earth Sci 33:49-68.

Keheila EA, El-Ayyat AAM (1990) Lower Eocene carbonate facies, environments and sedimentary cycles in Upper Egypt: evidence for global sea-level changes. Palaeogeogr Palaeoclimatol Palaeoecol 81:333-47.

Keheila EA, El-Ayyat AM (1992) Silicification and dolomitization of the Lower Eocene carbonates in the Eastern Desert between Sohag and Qena, Egypt. J Afr Earth Sci 14:341–349.

Krenkel E (1925) Geologie Afrikas. Gebrüder Bornträger, Berlin, pp 461.

Kuss J (1986) Facies development of Upper Cretaceous-Lower Tertiary sediments from the monastery of St. Anthony/Eastern Desert, Egypt. Facies 15:177-194.

Kuss J, Leppig U (1989) The early Tertiary (middle-late Paleocene) limestones from the western Gulf of Suez, Egypt. N Jahrb Geol Paläontol Abh 177:289-332.

Kuss J, Scheibner C, Gietl R (2000) Carbonate platform to basin transition along an Upper Cretaceous to Lower Tertiary Syrian Arc Uplift, Galala Plateaus, Eastern Desert, Egypt. GeoArabia 5:405-424.

Lee JW, D'Argenio B (1982) Controls on carbonate platforms and basin systems development. Geology 10:659-661.

Lighty RG (1985) Preservation of internal reef porosity and diagenetic sealing of submerged early Holocene barrier reef, southeast Florida shelf. In: Bricker OP (ed) Carbonate cements, John Hopkins Press, pp 123-151.

Loucks RG, Moody RTJ, Bellis JK, Brown AA (1998) Regional depositional setting and pore network systems of the El Garia Formation (Metlaoui Group, Lower Eocene), offshore Tunisia. In: Macgregor DS, Moody RTJ, Clark-Lowes DD (eds) Petroleum geology of North Africa, Geol Soc Lond Spec Publ 132: 355-374.

Lüning S, Marzouk AM, Kuss J (1998) The Paleocene of central East Sinai, Egypt: "sequence stratigraphy" in monotonous hemipelagites. J Foraminifer Res 28:19-39.

Luterbacher H (1984) Paleoecology of foraminifera in the Paleogene of the southern Pyrenees. Benthos´83, 2nd Int Symp Benthic Foraminifera, pp 389-392.

Martini E (1971) Standard Tertiary and Quaternary calcareous nannoplankton zonation. In: Farinacci A (ed) Proc II Plankton Conf, Roma, Ed Tecnosci Rome, Roma, pp 739-785.

McBride EF, Abdel-Wahab A, El-Younsy ARM (1999) Origin of spheroidal chert nodules, Drunka Formation (Lower Eocene), Egypt. Sedimentology 46:733-755.

Meshref WM (1990) Tectonic framework. In: Said R (ed) The Geology of Egypt, AA Balkema Publ, Rotterdam, pp 113-156.

Miller KG, Kominz MA, Browning JV, Wright JD, Mountain GS, Katz ME, Sugarman PJ, Cramer BS, Christie-Blick N, Pekar SF (2005) The Phanerozoic record of global sea-level change. Science 310:1293-1298.

Morsi AMM, Scheibner C (2009) Paleocene - Early Eocene ostracodes from the Southern Galala Plateau (Eastern Desert, Egypt): taxonomy, impact of paleobathymetric changes. Rev Micropaléontol 52:149–192.

Moustafa AR, El-Rey AK (1993) Structural characteristics of the Suez rift margins. Geol Rundschau 82:101-109.

Moustafa AR, Khalil MH (1995) Superposed deformation in the northern Suez Rift, Egypt: Relevance to hydrocarbons exploration. J Petrol Geol 18:245-266.

Murray JW (1991) Ecology and Paleoecology of Benthic Foraminifera. Longman Scientific and Technical, New York, pp 397.

Orue-Etxebarria X, Pujalte V, Bernaola G, Apellaniz E, Baceta JI, Payros A, Nunez-Betelu K., Serra-Kiel J, Tosquella J (2001) Did the Late Paleocene thermal maximum affect the evolution of larger foraminifers? Evidence from calcareous plankton of the Campo Section (Pyrenees, Spain). Mar Micropal 41:45-71.

Özgen-Erdem N, Inan N, Ajyazi M, Tunoglu C (2005) Benthonic foraminiferal assemblages and microfacies analysis of Paleocene-Eocene carbonate rocks in the Kastamonu region, Northern Turkey. J Asian Earth Sci 25:403-417.

Papazzoni C, Trevisani E (2006) Facies analysis, palaeoenvironmental reconstruction, and biostratigraphy of the “Pesciara di Bolca” (Verona, northern Italy): An early Eocene Fossil-Lagerstätte. Palaeogeogr Palaeoclimatol Palaeoecol 242:21-35.

Pearson PN, van Dongen BE, Nicholas CJ, Pancost RD, Schouten S, Singano JM, Wade BS (2007) Stable warm tropical climate through the Eocene Epoch. Geology 35: 211-214.

Pujalte V, Baceta JI, Payros A, Orue-Etxebarria X, Schmitz B (1999) Upper Paleocene-Lower Eocene strata of the W. Pyrenees, Spain: A shelf-to-basin correlation. In: Andreasson FP, Schmitz B, Thompson EI (eds) Early Paleogene warm climates and biosphere dynamics, Dep Mar Geol, Göteborg.

Pujalte V, Schmitz B, Baceta JI, Orue-Etxebarria X, Bernaola G, Dinares-Turell J, Payros A, Apellaniz E, Caballero F (2009) Correlation of the Thanetian-Illerdian turnover of larger foraminifera and the Paleocene-Eocene thermal maximum: confirming evidence from the Campo area (Pyrenees, Spain). Geol Acta 7:161-175.

Racey A (1994) Biostratigraphy and palaeobiogeographic significance of Tertiary nummulitids (Foraminifera) from northern Oman. In: Simmons MD (ed) Micropalaeontology and hydrocarbon exploration in the Middle East, Chapman and Hall, London, pp 343-367.

Rasser MW (1994) Facies and palaeoecology of rhodoliths and acervulinid macroids in the Eocene of the Krappfeld (Austria). Beitr Paläontol 19:191-217.

Rasser MW, Scheibner C, Mutti M (2005) A paleoenvironmental standard section for Lower Ilerdian tropical carbonate factories (Pyrenees, Spain; Corbieres, France). Facies 51:217-232.

Rea DK, Zachos JC, Owen RM, Gingerich PD (1990) Global change at the Paleocene-Eocene boundary: climatic and evolutionary consequences of tectonic events. Palaegeogr Palaeoclimatol Palaeoecol 79:117-128.

Reineck HE, Singh IB (1980) Depositional Sedimentary Environments. 2nd ed Springer, Berlin, pp 549.

Renema W (2006) Large benthic foraminifera from the deep photic zone of a mixed siliciclastic-carbonate shelf off East Kalimantan, Indonesia. Mar Micropaleontol 58:73-82.

Said R (1990) Cenozoic. In: Said R (ed) The geology of Egypt, Balkema, Rotterdam, pp 451-486.

Salem R (1976) Evolution of Eocene-Miocene sedimentation patterns in parts of northern Egypt. AAPG Bull 60:34-64.

Schäfer K (1969) Vergleichs-Schaubilder zur Bestimmung des Allochemgehalts bioklastischer Karbonatgesteine. N Jahrb Geol Paläontol Monatshefte 1969:173–184.

Schaub H (1992) The Campo Section (NE Spain) a Tethyan parastratotype of the Cuisian. N Jahrb Geol Paläontol Abh 186:63-70.

Scheibner C, Kuss J, Marzouk AM (2000) Slope sediments of a Paleocene ramp-to-basin transition in NE Egypt. Int J Earth Sci 88:708-724.

Scheibner C, Marzouk AM, Kuss J (2001a) Maastrichtian-Early Eocene litho- biostratigraphy and palaeogeography of the northern Gulf of Suez region, Egypt. J Afr Earth Sci 32:223-255.

Scheibner C, Marzouk AM, Kuss J (2001b) Shelf architectures of an isolated Late Cretaceous carbonate platform margin, Galala Mountains (Eastern Desert, Egypt). Sediment Geol 145:23-43.

Scheibner C, Kuss J, Speijer RP (2003) Stratigraphic modelling of carbonate platform-to-basin sediments (Maastrichtian to Paleocene) in the Eastern Desert, Egypt. Palaeogeogr Palaeoclimatol Palaeoecol 200:163-185.

Scheibner C, Speijer RP, Marzouk AM (2005) Larger foraminiferal turnover during the Paleocene/Eocene thermal maximum and paleoclimatic control on the evolution of platform ecosystems. Geology 33:493-496.

Scheibner C, Rasser MW, Mutti M (2007) Facies changes across the Paleocene-Eocene boundary: The Campo section (Pyrenees, Spain) revisited. Palaegeogr Palaeoclimatol Palaeoecol 248:145-168.

Scheibner C, Speijer RP (2008) Late Paleocene–early Eocene Tethyan carbonate platform evolution - A response to long- and short-term paleoclimatic change. Earth Sci Rev 90:71-102.

Scheibner C, Speijer RP (2009) Recalibration of the Tethyan shallow-benthic zonation across the Paleocene-Eocene boundary; the Egyptian record. Geol Acta 7:195-214.

Schütz KI (1994) Structure and stratigraphy of the Gulf of Suez, Egypt. In: Landon SM (ed) Interior rift basins, AAPG Mem, pp 57-96.

Serra-Kiel J, Hottinger L, Caus E, Drobne K, Ferrandez C, Jauhri AK, Less G, Pavlovec R, Pignatti J, Samso JM, Schaub H, Sirel E, Strougo A, Tambareau Y, Tosquella J, Zakrevskaya E (1998) Larger foraminiferal biostratigraphy of the Tethyan Paleocene and Eocene. Bull Soc Géol Fr 169:281-299.

Shahar J (1994) The Syrian Arc System: an overview. Palaeogeogr Palaeoclimatol Palaeoecol 112:125-142.

Speijer RP, Schmitz B (1998) A benthic foraminiferal record of Paleocene sea level and trophic/redox conditions at Gebel Aweina, Egypt. Palaeogeogr Palaeoclimatol Palaeoecol 137:79-101.

Speijer RP, Wagner R (2002) Sea-level changes and black shales associated with the late Paleocene thermal maximum; organic-geochemical and micropaleontologic evidence from the southern Tethyan margin (Egypt-Israel). In: Koeberl C, MacLeod KG (eds) Catastrophic Events & Mass Extinctions: Impacts and Beyond, Geol Soc Am Spec Pap, Boulder, pp 533-549.

Strougo A, Faris M (1993) Paleocene-Eocene stratigraphy of Wadi El Dakhl, Southern Galala plateau. Middle East Res Center, Ain Shams Univ, Earth Sci Serv 7:49-62.

Tripati AK, Delaney ML, Zachos JC, Anderson LD, Kelly DC, Elderfield H (2003) Tropical sea-surface temperature reconstruction for the early Paleogene using Mg/Ca ratios of planktonic foraminifera. Paleoceanography 18:doi:1110.1029/2003PA000937,002003.

Werner J (1963) Über die Bedeutung der Opal-Phytolithen als Mikrofossilien des Bodens. Eiszeitalter und Gegenwart 14:229.

Wielandt U (1996) Benthic foraminiferal paleoecology and microfacies investigations of Paleogene sediments from the Farafra Oasis, Western Desert, Egypt. Tübinger Mikropaläontol Mitteilungen 13:1-78.

Youssef MM (2003) Structural setting of central and south Egypt: An overview. Micropaleontology 49:1-13.

Zachos JC, Stott LD, Lohmann KC (1994) Evolution of early Cenozoic marine temperatures. Paleoceanography 9:353-387.

Zachos J, Pagani M, Sloan L, Thomas E, Billups K (2001) Trends, rhythms, and aberrations in global climate 65 Ma to present. Science 292:686-693.

Zachos JC, Dickens GR, Zeebe RE (2008) An early Cenozoic perspective on greenhouse warming and carbon-cycle dynamics. Nature 451:279-28.

Zamagni J, Mutti M, Kosir A (2008) Evolution of shallow benthic communities during the Late Paleocene-earliest Eocene transition in the Northern Tethys (SW Slovenia). Facies 54:25-43.

Second manuscript

INCREASING RESTRICTION OF THE EGYPTIAN SHELF DURING THE EARLY EOCENE? – NEW INSIGHTS FROM A SOUTHERN TETHYAN CARBONATE PLATFORM

Stefan Höntzsch [a], Christian Scheibner [a], Elisa Guasti [b], Jochen Kuss [a], Akmal M. Marzouk [c] and Michael W. Rasser [d]

[a] *Department of Geosciences, Bremen University, PO Box 330440, 28359 Bremen, Germany*

[b] *TNO, Princetonlaan 6, 3584 CB Utrecht, Netherlands*

[c] *Geology Department, Faculty of Science, Tanta University, Tanta 31527, Egypt*

[d] *Staatliches Museum für Naturkunde, Rosenstein 1, 70191 Stuttgart, Germany*

Published in Palaeogeography, Palaeoclimatology, Palaeoecology (2011, in press) pp. 1-18, doi:10.1016/j.palaeo.2011.01.022

Received: 17. September 2010 / Accepted: 22. January 2011

VII. INCREASING RESTRICTION OF THE EGYPTIAN SHELF DURING THE EARLY EOCENE? – NEW INSIGHTS FROM A SOUTHERN TETHYAN CARBONATE PLATFORM

Abstract The evolution of the isolated Galala carbonate platform has been studied intensively with respect to the Paleocene-Eocene Thermal Maximum (PETM) and the strong climatic variability from the Late Paleocene to the Early Eocene. In this study, we compare the results of different approaches which deal with the Early Palaeogene evolution of the Egyptian shelf, including new data from the Galala platform. Microfacies analyses along a platform to basin transect reveal a sedimentological response to a massive tectonic uplift along the Syrian Arc-Fold Belt in the Early Eocene. This uplift triggered the restriction of the Egyptian shelf by modulating and weakening Tethyan onshore currents from the North. The increasing deposition of quartz and proliferating gastropods, green algae and radiolaria, which indicate elevated nutrient levels, reflect an intensified eutrophication of shallow-marine platforms and deeper-marine shelf environments. Strongly depleted carbon isotope ratios in the sediments of the Galala succession strongly suggest the presence of restricted conditions throughout the Early Eocene. We assume that a strong climatic divergence with arid conditions on the shelf and humid conditions at the African hinterland triggered intensified chemical weathering at the Nubian-Arabian Craton. The enhanced riverine transport of terrestrial organic material to the North African shelf caused the increased availability of trophic resources and a strong negative shift of carbon isotope ratios between NP10 and NP14a. The recovery to open ocean conditions is linked to the termination of tectonic uplift along the Syrian Arc-Fold Belt in the latest Early Eocene and to stronger ocean currents, caused by increasing latitudinal temperature gradients.

Additionally, the post-PETM carbon isotope evolution at the Galala platform indicates at least two further negative carbon isotope excursions, which reflect hyperthermal events on a global scale. The associated reorganization of shallow-marine assemblages as described for example for the Larger Foraminifera Turnover at the PETM boundary event is, however, missing. We assume that the absence of a foraminiferal reorganization in this region can be linked to an increasing robustness of the major Early Eocene platform organisms (larger benthic foraminifera) and their adaption to unfavourable conditions and repeated environmental shifts.

VII.1 Introduction

The Early Palaeogene Tethys is represented by a tropical ocean basin with broad epicontinental shelf areas in the South (Bolle et al., 2000). Open seaways in the West and in the East enabled a nearly circum-tropical halothermal-driven water circulation, which kept the Tethys uniformly warm during times of global greenhouse climate (Lawver and Gahagan, 2003). This circulation pattern persisted until the collision of Greater India with southern Tibet and the continuing northward movement of Arabia resulting in the closure of the eastern Tethyan seaway in the Early Eocene (Lawver and Gahagan, 2003). As a consequence, the western Tethys, forming now the Proto-Mediterranean Sea, became more restricted and sensitive for the impact of global and regional environmental perturbations. In contrast to the open ocean, marginal shelf areas (e.g., the North African shelf) reveal complex regional environmental conditions regarding ocean circulations and local climate.

In the Early Palaeogene, major environmental perturbations are related to carbon isotope shifts, regional climate variability and tectonic uplift at the southern Tethyan shelf. Earlier studies proposed various mechanisms that affected environments at the southern Tethyan shelf with respect to the biotic and geochemical shifts of the Paleocene-Eocene Thermal Maximum (PETM; Speijer et al., 1996; Charisi and Schmitz, 1998; Speijer and Morsi, 2002; Berggren and Ouda, 2003; Alegret et al., 2005; Scheibner and Speijer, 2009) and regional climatic variations based on mineralogical investigations (Hendriks et al., 1990; Strouhal, 1993; Bolle et al., 2000; Bolle and Adatte, 2001; Ernst et al., 2006).

The main objective of this paper is the reconstruction of the Egyptian Tethyan shelf during the Early Palaeogene global greenhouse period (Zachos et al., 2001), focusing on the impact of Early Eocene carbon isotope perturbations on tropical carbonate platform development, as well as on causes and consequences of enhanced nutrient discharge and the local tectonic activity at the southern Tethyan shelf. We created a new palaeogeographic model, which re-evaluates the function of the Syrian Arc-Fold Belt (SAFB) regarding the increasing restriction of the Egyptian Tethyan shelf in the Early Palaeogene (Speijer and Wagner, 2002; Scheibner et al., 2003).

Previous studies dealing with the environmental response of post-PETM carbon isotope perturbations mainly focus on deep-sea environments (Lourens et al., 2005; Nicolo et al., 2007; Stap et al., 2009), whereas shallow-marine shelf areas and carbonate platform systems are still underrepresented in the geological record. The Upper Paleocene to late Early Eocene succession of the Galala Mountains (Eastern Desert, Egypt) provides new data for the geochemical and environmental evolution on a tectonically controlled isolated carbonate platform at the marginal southern Tethys. We link and compare our results with previous studies on Eocene hyperthermals, focussing on larger benthic foraminifera and on other benthic organisms.

VII.1.1 Early Palaeogene climate and carbon cycle perturbations

The early Cenozoic is known as a period in Earth's history which underwent repeated changes with respect to global climate variations. During the Middle Paleocene to the Early Eocene continuing global warming culminated in the Early Eocene Climatic Optimum (EECO, ~ 53 – 48 Ma) with the highest temperatures in the Cenozoic (Tripati et al., 2003; Zachos et al., 2008; Fig. VII.1). This global warming trend is superimposed by transient temperature perturbations (hyperthermals; Thomas and Zachos, 2000). The most prominent hyperthermal event is the Paleocene-Eocene Thermal Maximum (PETM; also Eocene Thermal Maximum 1, ETM1, ~ 55.5 Ma; Kennett and Stott, 1991; Zachos et al., 1993), which is a brief period (~170 k.y.) with a severe impact on many environments on Earth (Fig. VII.1). The PETM resulted in a transient rise in global temperature of 5°C (Zachos et al., 1993, 2003; Tripati and Elderfield, 2005) and enhanced continental runoff due to the major reorganization of the global hydrologic cycle (Ravizza et al., 2001; Zachos et al., 2006; Giusberti et al., 2007; Nicolo et al., 2007). Major biotic turnovers were recognized (i) in the deep sea (Benthic Extinction Event; Kaiho, 1991; Thomas and Shackleton, 1996), (ii) in shallow-marine realms (Larger Foraminifera Turnover; Orue-Etxebarria et al., 2001; Scheibner et al., 2005), (iii) at the sea surface (nannoplankton turnover and poleward migration of subtropical plankton: Kelly et al., 1996; Monechi et al., 2000; Gibbs et al., 2006); and (iv) in terrestrial environments (dispersal of mammals: Gingerich, 1989, 2003, 2006; expansion of vegetation: Beerling, 2000; Wing et al., 2005; Sluijs et al., 2006, 2009). The PETM is associated with a prominent negative carbon isotope excursion (CIE) of ~4 ‰ (Kennett and Stott, 1991), which reflects a massive input of $\delta^{13}C$-depleted carbon in the atmosphere (Fig. VII.1). Sources and processes responsable for this carbon injection are highly debated (Katz et al., 2001; Higgins and Schrag, 2006; Pagani et al., 2006; Sluijs et al., 2007). Various authors attribute the CIE of the PETM to methane hydrate degassing from sediments on the continental slope (Dickens et al., 1995, 1997; Bains et al., 1999). Alternative theories discuss the global conflagration of peatlands (Kurtz et al., 2003) or massive volcanism and gas expulsion in the North Atlantic (Storey et al., 2007).

The PETM is not a single hyperthermal event (Thomas and Zachos, 2000; Cramer et al., 2003). At least two other prominent hyperthermal events can be identified in the Early Eocene: (a) Two million years after the PETM another global CIE at 53.6 Ma is attributed to the Eocene Thermal Maximum 2 (ETM2, H1 or Elmo; Cramer et al., 2003; Lourens et al., 2005). Its characteristics are similar to those of the PETM but with a smaller magnitude (Fig. VII.1). A negative CIE between 0.4 ‰ and 2.5 ‰ is observed in deep-marine and marginal settings (Cramer et al., 2003: Lourens et al., 2005; Nicolo et al., 2007; Stap et al., 2009; Agnini et al., 2009). A global sea-surface temperature rise of 3-5 °C (Lourens et al., 2005; Nicolo et al., 2007; Sluijs et al., 2009) and a bottom-water temperature rise of 2-3 °C

(Kroon et al., 2007) are associated with warm and humid conditions at high latitudes (Sluijs et al., 2009) and enhanced continental runoff (Nicolo et al., 2007; Sluijs et al., 2009). Deep-water benthic foraminifera show a low diversity (Lourens et al., 2005); calcareous nannoplankton assemblages indicate enhanced nutrient availability (Raffi and De Bernardi, 2008). Recent studies have shown that the timing of the ETM2 coincides with the initial collision of Asia and India (Clementz et al., 2011).

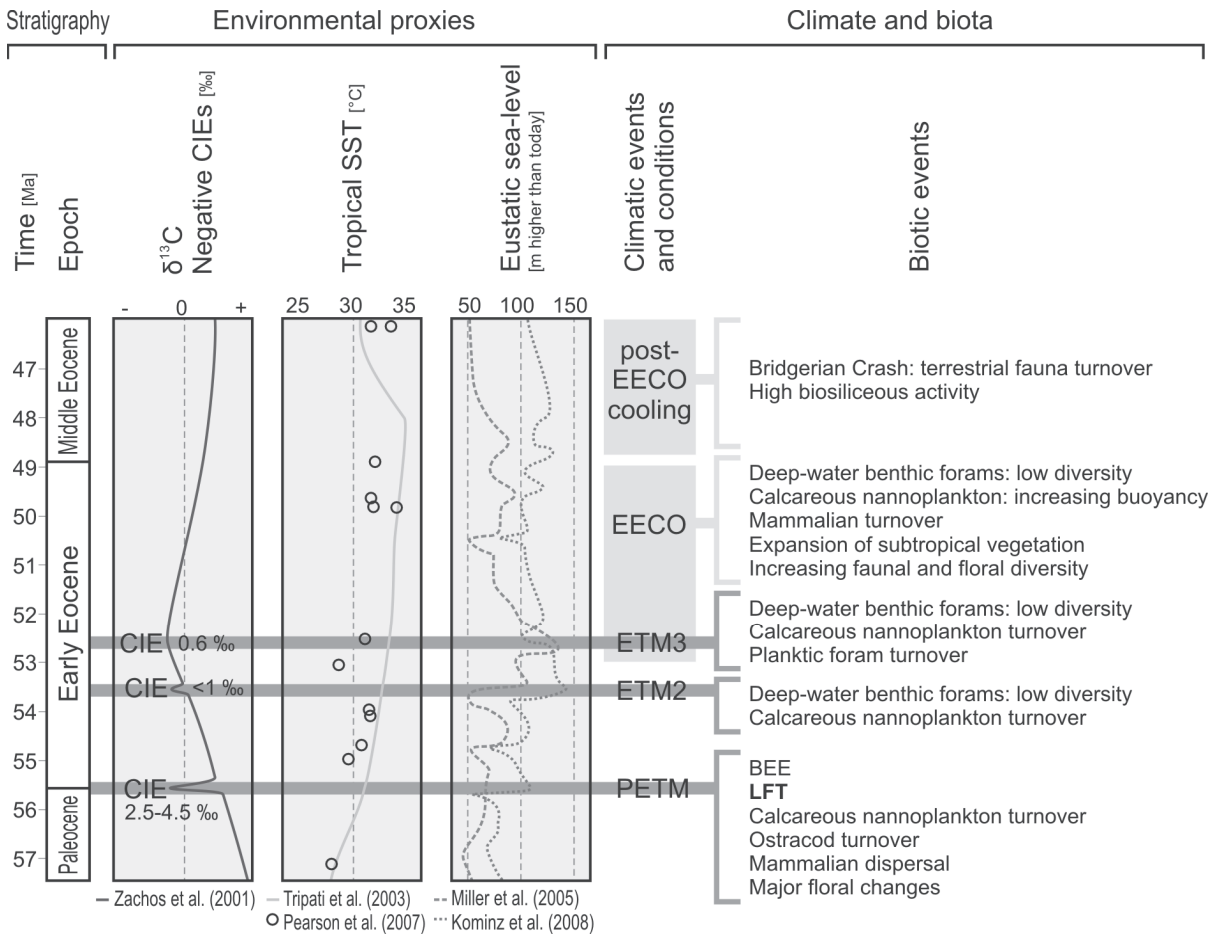

Figure VII.1 – Overview of the environmental changes during the latest Paleocene to early Middle Eocene (global carbon isotope evolution, tropical sea-surface temperatures, major climatic conditions and biotic events in terrestrial, shallow- and deep-marine environments). References to the associated biotic events are given in chapter 1.1. Abbreviations: CIE – carbon isotope excursion, SST – sea surface temperature, EECO – Early Eocene Climatic Optimum, ETM – Eocene Thermal Maximum, BEE – Benthic Extinction Event; LFT – Larger Foraminifera Turnover.

(b) The ETM3, K- or x-event at 52.5 Ma represents the third global hyperthermal event (Fig. VII.1). It shows a significantly smaller negative CIE (0.6 ‰ – 0.9 ‰) compared to the PETM and ETM2 (Cramer et al., 2003; Röhl et al., 2005). Deep-marine benthic foraminifera demonstrate a low diversity during the event; calcareous nannoplankton and planktic foraminifera show a turnover towards warmer and more eutrophic species (Röhl et al., 2005; Agnini et al., 2009).

CIEs with smaller magnitude (H2 at 53.5 Ma, I1 at 52.8 Ma and J at 52.3 Ma; according to Cramer et al., 2003) probably do not reflect hyperthermal events and only cause minor environmental perturbations. The latest recognized hyperthermal event was described at the marginal northern Tethys at around 45 Ma (NP15) by Ortiz et al. (2008). All periodic reoccurrences of negative CIEs are explained by orbital forcing (Lourens et al., 2005; Westerhold et al., 2007; Galeotti et al., 2010).

VII.1.2 The southern Tethyan shelf in the Early Palaeogene

In the Palaeogene, the Egyptian marginal Tethys consists of two major tectono-sedimentary environments, the unstable shelf and the stable shelf (Said, 1990; Fig. VII.2). The tectonically controlled unstable shelf traced the course of the SAFB, which formed a complex ENE-WSW striking framework of horst and graben structures, related to multiple intervals of uplift movements (Salem, 1976; Bowen and Jux, 1987; Shahar, 1994; Moustafa and Khalil, 1995; Hussein and Abd-Allah, 2001; Youssef, 2003). Deposits related to the unstable shelf are characterized by a heterogeneous assemblage of hemipelagic marls, platform limestones and siliciclastics (Salem, 1976). Uplift along the SAFB in the Early Palaeogene resulted in shallow palaeo-waterdepths < 100 m in the elongated basins and temporary subaerial exposure at the ridges (Fig. VII.2). The tectonically unaffected stable shelf south of the SAFB forms the Eastern Desert Intra-Shelf Basin (EDIB) with palaeo-waterdepths up to 600 m (Speijer and Wagner, 2002). Deposits of the EDIB are dominated by hemipelagic marls and chalks with minor terrestrial influence. The northern part of the EDIB is represented by the Southern Galala Subbasin (Kuss et al., 2000), which is probably still affected by Syrian Arc-related tectonism.

In the Early Palaeogene the Galala Mountains represent a mixed siliciclastic carbonate platform, which was situated at the unstable shelf, approximately 800 km north of the African craton (Fig. VII.2). Platform evolution is strongly controlled by the Early Eocene uplift along the SAFB, resulting in different tectono-sedimentary platform stages (Scheibner et al., 2003; Scheibner and Speijer, 2008; Höntzsch et al., 2011). The Eocene succession of the Galala Mountains is dominated by photo-autotrophic organisms, indicative for low-latitude environments with warm and arid conditions (Schlager, 2003; Mutti and Hallock, 2003; Höntzsch et al., 2011). The shallow-marine fauna is dominated by larger benthic foraminifera (LBF), co-occurring with other benthic biota (green algae, coralline red algae). Dominant species are represented by hyaline-walled rotaliids (nummulitids) and larger porcellaneous miliolids (alveolinids; Höntzsch et al., 2011).

VII.1.3 Study area

Today the study area is located about 100 km south of Suez in the Eastern Desert of Egypt (Fig. VII.3). The mountain range consists of two plateaus (N- and S-Galala Plateau) that are separated by the ENE-WSW striking Wadi Araba valley (Fig. VII.3). The northern margin of the Southern Galala Plateau reflects the ENE-WSW striking monocline of the Wadi Araba Fault, representing the SW branch of the SAFB (Fig. VII.2).

We studied eight sections in five areas along a N-S-striking inner ramp- to basin transect (Fig. VII.3). Inner ramp outcrops are only accessible at the Northern Galala Plateau (area 1 – Wadi Waida). Mid- to outer ramp environments are exposed in the Southern Galala Plateau (areas 2 – Wadi Ashkar, area 3 – Wadi B, area 4 – Bir Dakhl). The succession of area 5 (Wadi Tarfa) represents deposits of the lower outer ramp and the basin. The studied sections cover the latest Paleocene to the uppermost Early Eocene (Fig. VII.4). In the basin and at the outer ramp (area 5), the Upper Paleocene to lowermost Eocene is represented by hemipelagic marls and limestones of the Esna Formation (NP8 – NP12), which are followed by the chert-rich chalky marls of the Thebes Formation (NP12 – ?NP14a). At the middle ramp (areas 2, 3 and 4) the Thebes Formation interfingers with shallow-marine deposits of the Southern Galala Formation (NP6 – NP12). Area 1 represents the shallowest inner ramp environment of the Northern Galala Plateau. Detailed studies with respect to Early Palaeogene microfacies analyses and ramp evolution are documented by Scheibner et al. (2001, 2003), Scheibner and Speijer (2009) and Höntzsch et al. (2011).

Area 1 is characterized by various deeply incised Wadi valleys, situated 15 km SE of Ain Sukhna (Fig. VII.3). The studied succession (section 1) consists of alternating limestone and dolostone beds (Figs. VII.5 and VII.7). Limestones contain high amounts of LBF, *Nummulites* and *Alveolina*, as well as green algae, gastropods and smaller miliolids. Accumulations of larger alveolinids and nummulitids are interpreted as foraminiferal shoals, whereas limestones with smaller bioclasts point to inner ramp deposits (Scheibner et al., 2003; Höntzsch et al., 2011). The dolostones of area 1 are arranged in coarsening upward cycles of dolomitized fossiliferous limestones and conglomeratic dolostones with birdseyes and fenestral fabric, which were interpreted as tidal flat deposits.

Area 2 (section 2) and area 3 (section 3) are represented by deeply incised valleys, which run perpendicular to the WSW-ENE striking northern escarpment of the Southern Galala Plateau (Fig. VII.3). The Palaeogene successions of both areas contain highly fossiliferous quartz-rich limestones and sandstones with subordinated conglomerates, dolostones and marls (Figs. VII.5 and VII.7). Limestones are either peloidal wacke- to packstones with smaller biodetritus, green algae and miliolids or LBF-bearing wacke- to floatstones. Areas 2 and 3 are attributed to upper middle ramp environments with frequent proximal turbidites and debris flows (Scheibner et al., 2001, 2003; Höntzsch et al., 2011).

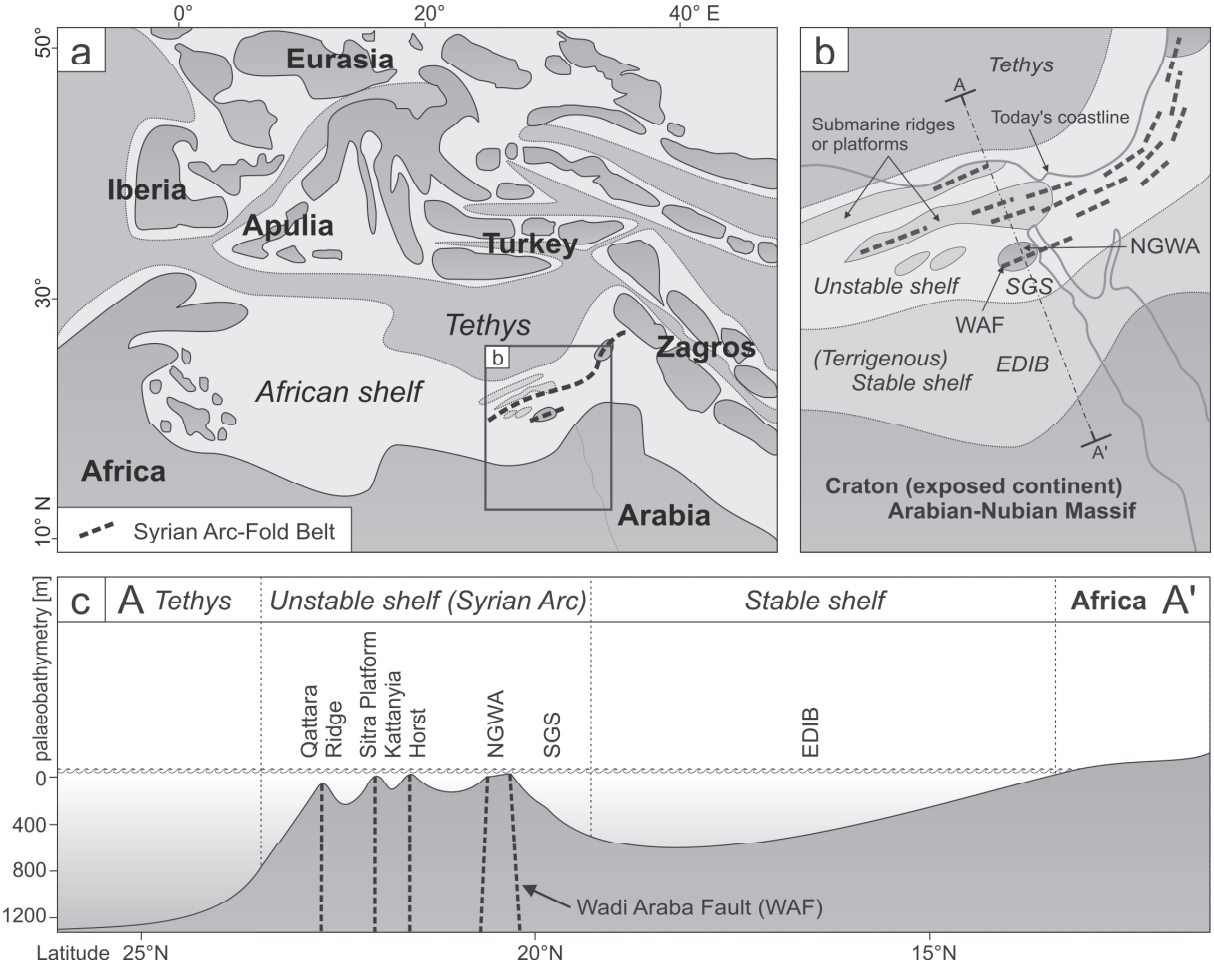

Figure VII.2 a – Palaeogeography of the western Tethys in the Early Eocene, including the main terranes, cratons and shelf areas (adapted and expanded from Blakey, http://www.jan.ucc.nau.edu/ ~rcb7/ eocenemed.jpg). The dashed line indicates the course of the SAFB according to Shahar (1994). **VII.2 b** - Simplified map of the Early Eocene southern Tethys margin of Egypt showing the location of the Northern Galala/Wadi Araba High (NGWA), the Southern Galala Subbasin (SGS) and the Eastern Desert Intra-Shelf Basin (EDIB, Kuss et al., 2000). The Southern Galala Subbasin represents the northern part of the EDIB which is distally influenced by Syrian Arc activity. The Wadi Araba Fault (WAF) forms the SW part of the SAFB (dashed lines). Submarine swells and plateaus are added according to Salem (1976), Said (1990) and Schütz (1994). The position of stable and unstable shelf was estimated by Meshref (1990) and was modified for the Early Palaeogene by Scheibner et al. (2001) and Speijer and Wagner (2002). A simplified cross section AA' is plotted in figure **VII.2 c**.

Area 4 is situated at the SE escarpment of the Southern Galala Plateau (Fig. VII.3, Bir Dakhl). Sections 4a and 4c are represented by steep valleys, which directly cut into the escarpment of the plateau. Sections 4b and 4d are rather outcrops at erosional hills. Deposits of area 4 (sections 4a, 4b, 4c and 4d) are represented by prevailing marls and marly limestones with intercalations of thin sandstone and quartz-rich limestone beds. Marls are occasionally slumped and become chert-bearing and chalkier towards the top of the succession. Limestone and sandstone intercalations contain bioclasts of varying size and origin and are interpreted as intermediate to distal turbidites at the middle ramp (Scheibner et al., 2003; Höntzsch et al., 2011). Trace fossils (*Zoophycos* sp.) prior to the Paleocene-

Eocene boundary suggest a palaeowater-depth of about 300 m (Seilacher, 1967; Everts, 1991).

Area 5 (Fig. VII.3, Wadi Tarfa) is situated at the SW branch of the Southern Galala Plateau. The studied section 5 is dominated by a monotonous succession of hemipelagic marls at the base and chert-bearing chalky marls with no limestone or sandstone intercalations at the top (Figs. VII.5 and VII.7). Prevailing organisms are planktic foraminifera and radiolaria, which indicate an outer ramp to basin environment.

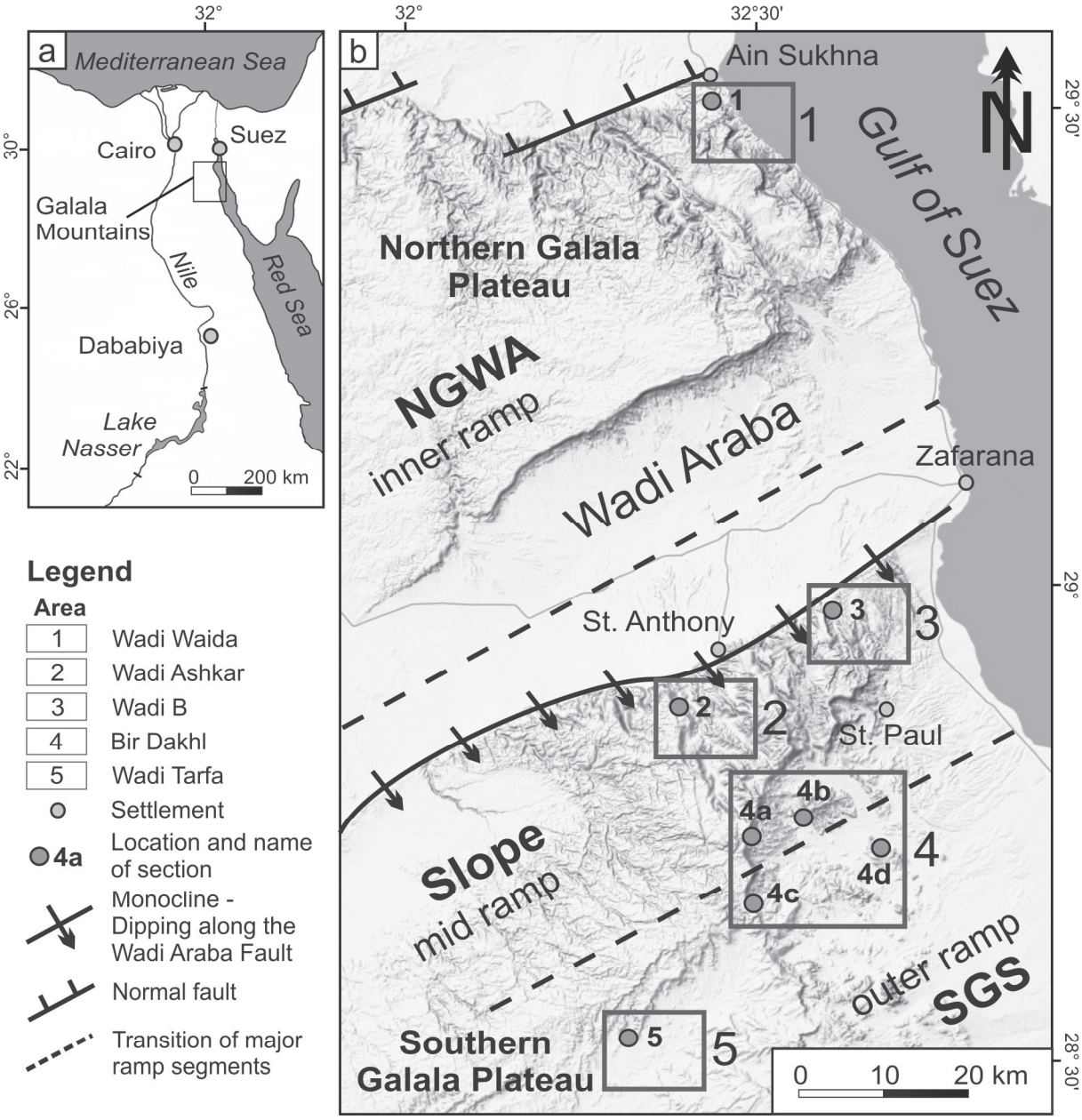

Figure VII.3 a – Simplified map of Egypt; the working area is marked by a rectangle. **VII.3 b** – Detailed map of the Galala Mountains with location of the sections, tectono-topographic features as well as the general ramp geometry of the carbonate platform (modified after Scheibner et al., 2001 and Höntzsch et al., 2011). Tectonic elements are added according to Moustafa and El-Rey (1993), Schütz (1994) and Moustafa and Khalil (1995).

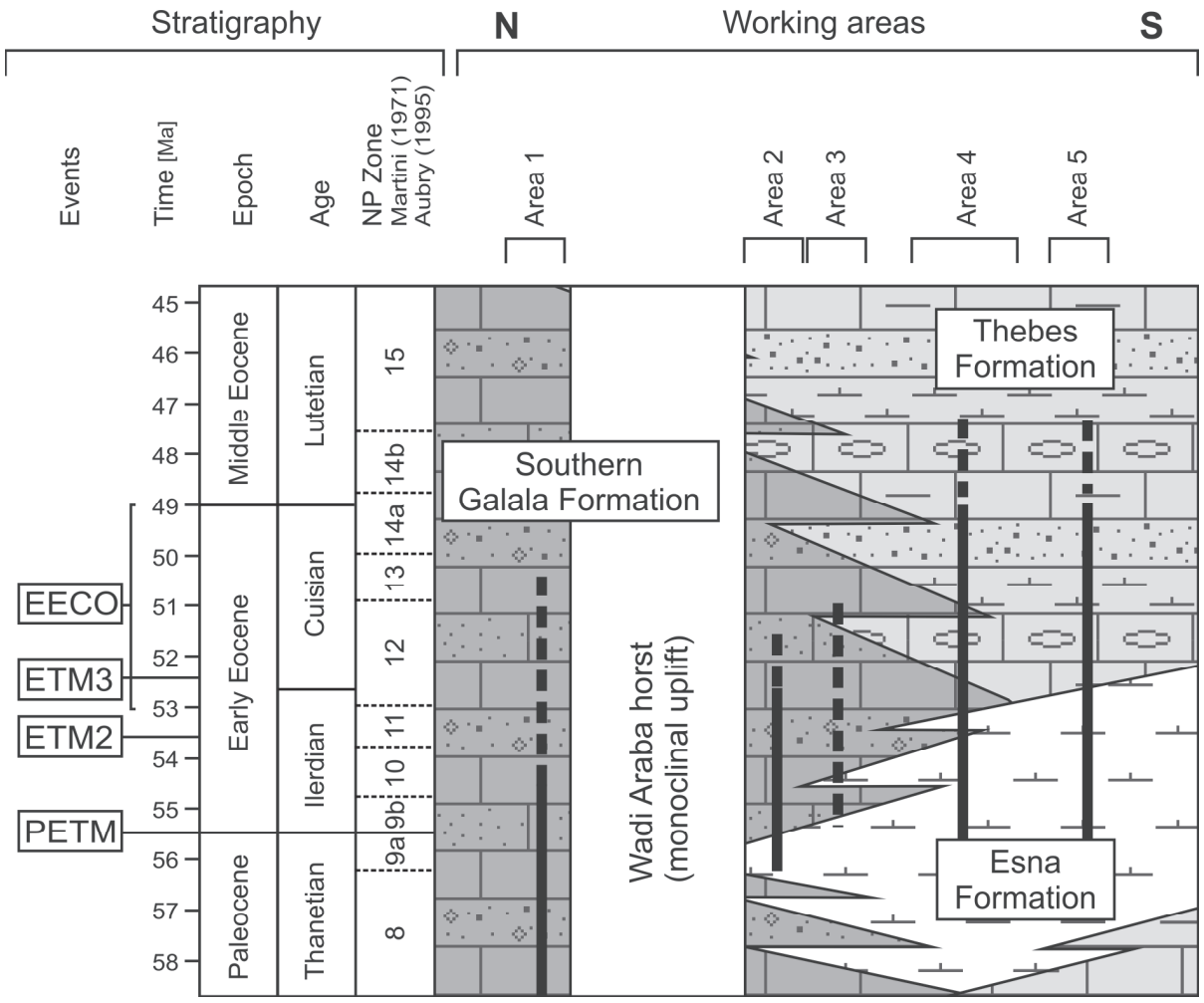

Figure VII.4 – Lithostratigraphy and biostratigraphy of the Palaeogene formations in the Galala Mountains along an S-N transect (modified after Höntzsch et al., 2011). The working areas (1-5) refer to figure VII.3 b. The vertical bold lines illustrate the stratigraphic range of the recorded sections. Dashed lines indicate an uncertain range.

VII.2 Methods

VII.2.1 Geochemical analyses

For this study, we present an integrated analysis of bulk rock carbon isotopes, weight percent of $CaCO_3$ and the long-term evolution of larger benthic foraminifera and other shallow-marine benthos.

Samples were prepared for thin section analysis as well as for geochemical and isotope investigations (sample weight 200 g to 400 g). Bulk rock total carbon (C_{total}) and total organic carbon (C_{TOC}) are determined with a Leco CS-300 analyzer at the University of Bremen (precision of measurement ±3 %). The bulk rock carbonate content is expressed in the formula $CaCO_3$ [%] = [(C_{total} – C_{TOC}) x 8.33]. Bulk rock carbon isotopes are determined with a Finnigan MAT 251 mass spectrometer at Marum, Bremen (Germany).

The recorded proxies show minor and major fluctuations, which result from global carbon cycle perturbations on the one hand, and from tectonically induced regional to local carbon contamination on the other hand. The challenge of this study is the impact of syndepositional tectonic activity along the SAFB, which caused the massive uplift and redeposition of Mesozoic and Palaeozoic siliciclastic material at the slope (Kuss et al., 2000; Scheibner et al., 2003; Höntzsch et al., 2011). To minimize the error of siliciclastic carbon contamination, we exclude bulk rock $\delta^{13}C$ values from samples, which exceed 20 weight percent (wt. %) of quartz. Marls and limestones with less than 20 wt. % of quartz do not show a significant deviation in the carbon isotope signature to adjacent quartz-free samples. Recrystallized planktic foraminifera in section 5 indicate a diagenetic overprint of the samples, which excludes the use of oxygen isotope data. In contrast to oxygen isotopes, stable carbon isotopes are less prone to alteration during diagenesis (Veizer, 1983; Marshall, 1992).

VII.2.2 Organisms as environmental indicators

Organisms of carbonate platforms record multiple geochemical signals depending on local and regional environmental conditions. LBF taxa are adapted to varying energetic, trophic and light conditions (Hallock, 1985, 1999; Hallock and Glenn, 1986; Beavington-Penney and Racey, 2004). The knowledge of the biology and the controlling factors of modern LBF helps to understand the environmental conditions of ancient forms. The distribution of LBF along the platform allows to estimate the palaeobathymetry and light conditions at the ramp. Gradual or abrupt changes in the prevailing LBF assemblages of a section help to recognize relative sea-level changes or depositional unconformities. Other biota reveal shifts in the trophic regime at the platform (e.g., corals, benthic green algae and gastropods; Wilson, 1975; Schlager, 1981; Hallock and Schlager, 1986; Leinfelder, 1994, 1997; Vecsei, 2003).

VII.3 Results

VII.3.1 Biostratigraphy

Highly varying lithologies in the studied sections require the application of several biostratigraphic concepts, regarding the prevailing fossil content. The marly sections of areas 4 and 5 are stratigraphically classified with the help of calcareous nannonplankton. Due to a decreasing preservation of calcareous nannoplankton towards the upper Lower Eocene and a general high diagenetic overprint of the studied rocks, planktic foraminifera are used to support the biostratigraphic framework in area 5. Sections of the inner and upper mid ramp

(areas 1, 2 and 3) are classified with the help of LBF (*Alveolina*), due to a lack of useable calcareous nannoplankton or missing marly intervals.

Calcareous nannoplankton

Biostratigraphy using calcareous nannoplankton follows the classification of Martini (1971), Aubry (1995) and Aubry (2000). 360 marl samples of sections 4a, 4b, 4c, 4d and 5 were prepared on standard smear slides for qualitative and semi-quantitative estimation of nannoplankton species, including their general abundance and preservation. The abundance of suitable specimen varies from rare (< 1 %) to very abundant (> 20 %). The preservation is generally good to moderate; some assemblages within carbonate depleted clay-rich units show a bad preservation and probably suffered dissolution. The extraction of useable specimen from the upper Lower Eocene chalky marls of sections 4a and 5 was difficult, due to a higher hardness of the rocks. The studied sections range from NP9 to NP14a (Fig. VII.4).

NP9: The occurrence of *Discoaster multiradiatus* in the lowermost parts of the studied sections indicates NP9 of Martini (1971). The thickness of NP9 ranges from 1 m (section 4d) to more than 10 m (section 4b). A discrimination of NP9a (Paleocene) and NP9b (Eocene) is possible with the help of the negative CIE of the PETM, which represents the boundary between both intervals (Aubry et al., 1996).

NP10: The subsequent nannofossil zone NP10 is defined by the first occurrence of *Tribrachiatus bramlettei* and ranges to the last occurrence of *T. contortus*. The thickness of the NP10 zone covers between 10 m and 20 m in the studied sections. A threefold subdivision of NP10 into NP10a, NP10b and NP10d, based on the distribution of species of the *Tribrachiatus* lineage (Aubry, 1995) was applied to the sections 4c and 4d.

NP11: The interval between the last occurrence of *T. contortus* and the presence of *D .lodoensis* defines NP11, which shows strongly varying thicknesses between 2 m (section 4c) and 18 m (section 4a). In section 4c the presence of multiple sandstone beds and the conjugated first occurrence of several nannofossil species within the sample, which define the onset of NP11 (*Ellipsolithus distichus*, *Sphenolithus moriformis*, *Discoaster deflandrei*, *Pontospaera multipora*), suggest a major hiatus prior to NP11.

NP12/13: The first occurrence of *D. lodoensis* marks the onset of NP12. The transition between NP12 and NP13 is represented by the last occurrence of *T. orthostylus*. However, *T. orthostylus* is still present in the nannofossil record of our sections, when the first occurrence of *D. sublodoensis* marks the onset of NP14a. Consequently, NP12 and NP13 are plotted as conjugated intervals in all studied sections. The thickness of both conjugated intervals ranges from 5 m (section 4d) to more than 20 m (section 4a).

NP14a: NP14 can be subdivided into two subzones: NP14a (*Discoasteroides kuepperi* zone) represents the uppermost Lower Eocene and is defined as the zone between the first occurrence of *D. sublodoensis* to the first occurrence of *Rhabdosphaera inflata*. NP14b representing the uppermost Lower Eocene and the lowermost Middle Eocene is defined by the occurrence of *Rhabdosphaera inflata* (Valentine, 1987; Aubry, 1991). The subdivision of NP14 can not be applied to the studied sections due to the absence of marker species *Rhabdosphaera inflata*. Thus, the base of the Lutetian (Middle Eocene) within lower NP14b is not recognized in the studied sections. Generally, NP14a is vertically expanded in all studied section with maximum thickness of more than 130 m in section 4a.

Alveolinids

Upper mid- and inner ramp deposits are dominated by bioclast-rich limestones and sandstones. Marl units, which provide sufficient material for nannoplankton analyses are rare. Thus, LBF are used for a detailed biostratigraphic classification of shallow-marine carbonate platform environments (Hottinger, 1960, 1974; Hottinger and Schaub, 1960).

A standardized classification was achieved with the help of the Tethyan Paleocene-Eocene Shallow Benthic Zonation (SBZ) of Serra-Kiel et al. (1998).

We studied 92 alveolinid-bearing samples in sections 1, 2, 3, 4a and 4b. Multiple erosional and tectonic unconformities as well as expanded intervals without suitable *Alveolina* specimen hamper a detailed biostratigraphic classification in all studied sections. Despite those limitations, a clear shift of alveolinid taxa is present between SBZ4 (~ NP9a) and SBZ5 (NP9b).

SBZ4/5: SBZ5 reflects the first appearance of true *Alveolina* species, whereas SBZ4 is still dominated by Paleocene glomalveolinids. This transition demonstrates the Larger Foraminifera Turnover (Hottinger, 1960; Orue-Extebarria et al., 2001) and coincides with the Paleocene-Eocene boundary (Scheibner et al., 2005). In section 3 this foraminiferal shift is supported by the negative CIE of the PETM. First recorded Eocene alveolinid is *Alveolina aramea aramea* (SBZ5, *A. cucumiformis* biozone).

SBZ6: SBZ6 (*A. ellipsoidalis* biozone, upper NP9) is represented by *A. pasticillata* and *A. ellipsoidalis* (sections 2 and 3) and *A. pasticilata* (section 1).

SBZ7/8: The subsequent SBZ7 (top NP9 – NP10c) was discriminated with the help of *A. moussoulensis*, *A. cucumiformis tumida* and *A. globosa* (section 3) as well as *A. decipiens* (section 1). Despite that the upper interval of section 2 comprises *A. decipiens* and *A. aragonensis* reflecting SBZ7 or SBZ8, a biostratigraphic classification of deposits beyond SBZ7/8 was not possible.

Planktic foraminifera

Planktic foraminifera biostratigraphy was performed on 16 samples collected in the upper interval of section 5. Samples are generally rich in planktic foraminifera, however well preserved specimen are only present in the lower part of section 5. In the upper interval of the section planktic foraminifera are characterized by a chalky preservation and strong recrystallization of secondary calcite.

The Early Eocene biozonation scheme is mainly characterized by the occurrences of *Morozovella* (Berggren et al., 1995; Berggren and Pearson, 2005). Morozovellids are generally absent in section 5. The lowermost interval contains rare questionable planktic foraminifera species, preventing the application of a biostratigraphic classification. However, a tentative assignment is suggested based on the general planktic foraminifera assemblages. In the lower part of the studied interval, the assemblage is mainly dominated by *Acarinina* associated with rare *Igorina*, *Subbotina* and only occasional *Globanomalina*. The presence of different species of *Acarinina*, such as *A. soldadoensis*, *A. coaligensis*, *A. esnaensis*, *A. angulosa* and *A. hornibrooki* suggests that this interval is assigned to Zones P6-P8 (Berggren et al., 1995), which corresponds to NP10 – NP12 (Martini, 1971). A possible presence of *Acarinina pentacamerata* 55.8 m above the Paleocene-Eocene boundary might indicate a zone not older than Zone P7 (Fig. VII.7; uppermost NP10 – lower NP12).

The occurrence of *Acarinina aspensis* 63.55 m above the Paleocene-Eocene boundary could indicate the presence of Zone P9 (Fig. VII.7; Berggren et al., 1995), which corresponds to NP13 – NP14a. The presence of Zone P9 68.10 m above the Paleocene-Eocene boundary is also confirmed with the occurrence of *Pseudohastigerina micra*. Samples in the uppermost interval of section 5 are very poorly preserved, preventing the recognition of any biozones.

VII.3.2 Bulk rock geochemistry of the lower Palaeogene Galala succession

Carbon isotope stratigraphy

Four of the six studied sections show clear trends regarding their long-term carbon isotope signature in the Early Palaeogene (sections 4a, 4b, 4c and 4d; Fig. VII.7). The latest Paleocene (NP9a) is represented by a rapid and constant shift from a $\delta^{13}C$ enriched to a $\delta^{13}C$ depleted signature. This trend culminates in a transient carbon isotope excursion (CIE) which refers to the PETM at the NP9a/NP9b boundary. The CIE of the PETM varies significantly in individual sections between 1.7 ‰ (section 4a) and 3.81 ‰ (section 4b) (Tab. VI.2). The absence of a major negative CIE indicating the PETM in the basinal section 5 remains enigmatic, despite that biostratigraphy and a significant 7 cm thick dark brown clay

layer with enriched organic carbon amounts strongly suggest the occurrence of the PETM horizon.

The post-PETM carbon isotope evolution is reflected by an increasing depletion in $\delta^{13}C$ from NP9b to NP13/14. Average $\delta^{13}C$ ratios range from +1 ‰ to -1 ‰. Some intervals within section 5 (NP14a) and section 3 (NP11/12) demonstrate depleted $\delta^{13}C$ ratios up to -3 ‰ over 20 m to 30 m. The general trend of the carbon isotope signature within NP14a is not clearly reconstructable due to highly fluctuating $\delta^{13}C$ ratios. However, sections 4a, 4b, 4d and 5 indicate a slight shift towards a $\delta^{13}C$ enriched signature (Fig. VII.7).

The long-term $\delta^{13}C$ trend in the Early Eocene is superimposed by multiple transient post-PETM CIEs which are summarized in table 1. At the basis of NP11 a CIE of 1.51 ‰ (section 4a) reflects the ETM2 or Elmo-horizon. Within NP12 a CIE of 1.6 ‰ (sections 4a, 4c) indicates the ETM3 or x-event. We do not correlate further negative CIEs beyond ETM3 with those described by Cramer et al. (2003), because of their small magnitudes and a supposed high background noise in the carbon isotope ratios at the Egyptian shelf. Solely section 4a demonstrates another transient CIE within NP11, which correlates with the I1-event (Cramer et al., 2003). The sections 4a, 4c, 4d and 5 show significant fluctuations with several negative CIEs within NP14a. Those fluctuations are probably not explained by hyperthermals, rather than higher carbon fluxes at the marginal shelf. Generally, the magnitudes of hyperthermal-related CIEs of the Galala succession decrease from the upper mid-ramp to the basin significantly.

Calcium Carbonate

Calcium carbonate content of the studied rocks shows high fluctuations in the Early Eocene, which is related to intensive siliciclastic dilution during Wadi Araba uplift and the redeposition of Mesozoic and Palaeozoic sandstones (Kuss et al., 2000; Scheibner et al., 2001; Höntzsch et al., 2011). Mixed siliciclastic-carbonate deposition with strongly depleted calcium carbonate ratios between NP9 and NP14a shifted to pure carbonate deposition during NP14a, when the activity of Syrian Arc tectonic processes decreases significantly (Moustafa and Khalil, 1995; Hussein and Abd-Allah, 2001; Höntzsch et al., 2011). However, beds which are supposed to reflect hyperthermals with a significant negative CIE show major transient shifts towards depleted calcium carbonate (Fig. VII.6). Calcium carbonate depletion ranges from 20 % (sections 4b and 5) to more than 75 % (section 4c) for the PETM. The ETM2 interval is associated with calcium carbonate depletion up to 23 % (section 4a); the ETM3 interval up to 85 % (section 4a). However, we cannot confirm a clear correlation of calcium carbonate depletion to hyperthermal events due to multiple siliciclastic dilution horizons.

Table VII.3 – Comparison of the recorded CIE of major presumed Palaeogene hyperthermal events. The strongly varying thicknesses between the individual events indicate major unconformities in the depositional sequence of the ramp. Section 2 and 3 are not considered in detail in the interpretation, due to doubtful biostratigraphic classification and assumed diagenetic alteration.

Section	Negative CIE of recorded hyperthermals				Height above PETM-CIE		
	PETM [‰]	ETM2 [‰]	I1 [‰]	ETM3 [‰]	ETM2 [cm]	I1 [cm]	ETM3 [cm]
2a	-	? 1.4	-	? 2,7	-	-	-
3a	3.3	? 2.4	-	? 3.0	2520	-	11410
4a	1.7	1.5	1.0	1.6	1435	1975	3210
4b	3.8	0.9	-	0.9	1635	-	2605
4c	2.1	0.7	-	> 1.6	1695	-	2440
4d	2.1	1.0	-	1.5	1910	-	3930
5a	0.4	0.9	-	0.9	880	-	1690

Total organic carbon (TOC)

Total organic carbon ratios of bulk rock samples range from 0.05 % to 0.1 % in average in all studied sections (Fig. VII.6). TOC enriched intervals are attributed to negative CIEs and calcium carbonate depletion and are well visible in section 4a for the PETM (TOC_{PETM} = 0.54 %) and for the ETM3 (TOC_{ETM3} = 0.53 %). The ETM3 horizon shows enriched TOC-values in section 5 (TOC_{ETM3} = 0.26 %) and in section 4c (TOC_{ETM3} = 0.41 %). In section 4c multiple TOC-peaks within NP14a are associated to minor negative CIEs and calcium carbonate depletion. A relation of those peaks to hyperthermal events is not evident.

VII.3.3 Regional environmental and biotic conditions at the Galala platform

The Early Palaeogene evolution of the Galala carbonate platform is strongly influenced and controlled by syndepositional tectonic activity along the Wadi Araba Fault. From the PETM (NP9a/b) to the latest Early Eocene (NP14a), three tectono-sedimentary platform stages were classified and discussed by Scheibner et al. (2003) and Höntzsch et al. (2011). A generalized view on lithofacies and calculated sedimentation rates indicate multiple erosional unconformities between NP9 and NP14a (Tab. VII.3). The termination of the Syrian Arc-related tectonic activity of the Wadi Araba Fault within NP14a is reflected by the absence of siliciclastics and by average sedimentation rates at the mid ramp (Figs. VII.6 and VII.7). The classification of 13 facies types along an Early Palaeogene inner to outer ramp transect yielded detailed information regarding environmental and biotic conditions of the platform system (Scheibner et al., 2001, 2005; Scheibner and Speijer, 2009; Höntzsch et al., 2011).

The shallow-marine inner ramp is dominated by photo-autotrophic larger benthic foraminifera (nummulitids, alveolinids and soritids), smaller benthic foraminifera (miliolids) and benthic green algae (Figs. VII.5 and VII.6). Typical low-latitude nutrient-depleted assemblages, which are dominated by corals, are absent. Other major taxa are heterotrophic gastropods, serpulid worm tubes and minor red algae.

At the mid ramp, shallow-marine inner ramp organisms can be found in repeated turbidites and debris flows (areas 2, 3 and 4). Individual turbidite beds accumulate in four major intervals, which are related to massive uplift along the Wadi Araba Fault (Fig. VII.6). In those intervals, taxa from adjacent environments of different depth and energetic regimes are frequently mixed. Turbidites are dominated by LBF, planktic foraminifera and smaller benthos from the platform.

At the PETM (NP9a/b boundary) a major shift in the LBF assemblages is recorded in all studied mid ramp sections. Paleocene ranikothalids, miscellanids and glomalveolinids are replaced by Eocene nummulitids and alveolinids, which are characterized by significant larger shell sizes and adult dimorphism (Larger Foraminifera Turnover). An interval with mixed Paleocene and Eocene LBF in section 4a is probably related to the sea-level or tectonically-controlled erosion and redeposition of Paleocene turbidites (Fig. VII.6).

Planktic organisms are more frequent in outer ramp to basin sections and are dominated by planktic foraminifera, calcareous nannoplankton and radiolaria. Accumulations of these organisms can be found in calciturbidite sequences and chert-bearing chalky marls of area 4 and 5. The occurrence of radiolaria increased from the marls of the earliest Eocene to the chalky marls of the late Early Eocene (Fig. VII.6). Planktic foraminifera assemblages within the chalky marls of section 5 indicate missing *Morozovella* species throughout the middle Lower Eocene (NP12 – NP14a).

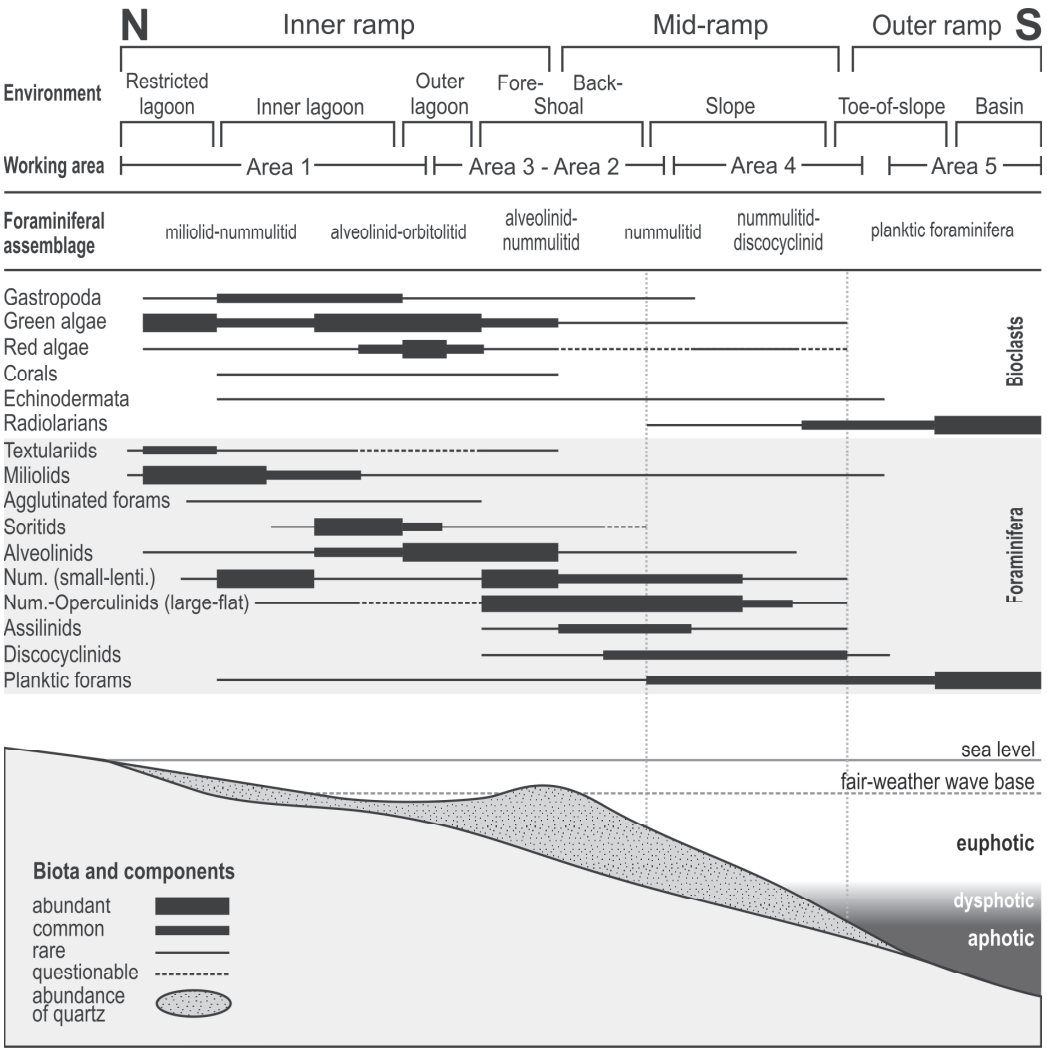

Figure VII.5 – Semi-quantitative distribution of the main microfossils combined with six foraminiferal assemblages on the Galala platform (modified after Höntzsch et al., 2011). The discrimination of inner ramp, mid ramp and outer ramp environments with the help of different bioclasts and larger foraminifera is only roughly demonstrated due to the lack of in situ deposits in the study area.

VII.4 Discussion

VII.4.1 Early Palaeogene hyperthermals – global vs. local record

Geochemical expression

The geochemical expression of hyperthermal events varies between shallow- and deep-marine environments due to their different palaeoceanographic position. Marginal shallow-marine environments are severely affected by sediment discharge of river systems from adjacent land masses, which may affect the trophic regime and the carbon cycle of (proximal) shelf areas.

On the other hand, shelf areas act as large carbon sinks during hyperthermals, due to sea-level rise (John et al., 2008). Swart (2008) demonstrated a strong relationship between Late Cenozoic sea-level changes and the carbon isotope signature in marginal platform systems.

The author argued that aragonite-rich sediments of marginal platforms, which are only produced during the flooding of the platform, reveal more positive $\delta^{13}C$ ratios, than pelagic deposits without major aragonite concentrations. Thus, positive bulk rock $\delta^{13}C$ ratios indicate periods with a high sea level, whereas depleted bulk rock $\delta^{13}C$ ratios indicate periods with a low sea level. This relation is decoupled from the isotopic changes of the global carbon cycle. The impact of $\delta^{13}C$ enrichment during sea level highstands requires the presence of major aragonite producing organism. However, the Egyptian shelf is dominated by organisms with calcite shells during the Early Palaeogene greenhouse (LBF; Hallock, 1999). Following the approach of Swart (2008), sea level highstand during hyperthermal events would shift the magnitude of the CIE towards more positive ratios, which is not the case in the Galala succession.

Moreover, periplatform settings are much stronger affected by diagenetic alteration than pelagic realms, which limits the use of oxygen isotope ratios for palaeoenvironmental interpretations of these deposits (Reuning et al., 2005). To compare our shallow-marine data with those described from open ocean environments we will focus on carbon isotopes, bulk rock calcium carbonate and total organic carbon.

Carbon isotope evolution

Global carbon isotope records for the Cenozoic, based on small benthic foraminifera compiled by Zachos et al. (2001) indicate a continuing depletion in $\delta^{13}C$ from Middle Paleocene to the Early Eocene, culminating at around 52 Ma with the onset of the EECO. Repeated transient perturbations in the global carbon cycle (CIEs) occur superimposed on this trend. Timing and magnitude of those perturbations are strongly linked to variations in the orbital parameters of the the Earth (Cramer et al., 2003; Lourens et al., 2005). After the onset of the EECO, the carbon isotope curve quickly recovered towards a $\delta^{13}C$-enriched signature. Other high-resolution, carbon isotope records based on bulk rock samples indicate similar trends (Exmouth Plateau, Eastern Indian Ocean; Thomas et al., 1992).

Bulk rock data of the sections 4a, 4b and 4d demonstrate a similar isotopic trend as the composite curve of Zachos et al. (2001) from NP9 to NP11. This trend suggests a certain coupling of the Egyptian shelf to open ocean condition and enhanced water-mass exchange with the Tethys (Charisi and Schmitz, 1995, 1998; Speijer and Schmitz, 1998; Fig. VII.7). Within upper NP11, the $\delta^{13}C$ ratios of the studied sections indicate a continuing depletion. This trend is in contrast with the data of Thomas et al. (1992) and Zachos et al. (2001), demonstrating a shift towards more positive $\delta^{13}C$ ratios during NP11. This deviation is probably related to the increasing restriction of the EDIB and a decoupling from open ocean conditions during the Early Eocene (Charisi and Schmitz, 1998; Bolle et al., 2000). Following the concept of Swart (2008), the massive global sea-level drop during the late Early Eocene

(~50 Ma; Haq and Al-Qahtani, 2005; Miller et al., 2005) can also cause the continuing depletion of the $\delta^{13}C$ ratios of the marginal Galala succession. Another possible cause for the increasing restriction of the southern Tethyan margin is the massive tectonic activity along the SAFB during the Early Eocene (Fig. VII.7, Tab. VII.3; Moustafa and Khalil, 1995; Kuss et al., 2000; Hussein and Abd-Allah, 2001). The repeated uplift of inner ramp environments along the Wadi Araba Fault between NP11 – NP14a caused the massive erosion and relocation of terrestrial Mesozoic and Palaeozoic siliciclastics of the Nubia Group (Amireh, 1991; Baioumy et al., 2003; Höntzsch et al., 2011). The isotopic composition of terrestrial organic material shows a more depleted signature than organic material from a marine source. Thus, tectonic uplift and the relocation of large amounts of isotopically depleted terrestrial organic-rich sediments may contribute to depleted bulk rock $\delta^{13}C$ ratios in marginal shallow-marine settings (Beck et al., 1995; Steurbaut et al., 2003). The termination of the uplift along the SAFB is indicated by the slight recovery from depleted to enriched carbon isotope ratios within NP14a, coinciding with the termination of siliciclastic dilution at the Galala platform (Hussein and Abd-Allah, 2001; Höntzsch et al., 2011). This shutdown of tectonic activity also concludes the recovery of the EDIB from a restricted basin to a basin with open-marine conditions.

In contrast to the clear isotopic trends of the sections 4a, 4b, 4c and 4d, section 3 is characterized by high transient fluctuations which hamper the recognition of long term isotopic trends. The proximity of section 3 to the Wadi Araba Fault as well as frequent thick-bedded siliciclastics and dolomites suggest a significant alteration of the in situ carbon isotope ratios.

Besides the overall trend in the Palaeogene carbon cycle, several significant transient perturbations in the isotope and geochemical record of the Galala succession suggest an impact of Early Palaeogene hyperthermals to shallow-marine environments (Figs. VII.6 and VII.7). In contrast to the deep-marine record, the magnitude of the CIEs of ETM2, ETM3 and the I1-event are significantly higher in the studied mid ramp sections of area 4. This amplification may result from syndepositional reworked Mesozoic and Palaeozoic siliciclastics that are depleted in $\delta^{13}C$. This hypothesis is supported by the frequent occurrence of quartz-rich deposits prior to and after the post-PETM CIEs. However, hyperthermal-related CIEs always occur within marl beds. Bioturbation can cause the mixing of marls and siliciclastic intervals, which is demonstrated by frequent quartz grains within marly intervals.

The missing negative CIE of the PETM in section 5 has also been recognized in other sections of the study area. Marzouk and Scheibner (2003) recorded numerous stratigraphic gaps around the Paleocene-Eocene boundary in area 5. Marzouk and Soliman (2004) explain similar hiati in drillings in Sinai as a result of Early Eocene tectonic uplift. However,

the presence of an organic carbon-enriched dark clay layer and significant depleted calcium carbonate ratios in section 5 suggest the presence of the PETM horizon. Significant unconformities which are related to tectonic uplift were not found in section 5 but in section 3 and 4c (Fig. VII.7). Furthermore, the sea level lowstand at the NP9b/NP10 boundary may trigger the release of mass flows and the erosion of distal intervals along the ramp (Speijer and Wagner, 2002).

Calcium carbonate ratios

In contrast to the deep sea, shelf deposits were largely unaffected by dissolution due to lysocline shallowing during Early Palaeogene hyperthermals (John et al., 2008). Depletion in calcium carbonate associated to CIEs is rather related to siliciclastic dilution (Nicolo et al., 2007). On the other hand, strongly varying sedimentation rates and bulk rock calcium carbonate fluctuations are interpreted to result from multiple tectonical unconformities and not from dissolution or dilution of carbonates (Zachos et al., 2005; Giusberti et al., 2007; Galeotti et al., 2010). The local environmental and tectonic constraints of the Galala succession reveal a combination of siliciclastic dilution and tectonic unconformities as major triggers for calcium carbonate depletion. Frequent beds with depleted calcium carbonate ratios coincide with the main activity of Syrian Arc uplift (NP10 – NP14a; Hussein and Abd-Allah, 2001; Höntzsch et al., 2011). After the termination of Syrian Arc uplift within NP14a, bulk rock calcium carbonate ratios quickly shifted towards constant values between 85 % and 95 % (Fig. VII.6).

TOC

The TOC amounts are low in all studied sections and can be related to higher sedimentation rates and siliciclastic dilution at the platform. Single marl beds which are significantly enriched in TOC correlate with the negative CIEs of post-PETM hyperthermal events and probably reflect transient productivity peaks (Hallock et al., 1991; Scheibner et al., 2005). Studies on Early Eocene calcareous phytoplankton assemblages demonstrated that productivity increases during hyperthermal events on the shelfs and decreases at the open ocean (Lourens et al., 2005; Gibbs et al., 2006). Organic carbon-rich marl horizons at Mead Stream (New Zealand), which coincide with the CIEs of PETM and ETM2, were attributed to excess terrigenous dilution (Nicolo et al., 2007). Black shales from the Early Eocene Arctic Ocean reveal transient euxinic conditions due to a high primary productivity and increased terrigenous input during hyperthermal events (Stein et al., 2006; Sluijs et al., 2009). Comparable TOC-rich horizons in the Early Palaeogene EDIB were interpreted as black shales, which are related to local upwelling regimes (Speijer and Wagner, 2002). Major black shale horizons at the Egyptian shelf correlate to the PETM and multiple Early Eocene

intervals. The dark grey marl layer of section 5 represents a distal equivalent of the described black shales. A correlation of post-PETM black shale horizons to Early Eocene hyperthermal events, described by Speijer and Wagner (2002), is possible but can not be proved in this study.

Biotic impact

Earlier studies reveal that the post-PETM hyperthermals had a major impact on various environments on Earth, however with a smaller magnitude (Thomas and Zachos, 2000; Lourens et al., 2005; Röhl et al., 2005; Agnini et al., 2009; Sluijs et al., 2009; Clementz et al., 2011). Similar to the Benthic Extinction Event at the PETM (Kaiho, 1991; Thomas and Shackleton, 1996), deep-sea benthic foraminifera show a massive decrease in diversity during ETM2 (Lourens et al., 2005; Stap et al., 2009) and ETM3 (Röhl et al., 2005). The distribution of calcareous nannoplankton reflects a massive shift in the trophic regime during the PETM (Kelly et al., 1996; Bralower, 2002; Raffi et al., 2005; Gibbs et al., 2006), at the ETM2 (Raffi and De Bernardi, 2008) and at the ETM3 (Röhl et al., 2005; Agnini et al., 2007). At higher latitudes, the poleward migration of subtropical dinoflagellate *Apectodinium* reveals major transient temperature anomalies during the PETM and the expansion of subtropical vegetation around the poles (Bujak and Brinkhuis, 1998; Crouch et al., 2001; Sluijs et al., 2006). Similar shifts were recorded for ETM2 (Crouch and Brinkhuis, 2005; Sluijs et al., 2009) and ETM3 (Agnini et al., 2009).

During the Paleocene (SBZ1 – SBZ3, NP1 – NP8) shallow-marine LBF are characterized by an increasing adaption to stable environments, resulting in a longer lifespan and decreasing reproduction rates (K-strategy). The environmental impact of the PETM (SBZ4/5; NP9a/b) caused a major shift in the prevailing LBF taxa (Orue-Extebarria et al., 2001). New taxa with different ecological strategies evolved (Scheibner et al., 2005). Paleocene Rotaliida (ranikothalids, miscellanids) were replaced by the first Eocene nummulitids. Porcellaneous alveolinids evolved from planspiral glomalveolinids to fusiform Eocene alveolinids (Hottinger, 2001). The diversification of LBF was linked to an overall increase in test size. The coeval evolving adult dimorphism of LBF is interpreted as an adaptation to the seasonality in warm and oligotrophic habitats (Hottinger, 1998, 2001). Scheibner et al. (2005) linked this Larger Foraminifera Turnover directly to the CIE of the PETM (Fig. VII.7). Despite the adaption of LBF to stable and oligotrophic environments, the newly evolved Eocene forms suggest an adaption to extreme climatic conditions. The climatically controlled shift from coral-dominated platforms to LBF-dominated platforms during the Early Palaeogene reveals a higher temperature tolerance of LBF (Scheibner et al., 2005; Scheibner and Speijer, 2009).

Evidence for an impact of post-PETM hyperthermals to LBF was not observed yet. According to Hottinger (1998), specific diversity of K-strategists peaks at 53.5 Ma (SBZ8, upper NP10)

and at around 48 Ma (SBZ12, NP14a). A subsequent decrease in the specific diversity of K-strategists is documented within SBZ13. The first subordinate peak at around 53.5 Ma correlates roughly with the ETM2, the second peak at 48 Ma coincides with late EECO in low latitude settings (Pearson et al., 2007). In contrast to the specific diversity, the genus diversity of K-strategists peaks in the upper Paleocene. After a subordinate decrease prior to the PETM, genus diversity remains almost constant until the Middle Eocene.

A relation between the peaks in the specific diversity of LBF and the Early Eocene climatic evolution is possible. However, the studied sections of the Galala platform do not show any impact of Eocene hyperthermals on the major carbonate platform building organisms (LBF, green algae), nor changes in the prevailing biotic assemblages. We assume, that LBF have adapted to the prevailing extreme climatic conditions during the Early Palaeogene as a result of increasing K-strategy.

The general negligible occurrence of corals in the studied sections reflects the non-recovery of these platform organisms in the Early Eocene, which is probably related to multiple environmental thresholds (Höntzsch et al., 2011; Fig. VII.6). Critical thresholds, which prevent coral recovery, are represented by the continuing warming during the Early Eocene, increased nutrient availability and surface water turbidity caused by algal blooms and continental runoff.

Figure VII.6 (next page) – Integrated geochemical, tectonical and microfacial comparison of section 4a from the latest Paleocene to uppermost Early Eocene. Carbon isotope data and calcium carbonate ratios are provided for marl and limestone samples with less than 20 % of quartz. Measured carbon isotope data are compared with data from Thomas et al. (1992) and Zachos et al. (2001). Additional total organic carbon (TOC) and calculated bulk rock calcium carbonate data indicate transient shifts, which reflect Early Eocene hyperthermal events (PETM, ETM2, ETM3). Platform stages are adapted from Höntzsch et al. (2011) and Scheibner and Speijer (2008). Grey shaded intervals indicate time of tectonic quiescence (TQ); white intervals represent tectonic uplift along the Wadi Araba Fault (WAF). The chart on the right hand site is based on thin section analyses of limestone and sandstone turbidites and includes %-values of the quartz and fossil content, as well as the semi-quantitative abundance of selected main biota (r...rare, f...few, c...common, a...abundant, v...very abundant). Due to strongly varying thicknesses and various preservation states, not all turbidites were sampled and included in the scheme. Note the Larger Foraminifera Turnover (LFT) at the CIE of the PETM and the rare abundance of corals in the whole section. The red circles indicate Paleocene and Eocene key species of the LFT. Black arrows show increasing abundances of LBF after the PETM. The diversity and abundance of the post-ETM3-LBF are higher during tectonically active periods, compared to the tectonically quiet periods.

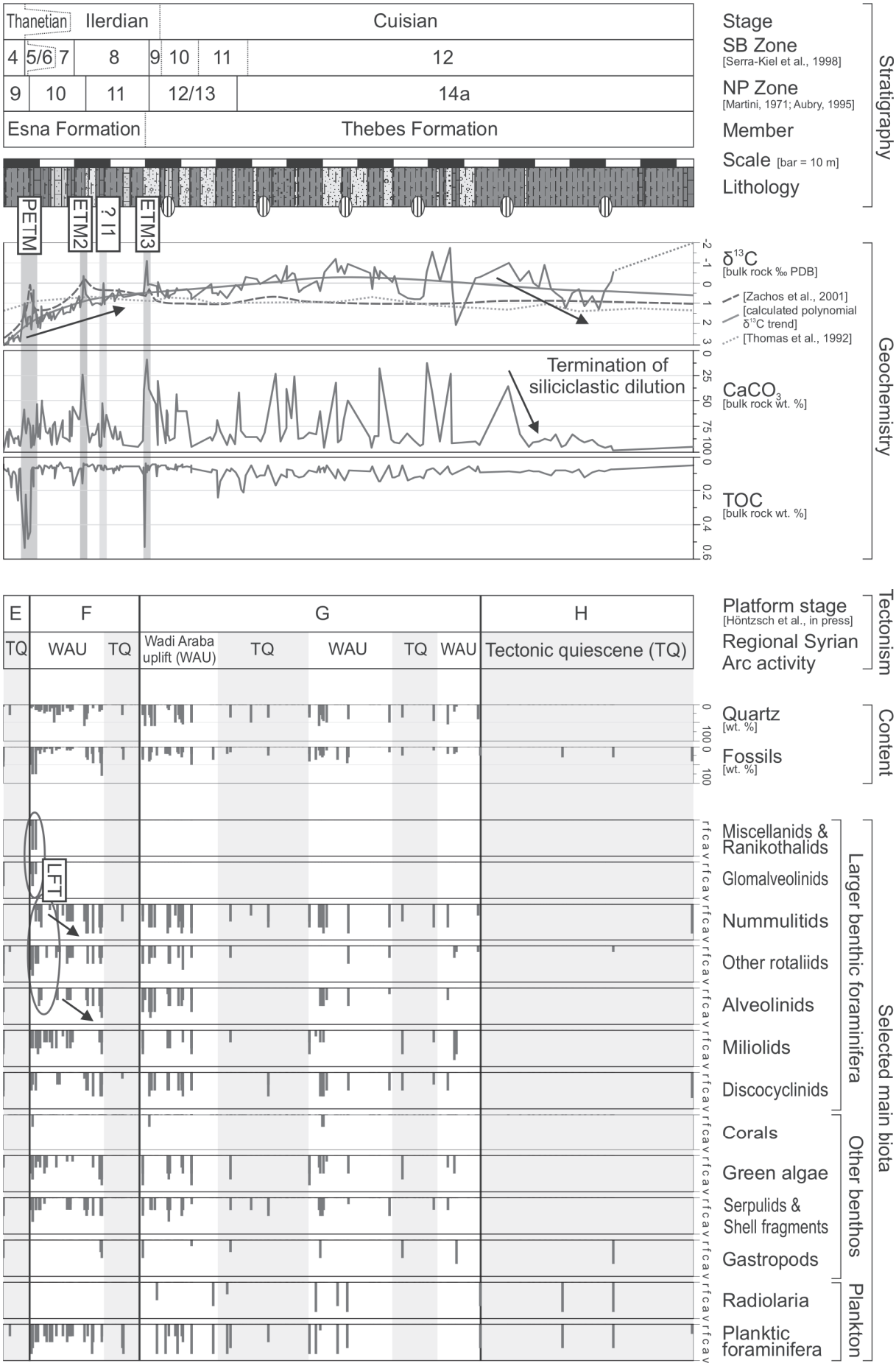
Thanetian
Ilerdian
Cuisian
4
5/6
7
8
9
10
11
12
9
10
11
12/13
14a
Esna Formation
Thebes Formation
PETM
ETM2
? I1
ETM3
Termination of siliciclastic dilution
E
F
G
H
TQ
WAU
TQ
Wadi Araba uplift (WAU)
TQ
WAU
TQ
WAU
Tectonic quiescene (TQ)
LFT
Stage
SB Zone
[Serra-Kiel et al., 1998]
NP Zone
[Martini, 1971; Aubry, 1995]
Member
Scale [bar = 10 m]
Lithology
Stratigraphy
δ13C
[bulk rock ‰ PDB]
[Zachos et al., 2001]
[calculated polynomial δ13C trend]
[Thomas et al., 1992]
CaCO3
[bulk rock wt. %]
TOC
[bulk rock wt. %]
Geochemistry
Platform stage
[Höntzsch et al., in press]
Regional Syrian Arc activity
Tectonism
Quartz
[wt. %]
Fossils
[wt. %]
Content
Miscellanids & Ranikothalids
Glomalveolinids
Nummulitids
Other rotaliids
Alveolinids
Miliolids
Discocyclinids
Larger benthic foraminifera
Corals
Green algae
Serpulids & Shell fragments
Gastropods
Other benthos
Radiolaria
Planktic foraminifera
Plankton
Selected main biota

Legend
Facies
Marl dominated
Marly limestone dominated
Sand-rich limestone dominated
Siliciclastic dominated
Debris flow dominated
Dolostone dominated
Depositional features
Undefined CIEs
ETM3 (x-event)
ETM2 (Elmo)
PETM/LFT interval
Chert nodules
Scale
10 m
Gulf of Suez
Wadi Araba
N-Galala
S-Galala
3
4a
4b
4c
4d
5
N
S
Wadi Araba Monocline
Area 3
Mid Ramp (Slope)
Area 4
Outer Ramp - Basin (SGS)
Area 5
Section 3
Section 4a
Section 4b
Section 4c
Section 4d
Section 5
δ13C [bulk rock ‰ PDB]
CaCO3 [bulk rock wt. %]
TOC [bulk rock wt. %]
ETM3
ETM2
PETM
NP Zone (Martini, 1971; Aubry, 1995)
SB Zone (Serra-Kiel et al., 1998)
Age
Epoch
Time [Ma]
Thanetian
Ilerdian
Cuisian
Lutetian
Early Eocene
M. Eocene
Paleocene

Figure VII.7 (previous page) – Biostratigraphic and geochemical correlation of six sections, along an outer ramp to upper mid ramp transect (area 3, 4 and 5). The basis of the correlation is the negative CIE of the PETM, which was found in all plotted sections (in section 5, the PETM is indicated by a dark brown TOC-enriched layer, whereas a significant negative CIE is missing). Note the strong variability in calcium carbonate content until NP14a generally strong $\delta^{13}C$-depleted bulk rock data in the Lower Eocene succession. A correlation of major siliciclastic units at the mid ramp is only roughly applicable, due to frequent tectonic unconformities.

VII.4.2 Regional climate and local tectonism – insights to enhanced nutrient availability and shelf basin restriction?

In contrast to the open ocean, marginal shelf areas reveal complex environmental conditions regarding ocean circulation, regional climate and tectonic activity. During the Early Palaeogene, the Egyptian shelf is affected by repeated environmental perturbations, which yield to enhanced nutrient availability and temporary shelf restriction.

Here we present an integrated palaeoenvironmental and palaeogeographic model, which reveals the evolution of the Egyptian shelf from the Late Paleocene (NP7) to the uppermost Early Eocene (NP14a; Figs. VII.8a-d). The processes which influence the study area during the Early Palaeogene are controlled by global and regional climatic constraints as well as by the local tectonic activity along the SAFB.

<u>Late Paleocene (NP7 – NP8): open ocean conditions on the shelf</u>

Late Paleocene climate is characterized by prevailing warm and arid conditions at the Egyptian shelf and at the African craton (Hendriks et al., 1990; Bolle et al., 2000). The shift from coral-dominated carbonate platforms to LBF-dominated platforms indicates rising temperatures at the southern Tethys (Scheibner and Speijer 2008; Höntzsch et al., 2011).

Shales and marls with low to moderate TOC amounts suggest open ocean conditions in the EDIB with low terrigenous influence from the African craton (Speijer and Wagner, 2002). Our results show that pure carbonate deposition prevailed at the shallow-marine unstable shelf. Carbonate mass flow deposits (slumps, debris flows) result from prograding platform systems that are triggered by the sea-level (Scheibner et al., 2000, 2003; Galala platform stage D, according to Scheibner and Speijer, 2008). Ocean currents from the open Tethys can penetrate the EDIB without significant modulation (Fig. VII.8a).

Latest Paleocene – earliest Eocene (NP9a – NP10/11): increasing climatic feedback and tectonic reactivation

The continuing global warming during the Early Palaeogene causes decreasing temperature gradients between equatorial areas and higher latitudes. Decreasing latitudinal temperature gradients result in weakened meridional ocean currents and reduced ocean mixing (Boersma et al., 1987, 1998). This weakening of ocean currents results in the reduced strength of onshore currents towards the southern Tethyan shelf (Fig. VII.8b). At the southern Tethyan margin, Early Palaeogene climate is characterized by an increasing aridity at the North African continental shelf, whereas stable warm and temporarily wet conditions with an increasing seasonality prevail at the continental hinterland (Fig. VII.8b; Aboul-Ela, 1989; Hendriks et al., 1990; Strouhal, 1993; Bolle et al., 2000; Bolle and Adatte, 2001; Ernst et al., 2006). This divergence between seasonal conditions in the hinterland and arid climates on the shelf results in intensified chemical weathering at the African continent and the drainage of terrigenous materials towards the EDIB (Hendriks et al., 1990).

At the shallow-marine unstable shelf, quartz-free calcareous turbidites and debris flows increase significantly. Possible mechanisms for the increasing deposition of mass wasting deposits during the latest Paleocene are highstand shedding due to an increasing productivity during sea-level highstands (Schlager et al., 1994) or the reactivation of the Wadi Araba Fault as SW branch of the SAFB (Galala platform stages E/F; according to Höntzsch et al., 2011). The uplift along the SAFB causes a further weakening of the southward currents from the open Tethys. However, open ocean conditions prevailed at the northern EDIB (Southern Galala Subbasin), which is indicated by comparable carbon isotope ratios of bulk rock samples from the southern Galala mid ramp and other open ocean environments (Thomas et al., 1992).

Early Eocene (NP10/11 – NP14a): shelf restriction and nutrient excess

In the Early Eocene, global warming continues, culminating in the EECO between 53 - 49 Ma (Zachos et al., 2001). The weakening of meridional currents due to decreasing latitudinal temperature gradients result in a global sluggish ocean (Boersma et al., 1998). Especially during times of transient extreme temperatures (hyperthermals), the global ocean circulation is reduced to a minimum (Fig. VII.8c; Sluijs et al., 2006).

At the marginal southern Tethys, perennial warm and humid conditions prevail on the African hinterland, whereas warm and arid climates dominate the African shelf (Hendriks, 1990; Bolle et al., 2000). Increasing chemical weathering in the hinterland causes enhanced drainage from the continent to the shelf, transporting dissolved terrestrial organic matter and sediment load towards the shelf. The mass wasting of terrestrial organic deposits with

strongly negative $\delta^{13}C$ ratios may shift the bulk rock carbon isotope signature of marginal shelf deposits on a regional scale (Nicolo et al., 2007).

Lower Eocene deposition at the unstable shelf is characterized by frequent siliciclastic mass flows, slumps and debris flows, reflecting a major phase of tectonic activity along the SAFB. The uplift along the SAFB causes erosion of Mesozoic and Palaeozoic siliciclastics, reflecting terrestrial and shallow-marine deposits of the Nubia Series (Galala platform stage G, according to Höntzsch et al., 2011). Drillings along the unstable Egyptian shelf reveal the emergence of various platform systems, forming a NE-SW striking palaeogeographic barrier, which modulates ocean currents from the northern Tethys (Fig. VII.8c; Salem, 1976). This modulation and the already weak ocean currents from the Tethys favour an increasing isolation of the Egyptian shelf. The onset of restricted conditions is supported by strongly depleted $\delta^{13}C$ ratios, compared to other open ocean records (Fig. VII.6; Thomas et al., 1992; Zachos et al., 2001).

Table VII.4 – Relation between calculated sedimentation rates, platform stages (Höntzsch et al., 2011; Scheibner and Speijer, 2008) and relevant tectonic events in the study area. Sedimentation rates are only calculated for the mid ramp and the outer ramp sections (areas 4 and 5). The effect of diagenetic compaction is not excluded in the calculation. The sedimentation rates of NP14 represent only an interval within NP14a due to the missing upper boundary of NP14a. Low sedimentation rates correlate to high tectonic activity and uplift along the SAFB, resulting in multiple erosional unconformities at the slope.

NP zone	Sed. rates [cm/ka]	Related events	Deposition and Erosion	Platform stage
NP9b	0.2 – 0.4	Recovery of PETM	? Unconformity	Stage F
NP10	0.9 – 1.7	Initial tectonic activity	Massive erosion	Stage F
NP11	2.0 – 2.5	? Reduced tectonic activity	Few hiati	Stage F/G
NP12/13	0.6 – 0.8	Massive tectonic activity	Massive erosion	Stage G
NP14a	> 2.0 – 6.0	Termination of tectonism	Little erosion	Stage H

Latest Early Eocene (NP14a – ?): recovery to open ocean conditions

The latest Early Eocene is characterized by increasing latitudinal temperature gradients, which result from the cooling of higher latitudes at the end of the EECO (~49 Ma, NP14a). Increasing temperature gradients re-enforce meridional ocean currents and terminate sluggish ocean conditions.

The termination of tectonic uplift along the SAFB is reflected by decreasing quartz-rich mass flow deposition and the transition from mixed siliciclastic to pure carbonate deposition during the uppermost Lower Eocene (Figs. VII.6, VII.8d; NP14a, Galala platform stage H according to Höntzsch et al., 2011). With the erosion of major platforms at the unstable shelf, ocean currents from the open Tethys can penetrate the EDIB. Thus, the disappearance of the

tectonically-controlled palaeogeographic barrier along the unstable shelf triggers the transition from a restricted basin to a basin with open ocean conditions at the Egyptian shelf. The transition to open ocean conditions is supported by a shift from strongly depleted $\delta^{13}C$ ratios to enriched $\delta^{13}C$ ratios, which are comparable to the open ocean bulk rock data of Thomas et al. (1992) (Fig. VII.6).

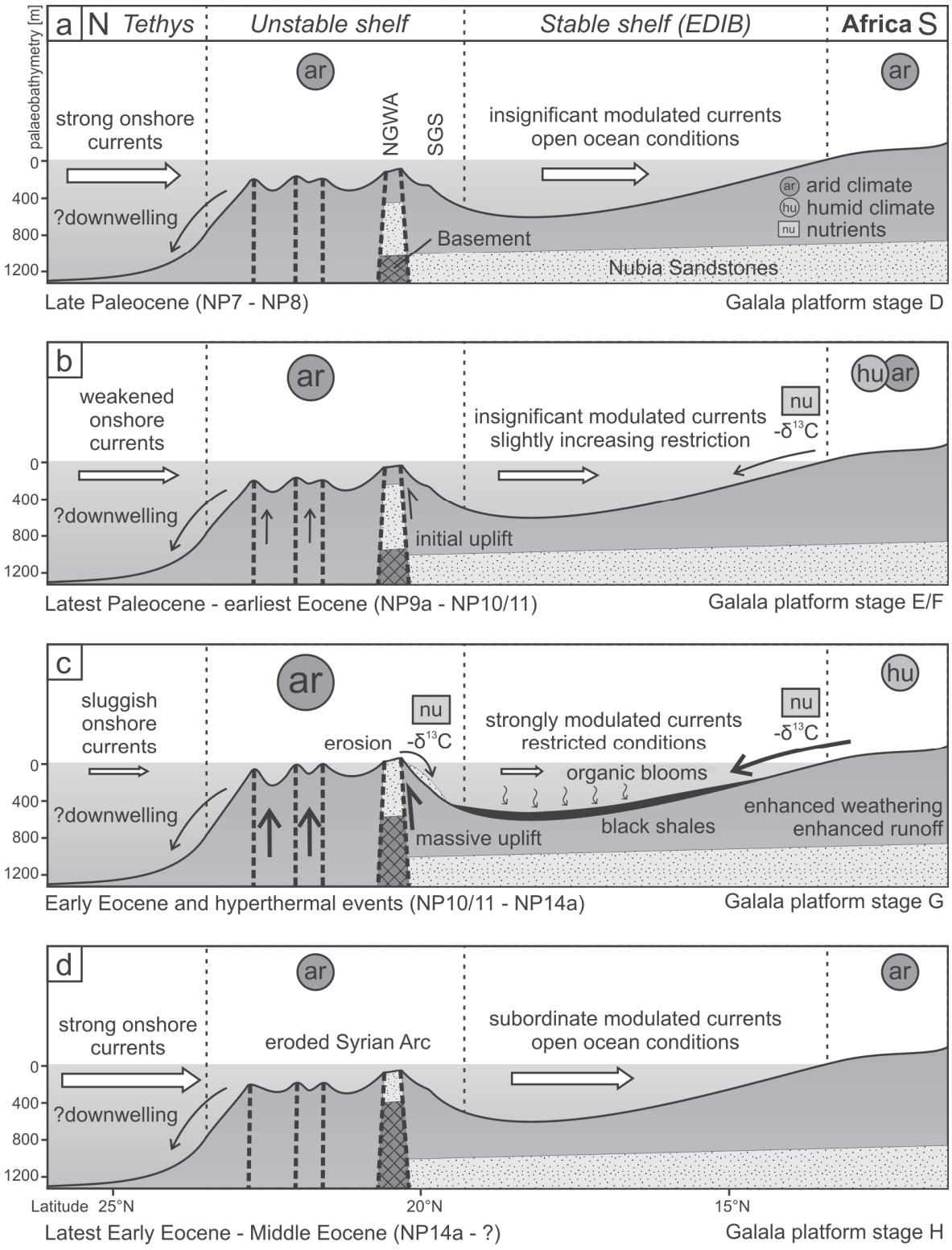

Figure VII.8 (previous page) – Palaeogeographic evolution of the Late Paleocene – Early Eocene stable and unstable shelf of Egypt (platform stages D – H after Scheibner and Speijer, 2008 and Höntzsch et al., 2011) plus oceanographic and climatic interpretations (ar - arid climate, hu - humid climate, nu - nutrients).
VII.8 a – Late Paleocene (NP7 – NP8): Only subordinated modulation of onshore Tethyan currents through the SAFB. Open ocean conditions prevailed in the EDIB. Warm-arid climate prevailed at the whole shelf system, including the African hinterland.
VII.8 b – Latest Paleocene – earliest Eocene (NP9a – NP10/11): The reactivation of the SAFB caused uplift along the Egyptian unstable shelf. Increased warming at high latitudes caused decreased latitudinal temperature gradients and weakened onshore currents. Warm arid climates prevailed on the shelf (including the EDIB). Alternating warm-arid and warm-humid conditions dominated the African hinterland and probably caused slightly enhanced chemical weathering rates.
VII.8 c – Early Eocene (NP10/11 – NP14a): Continuing global warming and decreasing temperature gradients between high and low latitudes resulted in strongly weakened Tethyan currents. Additionally, a massive uplift along the SAFB caused an increasing restriction of the EDIB. The subaerial exposure and erosion of Palaeozoic and Mesozoic sandstones at the NGWA yielded in strong siliciclastic admixtures at the ramp. A strong divergence between increasing aridity on the shelf and perennial warm-humid conditions in the hinterland caused enhanced chemical weathering and drainage from the continent. As a consequence, high amounts of nutrients were transported in the EDIB, enforcing high productivity and the local deposition of organic-rich black shales. ^{13}C-depleted organic material from the continent probably caused an amplification of CIE at the marginal African shelf. The described processes probably prevailed with varying strength in the Early Eocene and were exaggerated during the hyperthermal events.
VII.8 d – Latest Early Eocene (NP14a - ?): The termination of Syrian Arc-related uplift, the erosion of major platform systems and the decreasing drainage from the African continent caused a recovery of the carbon isotope signature within the EDIB. The termination of the EECO caused a rapid cooling at higher latitudes with increasing latitudinal temperature gradients and an enhanced oceanic circulation. The EDIB shifted from a restricted basin to a basin with well-oxygenated open ocean conditions.

VII.4.3 Causes and consequences of Early Eocene nutrient excess at the shelves

The Early Eocene warm and stagnating ocean is characterized by highly oligotrophic open ocean surface water masses and generally low productivity rates (Moore et al., 1978; Shackleton and Hall, 1984; Corfield and Shackleton, 1988; Hallock et al., 1991; Pak et al., 1997; Arkaah et al., 2006). In contrast to the open ocean, several marginal shelf basins are characterized by increased nutrient availability (Gibbs et al., 2006; Stein et al., 2006). In the EDIB and at the Galala platform, nutrient-sensitive organisms indicate prevailing meso- to eutrophic conditions. Possible sources of enhanced nutrient discharge are explained by three main processes:

a) Prevailing warm and humid conditions at the African hinterland result in enhanced chemical weathering and erosion of rocks, causing the massive transport of sediment load from the continent to the shelf. Higher sediment fluxes caused higher volumes of nutrients, transported as dissolved organic matter towards the shelf. Studies in modern marine environments show that enormous amounts of nutrients can be discharged by strong river currents (Williams and Follows, 2003). The environmental response of this major nutrient input is reflected by increasing productivity rates, flourishing of meso- to eutrophic organisms and higher phytoplankton densities in the

water column (Kouwenhoven et al., 1997; Speijer and Schmitz, 1998; Mutti and Hallock, 2003). Thus, in contrast to the scarcity of nutrients at the open ocean, continental shelves may be areas of high productivity and nutrient excess during the same time (Fig. VII.8c).

Speijer and Schmitz (1998) suggest that the riverine discharge of nutrients from the African continent can support the eutrophication of surface waters in the EDIB during the Late Paleocene. Similar conditions may have prevailed during the Early Eocene, and would be well comparable with results from general circulation models, which predict higher greenhouse gas concentrations in the atmosphere and an intensified hydrological cycle (Pierrehumbert, 2002; Huber and Caballero, 2003; Caballero and Langen, 2005, Zamagni et al., 2008). Radiolarians, which are enriched in chalky marl intervals of the Lower Eocene Thebes Formation in areas 4 and 5, possibly flourished due to increased nutrient supply by continental runoff (Bains et al., 2000). Especially during Early Eocene hyperthermals, sediment supply from the continental hinterlands and carbon burial at the shelves increased significantly (Fig. VII.8c). Comparable increasing sedimentation rates on the shelf were reported from the Iberian Peninsula (Schmitz and Pujalte, 2003), from New Zealand (Nicolo et al., 2007), from the Arctic Ocean (Stein et al., 2006; Sluijs et al., 2008, 2009), from the northern Para-Tethys (Agnini et al., 2009) and from the New Jersey coastal plain (John et al., 2008). On a global scale, similar interrelationships are demonstrated for the PETM (Kelly et al., 1998; Bains et al., 2000; Ravizza et al., 2001; Kelly et al., 2005; Guasti and Speijer, 2007) and Oceanic Anoxic Event 1a (OAE 1a) in the early Aptian (Larson and Erba, 1999; Leckie et al., 2002; Erba, 2004; Tremolada et al., 2007).

Nutrient excess and higher productivity rates result in increasing oxygen consumption of organisms in the ocean. Thus, organism blooms can cause the onset of oxygen minimum zones in the water column, which favours the deposition of black shales in somewhat restricted ocean basins (Arthur and Sageman, 1994). During the Early Eocene and especially at the PETM, black shale formation was documented in the EDIB (Schmitz et al., 1996; Speijer et al., 1997; Speijer and Wagner, 2002; Fig. VII.8c), in the northern Peri-Tethys (Gavrilov et al., 1997, 2003) and in the Arctic Ocean (Bujak and Brinkhuis, 1998; Stein et al., 2006; Boucsein and Stein, 2009). A TOC-rich layer in the basinal setting of area 5 represents the PETM and may indicate the marginal equivalent of the black shales in the EDIB. Other TOC-rich beds in the study area are associated to hyperthermal events (Fig. VII.5), although, they are not represented by macroscopically visible black shale sediments.

The absence of surface dwelling morozovellids in the basinal Thebes Formation (area 5) is probably also related to enhanced nutrient fluxes at the southern Tethyan shelf.

We assume that strong water column stratification due to pronounced nutrient-rich freshwater influence might have led to the disappearance of Morozovella, as it was speculated by Guasti (2005) for the Late Danian Event in the Nile Valley. Wade (2004) concluded, that the extinction of the genus Morozovella in the late Middle Eocene is probably related to increased surface water productivity. Alternatively, we do not exclude that strong dissolution affected the sampled intervals, and in particular Morozovella.

b) Speijer and Wagner (2002) link black shale formation at the PETM in the EDIB to local upwelling regimes, which provide nutrient-rich water masses to marginal shelf areas. Comparable processes of nutrient advection due to local upwelling were demonstrated in the present-day southern Caribbean (Hallock and Elrod, 1988), the Galapagos Islands (Feldman et al., 1984) and SE Asia (Wilson and Vecsei, 2005) and may represent an underrated approach for the nutrient supply at isolated carbonate platforms (Vecsei, 2003; Mutti and Hallock, 2003; Betzler et al., 2009; Reijmer et al., in press). However, the stagnating oceans during the Early Eocene global greenhouse are not efficient enough to establish major upwelling regimes (Muttoni and Kent, 2007), especially during hyperthermal events with low temperature gradients. Based on diatom distribution patterns in equatorial settings, Cervato and Burckle (2003) demonstrate reduced upwelling regimes and low productivity in lower latitudes throughout the Early Eocene. Seasonal upwelling, resulting in the episodic influx of nutrients may be sufficient enough to shift the biotic assemblages on the carbonate platform from a highly oligotrophic coral-dominated fauna to mesotrophic LBF- and algae-dominated assemblage (Reijmer et al., in press) but is not considered an important factor in the present study.

c) For the shallow-marine benthic assemblages of the Galala platform, the enhanced erosion of Mesozoic and Palaeozoic siliciclastics, triggered and controlled by the tectonic uplift along the Wadi Araba Fault, demonstrates a major mechanism of nutrient supply. The significant depletion of the carbon isotope signature from NP10 to NP14 as well as flourishing organisms, which reflect meso- to eutrophic conditions at the platform, indicate significantly higher nutrient concentrations at the Galala platform during the Early Eocene (Fig. VII.6).

VII.5 Conclusions and outlook

1) We have identified at least two post-PETM carbon isotope excursions (CIEs) at the marginal southern Tethys of Egypt, which are associated with bulk rock calcium carbonate depletion and organic carbon enrichment. Biostratigraphic classification assigns those perturbations to hyperthermal events, which previously have only been recorded in deeper marine environments.

2) A coupling of these hyperthermals to major shifts in the diversity with the abundance of benthic assemblages is not evident in the study area. It appears that the main platform building organisms, larger benthic foraminifera, have adapted to the extreme environmental conditions and perturbations during the Early Eocene.

3) New insights from the Galala carbonate platform at the southern Tethys reveal the increasing restriction of the Eastern Desert Intra-Shelf Basin (EDIB) during the Early Eocene, caused by climatic and tectonic processes.

   a) In the Late Paleocene the southern Tethyan margin is characterized by a warm-arid climate and open ocean conditions.

   b) The reactivation of the SAFB in the Early Eocene induced the massive uplift and erosion of Palaeozoic and Mesozoic siliciclastics along the Egyptian unstable shelf. As a consequence, the EDIB was enclosed by a SW-NE striking oceanographic barrier.

   c) Decreasing latitudinal temperature gradients during the Early Eocene global greenhouse and the closing of the Eastern Tethys seaway yielded to a more sluggish ocean with weak currents penetrating the EDIB.

   d) A strong climatic divergence between the warm-arid shelf and the perennial humid African hinterland prevailed during the Early Eocene. Strongly humid conditions at the African continent yielded intensified chemical weathering and an enhanced drainage towards the shelf in the North. The transport of terrestrial organic material caused the increased availability of trophic resources in the EDIB, which is reflected by the increased occurrence of radiolaria and absent *Morozovella* in the water column. Shallow-benthic assemblages at the Galala platform show a high abundance of benthic green algae and heterotrophic grazers.

      An increasing restriction of the EDIB is also reflected by strongly depleted bulk rock carbon isotope ratios, indicating a decoupling from open ocean conditions due to the increasing influence of regional environmental constraints.

e) The termination of the restriction of the EDIB is indicated by a shift of bulk rock carbon isotopes towards a $\delta^{13}C$-enriched signature. The recovery to open ocean conditions is coupled to the termination of Syrian Arc activity and the strengthening of Tethyan currents caused by the post-EECO cooling of higher latitudes in the late Early Eocene.

4) Future studies should focus on the post-PETM palaeoenvironmental evolution of deeper areas within the EDIB to refine the approach of increasing ocean basin restriction. Other carbonate platform successions along the SAFB (Syria and Jordan) will help to understand the timing of uplift and the related sea-level changes at the unstable shelf.

Acknowledgements The authors wish to thank John J.G. Reijmer (Amsterdam) and an anonymous reviewer for their comments, which greatly improved the manuscript. We appreciate the efforts of Dr. Abdel-Mohsen Morsi and Dr. Abdel-Monem Soltan and their help and organisation of our field trips in Egypt. We are grateful to Ralf Bätzel, Christian Sommerfeld, Patrick Simundic and Sarah Romahn for the excellent preparation of the samples, as well as Brit Kockisch and Monika Segl for the determination of the geochemical data. Robert J. Smith is thanked for his creative support. This project is funded by the German Science Foundation (DFG-KU 642/221).

VII.6 References

Aboul-Ela N (1989) Lower Tertiary microflora from the Esna Shale of the Red Sea Coast, Egypt. Revista Esp. Micropaleont. 21:189-206.

Agnini C, Fornaciari E, Rio D, Tateo F, J Backman, Giusberti L (2007) Responses of calcareous nannofossil assemblages, mineralogies and geochemistry to the environmental perturbations across the Paleocene/Eocene boundary in the Venetian Pre-Alps. Marine Micropaleontology 63:19-38.

Agnini C, Macrì P, Backman J, Brinkhuis H, Fornaciari E, Giusberti L, Luciani V, Rio D, Sluijs A, Speranza F (2009) An early Eocene carbon cycle perturbation at ~52.5 Ma in the Southern Alps: Chronology and biotic response. Paleoceanography 24:PA2209, doi:10.1029/2008PA001649.

Alegret L, Ortiz S, I Arenillas, Molina E (2005) Palaeoenvironmental turnover across the Palaeocene/Eocene boundary at the Stratotype section in Dababiya (Egypt) based on benthic foraminifera. Terra Nova 17:526-536.

Amireh BS (1991) Mineral composition of the Cambrian-Cretaceous Nubian Series of Jordan: Provenance, tectonic setting and climatological implications. Sedimentary Geology 71:99-119.

Arkaah AB, Kaminski M, Ogle N, Kalin RM, Atta-Petters D, Apaalse L, Wiafe G, Armah AK (2006) Early Paleogene climate and productivity of the Eastern Equatorial Atlantic, off the western coast of Ghana. Quaternary International 148:3-7.

Arthur M, Sageman B (1994) Marine Black Shales: Depositional Mechanisms and Environments of Ancient Deposits. Annu. Rev. Earth Planet. Sci. 22:499-551.

Aubry M-P (1991) Sequence Stratigraphy: Eustasy or Tectonic Imprint? J. Geophys. Res. 96:6641-6679.

Aubry MP (1995) Towards an upper Paleocene-lower Eocene high resolution stratigraphy based on calcareous nannofossil stratigraphy. Israel Journal of Earth Sciences 44:239-253.

Aubry MP, Berggren WA, Stott L, Sinha A (1996) The upper Paleocene-lower Eocene stratigraphic record and the Paleocene-Eocene boundary carbon isotope excursion: implications for geochronology. In: Knox, RWOB, Corfield, RM, Dunay, RE (ed) Correlation of the early Paleogene in northwest Europe, Geological Society, London, pp. 353-380.

Aubry MP (2000) Where should the Global Stratotype Section and Point (GSSP) for the Paleocene/Eocene boundary be located. Bulletin de la Societé Géologique de France 171:461-476.

Bains S, Corfield RM, Norris RD (1999) Mechanisms of climate warming at the end of the Paleocene. Science 285:724-727.

Bains S, Norris RD, Corfield RM, Faul KL (2000) Termination of global warmth at the Palaeocene/Eocene boundary through productivity feedback. Nature 407:171-174.

Baioumy H, Ismael I, Zidan I (2003) Clay Mineralogy of the Nubia Formation, Western Desert (Egypt). Geologica Carpathica 54:329-336.

Beavington-Penney SJ, Racey A (2004) Ecology of extant nummulitids and other larger benthic foraminifera: applications in palaeoenvrionmental analysis. Earth-Science Reviews 67:219-265.

Beck RA, Burbank DW, Sercombe WJ, Olson TL, Khan AM (1995) Organic carbon exhumation and global warming during the early Himalayan collision. Geology 23:387-390.

Beerling DJ (2000) Increased terrestrial carbon storage across the Palaeocene-Eocene boundary. Palaeogeography, Palaeoclimatology, Palaeoecology 161:395-405.

Berggren WA, Kent DV, Swisher III CC, Aubry MP (1995) A revised Cenozoic geochronology and chronostratigraphy. In: Berggren, WA, Kent, DV, Aubry, MP, Hardenbol, J (ed) Geochronology, time scales, and global stratigraphic correlation, SEPM Spec. Publ. 54, Tulsa, pp. 129-212.

Berggren WA, Ouda K (2003) Upper Paleocene-lower Eocene planktonic foraminiferal biostratigraphy of the Dababiya section, Upper Nile Valley (Egypt). Micropaleontology 49, supplement 1:61-92.

Berggren WA, Pearson PN (2005) A revised tropical to subtropical Paleogene planktonic foraminiferal zonation. Journal of Foraminiferal Research 35:279-298.

Betzler C, Hübscher C, Lindhorst S, Reijmer JJG, Römer M, Droxler AW, Fürstenau J, Lüdmann T (2009) Monsoon-induced partial carbonate platform drowning (Maldives, Indian Ocean). Geology 37:867-870.

Boersma A, Silva IP, Shackleton NJ (1987) Atlantic Eocene Planktonic Foraminiferal Paleohydrographic Indicators and Stable Isotope Paleoceanography. Paleoceanography 2:287-331.

Boersma A, Premoli Silva I, Hallock P (1998) Trophic models for the well-mixed and poorly mixed warm oceans across the Paleocene/Eocene epoch boundary. In: Aubry, MP, Lucas, SG, Berggren, WA (ed) Late Paleocene-early Eocene climatic and biotic events in the marine and terrestrial records, Columbia University Press, New York, pp. 204-213.

Bolle MP, Tantawy AA, Pardo A, Adatte T, Burns S, Kassab A (2000) Climatic and environmental changes documented in the upper Paleocene to lower Eocene of Egypt. Eclogae geol. Helv. 93:33-51.

Bolle MP, Adatte T (2001) Palaeocene-early Eocene climatic evolution in the Tethyan realm: clay mineral evidence. Clay Minerals 36:249-261.

Boucsein B, Stein R (2009) Black shale formation in the late Paleocene/early Eocene Arctic Ocean and paleoenvironmental conditions: New results from a detailed organic petrological study. Marine and Petroleum Geology 26:416-426.

Bowen R, Jux U (1987) Afro-Arabian Geology: a kinematic view. Chapman and Hall, London, pp. 250.

Bralower TJ (2002) Evidence of surface water oligotrophy during the Paleocene-Eocene thermal maximum: Nannofossil assemblage data from the Ocean Drilling Program Site 690, Maud Rise, Weddell Sea. Paleoceanography 17:10.1029/2001PA000662.

Bujak JP, Brinkhuis H (1998) Global warming and dinocyst changes across the Paleocene/Eocene epoch boundary. In: Aubry, MP, Lucas, S, Berggren, WA (ed) Late Paleocene - early Eocene climatic and biotic events in the marine and terrestrial records, Columbia University Press, New York, pp. 277-295.

Caballero R, Langen P (2005) The dynamic range of poleward energy transport in an atmospheric general circulation model. Geophys. Res. Lett. 32:L02705, doi:10.1029/2004GL021581.

Cervato C, Burckle L (2003) Pattern of first and last appearance in diatoms: Oceanic circulation and the position of polar fronts during the Cenozoic. Paleoceanography 18:1055.

Charisi SD, Schmitz B (1995) Stable (d13C, d18O) and strontium (87Sr/86Sr) isotopes through the Paleocene at Gebel Aweina, eastern Tethyan region. Palaeogeography, Palaeoclimatology, Palaeoecology 116:103-129.

Charisi SD, Schmitz B (1998) Paleocene to early Eocene paleoceanography of the Middle East; the d13C and d18O isotopes from foraminiferal calcite. Paleoceanography 13:106-118.

Corfield R, Shackleton N (1988) Productivity change as a control on planktonic foraminiferal evolution after the cretaceous/tertiary boundary. Historical Biology 1:323-343.

Cramer BS, Wright JD, Kent DV, Aubry MP (2003) Orbital climate forcing of d13C excursions in the late Paleocene-early Eocene (chrons C24n-C25n). Paleoceanography 18:1097, doi:10.1029/2003PA000909.

Crouch EM, Heilmann-Clausen C, Brinkhuis H, Morgans HEG, Rogers KM, Egger H, Schmitz B (2001) Global dinoflagellate event associated with the late Paleocene thermal maximum. Geology 29:315-318.

Crouch EM, Brinkhuis H (2005) Environmental change across the Paleocene-Eocene transition from eastern New Zealand: A marine palynological approach. Marine Micropaleontology 56:138-160.

Dickens G, O'Neil J, Rea D, Owen R (1995) Dissociation of oceanic methane hydrate as a cause of the carbon isotope excursion at the end of the Paleocene. Paleoceanography 10:965–971.

Dickens GR, Castillo MM, Walker JCG (1997) A blast of gas in the latest Paleocene: Simulating first-order effects of massive dissociation of oceanic methane hydrate. Geology 25:259-262.

Erba E (2004) Calcareous nannofossils and Mesozoic Oceanic Anoxic Events. Marine Micropaleontology 52:85-106.

Ernst SR, Guasti E, Dupuis C, Speijer RP (2006) Environmental perturbation in the southern Tethys across the Paleocene/Eocene boundary (Dababiya, Egypt): Foraminiferal and clay mineral records. Marine Micropaleontology 60:89-111.

Everts AJW (1991) Interpreting compositional variations of calciturbidites in relation to platform-stratigraphy: an example from the Paleogene of SE Spain. Sedimentary Geology 71:231-242.

Feldman G, Clark D, Halpern H (1984) Satellite color observations of the phytoplankton distribution in the eastern equatorial pacific during the 1982–1983 El Niño. Science 226:1069–1071.

Galeotti S, Krishnan S, Pagani M, Lanci L, Gaudio A, Zachos JC, Monechi S, Morelli G, Lourens L Orbital chronology of Early Eocene hyperthermals from the Contessa Road section, central Italy. Earth and Planetary Science Letters 290:192-200.

Gavrilov Y, Kodina L, Lubchenko I, Muzylev N (1997) The Late Paleocene Anoxic Event in epicontinental seas of Peri-Tethys and formation of the sapropelite unit: sedimentology and geochemistry. Lithology and Mineral Resources 32:427-450.

Gavrilov YO, Shcherbinina EA, Oberhänsli H (2003) Paleocene-Eocene boundary events in the northeaster Peri-Tethys. In: Wing, SL, Gingerich, PD, Schmitz, B, Thomas, E (ed) Causes and consequences of globally warm climates in the Early Paleogene, The Geological Society of America, Boulder, pp. 147-168.

Gibbs SJ, Bralower TJ, Bown PR, Zachos JC, Bybell LM (2006) Shelf and open-ocean calcareous phytoplankton assemblages across the Paleocene-Eocene Thermal Maximum: implications for global productivity gradients. Geology 34:233-236.

Gingerich PD (1989) New earliest Wasatchian mammalian fauna from the Eocene of northwestern Wyoming: composition and diversity in a rarely sampled high-floodplain assemblage. Univ. Mich. Pap. Paleontol. 28:1-97.

Gingerich PD (2003) Mammalian responses to climate change at the Paleocene-Eocene boundary: Polecat Bench record in the northern Bighorn Basin, Wyoming. In: Wing, SL, Gingerich, PD, Schmitz, B, Thomas, E (ed) Causes and consequences of globally warm climates in the Early Paleogene, The Geological Society of America, Boulder, pp. 463-478.

Gingerich PD (2006) Environment and evolution through the Paleocene-Eocene thermal maximum. Trends in Ecology and Evolution 21:246-253.

Giusberti L, Rio D, Agnini C, Backman J, Fornaciari E, Tateo F, Oddone M (2007) Mode and tempo of the Paleocene-Eocene thermal maximum in an expanded section from the Venetian pre-Alps. GSA Bulletin 119:391-412.

Guasti E (2005) Early Paleogene environmental turnover in the southern Tethys as recorded by foraminiferal and organic-walled dinoflagellate cysts assemblages. Berichte aus dem Fachbereich Geowissenschaften der Universität Bremen 241:1-191.

Guasti E, Speijer RP (2007) The Paleocene-Eocene Thermal Maximum in Egypt and Jordan: An overview of the planktic foraminiferal record. In: Monechi, S, Coccioni, R, Rampino, MR (ed) Large ecosystems perturbations: causes and consequences, Geological Society of America Special Paper 424, Tulsa, pp. 53-67.

Hallock P (1985) Why are larger foraminifera large? Paleobiology 11:195-208.

Hallock P, Glenn EC (1986) Larger foraminifera: a tool for paleoenvironmental analysis of Cenozoic carbonate depositional facies. Palaios 1:55-64.

Hallock P, Schlager W (1986) Nutrient excess and the demise of coral reefs and carbonate platforms. Palaios 1:389-398.

Hallock P, Elrod JA (1988) Oceanic chlorophyll around carbonate platforms in the western Caribbean; observations from CZCS data. Int. Coral Reef Symp. 449–454.

Hallock P, Premoli Silva I, Boersma A (1991) Similarities between planktonic and larger foraminiferal evolutionary trends through Paleogene paleoceanographic changes. Palaeogeography, Palaeoclimatology, Palaeoecology 83:49-64.

Hallock P (1999) Symbiont-bearing Foraminifera. In: Gupta, BS (ed) Modern Foraminifera, Kluwer, Amsterdam, pp. 123-139.

Haq BU, Al-Qahtani AM (2005) Phanerozoic cycles of sea-level change on the Arabian Platform. GeoArabia 10:127-160.

Hendriks F, Luger P, Strouhal A (1990) Early Tertiary marine palygorskite and sepiolite neoformation in SE Egypt. Z. dt. geol. Ges. 141:87-97.

Higgins J A, Schrag DP (2006) Beyond methane: Towards a theory for the Paleocene-Eocene thermal maximum. Earth and Planetary Science Letters 245:523-537.

Höntzsch S, Scheibner C, Kuss J, Marzouk A, Rasser M (2011) Tectonically driven carbonate ramp evolution at the southern Tethyan shelf: the Lower Eocene succession of the Galala Mountains, Egypt. Facies 57:51-72.

Hottinger L (1960) Über paleocaene und eocaene Alveolinen. Eclogae geol. Helv. 53:265-283.

Hottinger L, Schaub H (1960) Zur Stufeneinteilung des Paleocaens und des Eocaens. Eclogae geol. Helv. 53:453-479.

Hottinger L (1974) Alveolinids, Cretaceous Tertiary Larger Foraminifera, Exxon Research–European Laboratories. A. Schudel & Co, Riehen, Basel, pp. 85.

Hottinger L (1998) Shallow benthic foraminifera at the Paleocene-Eocene boundary. Strata, Serie 1 9:61-64.

Hottinger L (2001) Learning from the past? In: Box, E, Pignatti, S (ed) Volume IV: The living world. Part Two., Academic Press, San Diego, pp. 449-477.

Huber M, Caballero R (2003) Eocene El Nino: Evidence for robust tropical dynamics in the "Hothouse". Science 299:877-881.

Hussein IM, Abd-Allah AMA (2001) Tectonic evolution of the northeastern part of the African continental margin, Egypt. Journal of African Earth Sciences 33:49-68.

John CM, Bohaty SM, Zachos JC, Sluijs A, Gibbs S, Brinkhuis H, Bralower TJ (2008) North American continental margin records of the Paleocene-Eocene thermal maximum: Implications for global carbon and hydrological cycling. Paleoceanography 23:PA2217.

Kaiho K (1991) Global changes of Paleogene aerobic/anaerobic benthic foraminifera and deep-sea circulation. Palaeogeogr., Palaeoclimatol., Palaeoecol. 83:65-85.

Katz ME, Cramer BS, Mountain GS, Katz S, Miller KG (2001) Uncorking the bottle: What triggered the Paleocene/Eocene thermal maximum methane release? Paleoceanography 16:549-562.

Kelly DC, Bralower TJ, Zachos JC, Silva IP, Thomas E (1996) Rapid diversification of planktonic foraminifera in the tropical Pacific (ODP Site 865) during the late Paleocene thermal maximum. Geology 24:423-426.

Kelly DC, Bralower TJ, Zachos JC (1998) Evolutionary consequences of the latest Paleocene thermal maximum for tropical planktonic foraminifera. Palaeogeography, Palaeoclimatology, Palaeoecology 141:139-161.

Kelly DC, Zachos JC, Bralower TJ, Schellenberg SA (2005) Enhanced terrestrial weathering/runoff and surface ocean carbonate production during the recovery stages of the Paleocene-Eocene thermal maximum. Paleoceanography 20:Pa4023, doi:10.1029/2005PA001163.

Kennett J, Stott L (1991) Abrupt deep-sea warming, palaeoceanographic changes and benthic extinctions at the end of the Palaeocene. Nature 53:225-229.

Kominz MA, Browning JV, Miller KG, Sugarman PJ, Mizintseva S, Scotese CR (2008) Late Cretaceous to Miocene sea-level estimates from the New Jersey and Delaware coastal plain coreholes: an error analysis. Basin Research 20:211-226.

Kouwenhoven TJ, Speijer RP, van Oosterhout CWM, van der Zwaan GJ (1997) Benthic foraminiferal assemblages between two major extinction events: the Paleocene El Kef section, Tunisia. Marine Micropaleontology 29:105-127.

Kroon D, Zachos JC, Leg 208 Scientific Party (2007) Leg 208 synthesis: Cenozoic climate cycles and excursions. In: Kroon, D, Zachos, J C, Richter, C (ed) Proc. ODP, Sci. Results, 208, pp. 1-55, doi:10.2973/odp.proc.sr.208.201.2007.

Kurtz AC, Kump LR, Arthur MA, Zachos JC, Paytan A (2003) Early Cenozoic decoupling of the global carbon and sulfur cycles. Paleoceanography 18:1090, doi:10.1029/2003PA000908.

Kuss J, Scheibner C, Gietl R (2000) Carbonate platform to basin transition along an Upper Cretaceous to Lower Tertiary Syrian Arc Uplift, Galala Plateaus, Eastern Desert, Egypt. GeoArabia 5:405-424.

Larson RL, Erba E (1999) Onset of the Mid-Cretaceous Greenhouse in the Barremian-Aptian: Igneous Events and the Biological, Sedimentary, and Geochemical Responses. Paleoceanography 14:663–678.

Lawver LA, Gahagan LM (2003) Evolution of Cenozoic seaways in the circum-Antarctic region. Palaeogeography, Palaeoclimatology, Palaeoecology 198:11-37.

Leckie RM, Bralower T, Cashman R (2002) Oceanic Anoxic Events and plankton evolution: Biotic response to tectonic forcing during the mid-Cretaceous. Paleoceanography 17:doi: 10.1029/2001PA000623.

Leinfelder RR (1994) Karbonatplattformen und Korallenriffe innerhalb siliziklastischer Sedimentationsbereiche (Oberjura, Lusitanisches Becken, Portugal). Profil 6:1-207.

Leinfelder RR (1997) Coral reefs and carbonate platforms within a siliciclastic setting: General aspects and examples from the Late Jurassic of Portugal. Proc. 8th Int. Coral Reef Symp. 2:1737-1742.

Lourens LJ, Sluijs A, Kroon D, Zachos JC, Thomas E, Röhl U, Bowles J, Raffi I (2005) Astronomical pacing of late Palaeocene to early Eocene global warming events. Nature 435:1083-1087.

Marshall J (1992) Climatic and oceanographic isotopic signals from the carbonate rock record and their preservation. Geological Magazin 129:143-160.

Martini E (1971) Standard Tertiary and Quaternary calcareous nannoplankton zonation. In: Farinacci, A (ed) Proceedings of the II Plankton Conference, Roma, Edizioni Tecnoscienza Rome, Roma, pp. 739-785.

Marzouk AM, Scheibner C (2003) Calcareous nannoplankton biostratigraphy and paleoenvironment of the late Cretaceous-Paleogene of the Galala Mountains, Eastern Desert, Egypt. Courier Forschungsinstitut Senckenberg 244:11-35.

Marzouk AM, Soliman SIM (2004) Calcareous nannofossil biostratigraphy of the Paleogene sediments on an onshore-offshore transect of Northern Sinai, Egypt. Journal of African Earth Sciences 38:155-168.

Meshref WM (1990) Tectonic framework. In: Said, R (ed) The Geology of Egypt, A. A. Balkema Publishers, Rotterdam, pp. 113-156.

Miller KG, Kominz MA, Browning JV, Wright JD, Mountain GS, Katz ME, Sugarman PJ, Cramer BS, Christie-Blick N, Pekar SF (2005) The Phanerozoic record of global sea-level change. Science 310:1293-1298.

Monechi S, Angori E, von Salis K (2000) Calcareous nannofossil turnover around the Paleocene/Eocene transition at Alamedilla (southern Spain). Bulletin de la Societé Géologiue de France 171:477-489.

Moore T, Andel Tv, Sancetta C, Pisias N (1978) Cenozoic hiatuses in pelagic sediments. Micropaleontology 24:113-138.

Moustafa AR, El-Rey AK (1993) Structural characteristics of the Suez rift margins. Geologische Rundschau 82:101-109.

Moustafa AR, Khalil MH (1995) Superposed deformation in the northern Suez Rift, Egypt: Relevance to hydrocarbons exploration. Journal of Petroleum Geology 18:245-266.

Mutti M, Hallock P (2003) Carbonate systems along nutrient and temperature gradients: some sedimentological and geochemical constraints. International Journal of Earth Sciences 92:465-475.

Muttoni G, Kent DV (2007) Widespread formation of cherts during the early Eocene climate optimum. Palaegeography, Palaeoclimatology, Palaeoecology 253:348-362.

Nicolo MJ, Dickens GR, Hollis CJ, Zachos JC (2007) Multiple early Eocene hyperthermals: Their sedimentary expression on the New Zealand continental margin and in the deep sea. Geology 35:699-702.

Nisbet EG, Jones SM, Maclennan J, Eagles G, Moed J, Warwick N, Bekki S, Braesicke P, Pyle JA, Fowler CMR (2009) Kick-starting ancient warming. Nature Geosci 2:156-159.

Ortiz S, Gonzalvo C, Molina E, Rodríguez-Tovar FJ, Uchman A, Vandenberghe N, Zeelmaekers E (2008) Palaeoenvironmental turnover across the Ypresian-Lutetian transition at the Agost section, Southastern Spain: In search of a marker event to define the Stratotype for the base of the Lutetian Stage. Marine Micropaleontology 69:297-313.

Orue-Etxebarria X, Pujalte V, Bernaola G, Apellaniz E, Baceta JI, Payros A, Nunez-Betelu K, Serra-Kiel J, Tosquella J (2001) Did the Late Paleocene thermal maximum affect the evolution of larger foraminifers? Evidence from calcareous plankton of the Campo Section (Pyrenees, Spain). Marine Micropaleontology 41:45-71.

Pagani M, Caldeira K, Archer D, Zachos JC (2006) An ancient carbon mystery. Science 314:1556-1557.

Pak D, Miller K, Browning J (1997) Global significance of an isotopic record from the New Jersey coastal plain: linkage between the shelf and deep sea in the late Paleocene to early Eocene. In: Miller, KG, Snyder, SW (ed) Proceedings of the Ocean Drilling Program, Scientific Results, pp. 305-315.

Pearson PN, van Dongen BE, Nicholas CJ, Pancost RD, Schouten S, Singano JM, Wade BS (2007) Stable warm tropical climate through the Eocene Epoch. Geology 35:211-214.

Pierrehumbert RT (2002) The hydrologic cycle in deep-time climate problems. Nature 419:191-198.

Raffi I, Backman J, Pälike H (2005) Changes in calcareous nannofossil assemblages aacross the Paleocene/Eocene transition from the paleo-equatorial Pacific Ocean. Palaegeography, Palaeoclimatology, Palaeoecology 226:93-126.

Raffi I, De Bernardi B (2008) Response of calcareous nannofossils to the Paleocene-Eocene Thermal Maximum: Observations on composition, preservation and calcification in sediments from ODP Site 1263 (Walvis Ridge -- SW Atlantic). Marine Micropaleontology 69:119-138.

Ravizza G, Norris RN, Blusztajn J (2001) An osmium isotope excursion associated with the late Paleocene thermal maximum: evidence of intensified chemical weathering. Paleoceanography 16:155-163.

Reijmer JJG, Bauch T, Schäfer P (in press) Carbonate facies patterns in surface sediments of upwelling and non-upwelling shelf environments (Panama, East Pacific). Sedimentology

Reuning L, Reijmer JJG, Betzler C, Swart P, Bauch T (2005) The use of paleoceanographic proxies in carbonate periplatform settings--opportunities and pitfalls. Sedimentary Geology 175:131-152.

Röhl U, Westerhold T, Monechi S, Thomas E, Zachos JC, Donner B (2005) The third and final Early Eocene thermal maximum: characteristics, timing, and mechanisms of the "X"-event. GSA Abstracts with Programs 37:264.

Said R (1990) The geology of Egypt. Elsevier, Amsterdam, pp. 377.

Salem R (1976) Evolution of Eocene-Miocene sedimentation patterns in parts of northern Egypt. AAPG Bulletin 60:34-64.

Scheibner C, Kuss J, Marzouk AM (2000) Slope sediments of a Paleocene ramp-to-basin transition in NE Egypt. International Journal of Earth Sciences 88:708-724.

Scheibner C, Marzouk AM, Kuss J (2001) Maastrichtian-Early Eocene litho- biostratigraphy and palaeogeography of the northern Gulf of Suez region, Egypt. Journal of African Earth Sciences 32:223-255.

Scheibner C, Reijmer JJG, Marzouk AM, Speijer RP, Kuss J (2003) From platform to basin: The evolution of a Paleocene carbonate margin (Eastern Desert, Egypt). International Journal of Earth Sciences 92:624-640.

Scheibner C, Speijer RP, Marzouk AM (2005) Larger foraminiferal turnover during the Paleocene/Eocene thermal maximum and paleoclimatic control on the evolution of platform ecosystems. Geology 33:493-496.

Scheibner C, Speijer RP (2008) Late Paleocene–early Eocene Tethyan carbonate platform evolution — A response to long- and short-term paleoclimatic change. Earth-Science Reviews 90:71-102.

Scheibner C, Speijer RP (2009) Recalibration of the Tethyan shallow-benthic zonation across the Paleocene-Eocene boundary; the Egyptian record. Geologica Acta 7:195-214.

Schlager W (1981) The paradox of drowned reefs and carbonate platforms. Geological Society of America Bulletin, Part 1 92:197-211.

Schlager W, Reijmer J, Droxler A (1994) Highstand shedding of carbonate platforms. Journal of Sedimentary Research B 64:270-281.

Schlager W (2003) Benthic carbonate factories of the Phanerozoic. International Journal of Earth Sciences 92:445-464.

Schmitz B, Heilmann-Clausen C, King C, Steurbaut E, Andreasson FP, Corfield RM, Cartlidge J E (1996) Stable isotope and biotic evolution in the North Sea during the early Eocene: the Alb~ek Hoved section, Denmark. In: Knox, RWOB, Corfield, RM, Dunay, RE (ed) Correlation of the Early Paleogene in Northwest Europe, Geological Society, London, pp. 275-306.

Schütz KI (1994) Structure and stratigraphy of the Gulf of Suez, Egypt. In: Landon, SM (ed) Interior rift basins, AAPG Memoir, pp. 57-96.

Seilacher A (1967) Bathymetry of trace fossils. Marine Geology 5:413-428.

Serra-Kiel J, Hottinger L, Caus E, Drobne K, Ferrandez C, Jauhri AK, Less G, Pavlovec R, Pignatti J, Samso JM, Schaub H, Sirel E, Strougo A, Tambareau Y, Tosquella J, Zakrevskaya E (1998) Larger foraminiferal biostratigraphy of the Tethyan Paleocene and Eocene. Bulletin de la Société Géologique de France 169:281-299.

Shackleton N, Hall M (1984) Carbon isotope data from Leg 74 sediments. Initial Rep. Deep Sea Drill. Proj. 74:613-620.

Shahar J (1994) The Syrian Arc System: an overview. Palaeography, Palaeoclimatology, Palaeoecology 112:125-142.

Sluijs A, Schouten S, Pagani M, Woltering M, Brinkhuis H, Sinninghe Damste JS, Dickens GR, Huber M, Reichart GJ, Stein R, Matthiessen J, Lourens LJ, Pedentchouk N, Backman J, Moran K (2006) Subtopical arctic ocean temperatures during the Palaeocene/Eocene thermal maximum. Nature 441:610-613.

Sluijs A, Brinkhuis H, Schouten S, Bohaty SM, John CM, Zachos JC, Reichart GJ, Crouch EM, Dickens GR (2007) Environmental precursors to rapid light carbon injection at the Palaeocene/Eocene boundary. Nature 450:1218-1221.

Sluijs A, Röhl U, Schouten S, Brumsack HJ, Sangiorgi F, Sinninghe Damste JS, Brinkhuis H (2008) Arctic late Paleocene-early Eocene paleoenvironments with special emphasis on the Paleocene-Eocene thermal maximum (Lomonosov Ridge, Integrated Ocean Drilling Program Expedition 302. Paleoceanography 23:doi:10.1029/2007PA001495.

Sluijs A, Schouten S, Donders TH, Schoon PL, Rohl U, Reichart G-J, Sangiorgi F, Kim J-H, Sinninghe Damste JS, Brinkhuis H (2009) Warm and wet conditions in the Arctic region during Eocene Thermal Maximum 2. Nature Geosci 2:777-780.

Speijer RP, Zwaan GJ van d, Schmitz B (1996) The impact of Paleocene/Eocene boundary events on middle neritic benthic foraminiferal assemblages from Egypt. Marine Micropaleontology 28:99-132.

Speijer RP, Schmitz B, J van der Zwaan G (1997) Benthic foraminiferal extinction and repopulation in response to latest Paleocene Tethyan anoxia. Geology 25:683-686.

Speijer RP, Schmitz B (1998) A benthic foraminiferal record of Paleocene sea level and trophic/redox conditions at Gebel Aweina, Egypt. Palaeogeography, Palaeoclimatology, Palaeoecology 137:79-101.

Speijer RP, Morsi AMM (2002) Ostracode turnover and sea-level changes associated with the Paleocene-Eocene thermal maximum. Geology 30:23-26.

Speijer RP, Wagner R (2002) Sea-level changes and black shales associated with the late Paleocene thermal maximum; organic-geochemical and micropaleontologic evidence from the southern Tethyan margin (Egypt-Israel). In: Koeberl, C, MacLeod, KG (ed) Catastrophic Events & Mass

Extinctions: Impacts and Beyond, Geological Society of America Special Paper, Boulder, pp. 533-549.

Stap L, Sluijs A, Thomas E, Lourens L (2009) Patterns and magnitude of deep sea carbonate dissolution during Eocene Thermal Maximum 2 and H2, Walvis Ridge, southeastern Atlantic Ocean. Paleoceanography 24:A1211, doi:10.1029/2008PA001655.

Stein R, Boucsein B, Meyer H (2006) Anoxia and high primary production in the Paleogene central Artic Ocean: first detailed records from the Lomonosov Ridge. Geophysical Research Letters 33:10.1029/2006GL026776.

Storey M, Duncan RA, Swisher III CC (2007) Paleocene-Eocene thermal maximum and the opening of the Northeast Atlantic. Science 316:587-589.

Strouhal A (1993) Tongeologische Entwicklungstrends in kretazischen und tertiären Sedimenten Nordostafrikas: regionale Fallbeispiele. Berliner Geowissenschaftliche Abhandlungen 155:1-68.

Swart PK (2008) Global synchronous changes in the carbon isotopic composition of carbonate sediments unrelated to changes in the global carbon cycle. Proceedings of the National Academy of Sciences

Thomas E, Shackleton NJ (1996) The Paleocene-Eocene benthic foraminiferal extinction and stable isotope anomalies. In: Knox, RWOB, Corfield, RM, Dunay, RE (ed) Correlation of the Early Paleogene in Northwest Europe, Geological Society, London, pp. 401-441.

Thomas E, Zachos JC (2000) Was the late Paleocene thermal maximum a unique event? GFF 122:169-170.

Tremolada F, Erba E, Bralower TJ (2007) A review of calcareous nannofossil changes during the early Aptian oceanic anoxic event 1a and the Paleocene–Eocene thermal maximum: the influence of fertility, temperature, and pCO2. In: Monechi, S, Coccioni, R, Rampino, MR (ed) Large Ecosystem Perturbations: Causes and Consequences, Geol. Soc. Am. Special Paper, pp. 87–96.

Tripati A, Elderfield H (2005) Deep-sea temperature and circulation changes at the Paleocene-Eocene Thermal Maximum. Science 308:1894-1898.

Tripati AK, Delaney ML, Zachos JC, Anderson LD, Kelly DC, Elderfield H (2003) Tropical sea-surface temperature reconstruction for the early Paleogene using Mg/Ca ratios of planktonic foraminifera. Paleoceanography 18:1101, doi:10.1029/2003PA000937, 2003.

Valentine P (1987) Lower Eocene calcareous nannofossil biostratigraphy beneath the Atlantic slope and upper rise off New Jersey - New zonation based on Deep Sea Drilling Project sites 612 and 613. Initial Rep. Deep Sea Drill. Proj. 95:359-394.

Vecsei A (2003) Nutrient control of the global occurrence of isolated carbonate banks. International Journal of Earth Sciences 92:476-481.

Veizer J (1983) Trace elements and isotopes in sedimentary carbonates. Reviews in Mineralogy and Geochemistry 11:265-299.

Wade BS (2004) Planktonic foraminiferal biostratigraphy and mechanisms in the extinction of Morozovella in the late middle Eocene. Marine Micropaleontology 51:23-38.

Westerhold T, Röhl U, J Laskar, I Raffi, J Bowles, Lourens LJ, Zachos J C (2007) On the duration of magnetochrons C24r and C25n and the timing of early Eocene global warming events: implications from the Ocean Drilling Program Leg 208 Walvis Ridge depth transect. Paleoceanography 22:doi:10.1029/2006PA001322.

Williams RG, Follows MJ (2003) Physical transport of nutrients and the maintenance of biological production. In: Fasham, M (ed) Ocean Biogeochemistry: The role of the ocean carbon cycle in global change, Springer, pp. 19-51.

Wilson JL (1975) Carbonate facies in geologic history Springer, Berlin, New York, pp. 471.

Wilson MEJ, Vecsei A (2005) The apparent paradox of abundant foramol facies in low latitudes: their environmental significance and effect on platform development. Earth-Science Reviews 69:133-168.

Wing SL, Harrington GJ, Smith FA, Bloch JI, Boyer DM, Freeman KH (2005) Transient floral change and rapid global warming at the Paleocene-Eocene boundary. Science 310:993-996.

Youssef MM (2003) Structural setting of central and south Egypt: An overview. Micropaleontology 49, supplement 1:1-13.

Zachos J, Pagani M, Sloan L, Thomas E, Billups K (2001) Trends, rhythms, and aberrations in global climate 65 Ma to present. Science 292:686-693.

Zachos JC, Lohmann KC, Walker JCG, Wise SW (1993) Abrupt Climate Change and Transient Climates during the Paleogene: A Marine Perspective. The Journal of Geology 101:191-213.

Zachos JC, Wara MW, Bohaty S, Delaney ML, Petrizzo MR, Brill A, Bralower TJ, I Premoli-Silva (2003) A transient rise in tropical sea surface temperature during the Paleocene-Eocene Thermal Maximum. Science 302:1551-1554.

Zachos JC, Schouten S, Bohaty S, Quattlebaum T, Sluijs A, Brinkhuis H, Gibbs SJ, Bralower TJ (2006) Extreme warming of mid-latitude coastal ocean during the Paleocene-Eocene Thermal Maximum: Inferences from TEX86 and isotope data. Geology 34:737-740.

Zachos JC, Dickens GR, Zeebe RE (2008) An early Cenozoic perspective on greenhouse warming and carbon-cycle dynamics. Nature 451:279-283.

Zamagni J, Mutti M, Kosir A (2008) Evolution of shallow benthic communities during the Late Paleocene-earliest Eocene transition in the Northern Tethys (SW Slovenia). Facies 54:25-43.

Third manuscript

CIRCUM-TETHYAN CARBONATE PLATFORM EVOLUTION DURING THE PALAEOGENE – THE PREBETIC PLATFORM AS TEST CASE FOR CLIMATICALLY-CONTROLLED FACIES SHIFTS

Stefan Höntzsch [a], Johannes P. Brock [b], Christian Scheibner [a] and Jochen Kuss [a]

[a] *Department of Geosciences, Bremen University, PO Box 330440, 28359 Bremen, Germany*
[b] *Geo-Engineering.org GmbH, Hochschulring 40, 28359 Bremen*

To be submitted to Palaeogeography, Palaeoclimatology, Palaeoecology

VIII. CIRCUM-TETHYAN CARBONATE PLATFORM EVOLUTION DURING THE PALAEOGENE – THE PREBETIC PLATFORM AS TEST CASE FOR CLIMATICALLY-CONTROLLED FACIES SHIFTS

Abstract The distribution of selected shallow-benthic biota at circum-Tethyan carbonate platforms demonstrates an excellent proxy for the impact of latitudinal-controlled cooling and variations in the trophic resources during the Palaeogene. In this study we link and compare the spatial distribution and abundance of larger benthic foraminifera and hermatypic corals of Tethyan carbonate successions with new records from the Prebetic platform in SE Spain. The succession of the Prebetic platform is dominated by larger benthic foraminifera and coralline red algae throughout the Eocene, whereas corals were not recorded until the Late Eocene. High resolution carbon isotopes indicate conditions which are strongly decoupled from the global carbon cycle during the latest Eocene and Early Oligocene. A possible scenario is demonstrated by the increasing restriction of the Prebetic shelf due to the continuing convergence of the Betic domain towards Iberia during the Lower Oligocene.

Similar biotic trends were reported from ten selected circum-Tethyan carbonate platforms. Based on previous studies, we further develop earlier established Palaeogene platform stages, which pinpoint the evolution of shallow-benthic communities during the transition from global greenhouse to icehouse conditions. Global cooling yielded to the recovery of coral communities in the northern Tethyan realm during the Bartonian (stage IV). A prominent cooling event at the Bartonian-Priabonian boundary, associated with a demise of many symbiont-bearing larger foraminifera causes the proliferation of coral reefs in the northern Tethys and the recovery of corals in the southern Tethys (stage V). The massive temperature drop related to the Oi-1 glaciation represents the base of platform stage VI (Early Oligocene – ?). After a transient platform crisis during the lowermost Oligocene, coral reefs spread throughout the Tethys and proliferate with newley emerged larger benthic foraminifera.

VIII.1 Introduction

Carbonate platform systems represent an excellent example of ancient sediment archives, which provide crucial data regarding the reconstruction of continental margins. Platform evolution is influenced and controlled by multiple processes, including global and regional climate variability, global and local tectonics, eustatic sea-level variations and the changing dominance of platform biota through time. The interactions of those processes create highly dynamic and complex environmental scenarios. A main problem regarding the reconstruction of shallow-marine inner platform settings is the frequent subaerial exposure during sea-level lowstands, causing erosion, karstification and major hiati at the platform. To understand the evolution and the dynamics of carbonate platforms, mass flow deposits at the platform slope represent an excellent tool for the reconstruction of those systems. In contrast to the shallow-marine platform interior, mass flow deposits at the outer neritic and bathyal slope are less alterated and better preserved. Their composition and geochemical signature record environmental shifts from the remote platform interior, especially during times of climatic and tectonic instability.

The Palaeogene represents an epoch in Earth's history, which is characterized by high climatic variability and the reorganisation of major continental plates in the Mediterranean realm. The transition from the Early Cenozoic greenhouse to the Late Cenozoic icehouse, punctuated by multiple climatic perturbations is recorded by various environmental parameters and organisms at the marginal shelves (e.g. climatically-controlled facies shifts, shifts in the trophic regime, varying carbon isotope signatures). Furthermore, the continuing convergence of the African Craton and Eurasia, yielding to the reactivation and progradation of ancient fault systems, causes major incisions in the marginal marine environments in the Tethyan realm. Studying the impact of those pertubations on carbonate platforms will help to understand the dynamics of depositional processes at passive continental margins.

An excellent example for such a highly dynamic environment is represented by the South Iberian continental margin in the NW Tethys during the Palaeogene. The stratigraphic record of this passive margin reveals a complex framework of autochthonous and allochthonous units, which have been deformed during multiple phases of tectonic activity, culminating during the Miocene uplift of the Betic Cordillera. The pre-orogenic sedimentary record of the passive South Iberian margin contains a heterogenous suite of slope-related hemipelagites and shallow-marine platform carbonates. This succession has been studied intensively with respect to the tectono-stratigraphic evolution of the Betic domain since the Mesozoic. Various local studies reveal facies patterns and depositional processes, especially of the undisturbed marly successions of the deeper shelf. A coherent model of the detached carbonate platform regarding the fundamental biotic evolution during times of high climatic and tectonic variability is however missing. In this study we link and compare the data of ten

circum-Tethyan carbonate platforms with the succession of the South Iberian margin to achieve new information regarding timing and biotic impact of the Early Palaeogene greenhouse to Late Palaeogene icehouse transition. High resolution microfacies analysis of proximal and distal mass flow deposits, as well as new carbon isotope records will reveal the impact of long- and short-term climatic evolution to shallow-marine benthic assemblages, especially to larger benthic foraminifera and corals.

VIII.1.1 Climatic evolution during the Palaeogene

The Palaeogene is known as a period in Earth's history, which underwent fundamental long-term and transient climatic changes, resulting in the transition from a global greenhouse to icehouse conditions (Zachos et al., 2001). The Early Palaeogene (Paleocene – Middle Eocene) is characterized by global greenhouse conditions, culminating during the Early Eocene Climatic Optimum (EECO) between 53 – 49 Ma (Fig. VIII.1). Anomalous warm poles and low latitudinal temperature gradients caused strongly decreased ocean circulations with high oligotrophic open ocean conditions (Hallock et al., 1991; Gibbs et al., 2006). This Early Palaeogene "hothouse" is, however, superimposed by multiple transient climatic perturbations, which are attributed to significant negative shifts in the global carbon cycle ("hyperthermals" or Eocene Thermal Maxima [ETM]; Thomas and Zachos, 2000; Cramer et al., 2003; Lourens et al., 2005). The most prominent carbon cycle perturbation is the Paleocene-Eocene Thermal Maximum (PETM), resulting in a global transient temperature increase of 4 – 8°C and major environmental turnover in nearly all environments on Earth (e.g., Kennett and Stott, 1991; Beerling, 2000; Bowen et al., 2004).

The post-EECO climate is characterized by a cooling of higher latitudes, whereas the tropics remained warm (Pearson et al., 2007). The increasing latitudinal temperature gradients strengthened global ocean currents, causing the upwelling of cooler deep ocean waters and the eutrophication of the oceans (Hallock et al., 1991). The temperature decline during the Middle and Late Eocene is interrupted by the Middle Eocene Climatic Optimum (MECO) between ~41.5 – 40 Ma, affecting both surface and bathyal environments (Fig. VIII.1; Bohaty and Zachos, 2003, Bijl et al., 2010). This transient warming is however, not affected by a significant negative carbon isotope excursion (Jovane et al., 2007). The continuing cooling in the second half of the Eocene yielded to the occurrence of the first ephemeral Antarctic ice sheets in the second half of the Eocene. A major break in global climate since the end of the EECO is represented by the Oi-1 glaciation at ~34 Ma, coinciding with the Eocene-Oligocene boundary (Fig. VIII.1; Zachos et al., 2001, 2008; DeConto et al., 2008). A sharp global temperature drop is associated with a positive carbon isotope excurcion (CIE) of ~1 ‰ and a major biotic reorganization (Ivany et al., 2000; Zanazzi et al., 2007; Eldrett et al., 2009). The

Oi-1 glaciation demonstrates the onset of permanent Antarctic ice sheets and a strong demise in global carbonate platform systems. Thus, the Eocene-Oligocene boundary represents the final transition from climatic optimum conditions to icehouse conditions.

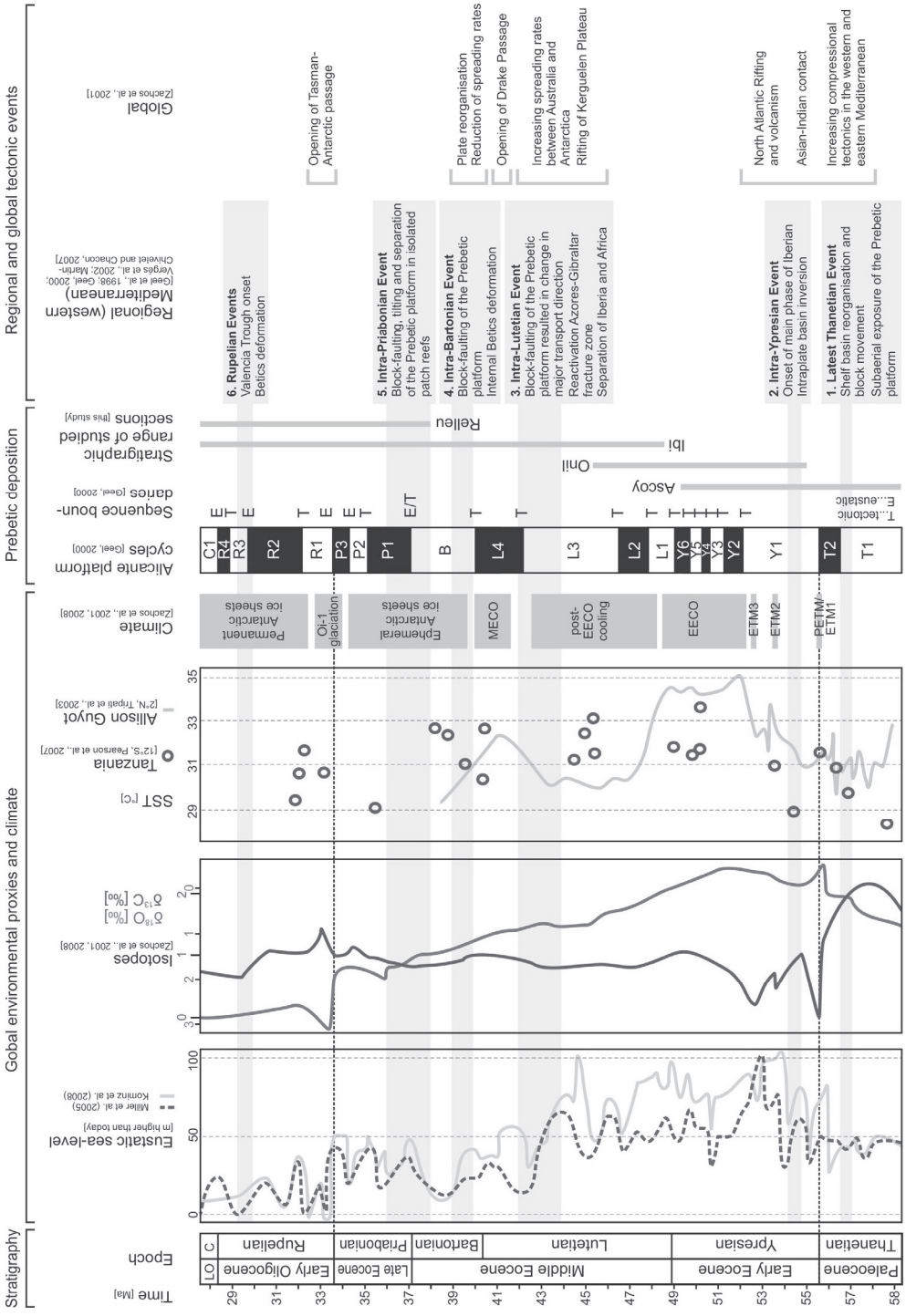

Figure VIII.1 – Global and regional climatic and tectonic evolution during the Palaeogene. The scheme includes the main depositional sequences and regional tectonic events (yellow bars) in the Prebetics (regional tectonic events according to Geel et al., 1998; Geel, 2000; Martin-Chivelet and Chacon, 2007). Abbreviations: LO – Late Oligocene. Alicante platform cycles of Geel (2000) are redefined regarding their stratigraphic occurrence: T – Thanetian, Y – Ypresian, L – Lutetian, B – Bartonian, P – Priabonian, R – Rupelian, C – Chattian.

VIII.1.2 Concepts on biotic shifts during Palaeogene platform evolution

The evolution of carbonate platform systems during the Palaeogene is strongly influenced by long term global climatic and tectonic turnover and transient perturbations. The spatial and quantitative distribution of platform-building organisms through time shows a clear connection to the environmental turnover in the Palaeogene (Hallock et al., 1991; McGowran and Li, 2001; Nebelsick et al., 2005). Timing and biotic effects of environmental transitions during the Palaeogene were raised in multiple bio-sedimentary concepts. Hallock et al. (1991) presented the first compilation of Palaeogene evolutionary events for larger benthic foraminifera and planktic foraminifera with respect to the effects of varying trophic resources in the oceans (trophic resource continuum). Hottinger (1997, 1998) and McGowran and Li (2001) link the evolution of Tethyan large neritic foraminifera to major changes in climate and define major Cenozoic LBF assemblages as chronofaunas (Fig. VIII.7). Brasier (1995) and Hottinger (2001) introduce the concept of global community maturation cycles (GCMC) for LBF. According to this approach, LBF evolution can be classified in four (Brasier) or five (Hottinger) phases of increasing habitat adaption and improving life strategies. Both authors suggest that each GCMC is terminated by a mass extinction.

The described concepts have been applied to selected critical intervals during the Palaeogene. Scheibner and Speijer (2008a) show that the global warming during the early Palaeogene caused a Tethyan-wide massive decline in coral reefs and a coeval shift to LBF dominated carbonate platforms. The authors define circum-Tethyan platform stages (Figs. VIII.6 and VIII.7) and link the evolutionary impact of the larger foraminifera turnover (LFT, Orue-Etxebarria et al., 2001) at the Paleocene-Eocene boundary directly to the Paleocene-Eocene Therma Maximum (PETM). Nebelsick et al. (2005) summarize changes of specific carbonate facies types in the circum-alpine area during the Middle Eocene to Oligocene and introduce the concept of facies dynamics. The authors argue that major carbonate platform organisms are controlled by phylogenetic, ecological and geological parameters.

The following paragraphs summarize the main steps in Palaeogene carbonate platform evolution with respect to the introduced concepts.

<u>Paleocene</u>

The global ocean crisis during the Cretaceous-Palaeogene transition at 65.5 Ma yielded to a massive specific decline in global shallow-benthic assemblages. Transient nutrient excess shortly after the Cretaceous-Palaeogene extinction shifted to increasing oligotrophy in the oceans during the Early Paleocene (Hallock et al., 1991). A long-term sea-level rise during the Early Paleocene created new shelf areas and vacant biological niches (Buxton and Pedley, 1989). The created vacant niches were occupied by LBF and corals, which became to a major part of shallow-benthic assemblages (1st phase of GCMC; Hottinger, 2001). At

around 60 Ma new LBF with complex morphologies appeared (2nd phase of GCMC; Hallock et al., 1991; Hottinger, 1998, 2001). Increasing oligotrophic conditions and a prominent sea level fall at 58.9 Ma (Hardenbol et al. 1998) favoured the proliferation of hermatypic coral built-ups throughout the Tethys (Tethyan platform stage I; Scheibner and Speijer, 2008a, 2008b). Increasing global temperatures at the end of the Paleocene caused a decline of many low-latitude coral communities (Tethyan platform stage II; Scheibner and Speijer 2008a, 2008b). The open niches were occupied by LBF. Platform stage II represents a transitional episode between coralgal and larger foraminifera dominance in the Tethyan realm. In the northern Tethyan and Peri-Tethyan realm coralgal assemblages still dominate the platfrom margin, whereas in lower latitudes (0 – 20°) first larger foraminifera communities, composed of ranikothalids and miscellanids proliferate. Duration is restricted to shallow benthic zone 4 (SBZ 4, Serra-Kiel et al. 1998).

Early Eocene

The Paleocene-Eocene boundary represents a major caesura in the evolution of shallow-marine benthic communities. The massive transient temperature peak during the PETM caused a Tethyan-wide decline of coral communities. Newly arisen LBF species are characterized by an increase in K-strategy, a significantely larger shell size, a longer life span and an adult dimorphism (Hottinger, 1998). Paleocene ranikothalids and miscellanids are replaced by Eocene nummulitids and alveolinids (Scheibner et al., 2005). This evolutionary trend, known as larger foraminifera turnover (LFT) is directly linked to the negative CIE of the PETM, Orue-Extebarria et al., 2001; Scheibner et al. 2005). Carbonate shelves were now dominated by photo-autotrophic LBF assemblages throughout the Tethys (3rd phase of GCMC; Hottinger, 2001; Tethyan platform stage III; Scheibner and Speijer, 2008a 2008b). Multiple Early Eocene hyperthermal events with a similar environmental impact as the PETM as well as an increasing warming culminating in the EECO (52 – 49 Ma; Zachos et al., 2001), prevented the recovery of temperature-sensitive Tethyan coral assemblages after the PETM. Studies from the Egyptian carbonate shelf suggest, that the impact of post-PETM hyperthermal events were of minor extent but may coincide with a peak in the specific diversity of larger foraminifera K-strategists (Hottinger, 1998; Höntzsch et al., in press). Furthermore, the size of LBF increased significantely from the Middle Ypresian to the Bartonian (4th phase of GCMC; Hottinger, 2001).

Middle Eocene

The global cooling subsequent to the terminantion of the EECO at ~49 Ma mainly affected higher latitudes, whereas equatorial realms remained stable warm (Pearson et al., 2007). However, specific diversity of K-strategist LBF continuously decreases from the base of the

Lutetian to the Priabonian (Hallock et al 1991; Hottinger, 1998). The extinction of Assilina in Lower Bartonian represents the termination of the Early Palaeogene GCMC (5th phase; Hottinger, 2001).

A transient period with increasing abundance of LBF K-strategist taxa is present during the Lower Bartonian and represents the onset of a new GCMC (Hottinger, 2001). This interval coincides with the transient warming during the Middle Eocene Climatic Optimum (MECO; Bohaty and Zachos, 2003; Bijl et al., 2010).

The Lower Bartonian is characterized by prevailing oligotrophic conditions at the shelves (Nebelsick et al., 2005). The general cooling trend favoured the recovery of patchy coral communities in higher latitudes (Perrin, 2002a). However, increasing latitudinal temperature gradients enforced the global ocean circulation yielded to strengthen upwelling regimes and a high biosilicious activity in the oceans (Cervato and Burckle, 2003).

Late Eocene

A significant global temperature drop in the uppermost Middle Eocene (Middle/Late Eocene cooling event; McGowran 2009) accompanied by prevailing meso- to eutrophic conditions at the shelfs caused a shift in the prevailing shallow-benthic facies assemblages and a prominent demise of K-strategists (Hallock et al 1991; Hottinger, 2001). Oligotrophic symbiont-bearing LBF (larger nummulitids, alveolinids and acervulinids) were replaced by meso- to eutrophic coralline algae (Priabonian chronofauna; McGowran and Li, 2001; Nebelsick et al., 2005). Early Palaeogene LBF which survived into the Oligocene are mostly represented by non-photosymbiontic smaller miliolids (Nebelsick et al., 2005). Despite the increasing availability of nutrients at the shelves, the recovery of coral communities continues especially in the northern Tethyan realm (Nebelsick et al., 2005).

Early Oligocene

The tectonic and climatic isolation of Antarctica during the latest Eocene caused a massive temperature drop and the onset of perennial icesheets at Antarctica (Oi-1 glaciation; Ivany et al., 2000; Zachos et al., 2001; Eldrett et al., 2009). Continuing cooling is accompanied by a strengthend ocean circulation and enhanced upwelling regimes (Hallock et al., 1991). This climtatic and evironmental caesura caused the extinction of LBF which survived the Middle/Late Eocene cooling event (e.g., discocyclinids; early Palaeogene *Nummulites*; Hallock et al., 1991; Prothero, 2003). The newly created niche favoured the evolution of modern LBF taxa and a slow diversification of Tethyan coral faunas (Hallock et al., 1991; Nebelsick et al., 2005). Newly emerged LBF are represented by lepidocyclinids (FO lowermost Rupelian) and miogypsinids (FO ?Chattian). Meso- to eutreuphic ocean conditions shifted to more oligotrophic habitats during the upper Rupelian (Hallock et al., 1991).

VIII.1.3 Regional geological framework

Tectono-stratigraphy at the south Iberian margin

The South Iberian continental margin underwent repeated changes and deformation since the Mesozoic, culminating with the uplift and deformation of the Betic Cordillera orogen in the Early Miocene (Fontboté and Vera, 1983; Blankenship, 1992; Geel et al., 1998; Alonso-Chaves et al., 2004). Classical tectono-stratigraphic classifications discriminate an external zone, representing the autochthonous deposits of the South Iberian margin, and an internal zone, characterized by an allochthonous unit which underwent repeated metamorphism prior to the Early Miocene orogeny.

The External Zone comprises a heterogenous suite of Mesozoic and Early Cenozoic passive continental margin deposits (Garcia-Hernandez et al., 1980; Everts, 1991). Those Triassic to Early Miocene sediments are detached from the Palaeozoic basement and have been thrusted northward onto the southern margin of the Iberian Craton (Blankenship, 1992). The deposits of the External Zone are subdivided into three units with respect to their position at the shelf: the Prebetic domain represents the shallow-marine shelf of the South Iberian margin, which is strongly affected by sea-level variations and terrigenous input from the Craton. Vast areas of the northern Prebetic were covered by a carbonate platform. The platform system represents a NE-SW striking belt of heterogenous shallow-marine sediments, which were attached to the Iberian Massif. The southern Prebetic is rather influenced by hemipelagic deposition and frequent mass flows (Fig. VIII.3). The contact between the lagoonal Prebetic platform (External Prebetic) and the hemipelagic Prebetic realm (Internal Prebetic) is referred to a major palaeogeographic barrier, called the Franja Anomala (e.g. de Ruig et al., 1991).

The Subbetic domain is characterized by deeper shelf deposits without major terrigenous influence. The contact between Prebetic and Subbetic domain points to a major thrust fault (e.g. Garcia-Hernandez et al., 1980). Besides the Prebetic and Subbetic domains, a third tectonostratigraphic unit is represented by the Guadalquivir allochthonous unit, which is characterized by the Neogene deposition of olistostromes and gravitational nappes from the Subbetic domain (García Rossell, 1973, Garcia-Hernandez et al., 1980).

The Internal Zone or Betic domain is characterized by a heterogenous stack of allochthonous complexes, containing thrust sheets of metamorphous Palaeozoic rocks (Geel 1996). It is part of the Alboran microplate, which collied with Africa and Eurasia during its westward migration, causing the uplift of the Betic Cordillera (Fig. VIII.2; Andrieux, 1971; Bouillin et al., 1986).

Tectonically-controlled platform evolution during the Palaeogene

During the Early Palaeogene the reactivation of major fault systems causes multiple phases of depositional instability and shelf reorganisation (Martin-Chivelet and Chacon, 2007). A first tectonic phase is demonstrated for the Late Thanetian (Latest Thanetian Event, ~57 Ma; Martin-Chivelet and Chacon, 2007) when far-field stress of strong compressional tectonics in the Pyrenean orogeny caused major block movement and a reorganization of the South Iberian shelf basin. During that interval a major depositional unconformity at the Prebetic platform indicates widespread subaerial exposure of the shallow-marine shelf. An acceleration of the collisional tectonics of Africa and Iberia as well as the onset of the main orogenic phase in the Pyrenees resulted in a second tectonic phase during the Middle Ypresian (Intra-Ypresian Event ~54.5 Ma; Martin-Chivelet and Chacon, 2007). During the late Lutetian (Intra-Lutetian Event, 44 – 42 Ma) a third tectonic phase resulted in the change of the major sediment transport direction along the platform from N-S to NE-SW and a significant progradation of the platform margin towards the S (Kenter et al., 1990). This tectono-sedimentary perturbation is caused by the reactivation of the Azores-Gibraltar Fault Zone and the separation of Iberia from Africa. The continuing convergence between Africa and Eurasia caused a fourth phase during the Bartonian (Intra-Bartonian Event, 40 – 39 Ma), resulting in the tilting of the Prebetic platform. A fifth phase of major tectonic activity during the Late Eocene resulted in complex block-faulting of the platform and its separation into several isolated fault-bounded patch reefs with different subsidence levels and complex block topography (Intra-Priabonian Event; De Ruig et al., 1991; Geel, 1996; Geel et al., 1998). During the Oligocene two more phases of tectonic activity have been suggested but not described in detail (Rupelian Events). Those events are probably related to the onset of the Valencia Trough and a phase of deformation in the Internal Betics (Lonergan, 1993; Torres et al., 1993; Geel et al., 1998; Maillard and Mauffret, 1999).

The phases of major tectonic activity reveal a significant cyclicity in the depositional record of the South Iberian margin throughout the Palaeogene but especially during the Eocene. Geel et al. (1998) distinguish fourteen 3rd-order cycles in the Prebetic realm from the latest Paleocene to the latest Eocene. Those cycles are mainly controlled by the tectonic processes, related to the African-Eurasian collision and the far field impact of Pyrenean orogeny. However, the beginning glaciation of the southern hemisphere at the late Middle Eocene increases the glacio-eustatic impact to the depositional record significantly.

Regional climate of Iberia during the Palaeogene

The Iberian Peninsula is characterized by a stable microclimate due to a strong influence of the Tethys in the south and emerging prominent orogenic system in the North (Postigo Mijarra et al., 2009). Early Cretaceous to Early Eocene conditions on the Iberian Peninsula

are characterized by a tropical climate with seasonal rainfalls, evidenced by palaeotropical forests with a high floral diversity (Lopez-Martınez, 1989; Gawenda et al., 1999; Adatte et al., 2000; Bolle and Adatte, 2001; Postigo Mijarra et al., 2009). The impact of multiple Palaeogene hyperthermal events has been recorded in the Pyrenees (Angori et al., 2007; Scheibner et al., 2007; Alegret et al., 2009), the Basque Basin (Schmitz et al., 2001; Schmitz and Pujalte, 2003) and the Betic realm (Alegret et al., 2010).

Large scale tectonic reorganization and the onset of the first ephemeral ice sheets in the southern hemisphere forced a global regression during the second half of the Eocene. This regression yielded to an increasing aridity and continentalization of the Iberian-Eurasian climate (Lopez-Martinez, 1989).

VIII.2 Methods

Selected sections along a platform to slope transect were recorded in order to establish a high resolution data set of various environments at the carbonate platform, comprising of selected samples of mass flow deposits and hemipelagic background sediments. Sample analysis focusses on three main approaches:

a) A detailed microfacies analysis of selected limestone samples based on the main platform organisms (larger benthic foraminifera, corals, algae) reveals the vertical and lateral evolution of the Prebetic carbonate platform through time. The spatial and temporal distribution of mass flow deposits along the slope allows recognizing high frequent sea level fluctuations and changes in the source area and transport direction of mass flows. Furthermore, intervals of increased tectonic activity in the hinterland can be recognized by increased amounts of detrical quartz grains.

b) Main platform organisms indicate multiple climatically-controlled facies shifts through the Palaeogene. The record of those evolutionary trends and perturbations helps to locate major phases of Palaeogene carbonate platform evolution, which have been explained and evaluated in different conceptional palaeontological studies. The application of those appraoches to the recorded succession of the Prebetic platform will help to refine and expand concepts and classifications regarding the evolution of shallow-benthic assemblages during the Palaeogene.

c) Limestones and marls from the lower slope section of Relleu were analysed with respect to record the long-term geochemical and carbon isotope evolution of a marginal shelf environment during times of major tectonic and climatic turnover. Bulk rock carbon isotopes ($\delta^{13}C$), total organic carbon (TOC) and calcite carbonate ratios were recorded and compared with data from open ocean and similar marginal

environments (Thomas et al., 1992; Zachos et al., 2001) in order to reveal either a coupling of the Prebetic platform to the global carbon cycle or the impact of regional processes which influence the Prebetic platform.

VIII.3 Study area and data set

The Prebetic domain extends as 130 km long and 60 km wide NE-SW striking fault-bounded block north and west of Alicante (Fig. VIII.3). It represents the NE most part of the Betic Cordillera in SE Spain. North of the Prebetic domain the Albacete low subsiding domain characterizes the southern branch of the Iberian Massif. The Balearic Islands probably reflect a continuation of the Prebetics prior to the Late Oligocene to Neogene opening of the Balearic Sea (Doblas and Oyarzun, 1990).

The Prebetic platform represents the NE most part of the External Betics. Outcrops of the Palaeogene platform interior are rare due to frequent erosional and tectonic unconformities as well as intense karstification. Generally, sea level lowstands are missing in the depositional record on the platform (Geel, 2000). In the SW most part of the Prebetic domain, various isolated mountain ranges expose Palaeogene rocks, reflecting the transition from inner shelf to the hemipelagic outer shelf (Carche, Benis, Enmedio; see Kenter et al., 1990). Outcrops along the deeper and more hemipelagic shelf are frequent in the areas of Relleu, Penaguila, Torremanzanas and Benifallim (e.g. Everts, 1991; Geel, 2000) as well as the Agost section, representing the Internal Prebetics (e.g. Molina et al., 2000; Ortiz et al., 2008; Monechi and Tori, 2010).

Most of the sections have been described and interpreted by various authors by means of different approaches. However, high-resolution microfacies and geochemical data are not available yet. Especially the evolution of the platform interior and the impact of the environmental perturbations during and after the Paleocene-Eocene boundary are still not described for the Prebetic platform. Thus we recorded the new section of Ascoy in the SW part of the Prebetic platform and the classical sections of Onil, Ibi and Relleu for detailed microfacies and biotic assamblage analysis, re-interpretation and comparison with other studies in order to achieve a coherent platform model with respect to depositional processes, climatic variability and tectonic impact.

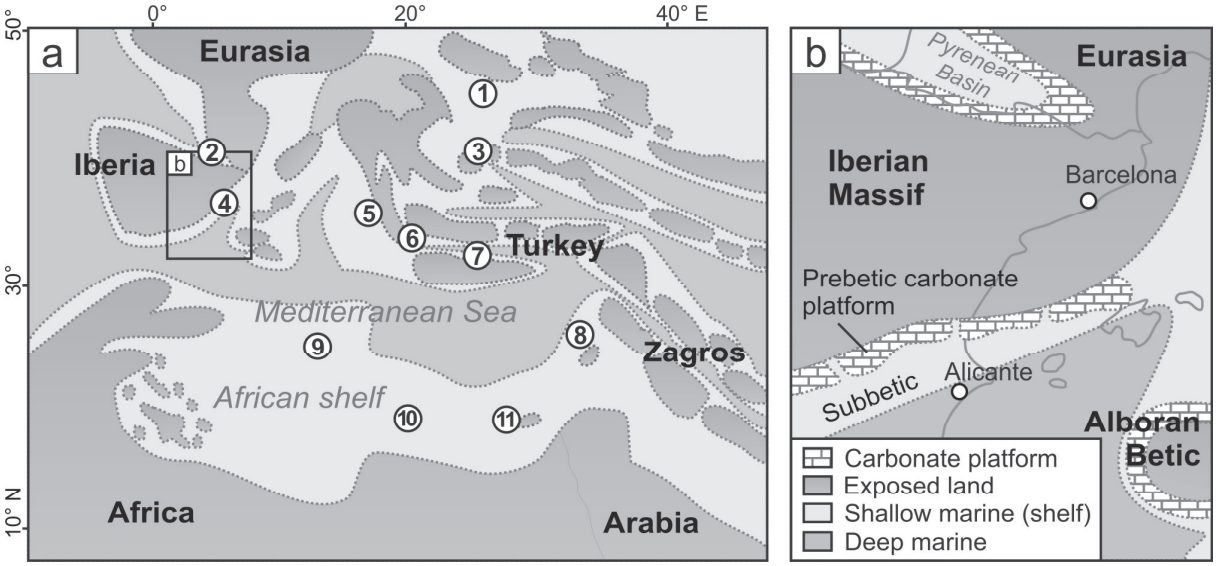

Figure VIII.2 a – Simplified palaeogeographic reconstruction of the Mediterranean realm in Early to Middle Eocene (Ypresian - Lutetian). Numbers indicate selected Eocene-Oligocene carbonate platform systems: 1) Northern Calcareous Alps, 2) Pyrenees, 3) North Adriatic platform, 4) Prebetic platform, 5) Maiella platform, 6) Greece, 7) Turkey, 8) NW Arabian platform (Syria, Israel), 9) Tunisia, 10) Libya (Sirte Basin), 11) Egypt (Galala platform). The position of the continents and ocean basins is adapted and expanded from Ziegler (1992), de Galdeano (2000), Meulenkamp and Sissingh, (2000, 2003) and Thomas et al. (2010). **VIII.2 b** – Early Palaeogene reconstruction of southern Iberian continental margin and the adjacent Alboran microplate, representing the (Internal) Betic domain.

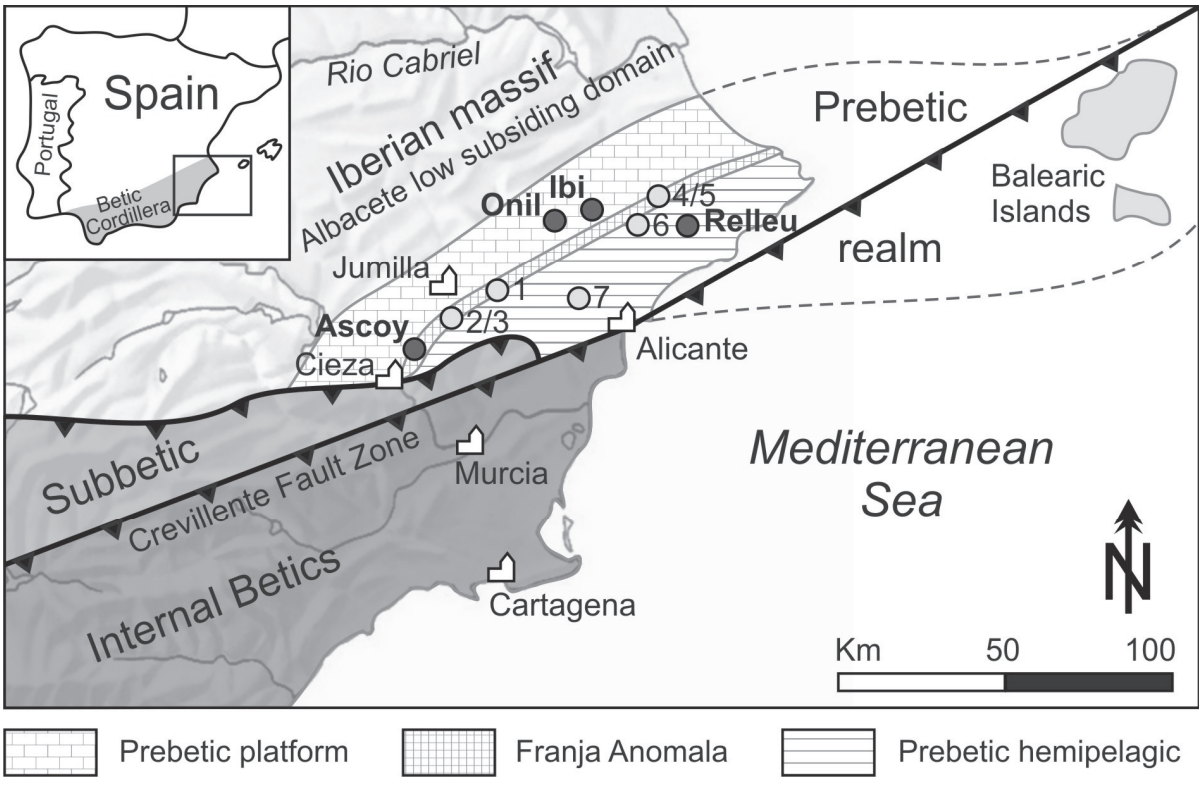

Figure VIII.3 – Location map of the eastern Betic Cordillera, including the main tectono-sedimentary units, major tectonic lineaments and selected sections (modified after Martin-Chivelet and Chacon, 2007). The contact between the Prebetic platform and the Prebetic hemipelagic realm is referred to the Franja Anomala (e.g. de Ruig et al., 1991). Red circles indicate the location of the studied section; grey circles demonstrate previously studied Palaeogene sections of other authors (1 – Carche, 2/3 – Benis/Caramucel, 4/5 – Penaguila/Torremanzanas, 6 – Benifallim, 7 – Agost).

VIII.3.1 Sections

We studied four sections of the Prebetic platform which are excellent examples for the coupled tectono-climatic impact on shallow-marine benthic assemblages during the transition from an Early Palaeogene greenhouse to Late Palaeogene icehouse conditions.

Ascoy (Paleocene – ?Middle Eocene, ~120 m total thickness)

The Sierra d'Ascoy represents a WSW-ENE striking mountain range NE of Cieza. The depositional sequence encompasses Lower Cretaceous to Miocene hemipelagic marls and carbonates, which are interrupted by several erosional unconformities (Kenter et al., 1990). Palaeogene rocks occur as a continuative suite of Paleocene to Middle Eocene carbonates of the platform interior, which merge into a transitional marine-continental facies during the Bartonian. Limestones comprise of larger benthic foraminifera, corals and coralline red algae. Few intervals show significant amounts of quartz grains. Paleogeographic reconstructions of the Palaeogene integrate the succession of Ascoy to the Franja Anomala (Martinez del Omo, 2003).

Onil (Lowermost Eocene – Middle Eocene, ~210 m total thickness)

At the section of Onil (~35 km N Alicante) limestones and marls which cover the lowermost Eocene to Middle Eocene are exposed. The rocks show a high abundance of larger benthic foraminifera (especially nummulitids and alveolinids) and reflect middle inner shelf settings during the Palaeogene. Geel (2000) describes eight depositional cycles, which are arranged in an overall shallowing-upward succession. The discrimination of the cycles is based on qualitative and quantitative variations in larger benthic foraminifera species as well as on detected erosional surfaces and hardgrounds. Few karstification horizons indicate temporarily subaerial exposure during sea-level lowstands. The upper interval of the section is represented by dolomitized limestones.

Ibi (Middle Eocene – Early Oligocene, ~360 m total thickness)

The section of Ibi represents a continuous succession of steep tilted Middle Eocene to Middle Oligocene limestones and dolomites with rare marl intercalations. The section is situated about 35 km N of Alicante and about 10 km NE of the section Onil. Geel (2000) describes eight Eocene cycles and four Oligocene cycles. The succession of Ibi is interpreted as platform interior or backreef environment and corresponds to the section of Onil (Geel, 2000).

Relleu (Upper Eocene – Upper Oligocene, ~215 m total thickness)

The road-cut section of Relleu is situated ~35 km NE of Alicante and encompasses an alternating succession of hemipelagic marls and mass-flow related limestones. Limestones show a great variety of depositional textures (normal grading, flute casts, rip-up clasts) which indicate a turbiditic origin. Furthermore frequent reworked larger benthic foraminifera from the inner platform (e.g. nummulitids, alveolinids) and autochthonous forms of orthophragminids are recorded. *Zoophycus* traces indicate a palaeo-water depth of ~300 m which refers to the lower slope (Seilacher, 1967; Everts, 1991). The succession of Relleu encompasses three depositional sequences during the Eocene and five depositional sequences during the the Oligocene (Geel, 2000).

The Eocene-Oligocene boundary and planktic foraminifera zone P18 are not recorded in the Relleu section. Geel (2000) relates this hiatus to a major erosional unconformity, caused by the massive glacio-eustatic regression during the Oi-1 glaciation.

VIII.4 Results

VIII.4.1 The Palaeogene succession of the Prebetic platform

The four recorded sections represent a continuous succession of Paleocene to Late Oligocene platform deposits and hemipelagic marls. Depositional cycles at the Prebetic platform compiled by Geel et al. (1998) and Geel (2000) are renamed and used to describe the stratigraphic range of the recorded stratigraphic intervals (Fig. VIII.1). The recorded sections can be correlated by their biostratigraphic range or major tectono-depositional intervals (Fig. VIII.4).

Paleocene (Thanetian)

Paleocene rocks are only recorded at the Sierra d'Ascoy in the SW part of the Prebetic platform. The succession consists of massive fossiliferous limestones with high abundances of smaller rotaliid foraminifera, orthophraminids (*Discocyclina* sp.), coralline red algae (e.g. *Distichoplax biserialis*), echinodermal fragments and highly disintegrated bioclasts. Smaller benthic foraminifera (miliolids) are rare. Detrital quartz accumulations up to 20 % are reported from a 15 m thick massive siliciclastic limestone interval in the upper Thanetian (Fig. VIII.4; cycle T1). The quartz-bearing interval is followed by limestones with high abundances of hermatypic corals (cycle T2).

The Paleocene-Eocene transition is represented in a significant shift in the shallow-benthic faunal assemblage. Small rotaliids are replaced by larger endosymbiont-bearing nummulitids (*Operculina* sp., *Nummulites* sp.) and alveolinids (*Alveolina* sp.).

Lower Eocene (Ypresian)

Lower Eocene rocks are recorded in the sections of Ascoy and Onil. The basal Eocene succession of Ascoy is dominated by massive fossiliferous limestones with abundant large nummulitids, alveolinids, orthophragminids and echinodermal fragments. Red algae are only common in the basal part of the lower Eocene succession of Ascoy (cycle Y1). Hermatypic corals are not recorded. In the section of Ascoy a significant quartz-bearing limestone bed in the middle Ypresian is strongly enriched in LBF, shell fragments and red algae (cycle Y1). During the upper Ypresian fossiliferous limestones are replaced by marls with a thickness up to 20 m (cycle Y2). Marls are intercalated by prominent 3 – 5 m thick massive limestone beds with reworked limestone nodules and high abundances of inner platform organisms (LBF, coralline red algae and echinodermal fragments).

The Lower Eocene succession of Onil is characterized by alternating highly fossiliferous limestones and marls. The recorded rocks are dominated by nummulitids (*Assilina* sp., *Nummulites* sp. and *Operculina* sp.), alveolinids (*Alveolina* sp.), orthophragminids (*Discocyclina* sp.) and echinodermal fragments. Soritids (*Orbitolites* sp.), miliolids and serpulid worm tube occur in varying amounts and accumulate in distinct intervals. Coralline red and green algae are rare. The dominance of orthophraminids decreases significantely during the middle Ypresian.

Middle Eocene (Lutetian – Bartonian)

Middle Eocene rocks are recorded from the sections of Onil and Ibi and can be discriminated in three major intervals. The basal Middle Eocene succession is characterized by partly dolomitized and quartz-rich limestones and marls without major fossil accumulations in the section of Onil but high fossil content in the section of Ibi (cycles L1 – L3).

Major benthic organisms in the limestones of Ibi are *Discocyclina* sp., *Nummulites* sp., *Alveolina* sp., and *Assilina* sp.; miliolids and soritids occur in varying amounts. The abundance of orthophragminids and nummulitids decreases significantely towards the upper part of the Middle Eocene succession (cycle L3). During cycle L4 an up to 30 m thick interval of massive to thick bedded quartz-rich limestones and debris flow deposits with reworked limestones nodules and multiple erosional unconformities represents a major break in the deposition at the platform. Depostion after this mass wasting event is characterized by thick bedded low fossiliferous nodular and dolomitized limestones (upper cycle L4/B). First specimen of *Solenomeris* sp. are recorded in cycle B. The monotonous deposition is interrupted by a 2 – 4 m thick interval of quartz-rich limestones (cycle B).

Upper Eocene (Priabonian)

Upper Eocene rocks are recorded from the sections Ibi and Relleu. In contrast to the low fossiliferous upper interval of the Middle Eocene, the Upper Eocene successions of both sections demonstrate limestones and marls with high amounts of LBF (*Nummulites* sp., *Discocyclina* sp., *Solenomeris* sp.), smaller foraminifers (miolids) and bioclastic debris from the platform interior (gastropods, shell debris, echinoids, coralline red algae). The first recorded specimen of *Heterostegina* sp. as well as the first Eocene coral fragments occurs in cycle P1. A 10 – 15 m thick interval of unconformitve bounded highly fossiliferous and partly quatz-rich limestones is recorded during cycle P1.

Lower Oligocene (Rupelian)

The Eocene-Oligocene boundary is only recorded at the section of Ibi and refers to major shift in the benthic assemblages. Post-Eocene shallow-benthic organisms are characterized by the first occurrence of lepidocyclinids (*Eulepidnia* sp.) and heterosteginids (*Heterostegina* sp.). Many Eocene LBF (e.g., *Nummulites* sp*., Discocyclina* sp., *Solenomeris* sp.) are not recorded from the Eocene-Oligocene boundary onwards, whereas miliolids and coralline red algae become more abundant. During cycle R2 first hermatypic coral fragments are recorded since the lowermost Eocene. In the section of Relleu at least three intervals with increased deposition of debris flows and quartz-rich limestones are recorded (cycle R2 – R4).

Upper Oligocene (Chattian)

The Upper Oligocene is only recorded in the uppermost intervals of the Relleu section and comprises of marls and fossiliferous limestones. Limestones are rich in LBF (*Eulepidina* sp., *Heterostegina* sp.), red algal fragments and coral debris.

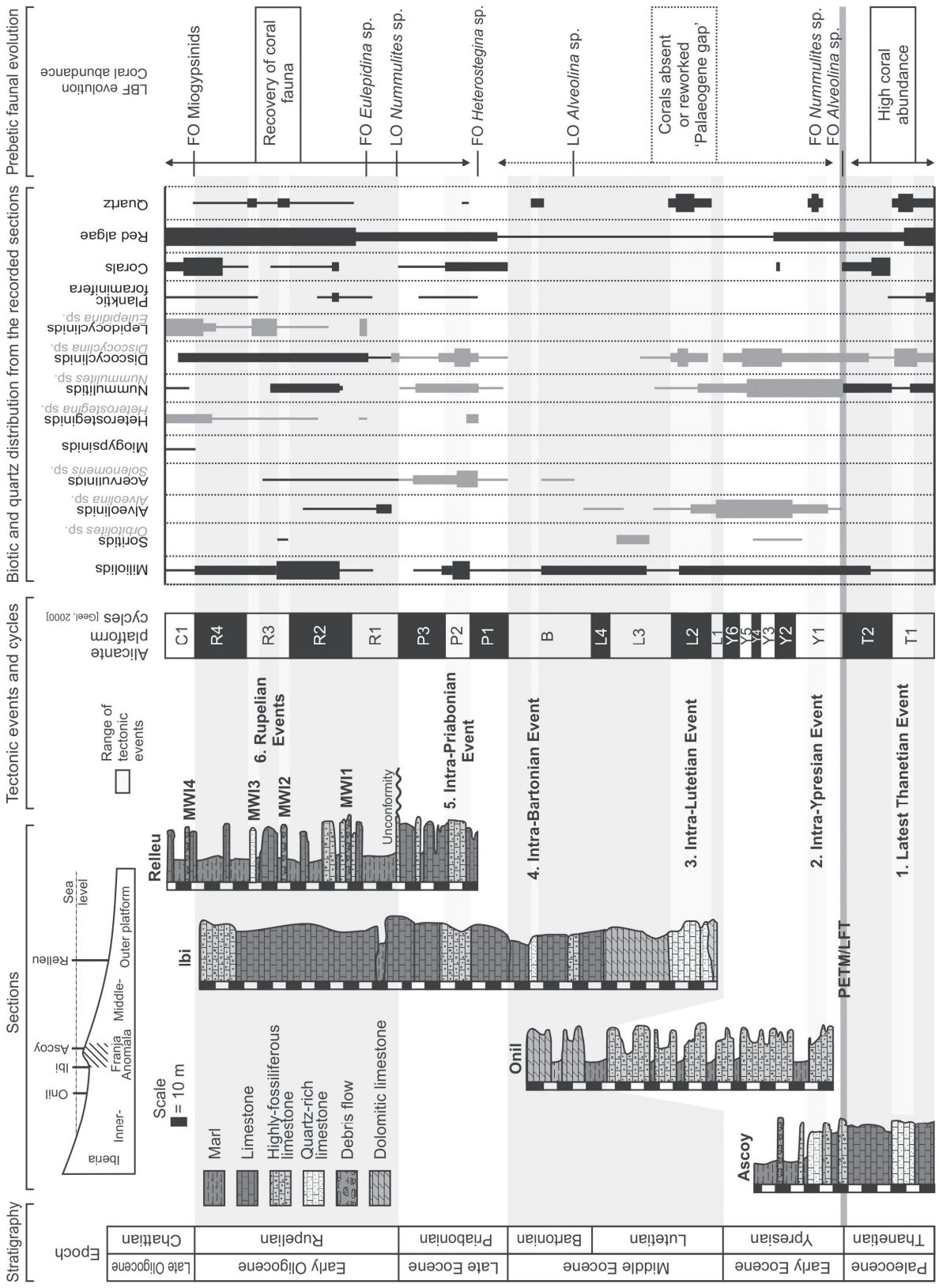

Figure VIII.4 – Faunal evolution of the Prebetic carbonate platform during the Palaeogene. The occurrence of selected LBF specimen, corals, red algae and quartz of four sections is summarized in order to demonstrate possible evolutionary turnover or extinctions. Paleocene to Early Oligocene faunal evolution can be subdivided into three main intervals: a Paleocene coral-dominated interval, an Early- to Middle Eocene interval without coral records and LBF-dominated assemblages, and a Late Eocene – Oligocene interval with increasing coral abundance but prevailing LBF assemblages. Abbreviations: FO – first occurrence, LO – last occurrence, MWI – mass wasting intervals (only for section Relleu), LFT – larger foraminifera turnover.

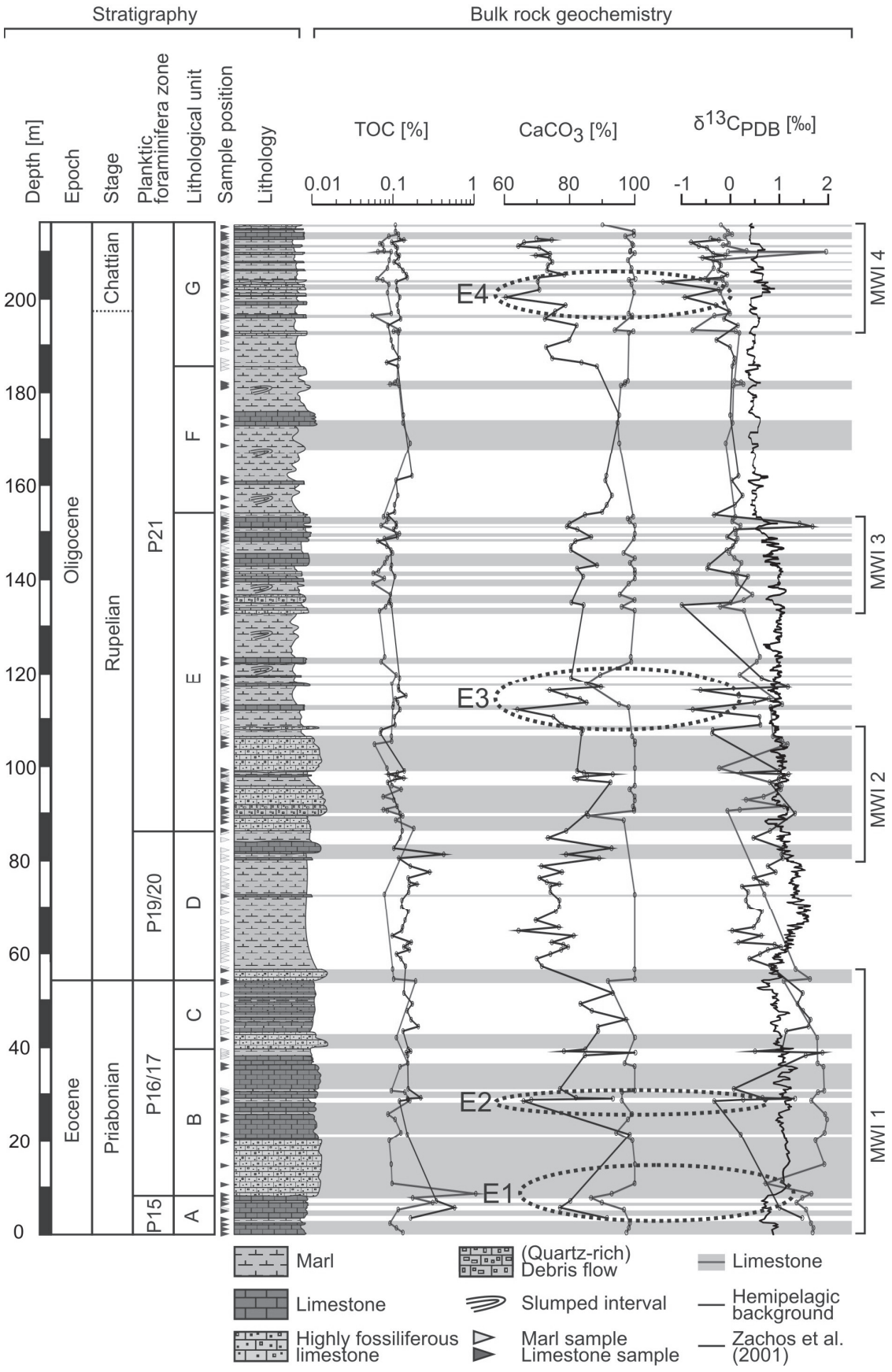

Figure VIII.5 – Bulk rock carbon isotopes and geochemistry for the Upper Eocene – Lower Oligocene outer ramp succession of Relleu. Data for hemipelagic background marls and limestones are plattet separately in order to show possible differences in source area and carbon burial. Gray bars indicate limestones. Mass wasting intervals (MWI) refer to periods of frequent turbidite deposition.

VIII.4.2 Carbon isotope stratigraphy and geochemical evolution

The long-term bulk rock carbon isotope trend was recorded for the Upper Eocene (Priabonian) – Upper Oligocene (Chattian) lower slope succession of Relleu (Fig. VIII.5). Carbonates and hemipelagic marls were examined separately in order to study possible variations between the platform-derived turbidites and basinal hemipelagites.

Carbon isotopes

Marls: Bulk rock carbon isotopes from the recorded hemipelagic background deposits (marls) range from -1.5 ‰ to 1.5 ‰. The discrimination of significant trends is doubtful due to highly fluctuating carbon isotope ratios. The Priabonian is characterized by a prominant shift from positive to negative $\delta^{13}C$ ratios, culminating with a negative excursion of -0.5 ‰ and a fast recovery to 1 ‰ (E2; Fig. VIII.5). From the latest Priabonian to the Rupelian the carbon isotope signature shifted from overall positive to negative ratios, superimposed by numerous minor positive and negative excursions. The depositional significance of those excursions is doubtful due to frequent slumping in the marl intervals. Chattian carbon isotopes ratios are characterized by a continuing shift towards negative $\delta^{13}C$ ratios with negative excursions in the lowermost interval of -1.5 ‰ (E4; Fig. VIII.5).

Limestones: The Priabonian is characterized by relatively stable positive $\delta^{13}C$ ratios (~1.5 ‰) with a negative excursion in the lower mass wasting interval 1 (MWI 1; E1; Fig. VIII.5). Carbon isotopes from the recorded Priabonian limestones indicate strong variations compared to the $\delta^{13}C$ of the measured hemipelagic marls. During the uppermost Priabonian carbon isotope ratios shift to more negative ratios in the limestones. This trend continues during the Rupelian with minor excursions during MWI 2. During the upper Rupelian and Chattian $\delta^{13}C$ ratios of both marl and limestone units converge and show only minor variatons.

Calcium carbonate ratios

Marls: Bulk rock calcium carbonate ratios vary significantely between the recorded limestones and marls. During the upper Priabonian (P16/17) marls show $CaCO_3$ ratios between 80 % and 96 % with transient drop to ~65 % (28 m above the basis of the section). This significant excursion correlates with a negative carbon isotope peak.

The Eocene-Oligocene transition is marked by a 10 % - 15% drop in the calcium carbonate ratios of the hemipelagic background marls. Average $CaCO_3$ ratios range from 70 % to 80 % in the lowermost Rupelian (P19/20) and increase to ~90 % during P21. During lower P21 a transient $CaCO_3$ drop from ~90 % to 63 % correlates with two minor negative carbon isotope peaks (E3; Fig. VIII.5). The calcium carbonate trend in the upper Rupelian and lowermost Chattian (upper P21) is characterized by a continuous decrease from >90 % to <70 %.

Limestones: The recorded limestones show only minor fluctuations in the $CaCO_3$ content with ratios between 95 % - 100 %. Three intervals with transient calcium carbonate drops to 85 % are recorded at the basis of P16 (E1; Priabonian), at the basis of P21 (Rupelian) and in the lower part of P21 (E3).

Total organic carbon (TOC)

Bulk rock TOC ratios neither show significant trends in the marls nor in the limestones throughout the recorded succession. Average TOC ratios range from 0.05 % to 0.15 %. A prominant excursion of 0.75 % in the TOC ratios is recorded at the base of P16 (Priabonian). This prominent TOC excursion correlates with a ~4 m thick interval of transient decreased $CaCO_3$ ratios and a significant negative CIE in the recorded limestones (E1; Fig. VIII.5).

VIII.5 Discussion

VIII.5.1 Circum-Tethyan carbonate platform evolution during the Palaeogene – the Prebetic platform as test case

The biotic evolution of the Prebetic carbonate platform can be characterized by major shifts in the prevailing benthic assemblages (Fig. VIII.4). Those shifts are related to climatic and environmental trends (temperature and nutrient availability) which cause the emergence, proliferation and demise of environmentally sensitive platform organisms. Excellent palaeoenvironmental indicators at the Prebetic platform are represented by corals, larger benthic foraminifera and coralline red algae. Coral reefs represent highly sensitive ecosystems with clearly defined tresholds regarding thermal stress, eutrophication and turbidity (Hallock, 2005; Payros et al., 2010). Increasing global temperatures during the Early Palaeogene (58 – 49 Ma) with low latitudinal gradients and generally low Mg/Ca-ratios in the ocean water hamper the growth of larger coral communities, while larger benthic foraminifera proliferate (Scheibner and Speijer 2008a, b). Furthermore, the aragonitic skeleton of corals is more prone to calcium carbonate dissolution than the calcitic tests of larger benthic foraminifera (Payros et al., 2010). The transition from coral-dominated assemblages to larger benthic foraminifera-dominated assemblages can be observed at the Prebetic platform and throughout the Tethys (Fig. VIII.4). Timing and distribution is, however, strongly linked to latitude (Fig. VIII.6). The three major circum-Tethyan platform stages arranged by Scheibner and Speijer (2008a) pinpoint the climatically-controlled trends in larger benthic foraminifera and coral evolution from the Late Paleocene to the Early Eocene. Platform stage I (58.9 - 56.2 Ma; SBZ 1 – 3) is represented by the dominance of coralgal assemblages throughout

the Tethys. Platform stage II (56.2 – 55.5 Ma; SBZ 4) represents a transitional stage with prevailing corals in the northern Tethyan realm but a significant demise of coral built-ups in the southern Tethys. During platform stage III (55.5 - ?; SBZ 5/6 - ?) LBF have replace corals as major platform organisms.

The demise of coral-dominated platforms during the Paleocene is rather an effect of coupled long-term climatic evolution and multiple transient environmental perturbations. With the pronounced sea-surface temperature rise at the PETM and the coeval eutrophication of shelf areas, the living conditions of corals have probably excessed a critical threshold throughout the Tethys, whereas the long-term coral demise during the Late Palaeogene is only an effect of increasing greenhouse conditions.

However, Scheibner and Speijer (2008a) only define platform stage III as tentative interval with a stratigraphic range of less than 500 ky. The timing of the recovery of the circum-Tethyan coral fauna and thus, the range of platform stage III is still under debate. Höntzsch et al. (in press) show that benthic foraminifera dominate in the low latitude carbonate shelf of Egypt at least until the end of the EECO (~ 49 Ma, SBZ 14a). New data from the Prebetic platform in SE Spain and compiled records from numerous Eocene-Oligocene shallow-marine successions reveal the evolution of circum-Tethyan carbonate platforms during the transition from a global greenhouse to an icehouse (Fig. VIII.6).

We selected eleven Paleocene to Oligocene carbonate platform systems in the Tethys which provide sufficiant data for a comparison between the abundance of corals and LBF. The selected environments range from temperate latitudes (~25°N – 43°N) to equatorial latitudes (<25°N). Especially in the northern cool temperate environments (e.g. Northern Calcareous Alps, Prebetic platform) carbonates are frequently dominated by coralline algae which are associated with LBF (Rasser, 1994; Rasser and Piller, 2004; Nebelsick et al., 2005). However, major platform organisms besides LBF and corals are not considered in this approach, due to their high tresholds to temperature and nutrient fluctuations.

1) Northern Calcareous Alps (43° N)

   Shallow-benthic assemblages in the Northern Calcareous Alps show a significant demise of hermatypic corals and a coeval increase in LBF after the PETM (Darga, 1992; Schuster, 1996b; Scheibner and Speijer, 2008b). However, the coral fauna did not disappear in the Early Eocene and persisted in rare small patch reefs until the Bartonian whereas LBF remain a major platform contributor. During the Priabonian the coral abundance increases significantely. Corals proliferate throughout the Northern Calcareous Alps and form major reefs (Nebelsick et al., 2005).

2) Pyrennes (38° N)

The Pyrenean succession is strongly affected by compressional tectonics of Iberia and Eurasia since the Mesozoic (Vergés et al., 2002). Continuous Palaoegene sections are rare and often influenced by terrigenous deposits. However various studies show flourishing coral patch reefs during the Early Eocene (Eichenseer and Luterbacher, 1992; Schuster, 1996a). Bartonian successions are rare and indicate LBF as major platform building organisms (Payros et al., 2010). During the Priabonian, abundant corals are described within siliciclastic mesotrophic prodelta settings (Morsilli et al., 2010). The ongoing Pyrenean orogeny yielded to an increasing continental infill of the Pyrenean basins and the destruction of the platform during the upper Priabonian and Oligocene (Vergés et al., 2002).

3) North Adriatic platform (38° N)

The Palaeogene succession of the North Adriatic platform reveals LBF-dominated assemblages without corals during the Ypresian and Lutetian (Ćosović et al., 2004; Zamagni et al., 2008). First post-PETM coral records point to the uppermost Lutetian (SBZ 16; Ćosović et al., 2004). A significant increase in coral abundance is recorded during the Early Oligocene in successions in Slovenia and in the Po Basin (Nebelsick et al., 2005).

4) Prebetic platform (36° N)

The Prebetic platform is dominated by LBF assemblages without coral records throughout the Early and Middle Eocene (Geel, 2000; this study). Increasing abundance of coral fragments and first post-PETM patch reefs are present during the Late Eocene (Geel, 2000; this study).

5) Maiella platform (35° N)

Platform deposits of the Maiella platform are dominated by LBF during the Early and Middle Eocene (Moussavian and Vecsei, 1995; Vecsei and Moussavian, 1997). Corals are generally present but are not referred as major platform contributor. Extend coral reefs are described from the Priabonian and Oligocene (Vecsei and Sanders, 1997). The timing of major coral abundance during the Priabonian coincides with coral-solenomeris assemblages in the Trentino in North Italy (SBZ 20; Bassi, 1998; Bosellini and Papazzoni, 2003)

6) Greece (32° N)

Accordi et al. (1998) describes LBF shoal dominated environments with colonial coral fragments during the Early Eocene. The first recorded reefal limestones with major coral abundance points to the Late Bartonian and Priabonian (Barattolo et al., 2007).

The Oligocene is characterized by an increasing restriction of the shallow-marine environment and the concurrent destruction of the platform (Barattolo et al., 2007).

7) Northern and Central Turkey (30° N)

Studies on carbonate platforms from the Palaeogene of northern and central Turkey reveal a strong tectonic influence and highly discontinuous sections. The Thrace Basin in NW Turkey is dominated by LBF during the Early Eocene. First coral records are dated from the Late Eocene (Kemper, 1966); other authors conclude the late Early Oligocene as period with the first coral records in the area (SBZ 21/22; Schuster, 2002; Harzhauser, 2004; İslamoğlu et al., 2010).

8) Northwestern Arabian platform (26° N)

The NW Arabian Platform (or Levant platform) is dominated by nummulitic limestones from the Early Eocene to the Priabonian (Ziegler, 2001; Daod, 2009). Small Early Eocene patch reefs are recorded in Israel (Benjamini, 1981). Krasheninnikov (2005) describes Upper Eocene and Oligocene coral-bearing reefal limestones in the Palmyrids of Syria. In Israel first post-PETM coral records refer to the Late Eocene (Benjamini and Zilberman, 1979).

9) Tunisia (26° N)

Early to Middle Eocene rocks are dominated by nummulitic limestones without hermatypic corals (Loucks et al., 1998; Taktak et al., 2010; Tlig et al., 2010). First rare coral records are present in the Priabonian (Tlig et al., 2010). The Lower Oligocene succession comprises of nummulitic limestones but no coralgal assemblages (Salaj and van Houten, 1988). During the Chattian the deposition at the Tunisian carbonate platform is characterized by increasing continentalization.

10) Libya (20° N)

Early Eocene deposits in the Libyan Sirte Basin are characterized by frequent Nummulitic limestones (Ahlbrandt, 2001). Tawadros (2001) reports on solitary corals in uppermost Lutetian to Priabonian limestones. The first extended reefal limestones are recorded from during the Early Oligocene (Abdulsamad and Barbieri, 1999).

11) Egypt (20° N)

Carbonate platform successions in Egypt are dominated by LBF limestones during the Early Eocene (Schuster, 1996a, b; Wielandt, 1996; Höntzsch et al., in press). Rare isolated coral fragments are found in the Eastern Desert during the Early Eocene (Galala platform; Höntzsch et al., in press) and in the Western Desert during the latest Lutetian, whereas Nummulitic limestones prevailed dominant throughout the Eocene (Tawadros, 2001). During the Oligocene major carbonate platforms of the Egyptian shelf are subaerial exposed and destroyed.

The compiled records of Palaeogene circum-Tethyan platform associations reveal a significant trend regarding timing and latitudinal distribution of LBF and hermatypic corals. Following the definition of circum-Tethyan platform stages of Scheibner and Speijer (2008a), we expand this classification from the Early Eocene to the Oligocene and redefine the stratigraphic range of platform stage III. We introduce three further circum-Tethyan platform stages which are characterized by a) the recovery of isolated coral faunas during the Bartonian in the northern Tethys (platform stage IV), the first larger reefal complexes at the northern Tethys and a recovery of the coral fauna in the southern Tethys during the Priabonian (platform stage V) and b) the Tethyan-wide coexistence of LBF and coral faunas in the Oligocene (platform stage VI).

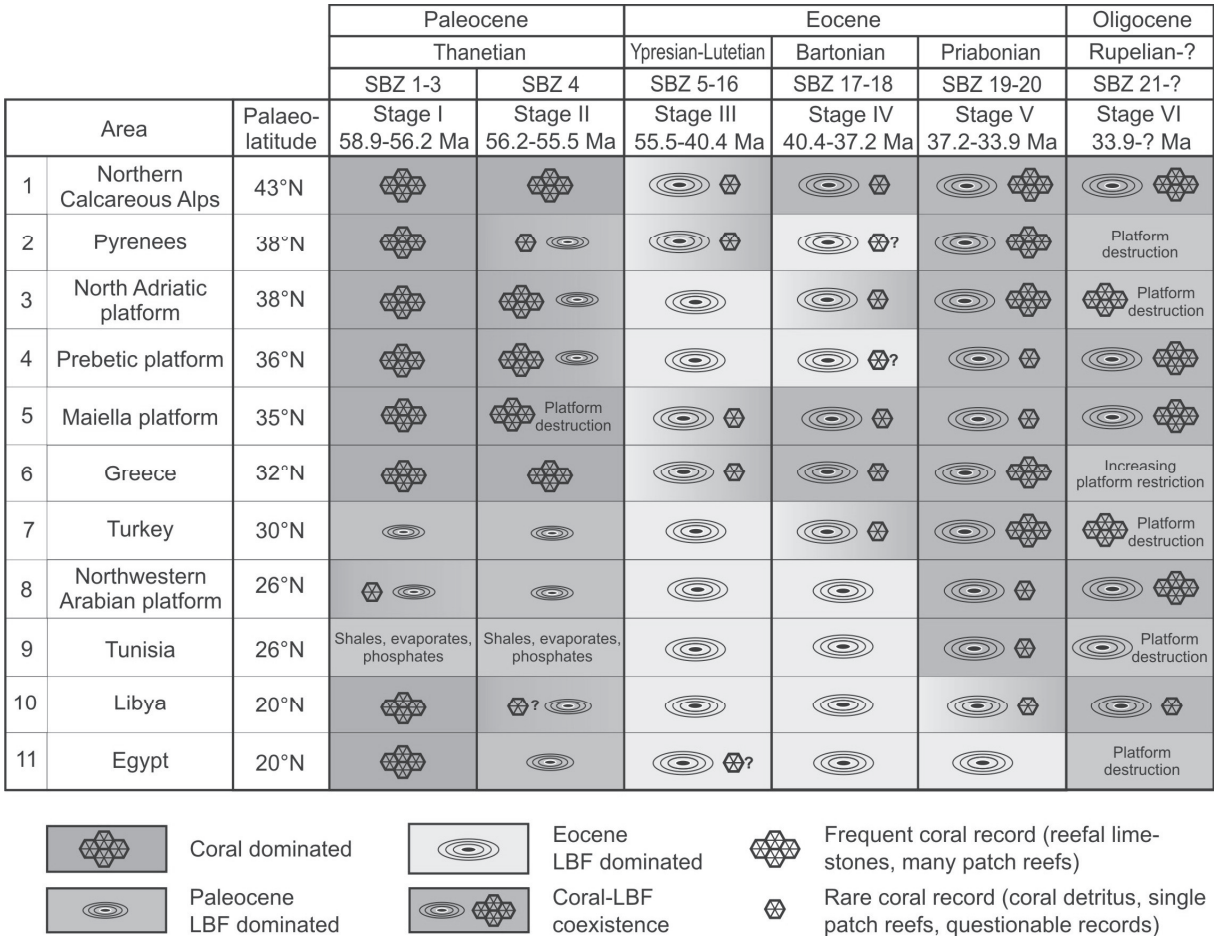

Figure VIII.6 – The evolution of circum-Tethyan carbonate platforms with respect to the latitudinal and quantitavive distribution of LBF and major coral built-ups. Questionsmarks refer to very rare or questionable coral records. Platform stages I-III according to Scheibner and Speijer (2008a). Shallow-benthic zonations (SBZ) refer to the classifications of Cahuzac and Poignant (1997) for the Oligocene and Serra-Kiel et al. (1998) for the Paleocene and Eocene.

Platform stage III (55.5 – 40.4 Ma; SBZ 5 – 16)

Platform stage III, introduced by Scheibner and Speijer (2008a) is defined by the occurrence of typical Eocene LBF assemblages (Early Palaeogene chronofauna: *Nummulites* sp., *Alveolina* sp., *Assilina* sp., *Discocyclina* sp., *Orbitolites* sp.; Buxton and Pedley, 1989; McGowran and Li, 2001) and rare or absent hermatypic coral built-ups (Fig. VIII.6; 'Palaeogene gap' in coral abundance; Wilson and Rosen, 1998). However in several areas in the northern-temperate Tethyan realm (Northern Calcareous Alps, Pyrenees, Maiella Platform) smaller coral patch reefs are recorded (Fig. VIII.6). Size and abundance of coral communities is significantly smaller than in the Paleocene in those areas. Exceptional warm temperatures in higher latitudes caused the expansion of the tropical reef belt >80°N (Kiessling, 2001).

Platform stage IV (40.4 – 37.2 Ma; SBZ 17 – 18)

Platform stage IV represents a transitional stage between circum-Tethyan LBF-dominated carbonate platforms during the Ypresian-Lutetian and the recovery of circum-Tethyan coral faunas during the Priabonian-Oligocene (Fig. VIII.6). The first larger Tethyan coral built-ups have been recorded during the latest Lutetian (Perrin, 2002b). During the Bartonian the occurrence of smaller patch reefs in overall LBF-dominated platforms increases in the northern Tethyan realm (43°N – 30°N). In contrast to the recovery of the coral fauna in the northern temperated-Tethys, the southern Tethyan realm remains coral-free.

Platform stage V (37.2 – 33.9 Ma; SBZ 19 – 20)

The global cooling event at the Bartonian-Priabonian boundary represents a major caesura in the evolution of Tethyan carbonate platform assemblages (Figs. VIII.1 and VIII.6). Many Early Eocene symbiont-bearing LBF have disappeard due to increasing trophic resources at the shelves (eutrophic Priabonian chronofauna; McGowran and Li, 2001). Besides the demise in LBF species, significantly lower temperatures during the Priabonian favoured the expansion of coral communities in the northern Tethys and yielded to the recovery of the coral fauna in the southern Tethys (Fig. VIII.6). Besides this latitudinal differentiation, increasing growth rates in coral reefs also vary beetween the Eastern and the Western Tethys. In the Western Tethys increasing coral growth has been dated during the Late Eocene, whereas coral growth in the Eastern Tethys has not been described until the Early Eocene (Wood, 1999). This observation is in contrast to the study of Kiessling (2001, 2002), who demonstrates a general slight constriction in coral reef growth during the Late Eocene and Early Oligocene. However, at the end of the Eocene the specific diversity of corals has increased significantly and all modern coral families have appeared (Wood, 1999).

Platform stage VI (33.9 – ?; SBZ 21 – ?)

The base of platform stage VI coincides with the massive temperature drope related to the Oi-1 glaciation. This climatic caesura caused the extinction of symbiont-bearing discocyclinids and strong decline in coral abundance but no extinction (Wood, 1999). New LBF emerge which are more tolerant to the cooler climate of the Late Palaeogene. This Oligocene-Miocene LBF chronofauna is dominated by lepidocylinids, smaller nummulitids and miogypsinids (Buxton and Pedley, 1989; McGowran and Li, 2001). Increasing oligotrophic conditions during the Early Oligocene favoured the proliferation of larger coral communities throughout the Tethys. However, the large-scale glacio-eustatic sea-level fall which coincides with the glaciation, caused the continuing continentalization and destruction of many Tethyan carbonate shelves (Fig. VIII.6).

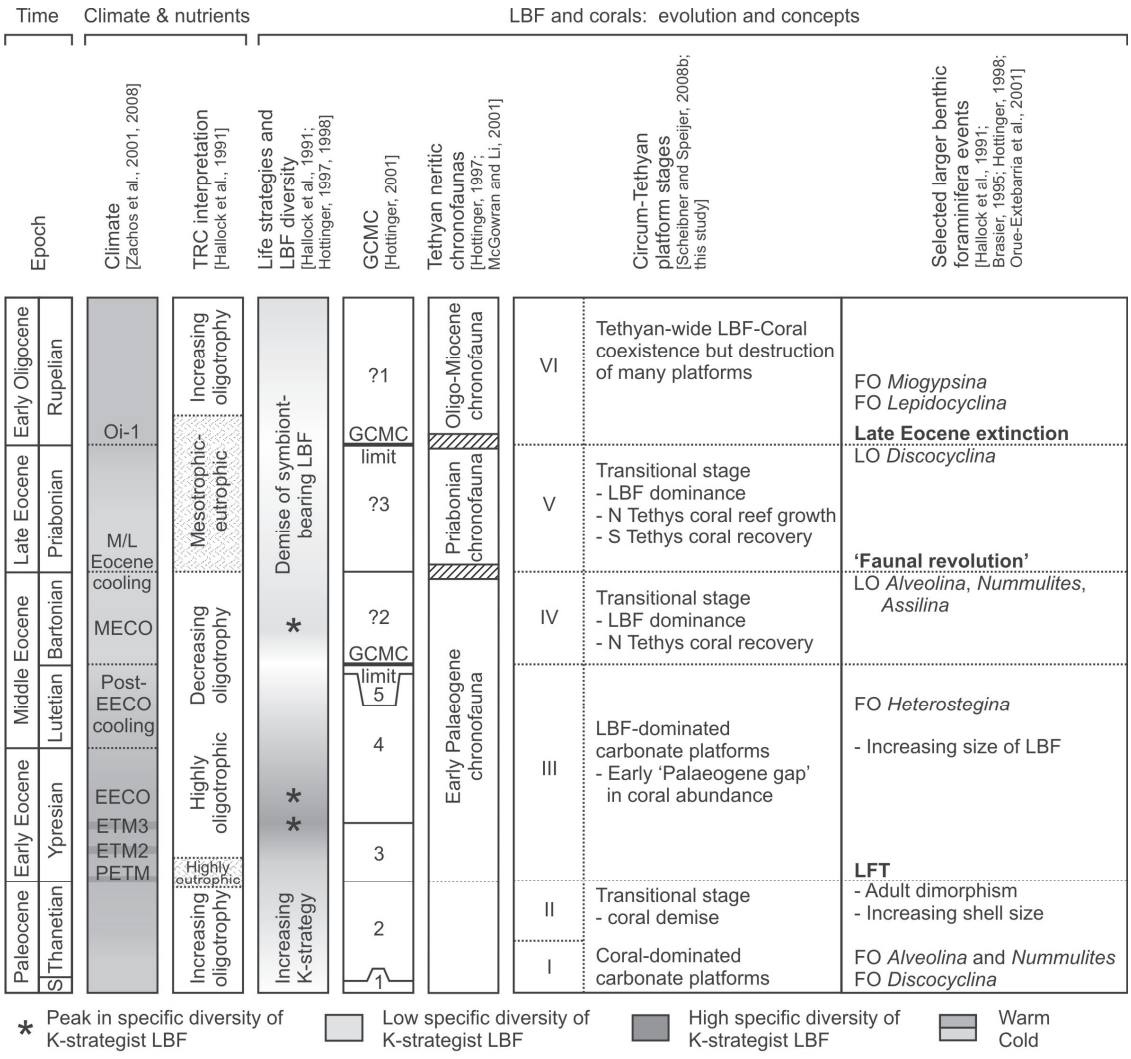

Figure VIII.7 – Relationship between climate, climatic events, trophic resources, LBF and coral evolution and circum-Tethyan platform stages during the Palaeogene. Main evolutionary caesuras are represented by major climatic events (PETM, Middle-Late Eocene cooling event, Oi-1 glaciation). The GCMC limit at the Lutetian-Bartonian boundary is propably linked to the increasing availablility of nutrients at the shelves. Abbreviations: S – Selandian, ETM – Eocene Thermal Maximum, FO – first occurrence, LO – last occurrence.

VIII.5.2 Variations in the evolution of LBF and corals at the Prebetic platform

The Prebetic carbonate platform represents an exception in the evolution of the Eocene coral fauna in the northern Tethys. The first coral records are found in the Late Eocene, whereas carbonate platforms in comparable latitudes reveal first frequent coral records during the Lutetian (Maiella Platform, Pyrenees) or Bartonian (North Adriatic Platform).

The causes for the absence of Middle Eocene coral faunas in the Prebetics are supposed to be related to repeated tectonic perturbations throughout the Palaeogene (Figs. VIII.1 and VIII.4). Frequent phases of tectonic deformation in the hinterland as well as the continuing convergence of the Betic domain towards the Prebetic shelf yielded to a high environmental instability. Repeated uplift at the Iberian hinterland linked to tropical humid to semi-humid climate causes the erosion and discharge of large amounts of terrigenous deposits toward the shelf (Postigo Mijarra et al., 2009). High-resolution carbon isotope records from the hemipelagic Relleu section indicate a depositional system, which is strongly decoupled from the global carbon cycle (Fig. VIII.5). This decoupling is related to increasing regional environmental impact in the Prebetic realm. Furthermore, the continuing convergence of the Betic domain may be related to an increasing isolation of the Prebetic shelf. A similar scenario has been described for the Early Eocene Egyptian shelf (Höntzsch et al., in press). Tectonic uplift along the SE Mediterranean Syrian Arc-Fold Belt associated with the closure of the Eastern Tethyan saeaway due to the initial contact between India and Eurasia yielded to an increasing restriction of the Egyptian Eastern Desert Intrashelf Basin (Höntzsch et al., in press). Assemblages of coralline red algae, green algae and LBF indicate higher trophic resources in the Egyptian platform succession (Hallock and Schlager, 1986; Vecsei, 2003; Bassi, 2005). A similar microfacies has been detected at the Palaeogene Prebetic succession. James et al. (1999) concluded that the combination of warm-temperated conditions and mesotrophic nutrient influx promotes coralline algae and bryozoan growth rather than the proliferation of reef-building corals. Recent studies have shown that increased terrestrial sediment influx decreses coral reef viability (Ryan et al., 2008). Copper (1994) links global coral reef crises in Earth history with periods of major tectonic reorganisation and climate change.

In contrast to the described scenario, enhanced nutrient availability and shelf restriction may not hinder the proliferation of corals. In the Pyrenees, Eocene non-framework coral built-ups have also developed in mesotrophic, turbid and poorly illuminated environments with high terrestrial sediment discharge (Morsilli et al., 2010). Leinfelder (1997) demonstrates the occurrence of coral reefs in siliciclastic settings in the Late Jurassic of Portugal. Pleistocene and Holocene mixed siliciclastic-carbonate settings with coral proliferation are described from volcanoclastic-influenced shelves in Indonesia (Wilson and Lokier, 2002).

The distribution of LBF at the Prebetic platform is comparable to the general evolution of LBF in the Tethys. The significant larger foraminifera turnover (LFT) at the Paleocene-Eocene boundary has been recorded for the first time in the Prebetic realm. Besides the prominent LFT, subsequent specific transitions are rather gradual than abrupt. Increasing records of LBF are often related to tectonically-driven mass wasting intervals (Fig. VIII.4). However, a prominent demise in the abundance of LBF and the dominance of miliolids and soritids during the upper Lutetian and Bartonian indicates the tectonically-driven restriction of the platform. The mass occurrence of *Solenomeris* sp. during the Priabonian has also been observed in the Early Eocene Pyrenean domain (Perrin, 1992; Plaziat and Perrin, 1992). The occurrence of *Solenomeris* built-ups is attributed to multikilometer-sized LBF reef bodys. Furthermore, ecological similarities between *Solenomeris* and coral reefs probably indicate environmental similarities of both organism groups. However, *Solenomeris* is attributed to tolerate more unfavourable conditions regarding light and trophic regime than corals. Plaziat and Perrin (1992) link the occurrence of *Solenomeris* to the northern limit of coral reef growth. In the Prebetics, the first post-PETM coral records are present in the Lower Oligocene (Fig. VIII.4). The mass occurrence of *Solenomeris* during the Late Eocene probably represents a transitional stage in coral recovery in the study area.

VIII.5.3 Global vs. regional carbon isotope trends and the relation to Late Eocene – Oligocene platform evolution

The evolution of the global carbon cycle, expressed in the ratio of stable carbon isotopes ($\delta^{13}C$) is controlled by major carbon fluxes driven by volcanism, tectonics, the expansion of ice sheets and changing Earth parameters. However, global signals are superimposed by regional carbon fluxes, which are related to changes in sea level, productivity and carbon burial, especially on marginal shelves.

Carbon isotope records based on bulk rock measurements indicate trends which are comparable to the high-resolution $\delta^{13}C$ records on deep-marine benthic foraminifera compiled by Zachos et al. (2001) (Exmouth Plateau, Eastern Indian Ocean; Thomas et al., 1992). The carbon isotope ratios of deep-marine bulk rock and benthic foraminifera reveal the evolution of the open ocean ocean reservoir. Carbon isotopes of peri-platform desposits are, however, strongly influenced by regional tectonic, oceanographic and climatic conditions and may significantly vary from those of the open ocean.

Carbon isotope trends of marginal hemipelagic and pelagic sediments have been used as proxy for Cenomanian – Turonian sea level flutuations since the late 1980s. Arthur et al. (1987) suggested a relationship between sediment erosion and decreasing $\delta^{13}C$ in the geological record. A shift to more negative $\delta^{13}C$ ratios requires the input of isotopical lighter

carbon (^{12}C), for example by the input of oxidized organic matter from sediments during sea level rises. This theorhetical approach was proven by Hilbrecht et al. (1986), who revealed a coupling of sea level fluctuations and long term carbon isotope trends in the Cenomanian and Turonian of NW Germany. Mitchell et al. (1996) and Voigt and Hilbrecht (1997) confirmed, that the long-term enrichment in heavier carbon isotopes is strongly related to long-term eustatic sea-level rise. Increases and positive maxima in $\delta^{13}C$ correspond to phases of sediment accumulation during sea level highstands and transgressions. A trend towards $\delta^{13}C$ depleted ratios and negative maxima in $\delta^{13}C$ correspond to phases of sediment erosion and reworking during sea level lowstands and regressions (Hilbrecht et al., 1986; Voigt and Hilbrecht, 1997).

Swart (2008) demonstrated a strong relationship between Late Cenozoic sea-level changes and the $\delta^{13}C$ trends in carbonate platform systems. Aragonite-producing organisms proliferate especially during transgressionas and high sea-levels at carbonate platforms. The chemical signature of aragonite reveals more positive $\delta^{13}C$ ratios, than pelagic deposits without major aragonite concentrations. Following this concept, positive bulk rock $\delta^{13}C$ ratios indicate periods with a high sea level at carbonate platforms, whereas depleted bulk rock $\delta^{13}C$ ratios indicate periods with a low sea level. This relation is decoupled from the isotopic changes of the global carbon cycle. The impact of $\delta^{13}C$ enrichment during sea level highstands requires the presence of major aragonite producing organism (benthic green and red algae, bivalve, gastropods, sepulid worm tubes; according to Van de Poel and Schlager, 1994; Lowenstam and Weiner, 1989; Flügel, 2004).

The Late Eocene – Early Oligocene carbon isotope evolution in the Prebetic realm reveals a prominent decoupling of the shelf from the global carbon cycle, especially during the latest Eocene and late Rupelian-early Chattian (Fig. VIII.4). The significant differences in the carbon isotope evolution are attributed to a strong regional impact on the Prebetic realm and are especially reflected in prominent variations in the carbon isotopes between turbiditic limestones and hemipelagic background marls.

The Relleu section reveals five intervals of frequent turbitidic limestone and debris flow deposition (mass wasting intervals: MWI 1 – 4; Fig. VIII.5). Limestones in the Priabonian MWI 1 are significantly enriched in heavier carbon. Microfacies indicate the predominance of aragonitic coralline red algae and calcitic LBF (Fig. VIII.4). Following the approach of Swart (2008), aragonitic organisms which flourish during times of relatively high sea-level favour the production of ^{13}C enriched carbon. Global sea-level and regional sequence stratigraphic reconstructions point to a flooding of the Prebetic platform prior to the Eocene-Oligocene boundary (Fig. VIII.1.; Geel, 2000; Miller et al., 2005). The significant shift towards more negative $\delta^{13}C$ ratios in the Early Oligocene is attributed to the massive glacio-eustatic sea-level of the Oi-1 glaciation, which caused a demise of aragonite producing organisms at the

platform. Microfacies from the sections of Ibi and Relleu do, however, not indicate a demise of red algae abundance during the Oligocene. The ^{13}C enriched turbidites of the Upper Eocene also indicate the negligible discharge of ^{12}C enriched organic matter to the Prebetic shelf.

Early Oligocene turbidite intervals (MWI 2 – 4) are characterized by converging carbon isotope ratios towards those of the hemipelagic background marls but a continuing depletion in the carbon isotope ratios (Fig. VIII.4). This depletion is in contrast to the open ocean data of Thomas et al. (1992) and Zachos et al. (2001). We suggest an increasing restriction of the Prebetic shelf basin, which is related to continuing sea-level drop during the Early Oligocene and the convergence of the Betic domain towards the Iberian massive. Continuing convergence of both domains causes the contraction of the Prebetic shelf and the Subbetic basin. Increasing deposition of terrestrial deposits during generally low Early Oligocene sea level may shift the carbon isotope signature towards more negative ratios (Höntzsch et al., in press).

VIII.6 Conclusions

The analysis of ten Tethyan carbonate platform successions supported by high resolution microfacies and geochemical data from the Prebetic platform in SE Spain reveals the following results regarding the palaeoenvironmental evolution of circum-Tethyan shallow-marine carbonate factories during the Palaeogene:

1) Palaeogene shallow-marine benthic assemblages of the Prebetic carbonate platform have been subdivided in distinct intervals which are related to major climatic thresholds. Paleocene platform deposits are characterized by dominating corals, coralline red algae and smaller benthic foraminifera. Increasing temperatures and decreasing trophic resources caused the demise of major coral and coralline red algae association during the Early and Middle Eocene and favoured the predominance of larger benthic foraminifera. Significant cooling and enhanced trophic resources during the Late Eocene and Oligocene favoured the recovery of corals and coralline red algae and caused major shifts in the larger bethic foraminifera assemblages at the Prebetic platform. However, frequent syn-depositional tectonic activity throughout the Palaeogene caused no significant impact on the prevailing benthic assemblages.

2) The distribution of larger benthic foraminifera and corals at ten Palaeogene circum-Tethyan carbonate platforms has been compared with the records of the Prebetic succession. Following the classification of circum-Tethyan platform stages (Scheiber

and Speijer, 2008b), the dominance of corals and larger foraminifera is strongly controlled by climatic variations during the Early Palaeogene.

We re-interpret platform stage III and introduce three new stages (IV - VI) which demonstrate the biotic evolution of carbonate platforms subsequent to the PETM.

Stage III is characterized by the predominance of LBF and rare or absent coral built-ups throughout the Tethys and ranges from the PETM to the Lutetian-Bartonian boundary (SBZ 5 – 16). During the subsequent platform stage IV (SBZ 17 – 18) carbonate platforms are dominated by LBF but corals also proliferate in the northern temperated Tethys. This trend is linked to the increasing cooling of higher latitudes whereas tropical realms remain warm. The Bartonian-Priabonian boundary represents another major cooling event, which coincides with the demise of many symbiont-bearing LBF and the expansion of coral faunas in the tropical southern Tethys (platform stage V; SBZ 19 – 20). Platform stage V coincides with the exceptional highly eutrophic Priabonian chronofauna in LBF evolution. The final step in the transition from greenhouse to icehouse conditions is represented by the Oi-glaciation at the Eocene-Oligocene boundary. This temperature drop favoured the proliferation of major coral builtups throughout the Tethys and their coexistence with newly emergered LBF (platform stage VI, SBZ 21 – ?).

3) Carbon isotope ratios from the Prebetic platform indicate an increasing decoupling of the Prebetic shelf from the global carbon cycle during the Oligocene. Strongly negative carbon isotope ratios suggest increasing carbon burial at the shelf, related to the massive sea level drop at the Eocene-Oligocene. Furthermore, the continuing convergence of the Betic domain and the Iberian Craton causes the restriction of the Prebetic shelf, which yields to increasing terrestrial sediment discharge.

Acknowledgements The authors would like to thank Ralf Bätzel and Karin Gesierich for the excellent preparation of the samples, as well as Brit Kockisch and Monika Segl for the determination of the geochemical parameters. Peter Gabriel is thanked for his creative support. This project is funded by the German Science Foundation (DFG-KU 642/221).

VIII.7 References

Abdulsamad EO, Barbieri R (1999) Foraminiferal distribution and palaeoecological interpretation of the Eocene and Miocene carbonates at Al Jabal al Akhdar (northeast Libya). Journal of Micropalaeontology 18:45-65.

Accordi G, Carbone F, Pignatti JS (1998) Depositional history of a Paleogene carbonate ramp (Western Cephalonia, Ionian Islands, Greece). Geologica Romana 34:131-205.

Adatte T, Bolle M-P, Kaenel ED, Gawenda P, Winkler W, Salis KV (2000) Climatic evolution from Paleocene to earliest Eocene inferred from clay-minerals: a transect from northern Spain (Zumaya) to southern (Spain, Tunisia) and southeastern Tethys margins (Israel, Negev). In: Schmitz, B, Sundquist, B, Andreasson, FP (ed) Early Paleogene Warm Climates and Biosphere Dynamics, Geol. Soc. Sweden, GFF, Uppsala, pp. 7-8.

Ahlbrandt TS (2001) The Sirte Basin Province of Libya - Sirte-Zelten total petroleum system. U.S. Geol. Surv. Bull., pp. 29.

Alegret L, Ortiz S, Arenillas I, Molina E What happens when the ocean is overheated? The foraminiferal response across the Paleocene-Eocene Thermal Maximum at the Alamedilla section (Spain). Geological Society of America Bulletin 122:1616-1624.

Alegret L, Ortiz S, Orue-Etxebarria X, Bernaola G, Baceta JI, Monechi S, Apellaniz E, Pujalte V (2009) The Paleocene-Eocene Thermal Maximum: new data on microfossil turnover at the Zumaia section, Spain. Palaios 24:318-328.

Alonso-Chaves F, Soto J, Orozco M, Kilias A, Tranos M (2004) Tectonic evolution of the Betic Cordillera: an overview. Bulletin of the Geological Society of Greece 35:1598-1607.

Andrieux J (1971) La structure du Rif central Étude des relations entre la tectonique de compression et les nappes de glissement dans un tronçon de la chaîne alpine. pp. 155.

Angori E, Bernaola G, Monechi S (2007) Calcareous nannofossil assemblages and their response to the Paleocene-Eocene Thermal Maximum event at different latitudes: ODP Site 690 and Tethyan sections. Geological Society of America Special Papers 424:69-85.

Arthur MA, Schlanger SO, Jenkyns HC (1987) The Cenomanian-Turonian Oceanic Anoxic Event, II. Palaeoceanographic controls on organic-matter production and preservation. Geological Society, London, Special Publications 26:401-420.

Barattolo F, Bassi D, Romano R (2007) Upper Eocene larger foraminiferal–coralline algal facies from the Klokova Mountain (southern continental Greece). Facies 53:361-375.

Bassi D (1998) Coralline algal facies and their palaeoenvironments in the Late Eocene of Northern Italy (Calcare di Nago, Trento). Facies 39:179-202.

Bassi D (2005) Larger foraminiferal and coralline algal facies in an Upper Eocene storm-influenced, shallow-water carbonate platform (Colli Berici, north-eastern Italy). Palaegeography, Palaeoclimatology, Palaeoecology 226:17-35.

Beerling DJ (2000) Increased terrestrial carbon storage across the Palaeocene-Eocene boundary. Palaeogeography, Palaeoclimatology, Palaeoecology 161:395-405.

Benjamini C, Zilberman E (1979) Late Eocene coral reefs of the western Negev, Israel. Isr Jour Earth Sci 28:42-46.

Benjamini C (1981) Limestone and chalk transitions inthe Eocene of the Western Negev, Israel. In: Neale, JW, Brasier, MD (ed) Microfossils from recent and fossil shelf seas, pp. 205-213.

Bijl PK, Houben AJP, Schouten S, Bohaty SM, Sluijs A, Reichart G-J, Sinninghe Damste JS, Brinkhuis H (2010) Transient Middle Eocene Atmospheric CO2 and Temperature Variations. Science 330:819-821.

Blankenship CL (1992) Structure and palaeogeography of the External Betic Cordillera, southern Spain. Marine and Petroleum Geology 9:256, 257-264.

Bohaty SM, Zachos JC (2003) Significant Southern Ocean warming event in the late middle Eocene. Geology 31:1017-1020.

Bolle MP, Adatte T (2001) Palaeocene-early Eocene climatic evolution in the Tethyan realm: clay mineral evidence. Clay Minerals 36:249-261.

Bosellini FR, Papazzoni CA (2003) Palaeoecological significance of coral–encrusting foraminiferan associations: A case–study from the Upper Eocene of northern Italy. Acta Palaeontologica Polonica 48:279-292.

Bouillin JP, Durand-Delga M, Olivier P (1986) Betic-Rifain and Tyrrhenian arcs: Distinctive features, genesis and development stages. In: Wezel, F (ed) The origin of arcs, Elsevier Science Publ., Amsterdam, pp. 281-304.

Bowen GJ, Beerling DJ, Koch PL, Zachos JC, Quattlebaum T (2004) A humid climate state during the Palaeocene/Eocene thermal maximum. Nature 452:495-499.

Brasier MD (1995) Fossil indicators of nutrient levels. 2: Evolution and extinction in relation to oligotrophy. Geological Society, London, Special Publications 83:133-150.

Buxton MWN, Pedley HM (1989) A standardized model for Tethyan Tertiary carbonate ramps. Journal of the the Geological Society, London 146:746-748.

Cahuzac B, Poignant A (1997) Essai de biozonation de l'Oligo-Miocene dans les bassins europeens a l'aide des grands foraminiferes neritiques. Bulletin de la Societe Geologique de France 168:155-169.

Cervato C, Burckle L (2003) Pattern of first and last appearance in diatoms: Oceanic circulation and the position of polar fronts during the Cenozoic. Paleoceanography 18:1055.

Copper P (1994) Ancient reef ecosystem expansion and collapse. Coral Reefs 13:3-11.

Ćosović V, Drobne K, Moro A (2004) Paleoenvironmental model for Eocene foraminiferal limestones of the Adriatic carbonate platform (Istrian Peninsula). Facies 50:61-75.

Cramer BS, Wright JD, Kent DV, Aubry MP (2003) Orbital climate forcing of d13C excursions in the late Paleocene-early Eocene (chrons C24n-C25n). Paleoceanography 18:1097, doi:10.1029/2003PA000909.

Daod H (2009) Carbonate Microfacies Analysis of Sinjar Formation from Qara Dagh Mountains, South–West of Sulaimani City, Kurdistan Region, Iraq. World Academie of Science, Engeneering and Technology 58:752-762.

Darga R (1992) Geologie, Paläontologie and Palökologie der südostbayrischen unter-Priabonen (Ober-Eozän) Riffkalkvorkommen des Eisenrichtersteins bei Hallthurm (Nördlichen Kalkalpen) und des Kirchberg bei Neubeuern (Helvetikum). pp. 166.

de Ruig MJ, Smit J, Geel T, Kooi H (1991) Effects of the Pyrenean collision on the Paleocene stratigraphic evolution of the southern Iberian margin (southeast Spain). Geological Society of Amercia Bulletin 103:1504-1512.

DeConto RM, Pollard D, Wilson PA, Palike H, Lear CH, Pagani M (2008) Thresholds for Cenozoic bipolar glaciation. Nature 455:652-656.

Doblas M, Oyarzun R (1990) The late Oligocene-Miocene opening of the North Balearic Sea (Valencia basin, western Mediterranean): A working hypothesis involving mantle upwelling and extensional detachment tectonics. Marine Geology 94:155-163.

Eichenseer H, Luterbacher H (1992) The marine Paleogene of the Tremp Region (NE Spain) - depositonal sequences, facies history, biostratigraphy and controlling factors. Facies 27:119-152.

Eldrett JS, Greenwood DR, Harding IC, Huber M (2009) Increased seasonality through the Eocene to Oligocene transition in northern high latitudes. Nature 459:969-973.

Everts AJW (1991) Interpreting compositional variations of calciturbidites in relation to platform-stratigraphy: an example from the Paleogene of SE Spain. Sedimentary Geology 71:231-242.

Flügel E (2004) Microfacies of carbonate rocks. Springer, Berlin, pp. 1-976.

Fontboté J, Vera J (1983) Introduccion de la Cordillera Betica. In: Comba, J (ed) Geologia de España Vol. 2, Instituto Geológico y Minero de España, Madrid, pp. 205-218.

Galdeano CSd (2000) Evolution of Iberia during the Cenozoic with special emphasis on the formation of the Betic Cordillera and its relation with the western Mediterranean. Ciencias da Terra 14:9-24.

Garcia-Hernandez M, Lopez-Garrido AC, Rivas P, Sanz de Galdeano C, Vera IA (1980) Mesozoic palaeogeographic evolution of the External Zones of the Betic Cordillera. Geologie en Mijnbouw 59:155-168.

Gawenda P, Winkler W, Schmitz B, Adatte T (1999) Climate and bioproductivity control on carbonate turbidite sedimentation (Paleocene to earliest Eocene, Gulf of Biscay, Zumaia, Spain). Journal of Sedimentary Research 69:1253-1261.

Geel T, Roep TB, Hinte JEv (1998) Eocene tectono-sedimentary patterns in the Alicante Region (southeastern Spain). In: de Graciansky, PC, Hardenbol, J, Jacquin, T, Vail, PR (ed) Mesozoic and Cenozoic sequence stratigraphy of European Basins, SEPM, Tulsa, pp. 289-302.

Gibbs SJ, Bralower TJ, Bown PR, Zachos JC, Bybell LM (2006) Shelf and open-ocean calcareous phytoplankton assemblages across the Paleocene-Eocene Thermal Maximum: implications for global productivity gradients. Geology 34:233-236.

Hallock P, Schlager W (1986) Nutrient excess and the demise of coral reefs and carbonate platforms. Palaios 1:389-398.

Hallock P, Premoli Silva I, Boersma A (1991) Similarities between planktonic and larger foraminiferal evolutionary trends through Paleogene paleoceanographic changes. Palaeogeography, Palaeoclimatology, Palaeoecology 83:49-64.

Hallock P (2005) Global change and modern coral reefs: new opportunities to understand shallow-water carbonate depositional processes. Sedimentary Geology 175:19-33.

Harzhauser M (2004) Oligocene gastropod faunas of the Eastern Mediterranean (Mesohellenic Through/ Greece and Isfahan-Sirjan Basin/ Central Iran. Courier Forschungsinstitut Senkenberg 248:93-181.

Hilbrecht H, Arthur M, Schlanger S (1986) The Cenomanian-Turonian boundary event: sedimentary, faunal and geochemical criteria developed from stratigraphic studies in NW-Germany. In: (ed) Global Bio-Events, Springer Berlin / Heidelberg, pp. 345-351.

Höntzsch S, Scheibner C, Guasti E, Kuss J, Marzouk AM, Rasser MW (in press) Increasing restriction of the Egyptian shelf during the Early Eocene? - New insights from a southern Tethyan carbonate platform. Palaeogeography, Palaeoclimatology, Palaeoecology:1-18.

Hottinger L (1997) Doktor Honoris Causa Lukas Hottinger.

Hottinger L (1998) Shallow benthic foraminifera at the Paleocene-Eocene boundary. Strata, Serie 1 9:61-64.

Hottinger L (2001) Learning from the past? In: Box, E, Pignatti, S (ed) Volume IV: The living world. Part Two, Academic Press, San Diego, pp. 449-477.

İslamoğlu Y, Harzhauser M, Gross M, Jiménez-Moreno G, Coric S, Kroh A, Rögl F, van der Made J From Tethys to Eastern Paratethys: Oligocene depositional environments, paleoecology and paleobiogeography of the Thrace Basin (NW Turkey). International Journal of Earth Sciences 99:183-200.

Ivany LC, Patterson WP, Lohmann KC (2000) Cooler winters as a possible cause of mass extinctions at the Eocene/Oligocene boundary. Nature 407:887-890.

James NP, Collins LB, Bone Y, Hallock P (1999) Subtropical carbonates in a temperate realm; modern sediments on the Southwest Australian shelf. Journal of Sedimentary Research 69:1297-1321.

Jovane L, Florindo F, Coccioni R, J Dinares-Turell, Marsili A, Monechi S, Roberts AP, Sprovieri M (2007) The middle Eocene climatic optimum event in the Contessa Highway section, Umbrian Apennines, Italy. GSA Bulletin 119:413-427.

Kemper E (1966) Beobachtungen an obereozänen Riffen am Nordrand des Ergene-Beckens (Türkisch-Thrazien). N. Jb. Geol. Paläont. Abh. 125:540-554.

Kennett J, Stott L (1991) Abrupt deep-sea warming, palaeoceanographic changes and benthic extinctions at the end of the Palaeocene. Nature 53:225-229.

Kenter JAM, Reymer JJG, van der Straaten HC, Peper T (1990) Facies patterns and subsidence history of the Jumilla-Cieza region (southeastern Spain). Sedimentary Geology 67:263-280.

Kiessling W (2001) Paleoclimatic significance of Phanerozoic reefs. Geology 29:751-754.

Kiessling W (2002) Secular variations in the Phanerozoic reef ecosystem. In: Kiessling, W, Flügel, E, Golonka, J (ed) Phanerozoic reef patterns, SEPM, Tulsa, pp. 625-690.

Krasheninnikov V (2005) Part II - Syria - Paleogene. In: Krasheninnikov, V, Hall, J, Hirsch, F, Benjamini, C, Flexer, A (ed) Geological Framework of the Levant. Volume I: Cyprus and Syria, Historical Productions-Hall, Jerusalem, pp. 299-342.

Leinfelder RR (1997) Coral reefs and carbonate platforms within a siliciclastic setting: General aspects and examples from the Late Jurassic of Portugal. Proc. 8th Int. Coral Reef Symp. 2:1737-1742.

Lonergan L (1993) Timing and kinematics of deformation in the Malaguide Complex, internal zone of the Betic Cordillera, southeast Spain. Tectonics 12:460-476.

Lopez-Martınez N (1989) Tendencias en plaeobiogeografia el futuro de la biogeografia del pasado In: Aguirre, E (ed) Paleontologia, Madrid, pp. 271-299.

Loucks RG, Moody RTJ, Bellis JK, Brown AA (1998) Regional depositional setting and pore network systems of the El Garia Formation (Metlaoui Group, Lower Eocene), offshore Tunisia. In: Macgregor, DS, Moody, RTJ, Clark-Lowes, DD (ed) Petroleum geology of North Africa, Geological Society, London, Spec. Publ. 132, London, pp. 355-374.

Lourens LJ, Sluijs A, Kroon D, Zachos JC, Thomas E, Röhl U, Bowles J, Raffi I (2005) Astronomical pacing of late Palaeocene to early Eocene global warming events. Nature 435:1083-1087.

Lowenstam HA, Weiner S (1989) On Biomineralization. Oxford University Press, New York, 324 pp.

Maillard, Mauffret (1999) Crustal structure and riftogenesis of the Valencia Trough (north-western Mediterranean Sea). Basin Research 11:357-379.

Martinez del Omo W (2003) La Plataforma Cretácica del Prebético y su falta de continuidad por el Margen Sudibérico. Cuadernos de Geología Ibérica, Volumen especial: Nuevas perspectivas sobre el Cretácico de España 29:111-133.

McGowran B, Li Q (2001) Evolutionary palaeoecology of Cainozoic foraminifera: Tethys, Indo-Pacific, Southern Australasia. Historical Biology: An International Journal of Paleobiology 15:3-27.

Meulenkamp JE, Sissingh Wea (2000) Early to Middle Ypresian, late Lutetian, late Rupelian, early Burdigalian, early Langhian, late Tortonian, Piacenzian/Gelasian. In: Dercourt, J, Gaetani, M. et al. (ed) Atlas Peri-Tethys, Palaeogeographical Maps, CCGM/CGMW, Paris, pp. 17-23.

Meulenkamp JE, Sissingh W (2003) Tertiary palaeogeography and tectonostratigraphic evolution of the Northern and Southern Peri-Tethys platforms and the intermediate domains of the African-Eurasian convergent plate boundary zone. Palaeogeography, Palaeoclimatology, Palaeoecology 196:209-228.

Miller KG, Kominz MA, Browning JV, Wright JD, Mountain GS, Katz ME, Sugarman PJ, Cramer BS, Christie-Blick N, Pekar SF (2005) The Phanerozoic record of global sea-level change. Science 310:1293-1298.

Mitchell SF, Paul CRC, Gale AS (1996) Carbon isotopes and sequence stratigraphy. Geological Society, London, Special Publications 104:11-24.

Molina E, Cosovic V, Gonzalvo C, Salis Kv (2000) Integrated biostratigraphy across the Ypresian/Lutetian Boundary at Agost, Spain. Revue de micropaléontologie 43:381-391.

Morsilli M, Bosellini F, Pomar L, Hallock P, Aurell M, Papazzoni CA (2010) Coral Buildups in Mesophotic, Siliciclastic Prodelta Settings (Late Eocene, Southern Pyrenees, Spain): An As Yet Unexplored Play? AAPG Search and Discovery Article #50311.

Moussavian E, Vecsei A (1995) Paleocene reef sediments from the Maiella carbonate platform, Italy. Facies 32:213-222.

Nebelsick J, Rasser M, Bassi D (2005) Facies dynamics in Eocene to Oligocene circumalpine carbonates. Facies 51:197-217.

Ortiz S, Gonzalvo C, Molina E, Rodríguez-Tovar FJ, Uchman A, Vandenberghe N, Zeelmaekers E (2008) Palaeoenvironmental turnover across the Ypresian-Lutetian transition at the Agost section, Southastern Spain: In search of a marker event to define the Stratotype for the base of the Lutetian Stage. Marine Micropaleontology 69:297-313.

Orue-Etxebarria X, Pujalte V, Bernaola G, Apellaniz E, Baceta JI, Payros A, Nunez-Betelu K, Serra-Kiel J, Tosquella J (2001) Did the Late Paleocene thermal maximum affect the evolution of larger foraminifers? Evidence from calcareous plankton of the Campo Section (Pyrenees, Spain). Marine Micropaleontology 41:45-71.

Payros A, Pujalte V, Tosquella J, Orue-Etxebarria X The Eocene storm-dominated foralgal ramp of the western Pyrenees (Urbasa-Andia Formation): An analogue of future shallow-marine carbonate systems? Sedimentary Geology 228:184-204.

Pearson PN, van Dongen BE, Nicholas CJ, Pancost RD, Schouten S, Singano JM, Wade BS (2007) Stable warm tropical climate through the Eocene Epoch. Geology 35:211-214.

Perrin C (1992) Signification Écologique des foraminifères acervulinidés et leur role dans la formation de faciès récifaux et organogènes depuis le Paléocène. Geobios 25:725-751.

Perrin C (2002) Tertiary: The Emergence of Modern Reef Ecosystems. In: (ed) Phanerozoic Reef Patterns, SEPM (Society for Sedimentary Geology), pp. 587-621.

Perrin C (2002) Tertiary: The emergence of modern reef ecosystems. In: Kiessling, W, Flügel, E, Golonka, J (ed) Phanerozoic reef patterns, SEPM, Tulsa, pp. 587-621.

Plaziat JC, Perrin C (1992) Multikilometer-sized reefs built by foraminifera (Solenomeris) from the early Eocene of the Pyrenean domain (S. France, N. Spain): Palaeoecologic relations with coral reefs. Palaeogeography, Palaeoclimatology, Palaeoecology 96:195-231.

Postigo Mijarra JM, Barrón E, Gómez Manzaneque F, Morla C (2009) Floristic changes in the Iberian Peninsula and Balearic Islands (south-west Europe) during the Cenozoic. Journal of Biogeography 36:2025-2043.

Prothero DR (2003) Chronostratigraphy of the Pacific Coast marine Eocene-Oligocene transition. In: Prothero, DR, Ivany, LC, Nesbitt, EA (ed) From Greenhouse to Icehouse: The Marine Eocene-Oligocene Transition, Columbia University Press, New York, pp. 1-12.

Rasser M (1994) Facies and palaeoecology of rhodoliths and acervulinid macroids in the Eocene of the Krappfeld (Austria). Beitr. Paläont. 19:191-217.

Rasser MW, Piller WE (2004) Crustose algal frameworks from the Eocene Alpine Foreland. Palaeogeography, Palaeoclimatology, Palaeoecology 206:21-39.

Ryan KE, Walsh JP, Corbett DR, Winter A (2008) A record of recent change in terrestrial sedimentation in a coral-reef environment, La Parguera, Puerto Rico: A response to coastal development? Marine Pollution Bulletin 56:1177-1183.

Salaj J, B. Van Houten F (1988) Cenozoic palaeogeographic development of northern Tunisia, with special reference to the stratigraphic record in the miocene trough. Palaeogeography, Palaeoclimatology, Palaeoecology 64:43-57.

Scheibner C, Speijer RP, Marzouk AM (2005) Larger foraminiferal turnover during the Paleocene/Eocene thermal maximum and paleoclimatic control on the evolution of platform ecosystems. Geology 33:493-496.

Scheibner C, Rasser MW, Mutti M (2007) Facies changes across the Paleocene-Eocene boundary: The Campo section (Pyrenees, Spain) revisited. Palaegeography, Palaeoclimatology, Palaeoecology 248:145-168.

Scheibner C, Speijer RP (2008a) Decline of coral reefs during late Paleocene to early Eocene global warming. eEarth 3:19-26.

Scheibner C, Speijer RP (2008b) Late Paleocene–early Eocene Tethyan carbonate platform evolution — A response to long- and short-term paleoclimatic change. Earth-Science Reviews 90:71-102.

Schmitz B, Pujalte V, Nunez-Betelu K (2001) Climate and sea-level perturbations during the Initial Eocene Thermal Maximum: evidence from siliciclastic units in the Basque Basin (Emua, Zumaia and Trabakua Pass), northern Spain. Palaeogeography, Palaeoclimatology, Palaeoecology 165:299-320.

Schmitz B, Pujalte V (2003) Sea-level, humidity, and land-erosion records across the initial Eocene thermal maximum from a continental-marine transect in northern Spain. Geology 31:689-692.

Schuster F (1996) Paleocene coral reefs and related facies associations, Kharga Oasis, Western Desert, Egypt. In: Reitner, J, Neuweiler, F, Gunkel, F (ed) Global and regional controls on biogenic sedimentation. I Reef evolution, Göttinger Arb. Geol. Paläont., Göttingen, pp. 169-174.

Schuster F (1996) Paleoecology of Paleocene and Eocene corals from the Kharga and Farafra Oases (Western Desert, Egypt) and the depositional history of the Paleocene Abu Tartur carbonate platform, Kharga Oasis. Tübinger Geowissenschaftliche Arbeiten A31:96.

Schuster F (2002) Scleractinian corals from the Oligocene of the Qom formation (Esfahan - Sirjan fore-arc basin, Iran). Courier Forschungsinstitut Senckenberg 239:5-55.

Seilacher A (1967) Bathymetry of trace fossils. Marine Geology 5:413-428.

Serra-Kiel J, Hottinger L, Caus E, Drobne K, Ferrandez C, Jauhri AK, Less G, Pavlovec R, Pignatti J, Samso JM, Schaub H, Sirel E, Strougo A, Tambareau Y, Tosquella J, Zakrevskaya E (1998) Larger foraminiferal biostratigraphy of the Tethyan Paleocene and Eocene. Bulletin de la Société Géologique de France 169:281-299.

Swart PK (2008) Global synchronous changes in the carbon isotopic composition of carbonate sediments unrelated to changes in the global carbon cycle. Proceedings of the National Academy of Sciences

Taktak F, Kharbachi S, Bouaziz S, Tlig S (2010) Basin dynamics and petroleum potential of the Eocene series in the gulf of Gabes, Tunisia. Journal of Petroleum Science and Engineering 75:114-128.

Tawadros EE (2001) the Geology of Egypt and Libya. Balkema, Rotterdam, pp. 468.

Thomas E, Zachos JC (2000) Was the late Paleocene thermal maximum a unique event? GFF 122:169-170.

Thomas MFH, Bodin S, Redfern J, Irving DHB (2010) A constrained African craton source for the Cenozoic Numidian Flysch: Implications for the palaeogeography of the western Mediterranean basin. Earth-Science Reviews 101:1-23.

Tlig S, Sahli S, Er-Raioui L, Alouani R, Mzoughi M (2010) Depositional environment controls on petroleum potential of the Eocene in the North of Tunisia. Journal of Petroleum Science and Engineering 71:91-105.

Torres J, Bois C, Burrus J (1993) Initiation and evolution of the Valencia Trough (Western Mediterranean) : constraints from deep seismic profiling and subsidence analysis. Tectonophysics 228:57-80.

Van de Poel HM, Schlager W (1994) Variations in Mesozoic-Cenozoic skeletal mineralogy. Geologie & Mijnbouw 74:31-51.

Vecsei A, Moussavian E (1997) Paleocene Reefs on the Maiella platform margin, Italy: an example of the effects of the Cretaceous/Tertiary boundary events on reefs and carbonate platforms. Facies 36:123-140.

Vecsei A, Sanders DGK (1997) Sea-level highstand and lowstand shedding related to shelf margin aggradation and emersion, Upper Eocene-Oligocene of Maiella carbonate platform, Italy. Sedimentary Geology 112:219-234.

Vecsei A (2003) Nutrient control of the global occurrence of isolated carbonate banks. International Journal of Earth Sciences 92:476-481.

Vergés J, Fernàndez M, Martìnez A (2002) The Pyrenean orogen: pre-, syn-, and post-collisional evolution. In: Rosenbaum, G, Lister, G (ed) Reconstruction of the evolution of the Alpine-Himalayan orogen, Journal of the Virtual Explorer, Electronic Edition, pp.

Voigt S, Hilbrecht H (1997) Late Cretaceous carbon isotope stratigraphy in Europe: Correlation and relations with sea level and sediment stability. Palaeogeography, Palaeoclimatology, Palaeoecology 134:39-59.

Wielandt U (1996) Benthic foraminiferal paleoecology and microfacies investigations of Paleogene sediments from the Farafra Oasis, Western Desert, Egypt. Tübinger Mikropaläontologische Mitteilungen 13:1-78.

Wilson MEJ, Rosen BR (1998) Implications of paucity of corals in the Paleogene of SE Asia: plate tectonics or centre of origin. In: Hall, R, Holloway, JD (ed) Biogeography and geological evolution of SE Asia, Backhuys Publishers, Leiden, pp. 165-195.

Wilson MEJ, Lokier SW (2002) Siliciclastic and volcaniclastic influences on equatorial carbonates: insights from the Neogene of Indonesia. Sedimentology 49:583-601.

Wood R (1999) Reef evolution. Oxford University Press, Oxford, pp. 1-414.

Zachos J, Pagani M, Sloan L, Thomas E, Billups K (2001) Trends, rhythms, and aberrations in global climate 65 Ma to present. Science 292:686-693.

Zachos JC, Dickens GR, Zeebe RE (2008) An early Cenozoic perspective on greenhouse warming and carbon-cycle dynamics. Nature 451:279-283.

Zamagni J, Mutti M, Kosir A (2008) Evolution of shallow benthic communities during the Late Paleocene-earliest Eocene transition in the Northern Tethys (SW Slovenia). Facies 54:25-43.

Zanazzi A, Kohn MJ, MacFadden BJ, Terry DO (2007) Large temperature drop across the Eocene-Oligocene transition in central North America. Nature 445:639-642.

Ziegler M (2001) Late Permian to Holocene Paleofacies Evolution of the Arabian Plate and its Hydrocarbon Occurrences. GeoArabia 6:445-505.

Ziegler PA (1992) Geological Atlas of Western and Central Europe (2nd Edition). Geological Society of London, London.

IX. SUMMARY AND CONCLUSIONS

The studied Palaeogene successions of the Galala platform in Egypt and the Prebetic platform in Spain are excellent examples for carbonate factories in a tectonically active setting. Both platform systems are influenced by strongly varying environmental parameters during times of long-term climatic change. The major outcomes of this multi-proxy approach, based on the analysis of the prevailing platform organisms, high-resolution carbon isotopes and geochemical data are summarized in the following paragraphs:

Distribution of platform biota – rather climatically- than tectonically-controlled

The distribution of the main platform organisms is rather controlled by the prevailing climatic conditions, than by local environmental parameters. The Prebetic and the Galala platform are dominated by larger benthic foraminifera during the Early Eocene, which have replaced corals as major platform contributors during the Late Paleocene. The absence of widespread Tethyan coral communities after the PETM is mainly related to the continuing warming trend, culminating during the EECO. The post-EECO cooling during the Middle Eocene is reflected by the first occurrence of corals in higher latitudes. Continuing cooling during the Late Eocene and the Early Oligocene causes the recovery of the coral fauna also in lower latitudes. Local environmental parameters (e.g., increased nutrient availability, syn-depositional tectonics and the proximity to the continent) may delay the recovery of the coral fauna.

Carbon isotope evolution at the shelves – decoupled from global carbon cycle

High resolution carbon isotopes from the Prebetic and the Galala platform have shown that marginal shallow-marine shelves may be strongly decoupled from the global carbon cycle. The causes of this decoupling are manifold and include a) increasing discharge of isotopically light carbon by continental runoff during times of enhanced chemical weathering at the continents, b) increasing tectonic activity at the hinterland and, c) increasing climatic and tectonic restriction of shelf basins. The input of isotopically light carbon is often related to increasing nutrient availability at the shelves, reflected by the occurrence of nutrient-indicative biota (gastropods, benthic green algae, radiolaria).

Hyperthermals – no impact to shallow-benthic communities?

Post-PETM Early Eocene hyperthermal events are recorded at the Galala platform for the first time in a shallow-marine tropical environment. Eocene Thermal Maxima (ETM) 2 and 3 are expressed by significant negative perturbations in the bulk rock carbon isotope signature, associated to shifts in the bulk rock calcium carbonate and total organic carbon ratios. A

significant impact of those perturbations to shallow-marine benthic assemblages, as recorded during the PETM, is, however, missing.

X. RESEARCH PERSPECTIVES

The investigation of Palaeogene circum-Tethyan carbonate platform systems is mainly focussed on the evolution of selected organism groups, biostratigraphy or the local impact of tectonic perturbations. Coharent palaeoenvironmental models which consider biotic and geochemical proxies are still rare. To understand timing, causes and consequences of climatically-controlled facies shifts, more Tethyan carbonate platforms need to be studied. Further studies should focus on the distribution of platform organisms through time. A latitudinal transect of Tethyan carbonate platforms will help to understand the driving mechanisms.

Repeated Early Eocene hyperthermal events are still underexplored with respect to their impact to shallow-marine environments. Especially the impact on the distribution and evolution of larger benthic foraminifera is still under debate and needs to be refined.

Repeated tectonic perturbations and their impact to shallow-marine carbonate platforms are still not studied in detail. Especially the link between climatically- and tectonically-controlled facies shifts need to be refined and proven with further case studies. A key area may be represented by the NW Arabian platform, the Zagros Belt and the Anatolian platform. Those areas a highly influenced by syn-depositional tectonic deformation and may represent an excellent example for a latitudinal platform transect. Especially the evolution of the NW Arabian platform, which is influenced and controlled by the northern branch of the Syrian Arc-Fold Belt, may be linked to the evolution of the Galala platform as SW counterpart of the Syrian Arc.

High resolution carbon isotopes from the Prebetic and the Galala platform have shown that shelves may be strongly decoupled from the global carbon cycle. The mechanisms, which cause this offset from the global carbon cycle, are manifold and need further investigation.

XI. APPENDIX

Supplementary material, including all recorded sections, sample lists, biostratigraphic and geochemical data, qualitative and quantitative microfacies, reprints of the already published manuscripts as well as a schedular overview of the main causes and consequences of Eocene hyperthermal events on different environments, is provided on an enclosed CD.

XII. REFERENCES

Agnini C, Macrì P, Backman J, Brinkhuis H, Fornaciari E, Giusberti L, Luciani V, Rio D, Sluijs A, Speranza F (2009) An early Eocene carbon cycle perturbation at ~52.5 Ma in the Southern Alps: Chronology and biotic response. Paleoceanography 24:doi:10.1029/2008PA001649.

Alonso-Chaves F, Soto J, Orozco M, Kilias A, Tranos M (2004) Tectonic evolution of the Betic Cordillera: an overview. Bulletin of the Geological Society of Greece 35:1598-1607.

Alonso-Zarza A, Armenteros I, Braga J, Munoz A, Pujalte V, Ramos E, Aguirre J, Alonso-Gavilán G, Arenas C, Baceta J, Carballeira J, Calvo J, Corrochano A, Fornos J, Gonzales A, Luzon A, Martin J, Pardo G, Payros A, Peres A, Pomar L, Rodriguez J, Villena J (2006) Tertiary. In: Gibbons, W, Moreno, T (ed) The Geology of Spain, The Geological Society, pp. 293-335.

Aubry MP (1995) Towards an upper Paleocene-lower Eocene high resolution stratigraphy based on calcareous nannofossil stratigraphy. Israel Journal of Earth Sciences 44:239-253.

Berggren WA, Kent DV, Swisher III CC, Aubry MP (1995) A revised Cenozoic geochronology and chronostratigraphy. In: Berggren, WA, Kent, DV, Aubry, MP, Hardenbol, J (ed) Geochronology, time scales, and global stratigraphic correlation, SEPM Spec. Publ. 54, Tulsa, pp. 129-212.

Berggren WA, Pearson PN (2005) A revised tropical to subtropical Paleogene planktonic foraminiferal zonation. Journal of Foraminiferal Research 35:279-298.

Bohaty SM, Zachos JC (2003) Significant Southern Ocean warming event in the late middle Eocene. Geology 31:1017-1020.

Bosellini A (1989) Dynamics of Tethyan carbonate platforms. In: Crevello, PD, Wilson, JL, Sarg, F, Read, JF (ed) Controls on carbonate platform and basin development, SEPM Spec. Publ. 44, Tulsa, pp. 3-13.

Bosence D (2005) A genetic classification of carbonate platforms based on their basinal and tectonic settings in the Cenozoic. Sedimentary Geology 175:49-72.

Bukry D (1973) Low-latitude coccolith biostratigraphic zonation. Initial Reports Deep Sea Drilling Projects 15:685-703.

Clementz M, Bajpai S, Ravikant V, Thewissen JGM, Saravanan N, Singh IB, Prasad V Early Eocene warming events and the timing of terrestrial faunal exchange between India and Asia. Geology 39:15-18.

Cramer BS, Wright JD, Kent DV, Aubry MP (2003) Orbital climate forcing of d13C excursions in the late Paleocene-early Eocene (chrons C24n-C25n). Paleoceanography 18:1097, doi:10.1029/2003PA000909.

Creech JB, Baker JA, Hollis CJ, Morgans HEG, Smith EGC Eocene sea temperatures for the mid-latitude southwest Pacific from Mg/Ca ratios in planktonic and benthic foraminifera. Earth and Planetary Science Letters 299:483-495.

Crevello P, Read JF, Sarg JF, Wilson JL (1989) Controls on carbonate platform and basin development. SEPM Special Publication 44:405.

de Ruig MJ, Smit J, Geel T, Kooi H (1991) Effects of the Pyrenean collision on the Paleocene stratigraphic evolution of the southern Iberian margin (southeast Spain). Geological Society of Amercia Bulletin 103:1504-1512.

Dickens G, O'Neil J, Rea D, Owen R (1995) Dissociation of oceanic methane hydrate as a cause of the carbon isotope excursion at the end of the Paleocene. Paleoceanography 10:965–971.

Eldrett JS, Greenwood DR, Harding IC, Huber M (2009) Increased seasonality through the Eocene to Oligocene transition in northern high latitudes. Nature 459:969-973.

Everts AJW (1991) Interpreting compositional variations of calciturbidites in relation to platform-stratigraphy: an example from the Paleogene of SE Spain. Sedimentary Geology 71:231-242.

Exon N, Kennett J, Malone M, Party atLSS (2000) The opening of the Tasmanian gateway drove global Cenozoic paleoclimatic and paleoceanographic changes: results of Leg 189. JOIDES J 26:11-17.

Flügel E (1978) Mikrofazielle Untersuchungen von Kalken. Springer, Berlin Heidelberg New York, pp. 453.

Flügel E (2004) Microfacies of carbonate rocks. Springer, Berlin, pp. 1-976.

Fournier F, Borgomano J, Montaggioni LF (2005) Development patterns and controlling factors of Tertiary carbonate buildups: Insights from high-resolution 3D seismic and well data in the Malampaya gas field (Offshore Palawan, Philippines). Sedimentary Geology 175:189-215.

Garcia-Hernandez M, Lopez-Garrido AC, Rivas P, Sanz de Galdeano C, Vera IA (1980) Mesozoic palaeogeographic evolution of the External Zones of the Betic Cordillera. Geologie en Mijnbouw 59:155-168.

Geel T, Roep TB, Hinte JEv (1998) Eocene tectono-sedimentary patterns in the Alicante Region (southeastern Spain). In: de Graciansky, PC, Hardenbol, J, Jacquin, T, Vail, PR (ed) Mesozoic and Cenozoic sequence stratigraphy of European Basins, SEPM, Tulsa, pp. 289-302.

Geel T (2000) Recognition of stratigraphic sequences in carbonate platform and slope deposits: Empirical models based on microfacies analysis of Palaeogene deposits in southeastern Spain. Palaeogeography, Palaeoclimatology, Palaeoecology 155:211-238.

Hallock P, Schlager W (1986) Nutrient excess and the demise of coral reefs and carbonate platforms. Palaios 1:389-398.

Hallock P (1999) Symbiont-bearing Foraminifera. In: Gupta, BS (ed) Modern Foraminifera, Kluwer, Amsterdam, pp. 123-139.

Hardenbol J, Thierry H, Farley MB, Jacquin T, de Graciansky P, Vail PR (1998) Mesozoic and Cenozoic sequence chronostratigraphic framework of European basins. In: de Graciansky, PC, Hardenbol, J, Jacquin, T, Vail, PR (ed) Mesozoic and Cenozoic sequence stratigraphy of European Basins, SEPM Spec. Publ. 60, Tulsa, pp. 3-13.

Hohenegger J (2004) Depth coenoclines and environmental considerations of Western Pacific larger foraminifera. Journal of Foraminiferal Research 34:9-33.

Hohenegger J (2005) Estimation of environmental paleogradient values basedon presence/absence data: a case study using benthic foraminifera for paleodepth estimation. Palaegeography, Palaeoclimatology, Palaeoecology 217:115-130.

Höntzsch S, Scheibner C, Guasti E, Kuss J, Marzouk AM, Rasser MW (in press) Increasing restriction of the Egyptian shelf during the Early Eocene? - New insights from a southern Tethyan carbonate platform. Palaeogeography, Palaeoclimatology, Palaeoecology In Press, Accepted Manuscript:

Hottinger L (1960) Über paleocaene und eocaene Alveolinen. Eclogae geol. Helv. 53:265-283.

Hottinger L (1974) Alveolinids, Cretaceous Tertiary Larger Foraminifera, Exxon Research–European Laboratories. A. Schudel & Co, Riehen, Basel, pp. 85.

Hussein IM, Abd-Allah AMA (2001) Tectonic evolution of the northeastern part of the African continental margin, Egypt. Journal of African Earth Sciences 33:49-68.

Ivany LC, Patterson WP, Lohmann KC (2000) Cooler winters as a possible cause of mass extinctions at the Eocene/Oligocene boundary. Nature 407:887-890.

John CM, Bohaty SM, Zachos JC, Sluijs A, Gibbs S, Brinkhuis H, Bralower TJ (2008) North American continental margin records of the Paleocene-Eocene thermal maximum: Implications for global carbon and hydrological cycling. Paleoceanography 23:PA2217.

Jovane L, Coccioni R, Marsili A, Acton G (2009) The late Eocene greenhouse-icehouse transition: Observations from the Massignano global stratotype section and point (GSSP). Geological Society of America Special Papers 452:149-168.

Katz ME, Pak DK, Dickens GR, Miller KG (1999) The source and fate of massive carbon input during the Latest Paleocene Thermal Maximum. Science 286:1531-1533.

Kennett J, Stott L (1991) Abrupt deep-sea warming, palaeoceanographic changes and benthic extinctions at the end of the Palaeocene. Nature 53:225-229.

Krenkel E (1925) Geologie Afrikas. Gebrüder Bornträger, Berlin, pp. 461.

Kurtz AC, Kump LR, Arthur MA, Zachos JC, Paytan A (2003) Early Cenozoic decoupling of the global carbon and sulfur cycles. Paleoceanography 18:1090, doi:10.1029/2003PA000908.

Kuss J, Herbig HG (1993) Biogeography, facies and taxonomy of Early Tertiary green algae from Egypt and Morocco. In: Barattolo, F, De Castro, P, e Parente, M (ed) Studies on fossil benthic algae, Bollettino della Società Paleontologica Italiana, Modena, pp. 249-280.

Kuss J, Scheibner C, Gietl R (2000) Carbonate platform to basin transition along an Upper Cretaceous to Lower Tertiary Syrian Arc Uplift, Galala Plateaus, Eastern Desert, Egypt. GeoArabia 5:405-424.

Kuss J, Bassiouni A, Bauer J, Bachmann M, Marzouk A, Scheibner C, Schulze F (2003) Cretaceous – Paleogene sequence stratigraphy of the Levant Platform (Egypt, Sinai, Jordan). In: Gili, E, Negra, H, Skelton, P (ed) North African Cretaceous Carbonate Platform Systems, Nato Science Series, pp. 171-187.

Lee J (1998) "Living sands" - Larger foraminifera and their endosymbiotic algae. Symbiosis 25:71-100.

Lourens LJ, Sluijs A, Kroon D, Zachos JC, Thomas E, Röhl U, Bowles J, Raffi I (2005) Astronomical pacing of late Palaeocene to early Eocene global warming events. Nature 435:1083-1087.

Martini E (1971) Standard Tertiary and Quaternary calcareous nannoplankton zonation. In: Farinacci, A (ed) Proceedings of the II Plankton Conference, Roma, Edizioni Tecnoscienza Rome, Roma, pp. 739-785.

McGowran B (1989) Silica burp in the Eocene ocean. Geology 17:857-860.

Masse JP, Montaggioni LF (2001) Growth history of shallow-water carbonates: control of accomodation on ecological and depositional processes. International Journal of Earth Sciences 90:452-469.

Moustafa AR, Khalil MH (1995) Superposed deformation in the northern Suez Rift, Egypt: Relevance to hydrocarbons exploration. Journal of Petroleum Geology 18:245-266.

Nicolo MJ, Dickens GR, Hollis CJ, Zachos JC (2007) Multiple early Eocene hyperthermals: Their sedimentary expression on the New Zealand continental margin and in the deep sea. Geology 35:699-702.

Nieto LM, Rey J (2004) Magnitude of lateral displacement on the Crevillente Fault Zone (Betic Cordillera, SE Spain): stratigraphical and sedimentological considerations. Geological Journal 39:95-110.

Nisbet EG, Jones SM, Maclennan J, Eagles G, Moed J, Warwick N, Bekki S, Braesicke P, Pyle JA, Fowler CMR (2009) Kick-starting ancient warming. Nature Geosci 2:156-159.

Orue-Etxebarria X, Pujalte V, Bernaola G, Apellaniz E, Baceta JI, Payros A, Nunez-Betelu K, Serra-Kiel J, Tosquella J (2001) Did the Late Paleocene thermal maximum affect the evolution of larger foraminifers? Evidence from calcareous plankton of the Campo Section (Pyrenees, Spain). Marine Micropaleontology 41:45-71.

Pearson PN, van Dongen BE, Nicholas CJ, Pancost RD, Schouten S, Singano JM, Wade BS (2007) Stable warm tropical climate through the Eocene Epoch. Geology 35:211-214.

Pujalte V, Robles S, Robador A, Baceta JI, Orue-Etxebarria X (2009) Shelf-to-Basin Palaeocene Palaeogeography and Depositional Sequences, Western Pyrenees, North Spain. Blackwell Publishing Ltd., pp. 369-395.

Rasser MW (2000) Coralline red algal limestones of the Late Eocene alpine foreland basin in upper Austria: component analysis, facies and palecology. Facies 42:59-92.

Rasser MW, Piller WE (2004) Crustose algal frameworks from the Eocene Alpine Foreland. Palaeogeography, Palaeoclimatology, Palaeoecology 206:21-39.

Röhl U, Westerhold T, Monechi S, Thomas E, Zachos JC, Donner B (2005) The third and final Early Eocene thermal maximum: characteristics, timing, and mechanisms of the "X"-event. GSA Abstracts with Programs 37:264.

Schaub H (1960) Über einige Nummuliten und Assilinen der Monographie und der Sammlung d´Archiae. Eclogae geol. Helv. 53:443-451.

Scheibner C, Reijmer JJG, Marzouk AM, Speijer RP, Kuss J (2003) From platform to basin: The evolution of a Paleocene carbonate margin (Eastern Desert, Egypt). International Journal of Earth Sciences 92:624-640.

Scheibner C, Speijer RP, Marzouk AM (2005) Larger foraminiferal turnover during the Paleocene/Eocene thermal maximum and paleoclimatic control on the evolution of platform ecosystems. Geology 33:493-496.

Scheibner C, Speijer RP (2008) Late Paleocene–early Eocene Tethyan carbonate platform evolution — A response to long- and short-term paleoclimatic change. Earth-Science Reviews 90:71-102.

Scheibner C, Speijer RP (2008) Decline of coral reefs during late Paleocene to early Eocene global warming. eEarth 3:19-26.

Scher HD, Martin EE (2006) Timing and Climatic Consequences of the Opening of Drake Passage. Science 312:428-430.

Searle MP, Windley BF, Coward MP, Cooper DJW, Rex AJ, Rex D, Tingdong LI, Xuchang X, Jan MQ, Thakur VC, Kumar S (1987) The closing of Tethys and the tectonics of the Himalaya. Geological Society of America Bulletin 98:678-701.

Serra-Kiel J, Hottinger L, Caus E, Drobne K, Ferrandez C, Jauhri AK, Less G, Pavlovec R, Pignatti J, Samso JM, Schaub H, Sirel E, Strougo A, Tambareau Y, Tosquella J, Zakrevskaya E (1998) Larger foraminiferal biostratigraphy of the Tethyan Paleocene and Eocene. Bulletin de la Société Géologique de France 169:281-299.

Shahar J (1994) The Syrian Arc System: an overview. Palaeography, Palaeoclimatology, Palaeoecology 112:125-142.

Sijp W, England M, Toggweiler JR (2009) Effect of Ocean Gateway Changes under Greenhouse Warmth. Journal of Climate 22:6639-6652.

Storey M, Duncan RA, Swisher III CC (2007) Paleocene-Eocene thermal maximum and the opening of the Northeast Atlantic. Science 316:587-589.

Thomas E, Zachos JC (2000) Was the late Paleocene thermal maximum a unique event? GFF 122:169-170.

Verdel C, Wernicke BP, Ramezani J, Hassanzadeh J, Renne PR, Spell TL (2007) Geology and thermochronology of Tertiary Cordilleran-style metamorphic core complexes in the Saghand region of central Iran. Geological Society of America Bulletin 119:961-977.

Wei W (2004) Opening of the Australia-Antarctica Gateway as dated by nannofossils. Marine Micropaleontology 52:133-152.

Wilson JL, D'Argenio B (1982) Controls on carbonate platforms and basin systems development. Geology 10:659-661.

Zachos J, Pagani M, Sloan L, Thomas E, Billups K (2001) Trends, rhythms, and aberrations in global climate 65 Ma to present. Science 292:686-693.

Zachos JC, Lohmann KC, Walker JCG, Wise SW (1993) Abrupt Climate Change and Transient Climates during the Paleogene: A Marine Perspective. The Journal of Geology 101:191-213.

Zachos JC, Röhl U, Schellenberg SA, Sluijs A, Hodell DA, Kelly DC, Thomas E, Nicolo M, I Raffi, Lourens LJ, McCarren H, Kroon D (2005) Rapid acidification of the ocean during the Paleocene-Eocene Thermal Maximum. Science 308:1611-1615.

Zanazzi A, Kohn MJ, MacFadden BJ, Terry DO (2007) Large temperature drop across the Eocene-Oligocene transition in central North America. Nature 445:639-642.

XIII. EPILOGUE

On the lapse of Time

"Independently of our not finding fossil remains of such infinitely numerous connecting links, it may be objected, that time will not have sufficed for so great an amount of organic change, all changes having been effected very slowly through natural selection. It is hardly possible for me even to recall to the reader, who may not be a practical geologist, the facts leading the mind feebly to comprehend the lapse of time. He who can read Sir Charles Lyell's grand work on the Principles of Geology, which the future historian will recognise as having produced a revolution in natural science, yet does not admit how incomprehensibly vast have been the past periods of time, may at once close this volume. Not that it suffices to study the Principles of Geology, or to read special treatises by different observers on separate formations, and to mark how each author attempts to give an inadequate idea of the duration of each formation or even each stratum. A man must for years examine for himself great piles of superimposed strata, and watch the sea at work grinding down old rocks and making fresh sediment, before he can hope to comprehend anything of the lapse of time, the monuments of which we see around us.

It is good to wander along lines of sea-coast, when formed of moderately hard rocks, and mark the process of degradation. The tides in most cases reach the cliffs only for a short time twice a day, and the waves eat into them only when they are charged with sand or pebbles; for there is reason to believe that pure water can effect little or nothing in wearing away rock. At last the base of the cliff is undermined, huge fragments fall down, and these remaining fixed, have to be worn away, atom by atom, until reduced in size they can be rolled about by the waves, and then are more quickly ground into pebbles, sand, or mud. But how often do we see along the bases of retreating cliffs rounded boulders, all thickly clothed by marine productions, showing how little they are abraded and how seldom they are rolled about! Moreover, if we follow for a few miles any line of rocky cliff, which is undergoing degradation, we find that it is only here and there, along a short length or round a promontory, that the cliffs are at the present time suffering. The appearance of the surface and the vegetation show that elsewhere years have elapsed since the waters washed their base."

Charles Robert Darwin
"On the Origin of Species by Means of Natural Selection"
Chapter 9: On the imperfection of the Geological record
London, 1859